STUDIES ON HADRON STRUCTURE FUNCTIONS AND GLDAP EVOLUTION EQUATIONS

Ms. Rasna Rajkhowa
Regn. No. 114 *of* 2004

A thesis submitted in
partial fulfillment of the
requirements
for the degree of Doctor of Philosophy

June, 2005

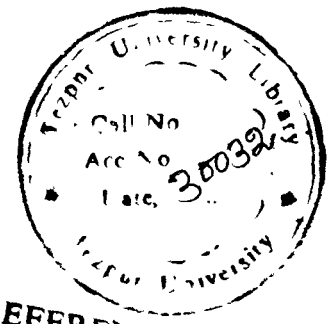

School of Science and Technology
Department of Physics
Tezpur University
Napaam, Tezpur – 784 028
Assam, India

Dedicated to
my beloved father
Late Parama Rajkhowa

And

my beloved mother
Mrs. Renu Rajkhowa

CERTIFICATE

Dr. Jayanta Kumar Sarma
Reader
Department of Physics
Tezpur University
Napaam, Tezpur- 784 028
Assam, India

This is to certify that **Ms. Rasna Rajkhowa** has worked under my supervision for the thesis entitled **Studies on Hadron Structure Functions and GLDAP Evolution Equations** which is being submitted to Tezpur University in partial fulfillment of the requirements for the degree of Doctor of Philosophy. The thesis is Ms. Rajkhowa's own work. She has fulfilled all the requirements under the Ph. D. rules and regulations of Tezpur University and to the best of my knowledge, the thesis as a whole or a part thereof has not been submitted to any other university for any degree or diploma.

Date : 27-06-2005
Place : Napaam, Tezpur

Jayanta Kr Sarma
(Dr. Jayanta Kumar Sarma)
Supervisor

PREFACE

This thesis deals with proton, neutron as well as deuteron structure functions determined from deep inelastic scattering experiments approximated for low-x region. Structure functions are calculated from complete, particular and unique solutions of GLDAP evolution equations which are deduced from pertubative quantum chromodynamics. t and x-evolutions of structure functions at low-x region are predicted. Theoretical predictions are compared with experimental data and recent global parameterizations.

With immense pleasure, I would like to express my profound sense of gratitude to Dr. Jayanta Kumar Sarma, Reader, Physics Department, Tezpur University under whose inspirational guidance this work has been carried out.

I would also like to extend my acknowledgement with gratitude to Professor A. Choudhury and Dr. A. Kumar, Reader, for providing me all necessary facilities of research as the heads of the Department of Physics, Tezpur University during my work.

I express my sincere thanks to Mr. Ganesh Pathak, Dr. Bipul Kr. Bora and all the faculty members of T. H. B. College and Physics Department of Tezpur University for their kind encouragement in performing the research work. I would like to acknowledge the help I received from Mr. Bipul Saikia, who was a constant source of inspiration to me.

I remember with happiness, Mamani ba, Bikash(Baba) da, Jyotshna(Matu) ba, Nabin da, Prasanta(Jitu) da, Suman, Buman, Eman, Sun, Bipasha and a number of friends and well wisher who extended their helpful hands in a variety of ways and for these, I offer my heartiest thanks to all of them. My warm appreciation goes to Panku, Jagat, Ashok da, Shantanu da, Samiran, Ghana da, Bhaskar da, Dipen da, Sanjib, Tulshi, Manisha, Rupa, Ranjit, Diganta, Abu, Naba, Juti, Syamalima, Angali ba, Mami, Nazir, Sanjib, Boby baidew, Babu for their love, inspiration and close friendship.

Financial support from the University Grants Commission, New Delhi, India as a minor research project is gratefully acknowledged.

Last but not least, I must acknowledge my all family members for extending their sympathy and more particularly my mother Mrs. Renu Rajkhowa, without whose constant encouragement and inspiration, I could not have completed this work in time.

Date : 27-06-2005
Place : Napaam, Tezpur

Rasna Rajkhowa
(Rasna Rajkhowa)

STUDIES ON HADRON STRUCTURE FUNCTIONS AND GLDAP EVOLUTION EQUATIONS

CONTENTS

Chapter–1

INTRODUCTION

1.1. Structure of Matter: A Historical Background

Extensive researches, since the start of nineteenth century, have been carried out by the scientists to conclude about the ultimate representatives of the matter that may be the basic building blocks – now a day called as elementary particles [1], also called sub-atomic particles.

In the beginning of nineteenth century, it was established that matter is composed of atoms and molecules. But soon it was found that atom has also a rich structure and in 1897, Joseph John Thomson, a professor of physics at Cambridge University in England, established the existence of a particle – the 'electron' that still is classified as an elementary particle. Six years later, Ernest Rutherford and Frederick Soddy, working at McGill University in Montreal, found that radioactivity occurs when atoms of one type transmute into those of another kind. The idea of atoms as immutable, indivisible objects had become completely untenable. The basic structure of the atom became apparent at the starting of twentieth century, when experiment and ideas of Rutherford and Niels Bohr established that atom consisted of a positively charged nucleus [2-6] with electrons revolving around it.

In 1932, James Chadwick identified 'neutron' and Werner Heisenberg suggested that atomic nuclei consist of 'neutrons' and 'protons' [2-6]. Thus atomic picture becomes somewhat clear with electron, neutron, proton and 'photon' as the basic building blocks. Photon has been added as a field particle for electromagnetic force such as exists between the nucleus and electrons in the atom, i.e., it is a quantum unit of radiation. It has zero rest mass and is uncharged. In the same year, Carl David Anderson found the positive electron or the 'positron' while studying cosmic ray showers. The discovery of this particle, being the antiparticle of electron, predicted the existence of antimatter. With this discovery it

was thought that the atomic picture could be completed, apart from four force – said particles with three possible antiparticles – anticlectrons, antiprotons and anti neutrons, thus including seven characters. While electron and proton are stable particles, the neutron disintegrates with a lifetime of 18 minutes into a proton with an ejection of β– particle and a 'neutrino'. A neutrino has zero rest mass and no charge. Study of cosmic ray showers led to the discovery of a number of elementary particles.

Quark, any of six types of particle that form the basic constituents of the elementary particles called hadrons, such as the proton, neutron and pion. The quark concept [7-8] was independently proposed in 1963 by the American physicists Murray Gell-Mann and George Zweig. The term 'quark' was taken from the novel by Irish writer James Joyce, 'Finnegans Wake'. Quarks were first believed to be of three kinds: up, down, and strange. The proton, for example, consisted of two up quarks and one down quark, while the neutron consisted of two down quarks and one up quark. Later theorists suggested that a fourth quark might exist; in 1974 the existence of this quark, named charm, was experimentally confirmed [9-10]. Thereafter a fifth and sixth quark-called bottom and top, respectively – were proposed for theoretical reasons of symmetry. Experimental evidence for the existence of the bottom quark [9-10] was obtained in 1977; the top quark eluded researchers until April 1994, when physicists at Fermi National Accelerator Laboratory (Fermilab) announced they had found experimental evidence for the top quark's existence. Confirmation came from the same laboratory in early March, 1995. Quarks have the extraordinary property of carrying electric charges that are fractions of the charge of the electron, previously believed to be the fundamental unit of charge. Whereas the electron has a charge of –1, a single negative charge, the up, charm, and top quarks have charges of +2/3, while the down, strange, and bottom quarks have charges of –1/3.

Each kind of quark has its antiparticle. Quantum chromodynamics (QCD) [11], physical theory of strong interaction, attempts to account for the behaviour of the elementary particles called quarks and gluons, which form the particles known as hadrons. Mathematically, QCD is quite similar to quantum electrodynamics (QED), the theory of electromagnetic interactions; it seeks to provide an equivalent basis for the strong nuclear force that binds particles into atomic nuclei. The prefix 'chromo' refers to 'colour', a

mathematical property assigned to quarks According to QCD each quark appears in three colours [7-10] – red (R), blue (B) and green (G). Antiquarks carry anticolours. Anti-red (Cyan), Anti-blue (Yellow) and Anti-green (magenta), i.e, ($\bar{R}$, $\bar{B}$, $\bar{G}$) . Colour has of course no relation to real colours of every day life; the terminology is just based on the analogy with the way all real colours are made up of three primary colours. Equal mixture

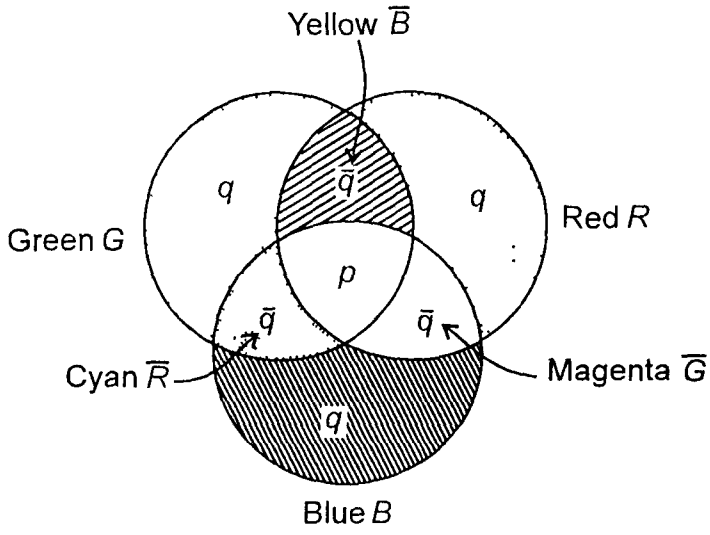

Fig.1.1: Colour composition of hadrons

of Red, Green, Blue (R, G, B) or Cyan, Yellow and magenta ($\bar{R}$, $\bar{B}$, $\bar{G}$) or equal mixture of color and complementary colour i. e. ($R\bar{R}$, $B\bar{B}$, $G\bar{G}$) are white or colourless. This explains why observed particle states – baryon and mesons in nature are colourless or white which means unchanged by rotation in R, B, G space i.e. colour space. It is easy to visualize the colour quantum number by associating the three possible colours of a quark with the three spots of primary red, green and blue light focused on a screen, as shown in figure 1.1. The antiquarks are assigned the complementary colours: Cyan $\bar{R}$, Yellow $\bar{B}$ and magenta $\bar{G}$ The colours assigned to the antiquarks appear in figure 1.1 in those parts of the screen where two and only two primary beams overlap. The analogy we have developed between the colour quantum number and colour is not perfect. The three $q\bar{q}$ states $R\bar{R}$, $G\bar{G}$ and $B\bar{B}$ are colourless, but it is only the combination $R\bar{R}+G\bar{G}-B\bar{B}$, unchanged by rotations in R, G, B colour space, which can form an observed meson. In other words, we use 'colourless' to mean a singlet representation of the colour group.

The carrier of the force between quarks is a particle called the gluon [7-10]. This strong

nuclear force is the strongest of the four fundamental forces. It has an extremely short range of about 10^{-15} m, less than the size of an atomic nucleus. The properties of the gluon come out of the standard model theory. Evidence for gluons comes in 1978 from an electron – positron machine at Hamburg in Germany. The machine, called PETRA [9-10], was able, like its Stanford twin PEP, to observe collisions up to 30 GeV and in the pattern of produced particles, the gluon was read.

Quarks cannot be separated from each other, for this would require far more energy than even the most powerful particle accelerator [2, 9-10] can provide. They are observed bound together in pairs, forming particles called mesons, or in threes, forming particles called baryons, which include the proton and neutron. However, at the colossal temperatures and pressures of the first millisecond following the birth of the universe in the big bang, quarks did exist singly. While the properties of quarks and other kinds of particle are partly accounted for by the so-called standard model of present-day physics, many problems remain. One of these is the question of why quarks have their particular masses. The mass of the top quark is particularly puzzling because it is so large. At approximately 188 times the mass of a proton, the top quark is as massive as an atom of the metal rhenium.

Elementary quarks, which feel the strong force, and leptons, such as electrons, form families, each containing two kinds of quarks and two kinds of leptons. Large Electron Positron (LEP) collider experiments at CERN have shown that there are just three such families, a classification encapsulated in the standard model. Three families of quarks and leptons [7-10, 12] are as follows:

Families of Quarks and Leptons

Particles	First family	Second family	Third family
Quarks	u , d	s , c	b , t
Leptons	e , ν_e	μ , ν_μ	τ , ν_τ

here u, d, s, c, b, t are up, down, strange, charm, bottom and top quarks and e, μ, τ, ν_e, ν_μ, μ_τ are electron, muon, tau, electron-neutrino, muon-neutrino and tau-neutrino respectively.

Apart from gravity, particles undergo three seemingly quite different types of interactions, the electromagnetic interaction of charged particles, the short-range weak interaction which is responsible for the β-decays [3-4] of nuclei, for example, and the strong or hadronic force which holds the quarks to one another and binds nucleons into nuclei. Because of small masses of single atom of particles, gravitational force is negligible at this level. Four forces [2-10] and their field particle's ranges, charges etc. are given below:

The Four Basic Forces

Name	Acts on	Particles of exchange	Range	Strength	Examples	
					Stable system	Reaction induced by force
Gravitational	All particles	Proposed gravition, g^*	Long, i.e. $F \propto 1/r^2$	$\sim 10^{-39}$	Solar system	Object falling
Weak nuclear	All particles except γ	Weak bosons, W and Z	$< 10^{-17}$m	10^{-5}	None	Neutron beta decay
Electro-magnetic	Particles with electric charge	Photon, γ	Long, i.e. $F \propto 1/r^2$	1/137	Atoms	Chemical reactions
Strong nuclear	Quarks and gluons	Gluon, g	10^{-15}	1	Hadrons, nucleons	Nuclear reactions

1.2. Lepton – Nucleon Interactions

Since the discovery of partons more than 30 years ago [13-14], deep inelastic lepton-nucleon scattering experiments [15-16] have provided important information on the structure of the hadrons or ultimately the structure of matter, and on the nature of the

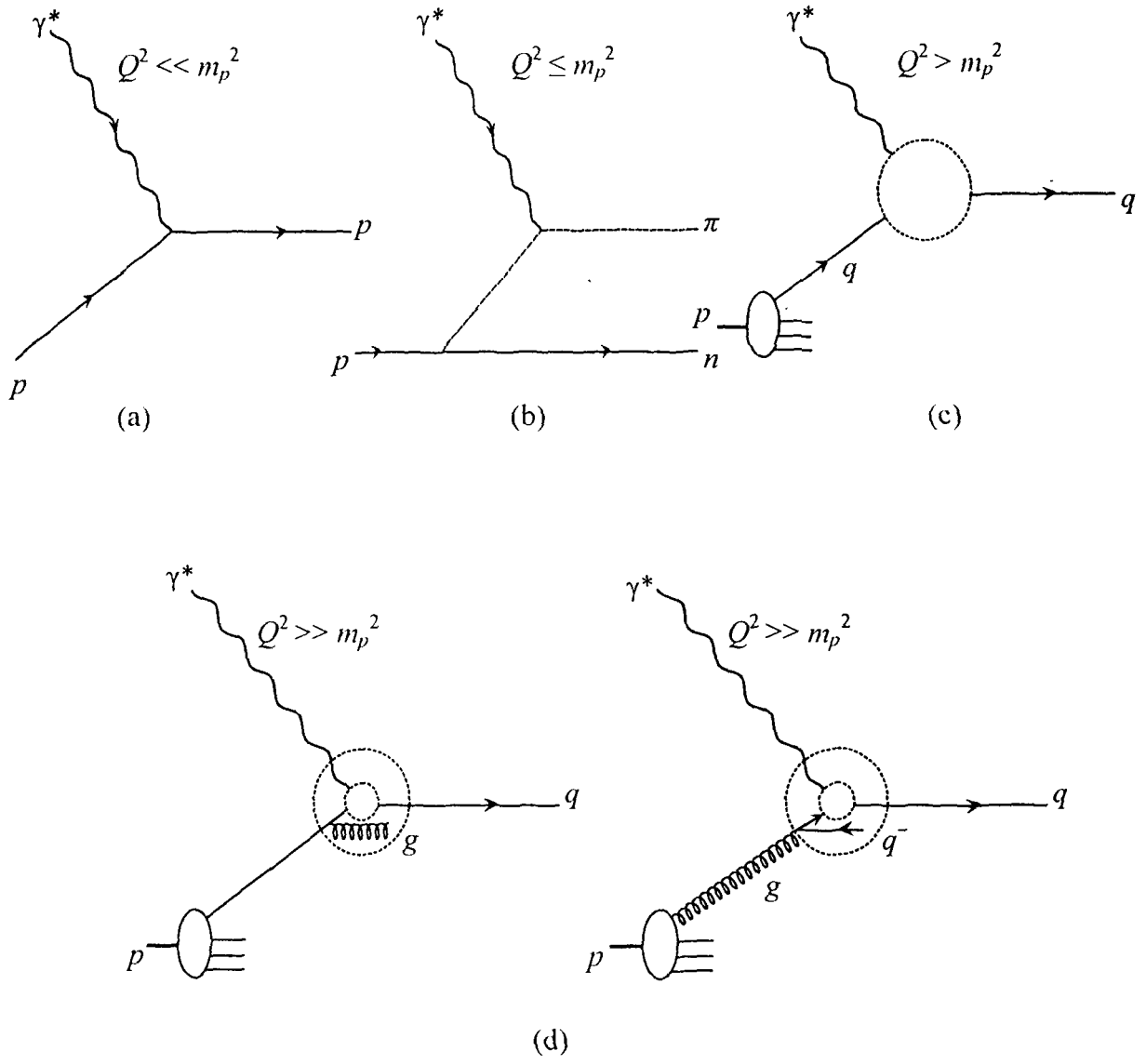

Fig.1.2: The hadron as seen by a 'microscope' ≡ virtual photon: as Q^2 increases, a quark may be resolved into a quark and bremsstrahlung gluon or into a quark - antiquark pair.

interactions between leptons and hadrons. When a very low mass virtual photon ($Q^2 = -q^2 << 1\text{GeV}^2$) scatters off a hadron, the photon 'sees' only the total charge and magnetic moment of the hadron and the scattering appears point-like (Fig.1.2(a)) [17]. A higher-mass photon of a few hundred MeV^2 is able to resolve the individual constituents of the

hadron's virtual pion cloud, as shown in Fig.1.2(b) [17], and the hadron appears as a composite extended object. At high momentum transfers the photon probes the fine structure of the hadron's charge distribution and sees its elementary constituents (Fig.1.2(c)) [17]. If quarks were non-interacting, no further structure would appear for increasing Q^2 and exact scaling would set in. However, in any renormalizable quantum field theory, we have to introduce a Bose-field (gluon) which mediates the interaction in order to form bound states of quarks, i.e. the observed hadrons. In such a picture, the quark is then always accompanied by a gluon cloud which will be probed as the momentum transfer is increased. The effect of gluons is then two-fold as illustrated in Fig. 1.2(d) [17].

When a lepton is scattered by a hadron, photon mediates interaction with quarks inside the hadron. The complete kinematics [18-22] of a deep inelastic scattering (DIS) process is given below:

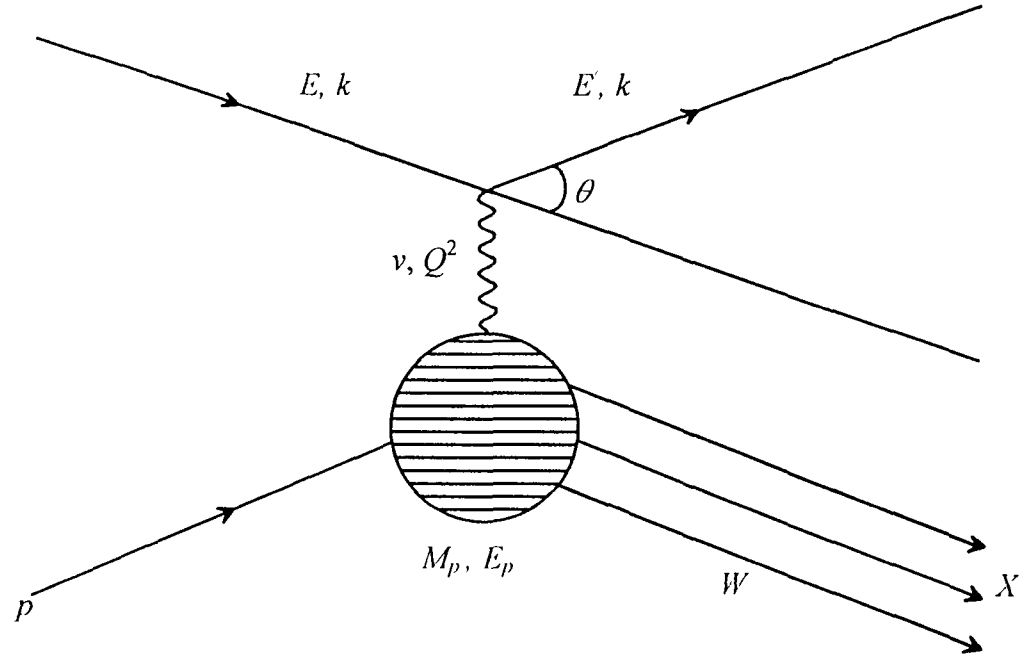

Fig.1.3: Deep inelastic lepton-nucleon scattering ep-eX, via photon exchange between the electron and a quark of the nucleon.

Here,

k = four momentum of the initial lepton,

k' = four momentum of the final lepton,

E = energy of the initial lepton,

E' = energy of the final lepton,

E_p = energy of the hadron,

M_p = rest mass of the hadron,

P = four momentum of the hadron,

S = centre of mass energy squared,

X = any set of outgoing particles,

W^2 = invariant mass squared of the final state hadrons,

θ = angle of the scattered lepton measured with respect to the nucleon direction.

$$S = (k+P)^2 \approx 4EE', \qquad Q^2 = -q^2 = -(k-k')^2 \approx 4EE'Cos^2\theta/2,$$

$$x = \frac{Q^2}{2p.q} = \frac{EE'Cos^2\theta/2}{E_p(E - E'Sin^2\theta/2)},$$

$$y = \frac{p.q}{p.k} \approx \frac{2p.q}{S} \approx \frac{E - E'Sin^2\theta/2}{E}.$$

A quark is carrying a fraction x of the longitudinal momentum of the hadron while y represents the fraction of the lepton energy transferred to the hadron in the nucleon rest frame. The relation between Q^2, x, y and S is $Q^2 \approx xyS$. The differential cross section for DIS from a nuclear target is completely calculable and is expressible in terms of two wave functions W_1 and W_2 which is

$$\sigma \equiv \frac{\partial^2\sigma}{\partial\Omega\,\partial E'} = \sigma^{mott}\left[W_1(\nu,Q^2) + 2W_1(\nu,Q^2)\tan^2\left(\frac{\phi}{2}\right)\right],$$

where

$$\sigma^{mott} = \frac{4\alpha^2 E'}{Q^4}Cos^2\left(\frac{\phi}{2}\right), \quad \nu = E - E' \text{ and, } \phi \text{ and } \theta \text{ are related by } \theta = \pi - \phi.$$

α = fine structure constant (dimensionless measure of strength of this interaction).

Observable structure functions are given by

$$F_1(x) \equiv M_p W_1 = \sum_i f_i(x) e_i^2 \quad \text{and} \quad F_2(x) \equiv \nu W_2 = x \sum_i f_i(x) e_i^2 ,$$

where, $f_i(x)$ is the probability density of finding the i-th parton with fractional momentum x and charge e_i. The Callan-Gross relation $F_2 = 2xF_1$ is a direct consequence of spin half partons and is strongly supported experimentally. A quark carrying a fraction x of the longitudinal momentum of the hadron will be seen by the high-Q^2 virtual photon with a momentum fraction smaller than x, just because the radiated gluon carries away some of the quark's original momentum. Similarly this photon may resolve the radiated gluon into a quark-antiquark pair – a process to be regarded as quark pair creation in the strong gluon field of the nucleon. Both effects will distort a given nucleon structure function $F(x)$ to lower x, and specifically quark pair creation will enhance the sea contribution at small-x. Thus, for a given structure function $F(x)$ of the nucleon, we have to calculate its dependence on Q^2, $F(x, Q^2)$, from radiative corrections as depicted in Fig.1.2 (d). To complete the identification of these partons with the quarks of Gell-Mann and Zweing, one compares electron and neutrino scattering results for F_1 and F_2 to infer the fractional charge assignment of the quark model.

1.3. Small-x Physics

Small-x physics is a new and exciting field of lepton-nucleon scattering. The behaviour of the parton distributions of the hadron in this small-x region is of considerable importance both theoretically and phenomenologicaly. First, the predictions of the rates of various processes at the high energy hadron colliders depend on the parton densities at small-x. From a theoretical point of view, the small-x behaviour is particularly interesting since novel effects are expected to emerge such as, at very low-x region (less than 10^{-3} to 10^{-4}), quarks and gluons radiate 'soft' gluons and thereby new phenomena with high gluon densities – recombination of gluon to form higher-x gluons, shading of gluons by each other, collective effects like condensation or super fluidity or formation of local region (known as hot spots) or something elsé can occur. These may have dominant effect of non-perturbative physics at small-x. Small-x physics represents an unexplored area in deep inelastic structure function of hadrons. Indeed a characteristic expectation of perturbative QCD in the small-x regime is the $x^{-\lambda}$ behaviour, which results from the summation of soft gluon emission via the Lipatov (or BKFL) equation [23-25], with $\lambda = 12\alpha_s \ln(2)/\pi$ for fixed coupling α_s. One consequence is that the gluon and sea quark

distributions are expected to behave as $xg(xq_{sea}) \sim x^{-\lambda}$, where λ may be as large as 0.5 [26-28]. As x decreases parton shadowing will become appreciable and suppresses this singular growth; and eventually we will enter the non-perturbative regime. The solution to this problem is to resum the leading logarithmic behavior of the cross section to all orders, thus rearranging the perturbative expansion into a more rapidly converging series. The GLDAP [29-32] evolution is the most familiar resummation strategy. Given that a cross section involving incoming hadrons is dominated by diagrams where successive emissions are strongly ordered in virtuality, the resulting large logarithms of ratios of subsequent virtualities can be resumed. The cross section can then be rewritten in terms of a process-dependent hard matrix element convoluted with universal parton density functions, the scaling violations of which are described by the GLDAP evolution. A new kinematics regime has opened up where the very small-x parts of the proton parton distributions are being probed. The hard scale, Q^2, is not very high in such events and it was expected that the GLDAP [29-32] evolution should break down. To some surprise, the GLDAP [29-32] evolution has been quite successful in describing the strong rise of the cross section with decreasing x.

At asymptotically large energies, it is believed that the theoretically correct description is given by the BKFL [23-25] evolution. Here, each emitted gluon is assumed to take a large fraction of the energy of the propagating gluon, $(1-z)$ for $z \rightarrow 0$, and large logarithms of $1/z$ are summed up to all orders. Recently, the next-to-leading logarithmic (NLL) corrections to the BKFL equation were calculated and found to be large [33]. This is related to the fact that at any finite energy, the cross section will also get contributions from emissions of gluons which take only a small fraction of the energy of the propagating gluon.

The CCFM [34-37] evolution equation resums also large logarithms of $1/(1-z)$ in addition to the $1/z$ ones. Here, z denotes the energy fraction of the emitted gluon. Furthermore it introduces angular ordering of emissions to correctly treat gluon coherence effects. In the limit of asymptotic energies, it is almost equivalent to BKFL [38-40], but also similar to the GLDAP evolution for large-x and high-Q^2. The cross section is still transverse momentum $k_\perp$ factorized into an off-shell matrix element convoluted with an unintegrated parton density, which now also contains a dependence on the maximum angle allowed in

emissions. An advantage of the CCFM evolution, compared to the BKFL evolution, is that it is fairly well suited for implementation into an event generator program, which makes quantitative comparison with data feasible also for non-inclusive observables.

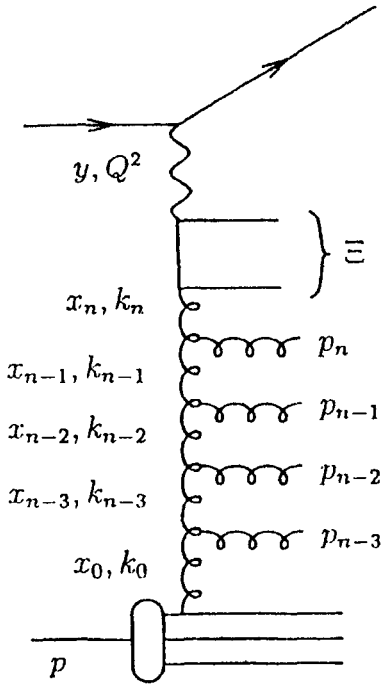

Fig1.3: Kinematic variables for multi-gluon emission. The t-channel gluon momenta are given by k_i and the gluons emitted in the initial state cascade have momenta p_i. The upper angle for any emission is obtained from the quark box, as indicated with Ξ. Here $z_{\pm i} = k_{\pm i} / k_{\pm(i\mp 1)}$ and $q_i = p_{\perp i} /(1 - z_{+i})$.

At small-x, the structure function $F_2(x, Q^2)$ is proportional to the sea quark density, which is driven by the gluon density. The standard QCD fits determine the parameters of the initial parton distributions at a starting scale Q_0^2. With the help of the GLDAP evolution equations these parton distributions are then evolved to any other scale Q^2, with the splitting functions still truncated at fixed $O(\alpha_s)$ at leading order (LO) or $O(\alpha_s^2)$ at next-to-leading order (NLO). Any physics process in the fixed order scheme is then calculated via collinear factorization into the coefficient functions $C^a(x/z)$ and collinear (independent of transverse momentum $k_\perp$) parton density functions $f_a(z, Q^2)$, $\sigma = \sigma_0 \int \frac{dz}{z} C^a(x/z) f_a(z, Q^2)$.

At large energies (small x) the evolution of parton distributions proceeds over a large region in rapidity $\Delta y \sim \log(1/x)$ and effects of finite transverse momenta of the partons

may become increasingly important. Cross sections can then be $k_\perp$-factorized [41-44] into an off-shell ($k_\perp$ dependent) partonic cross section $\hat{\sigma}(x/z, k_\perp)$ and a $k_\perp$-unintegrated parton density function $F(z, k_\perp)$, $\sigma = \int \frac{dz}{z} d^2k_\perp \hat{\sigma}(x/z, k_\perp^2) F(z, k_\perp^2)$. The unintegrated gluon density $F(z, k_\perp^2)$ is described by the BKFL [23-25] evolution equation in the region of asymptotically large energies (small x). An appropriate description valid for both small and large x is given by the CCFM evolution equation [34-37], resulting in an unintegrated gluon density $A(z, k_\perp^2, \bar{q}^2)$, which is a function also of the additional scale $\bar{q}$. The coefficient functions and also the GLDAP splitting functions leading to $f_a(z, Q^2)$ are no longer evaluated in fixed order perturbation theory but supplemented with the all-loop resummation of the $\alpha_s \log(1/x)$ contribution at small x. This all–loop resummation shows up in the regge form factor Δ_{regge} for BKFL or in the non-Sudakov form factor Δ_{ns} for CCFM.

Various high energy deep inelastic interactions give us different evolution equations [23-25, 29-37]. From these evolution equations we can obtain various structure functions which give us information about the number of partons i.e. quarks and gluons involved in different scattering processes. Actually structure function is a mathematical picture of the hadron structure at high-energy region. They are important inputs in many high-energy processes. The different evolution equations are:

A. Gribov-Lipatov-Dokshitzer-Altarelli-Parisi (GLDAP) evolution equation,

B. Balitskij-Kuraev-Fadin-Lipatov (BKFL) evolution equation,

C. Gribov-Levin-Ryskin (GLR) evolution equation, and

D. Ciafaloni-Catani-Fiorani-Marchesini (CCFM) evolution equation.

The exact form of these equations depends upon the accuracy with which one treats the large logarithms $\ln(Q^2/\Lambda^2)$ or $\ln(1/x)$, where Λ is the QCD cut off parameter. The GLDAP evolution equation is obtained in the leading $\ln Q^2$ (LLQ^2) approximation which corresponds to keeping only those terms in the perturbative expansion which has the leading power of $\ln Q^2$ that is $\alpha_s^n \ln^n Q^2$. The BKFL equation is obtained in the leading $\ln(1/x)$ ($LL(1/x)$) approximation instead of leading $\ln Q^2$. The GLR equation is obtained in

the leading power of $\ln Q^2$ and $\ln(1/x)$. GLR evolution equation is a non-linear integro-differential equation for structure function. The CCFM evolution equation resums also large logarithms of $1/(1-z)$ in addition to the $1/z$ ones.

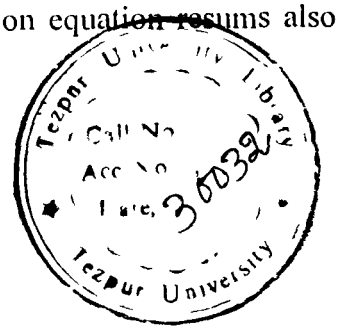

1.4. Evolution Equations

A. GLDAP Evolution Equation

The GLDAP evolution equation is obtained in the (LLQ^2) approximation which corresponds to keeping only those terms in the perturbative expansion which have the leading power of $\ln Q^2$, that is $\alpha_s^n ln^n Q^2$. The GLDAP evolution equation is

$$\frac{\partial q_i(x,Q^2)}{\partial t} = \frac{\alpha_s(Q^2)}{2\pi}\int_x^1 \frac{dy}{y}\left[P_{qq}(x/y)q_i(y,Q^2) + P_{qg}(x/y)G(y,Q^2)\right], \qquad (1.1)$$

for quark. In the above equation, first term mathematically expresses the fact that a quark with momentum fraction x [$q(x, Q^2)$ on the left hand side] could have come form a parent quark with a larger momentum fraction y [$q(y, Q^2)$ on the right-hand side] which has radiated a gluon. The probability that this happens is proportional to $\alpha_s P_{qq}(x/y)$. Second term considers the possibility that a quark with momentum fraction x is the result of $q\bar{q}$ pair creation by a parent gluon with momentum fraction y ($>x$). The probability is $\alpha_s P_{qg}(x/y)$. The integral in the equation is the sum over all possible momentum fractions y ($>x$) of the parent [7]. And for gluon we can give a symbolic representation of the gluon evolution equation as in Fig. 1.4:

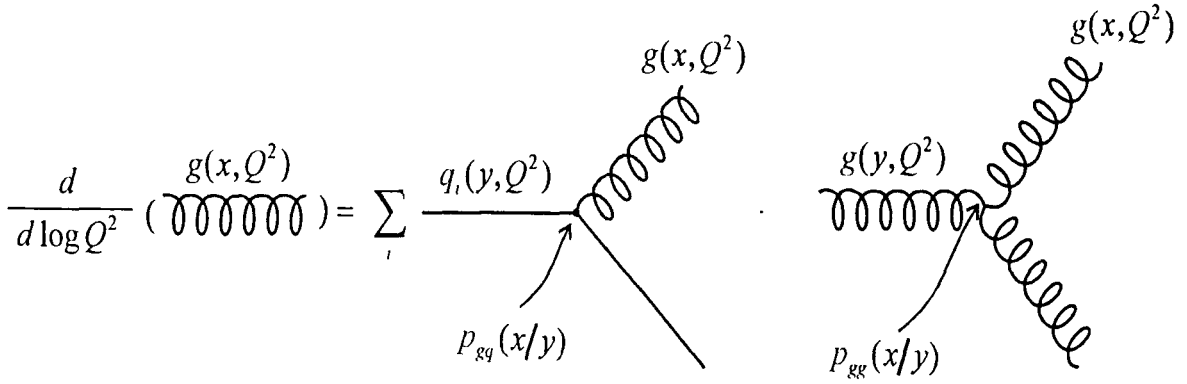

Fig.1.4: Symbolic representation of the gluon evolution equation.

which tells us that

$$\frac{\partial G(x,Q^2)}{\partial t}=\frac{\alpha_s(Q^2)}{2\pi}\int_x^1\frac{dy}{y}\left[\sum_i P_{gq}(x/y)q_i(y,Q^2)+P_{gg}(x/y)G(y,Q^2)\right], \tag{1.2}$$

where $t = \ln(Q^2/\Lambda^2)$ and P_{ab} denoting the splitting functions. The sum $i = 1.....2n_f$, n_f being the number of flavours, runs over quarks and antiquarks of all flavors. P_{gq} does not depend on the index i if the quark masses are neglected [7].

B. BKFL Evolution Equation

The BKFL evolution equation is obtained in the LL($1/x$) approximation instead of the LLQ^2 approximation. The BKFL evolution equation is

$$f(x,k^2)=f^0(x,k^2)+\frac{3\alpha_s(k^2)}{\pi}k^2\int_x^1\frac{dx'}{x'}\int_{k_0^2}^{\infty}\frac{dk'^2}{k'^2}\left\{\frac{f(x',k'^2)-f(x',k^2)}{|k'^2-k^2|}+\frac{f(x',k^2)}{\sqrt{4k'^4+k^4}}\right\}, \tag{1.3}$$

where, the function $f(x, k^2)$ is the nonintegrated gluon distribution, that is $f(x,k^2) = \partial xG(x,k^2)/\partial \ln k^2$, $f^0(x,k^2)$ is a suitably defined inhomogeneous term; k^2, k'^2 are the transverse momenta squared of the gluon in the final and initial states respectively, and k_o^2 is the lower limit cut-off. The important point here is that, unlike the case of the LLQ^2 approximation, the transverse momenta are no longer ordered along the chain.

C. GLR Evolution Equation

In the approximation where only leading power of $\ln Q^2$ and $\ln(1/x)$ are kept, that is the double logarithmic approximation (DLA), compact forms of GLR equations are shown in the recent literature [45-47]. Further approximation is that the coupling of $n \geq 2$ ladder to the hadron is proportional to the n-th power of a single ladder. As a result, the probability of finding two gluons (at low momentum Q_0^2) with momentum fraction x_1 and x_2 is proportional to $g(x_1, Q_0^2).g(x_2, Q_0^2)$. It leads to a non-linear integro-differential equation for structure function,

$$\frac{\partial F(y,\xi)}{\partial \xi} = \frac{1}{2}\int_0^y dy' F(y',\xi)[1 - 2C\exp\{-e^{-\xi} - \xi\}.F(y',\xi)] \quad (1.4)$$

with $C = (3\pi^2/4\beta_0).(Q_0^2/\Lambda^2)$, C representating the relevant coupling strength. A more accurate form of GLR equation reads

$$\frac{\partial \Phi(x,Q^2)}{\partial \ln(1/x)} = \int \hat{k}(q^2,q'^2)\Phi(x,q'^2).\frac{4N_f\alpha_s(q'^2)}{4\pi} - \frac{1}{4\pi R^2}\left(\frac{\alpha_s(q'^2)}{4\pi}\right)^2 .V.\Phi^2(x,Q^2) \quad (1.5)$$

where, $\Phi = \partial F(x, Q^2)/\partial Q^2$, R denotes the transverse radius of the hadron and V stands for the triple ladder vertex. However unlike GLDAP or BKFL equation, approximate analytic solutions of equations (1.4) and (1.5) are not available.

D. CCFM Evolution Equation

The CCFM [34-37] evolution equation with respect to the scale $\bar{q}_i^2$ can be written in a differential form [24]:

$$\bar{q}_i \frac{d}{d\bar{q}^2}\frac{xA(x,k_\perp^2,\bar{q}^2)}{\Delta_s(\bar{q}^2,Q_0^2)} = \int dz \frac{d\phi}{2\pi}\frac{\tilde{P}(z,(\bar{q}/z)^2,k_\perp^2)}{\Delta_s(\bar{q}^2,Q_0^2)} x' A(x',k_\perp'^2,(\bar{q}/z)^2), \quad (1.6)$$

where $A(x,k_\perp^2,\bar{q}^2)$ is the unintegrated gluon density, depending on longitudinal momentum fraction x, transverse momentum $k_\perp^2$ and the evolution variable μ^2 (factorization scale) $=\bar{q}^2$. The splitting variables are $z = x/x$ and $\vec{k}_\perp' = (1-z)/z\vec{q} + \vec{k}_\perp$, where the vector $\vec{q}$ is at an azimuthal angle ϕ. The Sudakov form factor Δ_s is given by

$$\Delta_s(\bar{q}^2,Q_0^2) = \exp(-\int_{Q_0^2}^{\bar{q}^2}\frac{dq^2}{q^2}\int_0^{1-Q_0/q} dz \frac{\bar{\alpha}_s(q^2(1-z)^2)}{1-z}, \text{ with } \bar{\alpha}_s = C_A\alpha_s/\pi = 3\alpha_s/\pi.$$

For inclusive quantities at leading logarithmic order the Sudakov form factor cancels against the $1/(1-z)$ collinear singularity of the splitting function. The splitting function $\tilde{P}$ for branching i is given by:

$$\tilde{P}_g(z_i,q_i^2,k_{\perp i}^2) = \frac{\alpha_s(q_i^2(1-z_i)^2)}{1-z_i} + \frac{\bar{\alpha}_s(k_{\perp i}^2)}{z_i}\Delta_{ns}(z_i,q_i^2,k_{\perp i}^2),$$

where the non-Sudakov form factor Δ_{ns} is defined as:

$$\log \Delta_{ns}(z_i, q_i^2, k_{\perp i}^2) = -\bar{\alpha}_s \int_{z_i}^{1} \frac{dz'}{z'} \int \frac{dq^2}{q^2} \Theta(k_{\perp i} - q)\Theta(q - z'q_i).$$

The unintegrated gluon density $A(x, k_\perp^2, \bar{q}^2)$ is a function also of the angular variable $\bar{q}^2$, ultimately limited by an angle, $\bar{q}^2 = x_{n-1}^2 \Xi_s$, defined by the hard interaction, and the two scales $k_\perp^2, \bar{q}^2$ in $A(x, k_\perp^2, \bar{q}^2)$.

1.5. Experimental Overview

The study of the DIS of leptons on hadrons has been of profound importance to the development of particle physics. Electroweak theory, which describes the electromagnetic and weak nuclear forces, and QCD, the gauge theory of the strong nuclear force, together form what particle physicists call the 'standard model'. The model works well, as far as can be measured using present technology, but several points still await experimental verification or clarification. Furthermore, the model is incomplete. Prior to 1994, one of the main missing ingredients of the standard model was the top quark, which was required to complete the set of three pairs of quarks. Searches for this sixth and heaviest quark failed repeatedly, until in April 1994 a team working on the Collider Detector Facility (CDF) at Fermi National Accelerator Laboratory (Fermilab), announced tentative evidence for the top quark. This was confirmed the following year, when not only the CDF team but also an independent team working on a second experiment at Fermi lab, code-named DZero, or D0, published more convincing evidence. The discovery had required the highest-energy particle collisions available those at Fermi lab's Tevatron, which collides protons with antiprotons at a total energy of 1,800 GeV, or 1.8 tera electron volts (TeV).

The discovery of the top quark in a sense not only completed one chapter in the history of particle physics but also focused the attention of experimenters on other questions unanswered by the standard model. For instance, why there are six quarks and not more or less. It may be that only this number of quarks allows for the subtle difference between particles and antiparticles. This asymmetry between particle and antiparticle could in turn

be related to the domination of matter over antimatter in the universe. Experiments studying neutral *B* mesons, which contain a *b* quark or its antiquark, may eventually reveal such effects and so cast light on this fundamental problem that links particle physics with cosmology and the study of the origin of matter in the universe. Much of current research, meanwhile, is centred on important precision tests which may reveal effects that lie outside the standard model in particular, those that are due to super symmetry. These studies include measurements based on millions of *Z* particles produced at the LEP collider at CERN and the Stanford Linear Collider (SLC) at the Stanford Linear Accelerator Center (SLAC) in California, and on large numbers of *W* particles produced at the Tevatron and later at LEP [9-10]. The precision of these measurements is such that comparisons with the predictions of the standard model constrain the allowed range of values for quantities that are otherwise unknown. The predictions depend, for example, on the mass of the top quark, and in this case comparison with the precision measurements indicates a value in good agreement with the mass measured at Fermilab. This agreement makes another comparison all the more interesting, for the precision data also provide hints as to the mass of the Higgs particle a major ingredient of the standard model that has yet to be discovered. The Higgs particle is the particle associated with the mechanism that allows the symmetry of the electroweak force to be broken, or hidden, at low energies and that gives the *W* and *Z* particles, the carriers of the weak force, their masses. Theory provides a poor guide as to the particle's mass or even the number of different varieties of Higgs particles involved. However, comparisons with the precision measurements from LEP suggest that the mass of the Higgs particle may be quite light.

Further new particles are predicted by theories that include super symmetry. This symmetry relates quarks and leptons, which have spin 1/2 and are collectively called fermions, with the bosons of the gauge fields, which have spins 1 or 2, and with the Higgs particle, which has spin 0. This symmetry appeals to theorists in particular because it allows them to bring together all the particles-quarks, leptons, and gauge bosons-in theories that unite the various forces. The price to pay is a doubling of the number of fundamental particles, as the new symmetry implies that the known particles all have super symmetric counterparts with different spins. Thus the leptons and quarks with spin 1/2 have super symmetric partners, dubbed sleptons and squarks, with integer spins, and the photon, *W*, *Z*, gluon, and graviton have counterparts with half-integer spins, known as

the photino, wino, zino, gluino, and gravitino, respectively. If they indeed exist, all these new super symmetric particles must be heavy to have escaped detection so far. Theory suggests that some of the lightest of them could be created in collisions at the particle accelerators with the highest energies-that is, at LEP, at the Tevatron, and at the Hadron-Electron Ring Accelerator (HERA) and at the DESY (German Electron Synchrotron)

There is still more chance of discoveries, including that of one or more Higgs particles, at the Large Hadron Collider (LHC) planned to start up at CERN about 2005. This machine, built in the same tunnel that houses the LEP collider, is designed to collide protons at energies of 7 TeV per beam [9-10]. Other hints of physics beyond the present standard model concern the neutrinos. In the standard model, these particles have zero mass. So any measurement of a nonzero mass, however small, would indicate the existence of processes that are outside the standard model. Experiments to measure directly the masses of the three neutrinos yield only limits; that is, they give no sign of a mass for the particular neutrino type but do rule out any values above the smallest mass the experiments can measure.

Within the region where the parton modal is applicable (i.e. for $Q^2 > 3\text{GeV}^2$ or so), the small values of x can be measured only in high energy experiments. However, for the exciting fixed target experiments, the low-x condition can only be obtained at the expense of lowering Q^2 below 1 GeV^2. This in turn means that the outgoing lepton is scattered at very small angles, usually equal a few milliradians, i.e. practically within the lepton beam divergence limits. Moreover, the extraction of the inelastic single photon exchange cross sections (or extraction of the structure functions) from the data requires corrections of the experimental yield for the radiative processes, i.e. separating the cross section due to the reaction from the higher order electromagnetic and weak effects faking and distorting the interesting events. Radiative processes may account for a substantial part of the measured low-x cross-section especially for nuclear targets. Listed below are the some experiments of the presently available low-x data.

A. Muon (Electron) Scattering Experiments

1. The Cambridge-Chicago-Illinois-Oxford (CHIO) Collaboration experiment performed

at the Fermilab accelerator with 96, 147, 219 GeV muons scattering off hydrogen and 147 GeV muons off deuterium. The structure function F_2 was measured for $0.0005 < x < 0.7$, $0.2 < Q^2 < 80$ GeV^2 and R for $0.003 < x < 0.10$, $0.4 < Q^2 < 30$ GeV^2 [49]. Observe that in this experiment low values of x were obtained by using data at high values of y where systematic effects are most significant.

2. A dedicated, low scattering angle experiment numbered NA28 performed by the European Muon Collaboration (EMC), at the CERN SPS with a positive muon beam of nominal energy 280 GeV. Structure functions F_2 were measured on deuterium, carbon and calcium targets for $0.002 < x < 0.17$ and $0.2 < Q^2 < 8$ GeV^2 [50-51].

3. The New Muon Collaboration (NMC) perfomed experiment at the CERN SPS with muon beams of energies 90, 120, 200 and 280 GeV. The target materials were ^1H, ^2D, ^4He, ^6Li, ^{12}C, ^{40}Ca, ^{56}Fe, ^{120}Sn, ^{208}pb, and the kinematical range of measurements $0.006 < x < 0.6$, $0.8 < Q^2 < 75$ GeV^2 for $F_2(H)$ and $F_2(D)$ [52], $0.003 < x < 0.7$, $0.12 < Q^2 < 100$ GeV^2 for the ratio $F_2(D)/ F_2(H)$ [53-55] and $0.007 < x < 0.8$, $0.6 < Q^2 < 18.3$ GeV^2 for the $F_2(Ca)/ F_2(Li)$, $F_2(C)/ F_2(Li)$ and $F_2(Ca)/ F_2(C)$ ratios [56] and $0.0035 < x < 0.65$, $0.5 < Q^2 < 90$ GeV^2 for the $F_2(He)/ F_2(D)$, $F_2(C)/ F_2(D)$ and $F_2(Ca)/ F_2(D)$ [57].

4. The experiment of the E665 Collaboration under way at FNAL uses a 490 GeV positive muon beam and ^1H, ^2D, ^{12}C, ^{40}Ca, ^{131}Xe and ^{208}Pb targets. Preliminary results for the $F_2(Xe)/ F_2(D)$ structure function ratio at Q^2 down to 0.01 GeV^2 and x down to 0.00002 have been presented [58-59].

Several low energy electro production experiments have been done both on hydrogen and nuclear targets [60]. In particular, extensive studies were carried out in 1970-1985 at SLAC experiments E49a [61], E62 [62], E87 [63], E139 [64], E140 [65] using a variety of targets. The data were recently reanalyzed [66] using the improved versions of the radiative correction procedure and were normalized to those from the high-precision experiment E140. The reanalysis permitted to extract $R(x, Q^2)$ and $F_2(x, Q^2)$ for proton and deuteron over the range $0.1 < x < 0.9$, $0.6 < Q^2 < 20$ GeV^2 [66].

B. Neutrino Scattering Experiments

1. The California-Columbia-FNAL-Rochester-Rockefeller (CCFRR) Collaboration

measured the neutrino (antineutrino)-iron scattering in the FNAL quadrupole focused beam of energies 120, 140, 168, 200 and 200 GeV [67]. F_2 and xF_3 were extracted for $0.015 < x < 0.65$ and $1.3 < Q^2 < 200$ GeV^2. New, precise results in the same kinematic limits were presented recently by the Wisconsin-Chicago-Columbia-FNAL-Rochester (CCFR) Collaboration [68].

2. The CERN-Dortumund-Heidelberg-Saclay-Warsaw (CDHSW) Collaboration performed the neutrino (antineutrino)-iron scattering experiments at the CERN SPS using the wide-band beam of energy up to about 280 GeV. Measured were F_2, xF_3 for $0.015 < x < 0.65$ and $0.19 < Q^2 < 196$ GeV^2 and F_L, $\overline{q}^{\upsilon}$ in somewhat narrower Q^2 intervals [69].

3. The Big European Bubble Chamber (BEBC) Collaboration at CERN measured the neutrino (antineutrino)-deuteron interaction using the wide-band beam of energy up to 200GeV. Both F_2 and xF_3 isoscalar functions were measured in the range $0 < Q^2 < 64$ GeV^2, $0.028 < x < 0.7$ on neon in BEBC [70].

Some Important Experimental Research Centres

1. CERN (Conseil Europeen pour la Recherche Nucleaire)

byname of ORGANISATION EUROPÉENE POUR LA RECHERCHE NUCLÉAIRE, formerly (1952-54) CONSEIL EUROPÉEN POUR LA RECHERCHE NUCLÉAIRE, English EUROPEAN ORGANIZATION FOR NUCLEAR RESEARCH, is the international scientific organization established for the purpose of collaborative research in sub-nuclear physics (high-energy, or particle physics). The organization operates expressly for research of a 'pure scientific and fundamental character', and the results of its experimental and theoretical work are made generally available. Headquarter of CERN is in Geneva, Switzerland. In the late 20th century, it had a membership of 14 European nations, in addition to several nations those maintained 'observer' status. CERN has the most powerful and versatile facilities of its kind in the world. The site covers more than 100 hectares in Switzerland and, since 1965, more than 450 hectares in France. The activation of a 600-mega volt synchrocyclotron in 1957 enabled CERN physicists to observe the decay of a pion, into an electron and a neutrino. The event was instrumental in the development of the theory of weak interaction. The laboratory grew steadily, activating the particle accelerator known as the Proton Synchrotron (1959), which used 'strong focusing' of particle beams; the Intersecting Storage Rings (ISR; 1971), enabling

head-on collisions between protons; and the Super Proton Synchrotron (SPS; 1976), with a 7-kilometre circumference. With the addition of an Antiproton Accumulator Ring, the SPS was converted into a proton-antiproton collider in 1981 and provided experimenters with the discovery of the *W* and *Z* particles in 1983 by Carlo Rubbia and Simon van der Meer. In November 2000 the Large Electron-Positron Collider (LEP), a particle accelerator installed at CERN in an underground tunnel 27 km in circumference, closed down after 11 years service. LEP was used to counter-rotate accelerated electrons and positrons in a narrow evacuated tube at velocities close to that of light, making a complete circuit about 11,000 times per second. Their paths crossed at four points around the ring. DELPHI, one of the four LEP detectors, was a horizontal cylinder about 10 m in diameter, 10 m long and weighing about 3,000 tones. It was made of concentric sub-detectors, each designed for a specialized recording task. The LEP tunnel will now house the Large Hadron Collider (LHC), a proton-proton collider due to be completed in the early years of the 21st century [71-72].

2. FNAL (Fermi National Accelerator Laboratory)

also called FERMILAB, centre for particle-physics research located at Batavia, Illions in USA, about 43 km west of Chicago. The laboratory is named after the Italian-American physicist Enrico Fermi, who headed the team that first achieved a controlled nuclear reaction. The facility is operated for the United States Department of Energy by the Universities Research Association, a consortium of American and Canadian institutions. The major components of Fermilab are two large particle accelerators called proton synchrotrons, configured in the form of a ring with a circumference of 6.3 km. The first, which went into operation in 1972, is capable of accelerating particles to 400 billion electron volts. The second, called the Tevatron, is installed below the first and incorporates more powerful superconducting magnets; it can accelerate particles to 1 trillion electron volts. The older instrument, operating at lower energy levels, now is used as an injector for the Tevatron. The high-energy beams of particles (notably muons and neutrinos) produced at the laboratory, have been used to study the structure of protons in terms of their most fundamental components, the quarks. In 1977 a team led by Leon Lederman discovered the upsilon meson, which revealed the existence of the bottom quark and its accompanying antiquark. Since 1987 the Tevatron also has operated as a proton-antiproton collider and can achieve total collision energies of 2 TeV. Antiprotons

are produced and stored in a smaller ring before being injected into the main rings for acceleration and collision with protons circulating in the opposite direction. In 1972 a team of scientists at Fermilab isolated the bottom quark and its associated antiquark. The existence of the top quark, the heaviest and most elusive quark predicted by the standard model, was established at Fermilab, and announced in March 1995 [71-73].

3. SLAC (Stanford Linear Accelerator Center)

acronym of STANFORD LINEAR ACCELERATOR CENTER is located in Stanford, California, USA. An exemplar of post World War II Big Science, SLAC is a laboratory for research in particle physics. It is run by Stanford University for the U.S. Department of Energy, but used by physicists from across the United States and from other countries. It houses the longest linear accelerator (linac) in the world-a machine 3.2 km long that accelerates electrons up to energies of 50 giga electron volts. The concept of a multi-GeV electron linac grew from the successful development of smaller electron linacs at Stanford University, culminating in the early 1950s in a 1.2 GeV machine. In 1961 plans for the new machine, designed to reach 20 GeV, were authorized, and the 3.2 km linac was completed in 1966. In 1968 experiments at SLAC found the first direct evidence for further structure (i.e., quarks) inside protons and neutrons. As early as 1961, design work began for an additional machine at SLAC, an electron-positron collider called SPEAR (Stanford Positron-Electron Asymmetric Rings). Construction did not begin until 1970, but the machine was completed within two years, producing collisions at energies of 2.5 GeV per beam. In 1974 SPEAR was upgraded to reach 4.0 GeV per beam, and physicists working with it soon discovered a new type of quark, which became known as charm, and a new, heavy leptons relative of the electron, called the tau. SPEAR was followed by a larger, higher-energy colliding-beam machine, the PEP (Positron-Electron Project), which began operation in 1980 and took electron-positron collisions to a total energy of 36 GeV. The SLAC Linear Collider (SLC) was completed in 1987. SLC uses the original linac, upgraded to reach 50 GeV, to accelerate electrons and positrons before sending them in opposite directions around a 600-metre loop, where they collide at a total energy of 100 GeV. This is sufficient to produce the Z particle, the neutral carrier of the weak nuclear force that acts on fundamental particles [71-73].

4. DESY (Deutsches Elektronen-Synchrotron)

byname of DEUTSCHES ELEKTRONEN-SYNCHROTRON, English German ELECTRON-SYNCHROTRON, the largest centre for particle-physics research in Germany, is located in Hamburg. DESY is funded jointly by the German federal government and the city of Hamburg; in addition, scientists from other countries who participate in the experiments there donate equipments. The laboratory was founded in 1959, when construction began on an electron synchrotron, which was completed in 1964 and eventually could generate an energy level of 7.4 billion electron-volts. The Double Ring Storage Facility (DORIS) was completed 10 years later and was capable of colliding beams of electrons and positrons at 3.5 GeV per beam; in 1978 its power was upgraded to 5 GeV per beam. DORIS is no longer used as a collider, but its electron beam provides synchrotron radiation (mainly at *X*-ray and ultraviolet wavelengths) for experiments on a variety of materials. A larger collider capable of reaching 19 GeV per beam, the Positron-Electron Tandem Ring Accelerator (PETRA), began operation in 1978. Experiments with PETRA in the following year gave the first direct evidence of the existence of gluons, the particles that carry the strong force between quarks. The laboratory's newest facility, completed in 1992, is the Hadron-Electron Ring Accelerator (HERA), the first machine capable of colliding electrons and protons. HERA consists of two rings in a single tunnel with a circumference of 6.3 km, one ring accelerates electrons to 30 GeV and the other protons to 820 GeV. It is being used to continue the study of quarks [71-73].

5. KEK (Koh - Ene - Ken)

stands for 'KOH-ENE-KEN, an abbreviation for a Japanese name of NATIONAL LABORATORY FOR HIGH ENERGY PHYSICS. The High Energy Accelerator Research Organization (KEK) facilitates a wide range of research programs based on high-energy accelerators for users from universities. Both proton accelerators and electron/positron accelerators, including storage rings and colliders, are in operation to support various activities, ranging from particle physics to structure biology. Besides the operation of these accelerators, the laboratory began construction work of newly approved high-intensity proton accelerators in collaboration with Japan Atomic Energy Research Institute for the future development of current research activities. KEK is one of the fourteen Inter-University Research Institutes belonging to MECSST (Ministry of Education, Culture, Sports, Science and Technology). It consists of two research

institutes, Institute of Particle and Nuclear Studies (IPNS) and Institute of Materials Structure Science (IMSS), and two laboratories, Accelerator Laboratory and Applied Research Laboratory, as well as the Engineering Department and the Administration Bureau. IPNS carries out research programs in particle physics and nuclear physics. The Belle collaboration at the KEK B-factory was highlighted by its observation of the CP violation of B-mesons. While most of these experiments are being carried out by international collaborations, international cooperation at oversea institutions is also an important activity of the institute in order to expand the research frontiers for the university staff. The theory group continued activities in fundamental field theory, particle and nuclear phenomenological theory, and computational physics. IMSS offers three types of probes for research programs in material science. The photon factory operates two storage rings for synchrotron radiation, the 2.5 GeV ring with 61 experimental stations and the new 6.5 GeV ring with 6 stations, which was used to be the positron accumulator ring for TRISTAN in former days but was converted to a synchrotron radiation ring. The new ring has a unique capability for single-bunch operation. The Accelerator Laboratory achieved an outstanding success in operating and improving the running accelerators, in designing and constructing the new High Intensity Proton Accelerator (HIPA) project and in pushing R & D work for the future linear-collider project. The luminosity of the KEKB electron-positron collider was steadily improved and its own world-record was kept being renewed. The 8 GeV electron linac was operated extremely efficiently, while providing beams periodically into 3 facilities: KEKB and the 2 SR rings. The Applied Research Laboratory, which has four research centers (Radiation Science Center, Computing Research Center, Cryogenics Science Center and Mechanical Engineering Center), provide basic technical support for all KEK activities with their high-level technologies. In addition to basic support tasks, they also played key roles in front-end programs. One year has already past since KEK became an Inter-University Research Institute Corporation. In 2004, they focused on the construction of the crab cavity which doubles the performance of KEKB electron-positron collider. By the early spring in 2006, they will construct the two crab cavities, which will bring further improvements on KEKB performance [74].

6. VECC (Variable Energy Cyclotron Centre)

acronym of VARIABLE ENERGY CYCLOTRON CENTRE located in Kolkata, India is

a national centre for accelerator based research. The variable energy cyclotron (VEC) set up here is used for research in nuclear sciences, condensed matter physics, accelerator physics, computer science and theoretical physics. Operated by the Department of Atomic Energy (DAE), the centre houses the variable-energy cyclotron built in 1978 and is building a KV500 super conducting cyclotron in conjunction with Bhabha Atomic Research Centre (BARC). VECC is also a major producer of accelerator-generated radioisotopes. The centre is setting up a Superconducting Cyclotron and a Radioactive Ion Beam Facility. VECC is used to conduct primarily peaceful scientific research but the facility's cyclotrons have potential for weapons-related research. In VECC, the production of exotic nuclei in deep inelastic collisions and structure of proton halo nuclei were studied. The effectiveness of stochastic resonances in enhancement of signals over the noise was investigated with interesting results. Relativistic Mean Field theory was used to investigate shape transitions and liquid to gas phase transitions in nuclei. An accurate description of fission width of nuclei using the Longevin dynamics was obtained. The year 2001-2002 marked a major advance towards the global recognition of the Indian built Photon Multiplicity Detector (PMD) in the STAR Experiment at the Relativistic Heavy Ion Collider (RHIC) at Brookhaven national Laboratory (USA) and the signing of the MoU with BNL. The STAR PMD, a smaller version of the PMD detector for the ALICE Project at CERN LHC, was installed in September-October, 2002. Fabrication of the detector is in progress at VECC [75].□

Chapter-2

COMPLETE AND PARTICULAR SOLUTIONS OF FIRST ORDER LINEAR PARTIAL DIFFERENTIAL EQUATIONS

We solve GLDAP evolution equations to obtain t and x distributions of various structure functions using Taylor expansion method. For these, we use method of solution of first order linear partial differential equation to obtain complete and particular solutions, and for x evolutions we use numerical integration. In this chapter, we explain different methods, which are used to obtain the results of our works.

2.1. Taylor Expansion Method

If a function f is such that

(i) the $(n\text{-}1)$th derivative f^{n-1} is continuous in $[a, a + h]$,

(ii) the nth derivative f^n exists in $]a, a + h[$, and

(iii) p is a given positive integer,

then there exists at least one number, θ, between 0 and 1 [76-77] such that

$$f(a+h)=f(a)+hf'(a)+\frac{h^2}{2!}f''(a)+.....+\frac{h^{n-1}}{(n-1)!}f^{n-1}(a)+\frac{h^{n-p}}{(n-1)!p}f^n(a+\theta h). \qquad (2.1)$$

The condition (i) implies the continuity of $f, f', f'', ...f^{n-1}$ in $[a, a + h]$. Let a function Φ be defined by

$$\Phi(x)=f(x)+(a+h-x)f'(x)+\frac{(a+h-x)^2}{2!}f''(x)+.....+\frac{(a+h-x)^{n-1}}{(n-1)!}f^{n-1}(x)+A(a+h-x)^p,$$

where A is a constant to be determined such that $\Phi(a) = \Phi(a + h)$. Thus A is given by

$$f(a+h)=f(a)+hf'(a)+\frac{h^2}{2!}f''(a)+.....+\frac{h^{n-1}}{(n-1)!}f^{n-1}(a)+Ah^p. \qquad (2.2)$$

The function Φ is continuous in $[a, a + h]$, derivable in $] a, a + h [$ and $\Phi(a) = \Phi(a + h)$. Hence, by Rolle's Theorem [76], there exists at least one number, θ, between 0 and 1 such that $\Phi'(a + \theta h) = 0$. But,

$$\Phi'(x) = \frac{(a+h-x)^{n-1}}{(n-1)!} f^n(x) - pA(a+h-x)^{p-1}.$$

$$0 = \Phi'(a + \theta h) = \frac{h^{n-1}(1-\theta)^{n-1}}{(n-1)!} f^n(a + \theta h) - pA(1-\theta)^{p-1} h^{p-1},$$

$$\Rightarrow A = \frac{h^{n-p}(1-\theta)^{n-p}}{p.(n-1)!} . f^n(a + \theta h), \text{ for } (1-\theta) \neq 0 \text{ and } h \neq 0.$$

Substituting the value of A in (2.2), we get the required result (2.1).

Let x be a point of the interval $[a, a + h]$. Let f satisfy the condition of Taylor's theorem in $[a, a + h]$ so that it satisfies the conditions for $[a, x]$ also. Changing $a + h$ to x that is, h to $x - a$, in (2.1) we obtain

$$f(x) = f(a) + (x-a)f'(x) + \frac{(x-a)^2}{2!} f''(x) + \frac{(x-a)^3}{3!} f'''(x) + \ldots\ldots +$$

$$\frac{(x-a)^{n-1}}{(n-1)!} f^{n-1}(x) + \frac{(x-a)^n(1-\theta)^{n-p}}{p.(n-1)!} f^n[a+\theta(x-a)], \; 0 < \theta < 1.$$

The remainder after n terms can thus written as

$$R_n = \frac{(x-a)^n(1-\theta)^{n-p}}{p[(n-1)!]} f^n(c),$$

where, c lies between a and x, and depends on the selection of x. We have seen that

$$f(a+h) = f(a) + hf'(a) + \frac{h^2}{2!} f''(a) + \ldots\ldots + \frac{h^{n-1}}{(n-1)!} f^{n-1}(a) + R_n .$$

The result can be interpreted in two ways:

(i) The value $f(a + h)$ of the function at a point may be approximated by a summation of the terms like $(h^r/r!) f^r(a)$ involving values of the function and its derivatives at some other point of the domain of definition, and

(ii) The value $f(a + h)$ of the function may be expanded in powers of h.

Here we use Taylor expansion method for solving GLDAP evolution equation in leading order and next-to-leading order.

2.2. Complete and Particular Solutions of First Order Linear Partial Differential Equations

The standard form of linear partial differential equation of first order [78-80] involving x and y as independent variables and z as dependent variable is

$$Pp + Qq = R, \tag{2.3}$$

where P, Q, R are functions of x, y, z and $p = \partial z/\partial x$, $q = \partial z/\partial y$. We have seen that Lagrange's method [78-82] of solving a linear partial differential equation of the first order leads to the general integral

$$\Phi(U, V) = 0, \tag{2.4}$$

where Φ is an arbitrary function of the arguments $U(x, y, z)$ and $V(x, y, z)$ and $U = a$, $V = b$ are two independent integrals of the subsidiary equations

$$\frac{dx}{P} = \frac{dy}{Q} = \frac{dz}{R}. \tag{2.5}$$

In some instances, we can deal with particular solutions more conveniently than with the general integral. The most important type of particular solution obtainable from the general integral is that containing two arbitrary constants, say α and β. Such a solution [81] of equation (2.3) may be denoted by

$$f(x, y, z, \alpha, \beta) = 0, \tag{2.6}$$

which is called a complete integral.

If $U = a$ and $V = b$ are two independent solutions of the subsidiary equation (2.5), then the complete integral [80-81] may be taken as

$$V = \alpha U + \beta. \tag{2.7}$$

Because, since U and V separately satisfy equation (2.3), then equation (2.7) will be a solution and since equation (2.7) contains two arbitrary constants α and β, it is a complete integral. Complete solution (2.7) represents a two parameter family of surfaces which does not have an envelope, since the arbitrary constants enter linearly [80]. Differentiating equation (2.7) with respect to β we get $0 = 1$, which is absurd. Hence there

is no singular solution. From this two-parameter family of surfaces, select a one-parameter family by setting $\beta = g(\alpha)$, where g is a given function of α. Then

$$V = \alpha U + g(\alpha). \tag{2.8}$$

This relation gives a solution of the partial differential equation (2.3) and the surfaces (2.8) will in general possess an envelope. If we differentiate equation (2.8) with respect to α we get

$$0 = U + g'(\alpha). \tag{2.9}$$

From equation (2.9), α may usually be obtained in terms of U, and inserting this value of α in equation (2.8) we fined a relation

$$V = \Psi(U) \tag{2.10}$$

which is merely a particular solution of the general solution $\Phi(U, V) = 0$ and it will satisfy the Lagrange's equation (2.3). So it does not furnish us with a new solution. Thus situation here is different from that of ordinary differential equation. In case of ordinary differential equation of first order, the envelope, when it exists in a one parameter family of curves (or surfaces), gives a singular solution which is not a part of the general solution.

It is to be noted that when β is an arbitrary function of α, then the elimination of α in equation (2.8) and (2.9) is not possible. Thus the general solution can not be obtained from the complete solution [80-81]. Actually, the general solution of a linear partial differential equation of order one is the totality of envelopes of all one parameter families (2.8) obtained from a complete solution. We use this method to obtain t and x-evolutions of structure functions.

2.3. Numerical Integration

In applied mathematics, the solution of problems generally consists of numbers which satisfy some kind of equation. Theoretically these numbers may be specified by the equation; but in practice, it is found that even in the simplest cases it is not possible to write down an exact decimal representative of the solution. Numerical methods are very important tools to provide practical methods for calculating the solutions of problems in applied mathematics to a desired degree of accuracy. The wide use of electronic

computers for solving problems in various fields of engineering, scientific, industry etc. has further enhanced the scope of numerical methods. Before doing discussion about numerical integration, it is necessary to know differences, interpolation and interpolation formula.

Differences: If $y_0, y_1, y_2, \ldots\ldots\ldots\ldots, y_n$ denote a set of any function $y(x)$, then $y_1 - y_0, y_2 - y_1, \ldots\ldots\ldots\ldots, y_n - y_{n-1}$ are called the first differences of the function y [83-85]. Denoting these differences by $\Delta y_0, \Delta y_1, \ldots\ldots\ldots\ldots, \Delta y_n$. The differences of first differences are called second differences. Denoting them by $\Delta^2 y_0, \Delta^2 y_1$ etc. we have $\Delta^2 y_0 = \Delta y_1 - \Delta y_0$, $\Delta^2 y_1 = \Delta y_2 - \Delta y_1$ etc. In like manner, the third differences are $\Delta^3 y_0 = \Delta^2 y_1 - \Delta^2 y_0$, $\Delta^3 y_1 = \Delta^2 y_2 - \Delta^2 y_1$ etc.

Interpolation and interpolation formula: Interpolation means insertion or filling up intermediate terms of a series. It is the technique of estimating the value of a function for any intermediate value of the independent variable when the values of the function corresponding to a number of the values of the variable are given. Let $y = f(x)$ be a function given by the values $y_0, y_1, y_2, \ldots\ldots\ldots\ldots, y_n$ which it takes for the values $x_0, x_1, x_2, \ldots\ldots\ldots\ldots, x_n$ of the independent variable x respectively, and let $\Phi(x)$ denote an arbitrary simpler function so constructed that it takes the same values as $f(x)$ for the values $x_0, x_1, x_2, \ldots\ldots\ldots\ldots, x_n$. Then if $f(x)$ is replaced by $\Phi(x)$ over a given interval, the process constitutes interpolation, and the function $\Phi(x)$ is a formula of interpolation [83-85].

Numerical integration: It is the process of computing the value of a definite integral from a set of numerical values of the integrand. When applied to the integration of a function of a single variable, the process is sometimes called mechanical quadrature; when applied to the computation of a double integral of a function of two independent variables it is called mechanical cubature. The problem of numerical integration is solved by representing integrand by an interpolation formula and then integrating this formula between the desired limits. We have a variety of quadrature formulas [83-85], like General quadrature formula, The Trapezoidal rule, Simpson's one – third rule, Simpson's three – eight rule, Weddle's rule, Cotes method, The Euler – Maclaurin's, Summation and Quadrature

formula, The central Difference Quadrature formula, Gauss's Quadrature formula, Labatto's formula, Tchebycheff's formula, Prisomoidal formula (Special and oldest form of Simpson's rule.) etc. We shall now mention some quadrature formulas as an example.

General quadrature formula for equidistant ordinates: Let us consider a function $y = f(x)$. We interpolate y by a Newton's forwarded interpolation formula as

$$\Phi(x) = y_o + u\Delta y_o + \frac{u(u-1)}{2!}\Delta^2 y_o + \frac{u(u-1)(u-2)}{2!}\Delta^3 y_o + \ldots\ldots, \qquad (2.11)$$

where $u = (x-x_0)/h$ and $du = (1/h)dx$. Now, we integrate (2.11) over n equidistant intervals of width h ($= \Delta x$). The limits of integration for x are x_0 and $x_0 + nh$. Therefore, the corresponding limits for u are 0 and n. We now have,

$$\int_{x_o}^{x_n} y dx = \int_{x_o}^{x_o+nh} y dx$$

$$= \int_o^n h\left[y_o + u\Delta y_o + \frac{u(u-1)}{2!}\Delta^2 y_o + \frac{u(u-1)(u-2)}{3!}\Delta^3 y_o + \ldots\ldots \right] du$$

$$= h\left[uy_o + \frac{u^2}{2}\Delta y_o + \frac{1}{2!}\left(\frac{u^3}{3} - \frac{u^2}{2}\right)\Delta^2 y_o + \frac{1}{3!}\left(\frac{u^4}{4} - \frac{3u^3}{3} + \frac{2u^3}{2}\right)\Delta^3 y_o + \ldots\ldots \right]_0^n$$

$$= h\left[ny_o + \frac{n^2}{2}\Delta y_o + \left(\frac{n^3}{6} - \frac{n^2}{4}\right)\Delta^2 y_o + \left(\frac{n^4}{24} - \frac{n^3}{6} + \frac{n^3}{6}\right)\Delta^3 y_o + \ldots\ldots \right] \qquad (2.12)$$

This is called general quadrature formula [83-85]. From this general formula we can obtain a variety of quadrature formulas by putting n = 1, 2, 3..... etc. The best two are found by putting $n = 2$ and $n = 6$.

Simpson's one – third rule: Putting $n = 2$ in equation (2.12) and neglecting all differences above the second, we get

$$\int_{x_o}^{x_o+2h} y dx = h\left[2y_o + 2\Delta y_o + \left(\frac{8}{3} - 2\right)\frac{\Delta^2 y_o}{2} \right]$$

$$= h\left[2y_o + 2\Delta y_o + \left(\frac{8}{3} - 2\right)\frac{\Delta^2 y_o}{2}\right]$$

$$= h\left[2y_o + 2y_1 - 2y_o + \frac{1}{3}(y_2 - 2y_1 + y_o)\right]$$

$$= \frac{h}{3}[y_o + 4y_1 + y_2].$$

For the next two intervals from x_2 to $x_2 + 2h$ we get in like manner

$$\int_{x_2}^{x_2+2h} ydx = \frac{h}{3}[y_2 + 4y_3 + y_4].$$

Similarly for the third pair of intervals we have

$\int_{x_4}^{x_4+2h} ydx = \frac{h}{3}[y_4 + 4y_5 + y_6]$; and so on. Adding all such expressions as these from x_o to x_n, where n is even, we get

$$\int_{x_o}^{x_o+nh} ydx = \frac{h}{3}[y_0 + 4y_1 + y_2 + y_2 + 4y_3 + y_4 + y_4 + 4y_5 + y_6 + \ldots\ldots].$$

Therefore,

$$\int_{x_o}^{x_o+nh} ydx = \frac{h}{3}[y_0 + 4(y_1 + y_3 + \ldots\ldots + y_{n-1}) + 2(y_2 + y_4 + \ldots\ldots + y_{n-2}) + y_n]$$

$$= \frac{h}{3}[y_0 + 2(y_1 + y_3 + \ldots\ldots + y_{n-1}) + 2(y_1 + y_2 + y_3 + y_4 + \ldots\ldots + y_{n-1}) + y_n].$$

This formula is known as Simpson's one third rule and we use this formula to obtain x evolution of structure functions in leading and next-to-leading orders.

Weddle's rule: Putting $n = 6$ in equation (2.12) and neglecting all differences above the sixth, we have

$$\int_{x_o}^{x_o+6h} ydx = h\left[6y_o + 18\Delta y_o + 27\Delta^2 y_o + 24\Delta^3 y_o + \frac{123}{10}\Delta^4 y_o + \frac{33}{10}\Delta^5 y_o + \frac{41}{140}\Delta^6 y_o\right].$$

Suppose h is chosen in such a way that $(h/140)\,\Delta^6 y_0$ is negligible. The $(41/140)\,\Delta^6 y_0$ is replaced by $(3/10)\,\Delta^6 y_0$ and thus we have

$$\int_{x_o}^{x_o+6h} y\,dx = \frac{3h}{10}\left[y_0 + 5y_1 + y_2 + 6y_3 + y_4 + 5y_5 + y_6\right].$$

For the next set of six intervals from x_6 to x_{12}, we get in the same way

$$\int_{x_6}^{x_{12}} y\,dx = \frac{3h}{10}\left[y_6 + 5y_7 + y_8 + 6y_9 + y_{10} + 5y_{11} + y_{12}\right]$$ and so on. Adding all such

expressions as these from x_0 to x_n, where n is now a multiple of six, we get

$$\int_{x_o}^{x_o+nh} y\,dx = \frac{3h}{10}\left[\begin{array}{l} y_0 + 5y_1 + y_2 + 6y_3 + y_4 + 5y_5 + 2y_6 + 5y_7 + y_8 + 6y_9 + y_{10} + 5y_{11} \\ + 2y_{12} + \ldots\ldots + 2y_{n-6} + 5y_{n-5} + y_{n-4} + 6y_{n-3} + y_{n-2} + 5y_{n-1} + y_n \end{array}\right].$$

This formula is known as Weddle's rule. It requires at least seven consecutive values of the function.□

Chapter-3

t AND x-EVOLUTIONS OF GLDAP EVOLUTION EQUATIONS IN LEADING ORDER

In this chapter, we obtain particular solutions of Gribov–Lipatov–Dokshitzer–Altarelli–Parisi (GLDAP) [29-32] evolution equations computed from complete solutions in leading order (LO) at low-x and thereby we obtain t and x-evolutions for singlet and non-singlet structure functions and hence t-evolutions of deuteron, proton, neutron, difference and ratio of proton and neutron structure functions and x-evolutions of deuteron structure functions. In calculating structure functions, input data points have been taken from experimental data directly unlike the usual practice of using an input distribution function introduced by hand. Results of proton and neutron structure functions are compared with the HERA low-x low-Q^2 data and those of deuteron structure functions are compared with the NMC low-x low-Q^2 data. Comparisons are also made with the results of earlier approximated solutions [86-88] of GLDAP evolution equations. We also compare our results of t-evolution of proton structure functions with a recent global parameterization.

3.1. Theory

The GLDAP evolution equations in LO for singlet and non-singlet structure functions in the standard forms are [89]

$$\frac{\partial F_2^S(x,t)}{\partial t} - \frac{A_f}{t}\left[\{3+4\ln(1-x)\}F_2^S(x,t) + I_1^S(x,t) + I_2^S(x,t)\right] = 0 \tag{3.1}$$

and

$$\frac{\partial F_2^{NS}(x,t)}{\partial t} - \frac{A_f}{t}\left[\{3+4\ln(1-x)\}F_2^{NS}(x,t) + I^{NS}(x,t)\right] = 0, \tag{3.2}$$

where

$$I_1^S(x,t) = 2\int_x^1 \frac{dw}{1-w}\left\{\left(1+w^2\right)F_2^S(x/w,t) - 2F_2^S(x,t)\right\}, \tag{3.3}$$

$$I_2^S(x,t) = \frac{3}{2}N_f\int_x^1 \left\{w^2 + (1-w)^2\right\}G(x/w,t)dw \tag{3.4}$$

and

$$I_1^{NS}(x,t) = 2\int_x^1 \frac{dw}{1-w}\left\{\left(1+w^2\right)F_2^{NS}(x/w,t) - 2F_2^{NS}(x,t)\right\}. \tag{3.5}$$

Here, $t = \ln(Q^2/\Lambda^2)$ and $\Lambda_f = 4/(33-2N_f)$, N_f being the number of flavours and Λ is the QCD cut off parameter.

Let us introduce the variable $u = 1-w$ and note that [90]

$$\frac{x}{w} = \frac{x}{1-u} = x\sum_{k=0}^{\infty} u^k. \tag{3.6}$$

The series (3.6) is convergent for $|u| < 1$. Since $x < w < 1$, so $0 < u < 1-x$ and hence the convergence criterion is satisfied. Now, using Taylor expansion method [80] we can rewrite $G(x/w, t)$ as

$$G(x/w,t) = G\left(x + x\sum_{k=1}^{\infty} u^k, t\right)$$

$$= G(x,t) + x\sum_{k=1}^{\infty} u^k \frac{\partial G(x,t)}{\partial x} + \frac{1}{2}x^2\left(\sum_{k=1}^{\infty} u^k\right)^2 \frac{\partial G(x,t)}{\partial x^2} + \ldots\ldots, \tag{3.7}$$

which covers the whole range of u, $0 < u < 1-x$. Since x is small in our region of discussion, the terms containing x^2 and higher powers of x can be neglected [86-88, 91-93] and $G(x/w, t)$ can be approximated for small-x as

$$G(x/w,t) \cong G(x,t) + x\sum_{k=1}^{\infty} u^k \frac{\partial G(x,t)}{\partial x}. \tag{3.8}$$

Similarly, $F_2^S(x/w, t)$ and $F_2^{NS}(x/w, t)$ can be approximated for small-x as

$$F_2^S(x/w,t) \cong F_2^S(x,t) + x\sum_{k=1}^{\infty} u^k \frac{\partial F_2^S(x,t)}{\partial x} \tag{3.9}$$

and

$$F_2^{NS}(x/w,t) \cong F_2^{NS}(x,t) + x\sum_{k=1}^{\infty} u^k \frac{\partial F_2^{NS}(x,t)}{\partial x} \quad (3.10)$$

Using equations (3.8), (3.9) and (3.10) in equations (3.3), (3.4) and (3.5) and performing u-integrations we get

$$I_1^S = -[(1-x)(x+3)]F_2^S(x,t) + \left[2x\ln(1/x) + x\left(1-x^2\right)\right]\frac{\partial F_2^S(x,t)}{\partial x}, \quad (3.11)$$

$$I_2^S = N_f\left[\frac{1}{2}(1-x)\left(2-x+2x^2\right)G(x,t) + \left\{-\frac{1}{2}x(1-x)\left(5-4x+2x^2\right) + \frac{3}{2}x\ln(1/x)\right\}\frac{\partial G(x,t)}{\partial x}\right] \quad (3.12)$$

and

$$I^{NS} = -[(1-x)(x+3)]F_2^{NS}(x,t) + \left[2x\ln(1/x) + x\left(1-x^2\right)\right]\frac{\partial F_2^{NS}(x,t)}{\partial x}. \quad (3.13)$$

Now using equations (3.11) and (3.12) in equation (3.1) we have,

$$\frac{\partial F_2^S(x,t)}{\partial t} - \frac{A_f}{t}\left[A(x)F_2^S(x,t) + B(x)\frac{\partial F_2^S(x,t)}{\partial x} + C(x)G(x,t) + D(x)\frac{\partial G(x,t)}{\partial x}\right] = 0. \quad (3.14)$$

Let us assume for simplicity [86-88]

$$G(x, t) = K(x)\, F_2^S(x, t), \quad (3.15)$$

where $K(x)$ is a function of x. Then equation (3.14) gives

$$\frac{\partial F_2^S(x,t)}{\partial t} - \frac{A_f}{t}[L(x)F_2^S(x,t) + M(x)\frac{\partial F_2^S(x,t)}{\partial x}] = 0, \quad (3.16)$$

where

$A(x) = 3 + 4\ln(1-x) - (1-x)(3+x)$,

$B(x) = x(1-x^2) + 2x\ln(1/x)$,

$C(x) = (1/2)N_f(1-x)(2-x+2x^2)$,

$D(x) = N_f x[-(1/2)(1-x)(5-4x+2x^2) + (3/2)\ln(1/x)$,

$L(x) = A(x) + K(x)C(x) + D(x)\frac{\partial K(x)}{\partial x}$ and

$M(x) = B(x) + K(x)\, D(x)$.

Secondly using equation (3.13) in equation (3.2) we have

$$\frac{\partial F_2^{NS}(x,t)}{\partial t} - \frac{A_f}{t}\left[P(x)F_2^{NS}(x,t) + Q(x)\frac{\partial F_2^{NS}(x,t)}{\partial x}\right] = 0, \tag{3.17}$$

where

$P(x) = 3 + 4 \ln (1-x) - (1-x)(x+3)$ and $Q(x) = x(1-x^2) - 2x \ln x$.

The general solutions of equations (3.16) is [80-81] $F(U, V) = 0$, where F is an arbitrary function and $U(x, t, F_2^S) = C_1$ and $V(x, t, F_2^S) = C_2$ form a solution of equations

$$\frac{dx}{A_f M(x)} = \frac{dt}{-t} = \frac{dF_2^S(x,t)}{-A_f L(x) F_2^S(x,t)}. \tag{3.18}$$

Solving equation (3.18) we obtain,

$$U\left(x,t,F_2^S\right) = t\exp\left[\frac{1}{A_f}\int\frac{1}{M(x)}dx\right] \quad \text{and} \quad V\left(x,t,F_2^S\right) = F_2^S(x,t)\exp\left[\int\frac{L(x)}{M(x)}dx\right].$$

If U and V are two independent solutions of equation (3.18) and if α and β are arbitrary constants, then $V = \alpha U + \beta$ may be taken as a complete solution of equation (3.17). We take this form as this is the simplest form of a complete solution which contains both the arbitrary constants α and β. Earlier few papers [86-88] considered a solution $AU + BV = 0$, where A and B are arbitrary constants. But that is not a complete solution having both the arbitrary constants as this equation can be transformed to the form $V = CU$, where $C = -A/B$, i.e., the equation contains only one arbitrary constant. Now the complete solution [80-81]

$$F_2^S(x,t)\exp\left[\int\frac{L(x)}{M(x)}dx\right] = \alpha t\exp\left[\frac{1}{A_f}\int\frac{1}{M(x)}dx\right] + \beta \tag{3.19}$$

is a two-parameter family of surfaces, which does not have an envelope, since the arbitrary constants enter linearly [80]. Differentiating equation (3.19) with respect to β we get $0 = 1$, which is absurd. Hence there is no singular solution. The one parameter family determined by taking $\beta = \alpha^2$ has equation

$$F_2^S(x,t)\exp\left[\int\frac{L(x)}{M(x)}dx\right]=\alpha t\exp\left[\frac{1}{A_f}\int\frac{1}{M(x)}dx\right]+\alpha^2. \tag{3.20}$$

Differentiating equation (3.20) with respect to α, we get

$$\alpha=-\frac{1}{2}t\exp\left[\frac{1}{A_f}\int\frac{1}{M(x)}dx\right].$$

Putting the value of α in equation (3.20), we obtain the envelope

$$F_2^S(x,t)=-\frac{1}{4}t^2\exp\left[\int\left(\frac{2}{A_fM(x)}-\frac{L(x)}{M(x)}\right)dx\right], \tag{3.21}$$

which is merely a particular solution of the general solution. Unlike the case of ordinary differential equations, the envelope is not a new locus. It is to be noted that when β is an arbitrary function of α, then the elimination of α in equation (3.20) is not possible. Thus the general solution can not be obtained from the complete solution [81]. Actually, the general solution of a linear partial differential equation of order one is the totality of envelopes of all one parameter families (3.21) obtained from a complete solution.

Now, defining

$$F_2^S(x,t_0)=-\frac{1}{4}t_0^2\exp\left[\int\left(\frac{2}{A_fM(x)}-\frac{L(x)}{M(x)}\right)dx\right],$$

at $t=t_0$, where, $t_0=\ln(Q_0^2/\Lambda^2)$ at any lower value of $Q=Q_0$, we get from equation (3.21)

$$F_2^S(x,t)=F_2^S\left(x,t_0\right)\left(\frac{t}{t0}\right)^2, \tag{3.22}$$

which gives the t-evolution of singlet structure function $F_2^S(x, t)$. Proceeding exactly in the same way, and defining

$$F_2^{NS}(x,t_0)=-\frac{1}{4}t_0^2\exp\left[\int\left(\frac{2}{A_fQ(x)}-\frac{P(x)}{Q(x)}\right)dx\right], \text{ we get}$$

$$F_2^{NS}(x,t)=F_2^{NS}\left(x,t_0\right)\left(\frac{t}{t0}\right)^2, \tag{3.23}$$

which gives the t-evolution of non-singlet structure function $F_2^{NS}(x, t)$.

Again defining

$$F_2^S(x_0,t) = -\frac{1}{4}t^2 \exp\left[\int\left(\frac{2}{A_f M(x)} - \frac{L(x)}{M(x)}\right)dx\right]_{x=x_0},$$

$x = x_0$, we obtain from equation (3.21)

$$F_2^S(x,t) = F_2^S(x_0,t)\exp\left[\int_{x_0}^{x}\left(\frac{2}{A_f M(x)} - \frac{L(x)}{M(x)}\right)dx\right], \tag{3.24}$$

which gives the x-evolution of singlet structure function $F_2^S(x, t)$. Similarly defining

$$F_2^{NS}(x_0,t) = -\frac{1}{4}t^2 \exp\left[\int\left(\frac{2}{A_f Q(x)} - \frac{P(x)}{Q(x)}\right)dx\right]_{x=x_0},$$

we get

$$F_2^{NS}(x,t) = F_2^{NS}(x_0,t)\exp\left[\int_{x_0}^{x}\left(\frac{2}{A_f Q(x)} - \frac{P(x)}{Q(x)}\right)dx\right]_{x=x_0}, \tag{3.25}$$

which gives the x-evolution of non-singlet structure function $F_2^{NS}(x, t)$.

Deuteron, proton and neutron structure functions measured in deep inelastic electro-production can be written [7] in terms of singlet and non-singlet quark distribution functions in leading order as

$$F_2^d(x, t) = (5/9)\, F_2^S(x, t), \tag{3.26}$$

$$F_2^p(x, t) = (5/18)\, F_2^S(x, t) + (3/18)\, F_2^{NS}(x, t), \tag{3.27}$$

$$F_2^n(x, t) = (5/18)\, F_2^S(x, t) - (3/18)\, F_2^{NS}(x, t) \tag{3.28}$$

and

$$F_2^p(x, t) - F_2^n(x, t) = (1/3)\, F_2^{NS}(x, t). \tag{3.29}$$

Now using equations (3.22) and (3.24) in equation (3.26) we will get t and x-evolutions of

deuteron structure function $F_2^d(x, t)$ at low-x as

$$F_2^d(x,t) = F_2^d(x,t_0)\left(\frac{t}{t_0}\right)^2 \tag{3.30}$$

and

$$F_2^d(x,t) = F_2^d(x_0,t)\exp\left[\int_{x_0}^{x}\left(\frac{2}{A_f M(x)} - \frac{L(x)}{M(x)}\right)dx\right], \tag{3.31}$$

where the input functions are

$$F_2^d(x,t_0) = \frac{5}{9}F_2^S(x,t_0) \quad \text{and} \quad F_2^d(x_0,t) = \frac{5}{9}F_2^S(x_0,t).$$

The corresponding results for a particular solutions from the linear combination of U and V of general solutions $F(U, V) = 0$ of GLDAP evolution equations obtained earlier [86-88] are

$$F_2^d(x,t) = F_2^d(x,t_0)\left(\frac{t}{t_0}\right) \tag{3.32}$$

and

$$F_2^d(x,t) = F_2^d(x_0,t)\exp\left[\int_{x_0}^{x}\left(\frac{1}{A_f M(x)} - \frac{L(x)}{M(x)}\right)dx\right]. \tag{3.33}$$

These were obtained by taking arbitrary linear combination $AU + BV = 0$ of general solution $F(U, V) = 0$, where A and B are two arbitrary constants as discussed earlier.

Similarly using equations (3.22) and (3.23) in equations (3.27), (3.28) and (3.29) we get the t-evolutions of proton, neutron, and difference and ratio of proton and neutron structure functions at low-x as

$$F_2^p(x,t) = F_2^p(x,t_0)\left(\frac{t}{t_0}\right)^2, \tag{3.34}$$

$$F_2^n(x,t) = F_2^n(x,t_0)\left(\frac{t}{t_0}\right)^2, \tag{3.35}$$

$$F_2^p(x,t) - F_2^n(x,t) = [F_2^p(x,t_0) - F_2^p(x,t_0)]\left(\frac{t}{t_0}\right)^2 \tag{3.36}$$

and

$$\frac{F_2^p(x,t)}{F_2^n(x,t)} = \frac{F_2^p(x,t_0)}{F_2^n(x,t_0)} = R(x), \tag{3.37}$$

where $R(x)$ is a constant for fixed-x. Here the input functions are

$$F_2^p(x,t_0) = \frac{5}{18}F_2^S(x,t_0) + \frac{3}{18}F_2^{NS}(x,t_0), \quad F_2^n(x,t_0) = \frac{5}{18}F_2^S(x,t_0) - \frac{3}{18}F_2^{NS}(x,t_0) \text{ and}$$

$$F_2^p(x,t_0) - F_2^n(x,t_0) = \frac{1}{3}F_2^{NS}(x,t_0).$$

The corresponding results for earlier solutions of GLDAP evolution equations [86-88] are

$$F_2^p(x,t) = F_2^p(x,t_0)\left(\frac{t}{t_0}\right), \tag{3.38}$$

$$F_2^n(x,t) = F_2^n(x,t_0)\left(\frac{t}{t_0}\right), \tag{3.39}$$

$$F_2^p(x,t) - F_2^n(x,t) = [F_2^p(x,t_0) - F_2^p(x,t_0)]\left(\frac{t}{t_0}\right) \tag{3.40}$$

and

$$\frac{F_2^p(x,t)}{F_2^n(x,t)} = \frac{F_2^p(x,t_0)}{F_2^n(x,t_0)} = R(x), \tag{3.41}$$

where $R(x)$ is a constant for fixed-x.

But the x-evolutions of proton and neutron structure functions like those of deuteron structure function is not possible by this method, because to extract the x-evolutions of proton and neutron structure functions we are to put equations (3.24) and (3.25) in equations (3.27) and (3.28). But as the functions inside the integral sign of equations (3.24) and (3.25) are different, we need to separate the input functions $F_2^S(x_0, t)$ and

$F_2^{NS}(x_0, t)$ from the data points to extract the x-evolutions of the proton and neutron structure functions, which will contain large errors.

For the particular solution of equation (3.16), we take $\beta = \alpha^2$ in equation (3.19). If we take $\beta = \alpha$ in equation (3.19) and differentiating with respect to α as before, we get

$$0 = t \exp\left[\frac{1}{A_f}\int\frac{1}{M(x)}dx\right]+1$$

from which we can not determine the value of α. But if we take $\beta = \alpha^3$ in equation (3.19) and differentiating with respect to α, we get

$$\alpha = \sqrt{-\frac{1}{3}t\exp\left[\frac{1}{A_f}\int\frac{1}{M(x)}dx\right]}$$

which is imaginary. Putting this value of α in equation (3.19) we get ultimately

$$F_2^S(x,t) = t^{3/2}\left\{\left(-\frac{1}{3}\right)^{1/2}+\left(-\frac{1}{3}\right)^{3/2}\right\}\exp\left[\int\left(\frac{3/2}{A_f M(x)}-\frac{L(x)}{M(x)}\right)dx\right].$$

Now, defining

$$F_2^S(x,t_0) = t_0^{3/2}\left\{\left(-\frac{1}{3}\right)^{1/2}+\left(-\frac{1}{3}\right)^{3/2}\right\}\exp\left[\int\left(\frac{3/2}{A_f M(x)}-\frac{L(x)}{M(x)}\right)dx\right],$$

we get,

$$F_2^S(x,t) = F_2^S(x,t_0)\left(\frac{t}{t_0}\right)^{3/2}.$$

Proceeding exactly in the same way we get for non-singlet structure function also

$$F_2^{NS}(x,t) = F_2^{NS}(x,t_0)\left(\frac{t}{t_0}\right)^{3/2}.$$

Then using equations (3.26), (3.27), (3.28) and (3.29) we get t-evolutions of deuteron, proton, neutron and difference of proton and neutron structure functions

$$F_2^{d,p,n,p-n}(x,t) = F_2^{d,p,n}(x,t_0)\left(\frac{t}{t_0}\right)^{3/2}.$$

Proceeding in the same way we get x-evolutions of deuteron structure function

$$F_2^d(x,t) = F_2^d(x_0,t)\exp\left[\int_{x_0}^{x}\left(\frac{3/2}{A_f M(x)} - \frac{L(x)}{M(x)}\right)dx\right].$$

But the determination of x-evolutions of proton and neutron structure functions like those of deuteron structure function is not possible by this method as discussed earlier.

Proceeding exactly in the same way we can show that if we take $\beta = \alpha^4$ we get

$$F_2^{d,p,n,p-n}(x,t) = F_2^{d,p,n}\left(x,t_0\left(\frac{t}{t_0}\right)^{4/3}\right.$$

and

$$F_2^d(x,t) = F_2^d(x_0,t)\exp\left[\int_{x_0}^{x}\left(\frac{4/3}{A_f M(x)} - \frac{L(x)}{M(x)}\right)dx\right],$$

and so on. So in general, if we take $\beta = \alpha^y$, we get

$$F^{d,p,n,p-n}(x,t) = F^{d,p,n,p-n}\left(x,t_0\left(\frac{t}{t_0}\right)^{y/(y-1)}\right.$$

and

$$F_2^d(x,t) = F_2^d(x_0,t)\exp\left[\int_{x_0}^{x}\left(\frac{y/(y-1)}{A_f M(x)} - \frac{L(x)}{M(x)}\right)dx\right],$$

which are t-evolutions of deuteron, proton, neutron and difference of proton and neutron structure functions and x-evolution of deuteron structure function for $\beta = \alpha^y$. We observe that if $y \to \infty$ (very large), $y/(y-1) \to 1$.

Thus we observe that if we take $\beta = \alpha$ in equation (3.19) we can not obtain the value of α and also the required solution. But if we take $\beta = \alpha^2, \alpha^3, \alpha^4, \alpha^5$..... and so on, we see that the powers of (t/t_0) in t-evolutions of deuteron, proton, neutron and difference of proton and neutron structure functions are 2, 3/2, 4/3, 5/4....and so on respectively as discussed above. Similarly, for x-evolutions of deuteron structure functions, we see that the

numerators of the first term inside the integral sign are 2, 3/2, 4/3, 5/4....and so on respectively for the same values of α. We observe that if in the relation $\beta = \alpha^y$, y varies between 2 to a maximum value, the powers of (t/t_0) and the numerators of the first term in the integral sign vary between 2 to 1. Then it is understood that the solutions of equations (3.16) and (3.17) obtained by this method are not unique and so the t-evolutions of deuteron, proton and neutron structure functions, and x- evolution of deuteron structure function obtained by this methodology are not unique. Thus by this methodology, instead of having a single solution we arrive a band of solutions, of course the range for these solutions is reasonably narrow.

3.2. Results and Discussion

We compare our results of t-evolutions of deuteron, proton, neutron and difference and ratio of proton and neutron structure functions from equations (3.30), (3.34), (3.35), (3.36) and (3.37) respectively with the HERA and NMC low-x, low-Q^2 data [94-95]. Here proton structure functions $F_2^p(x, Q^2, z)$ measured in the range $2 \leq Q^2 \leq 50$ GeV^2, $0.73 \leq z \leq 0.88$ and neutron structure functions $F_2^n(x, Q^2, z)$ measured in the range $2 \leq Q^2 \leq 50$ GeV^2, $0.3 \leq z \leq 0.9$ have been used. Moreover here $P_T \leq 200$ MeV, where P_T is the transverse momentum of the final state baryon and $z = 1\text{-}q.(p\text{-}p')\ /\ (q\ .\ p)$, where p, q are the four momenta of the incident proton and the exchanged vector boson coupling to the positron and p' is the four-momentum of the final state baryon. And also we compare our results of t-evolution of proton structure functions with a recent global parameterization [96]. This parameterization includes data from H1, ZEUS, NMC, E665 experiment [95, 97-102]. Though we compare our results with $y = 2$ in $\beta = \alpha^y$ relation with data, our results with y maximum, which are equivalent to earlier results of approximate solutions [86-88] are equally valid. For t-evolutions of deuteron, proton, neutron and difference of proton and neutron structure functions, the results will be the range bounded by the curves for $y = 2$ and $y =$ maximum (= infinity). But for x- evolutions of deuteron structure functions, both results have not any significant difference.

In figure 3.1, we present our results of t-evolutions of deuteron structure functions F_2^d (solid lines) for the representative values of x given in the figure for $y = 2$ in the $\beta = \alpha^y$ relation. Data points at lowest-Q^2 values in the figure are taken as inputs to test the

evolution equation (3.30). Agreement is found to be good. In the same figure, we also plot the results of t-evolutions of deuteron structure functions F_2^d (dashed lines) for y maximum in the $\beta = \alpha^y$ relation. The results of approximate solution [86-88] from equation (3.32) of GLDAP evolution equations are similar to that of our LO results for y maximum in $\beta = \alpha^y$ relation. We observe that the LO results for $y = 2$ are of better

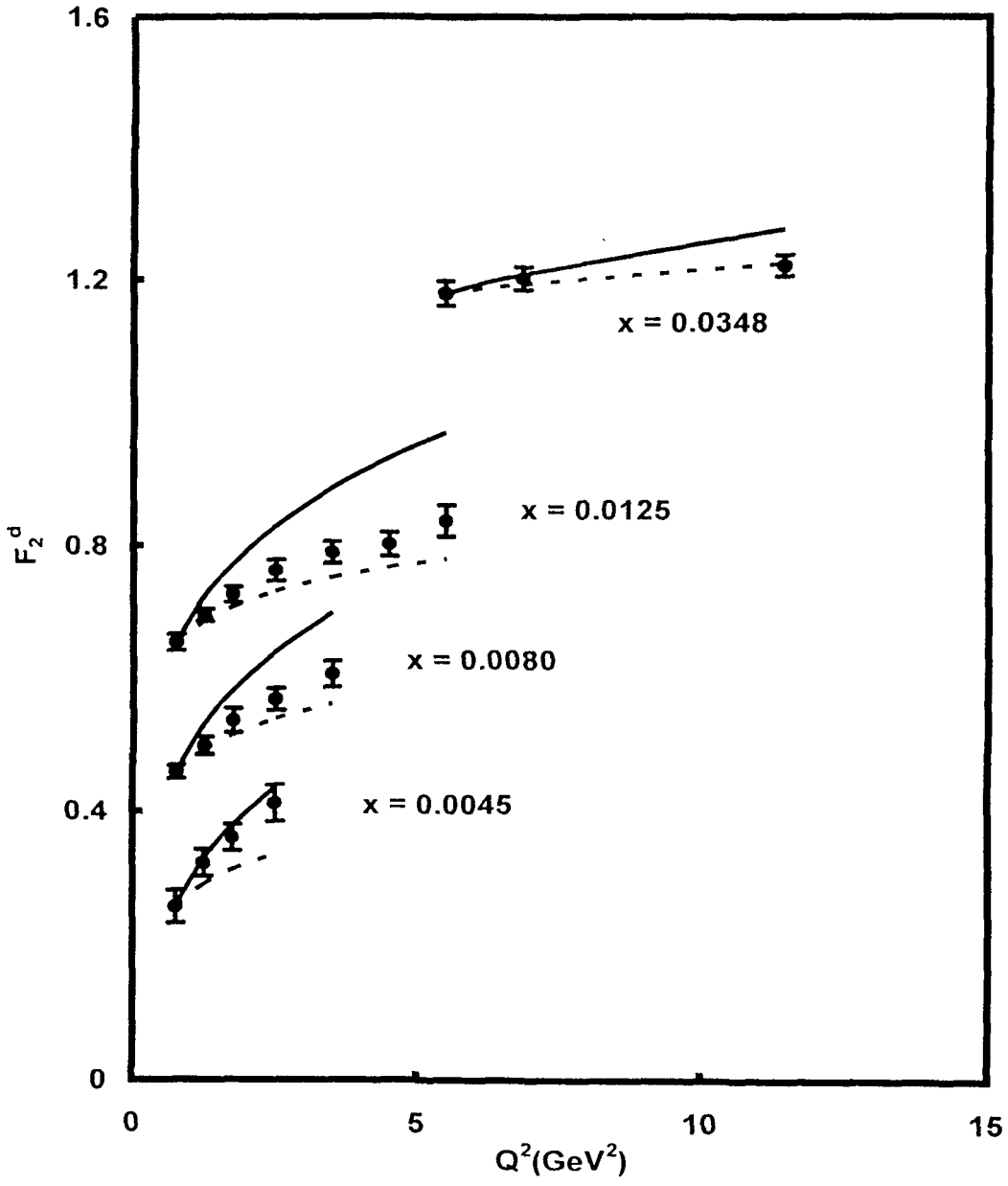

Fig.3.1: t-Evolution of deuteron structure functions in leading order.

agreement with experimental data in general. For convenience, value of each data point is increased by adding $0.2i$, where i = 0, 1, 2, 3... are the numberings of curves counting from the bottom of the lowermost curve as the 0-th order.

In figure 3.2, we present our results of t-evolutions of proton structure functions F_2^p (solid lines) for the representative values of x given in the figure for $y = 2$. Data points at lowest-Q^2 values in the figure are taken as input to test the evolution equation (3.34). Agreement is found to be excellent. In the same figure we also plot the results of t-evolutions of

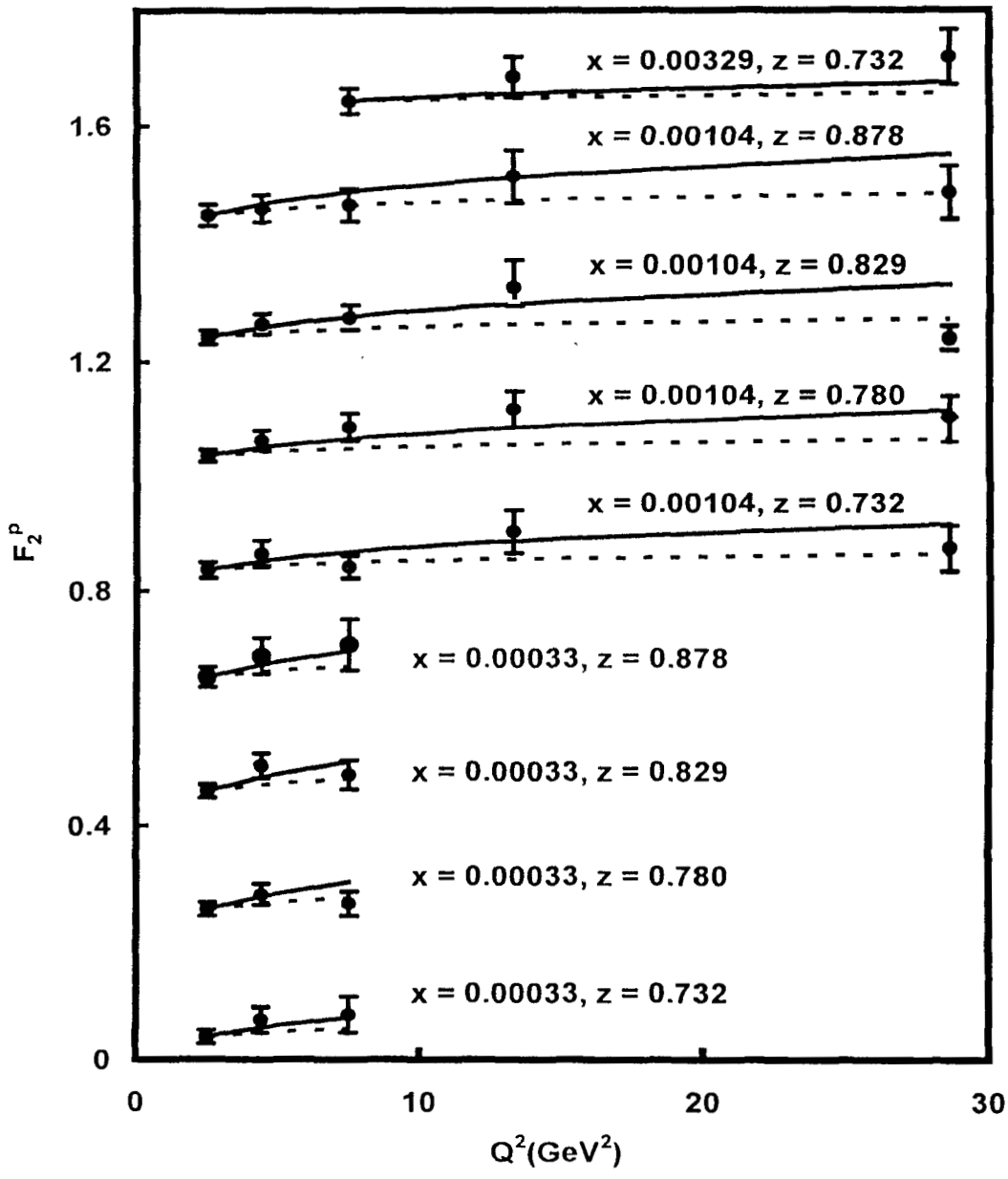

Fig.3.2: t-Evolution of proton structure functions in leading order

proton structure functions F_2^p (dashed lines) for y maximum in $\beta = \alpha^y$ relation. The results of earlier approximate solution [86-88] from equation (3.38) of GLDAP [29-32] evolution equations are similar to that of our LO results for y maximum in the $\beta = \alpha^y$ relation. We observe that the LO results for $y = 2$ are of better agreement with experimental data in general. For convenience, value of each data point is increased by adding $0.2i$, where $i =$

0, 1, 2, 3... are the numberings of curves counting from the bottom of the lowermost curve as the 0-th order.

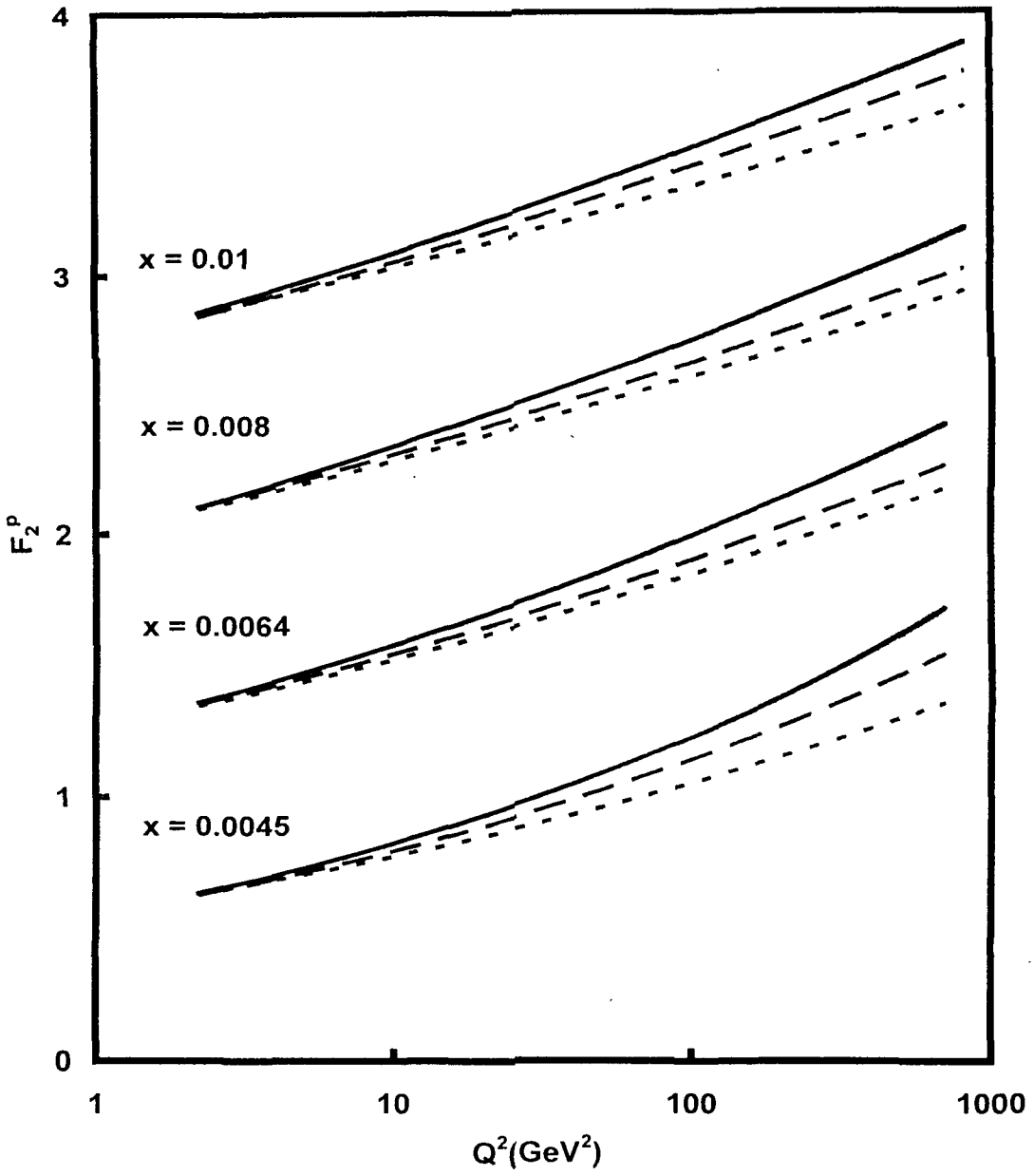

Fig.3.3: t-Evolution of proton structure functions in leading order .

In figure 3.3, we compare our results of t-evolutions of proton structure functions F_2^p with recent global parameterization [96] (long dashed lines) for the representative values of x given in the figures for $y = 2$ (solid lines) and y maximum (dashed lines) in the $\beta = \alpha^y$ relation. Data points at lowest-Q^2 values in the figures are taken as inputs to test the evolution equation. Agreement is found to be good. For convenience, value of each data point is increased by adding $0.5i$, where $i = 0, 1, 2, 3$ ... are the numberings of curves

counting from the bottom of the lowermost curve as the 0-th order.

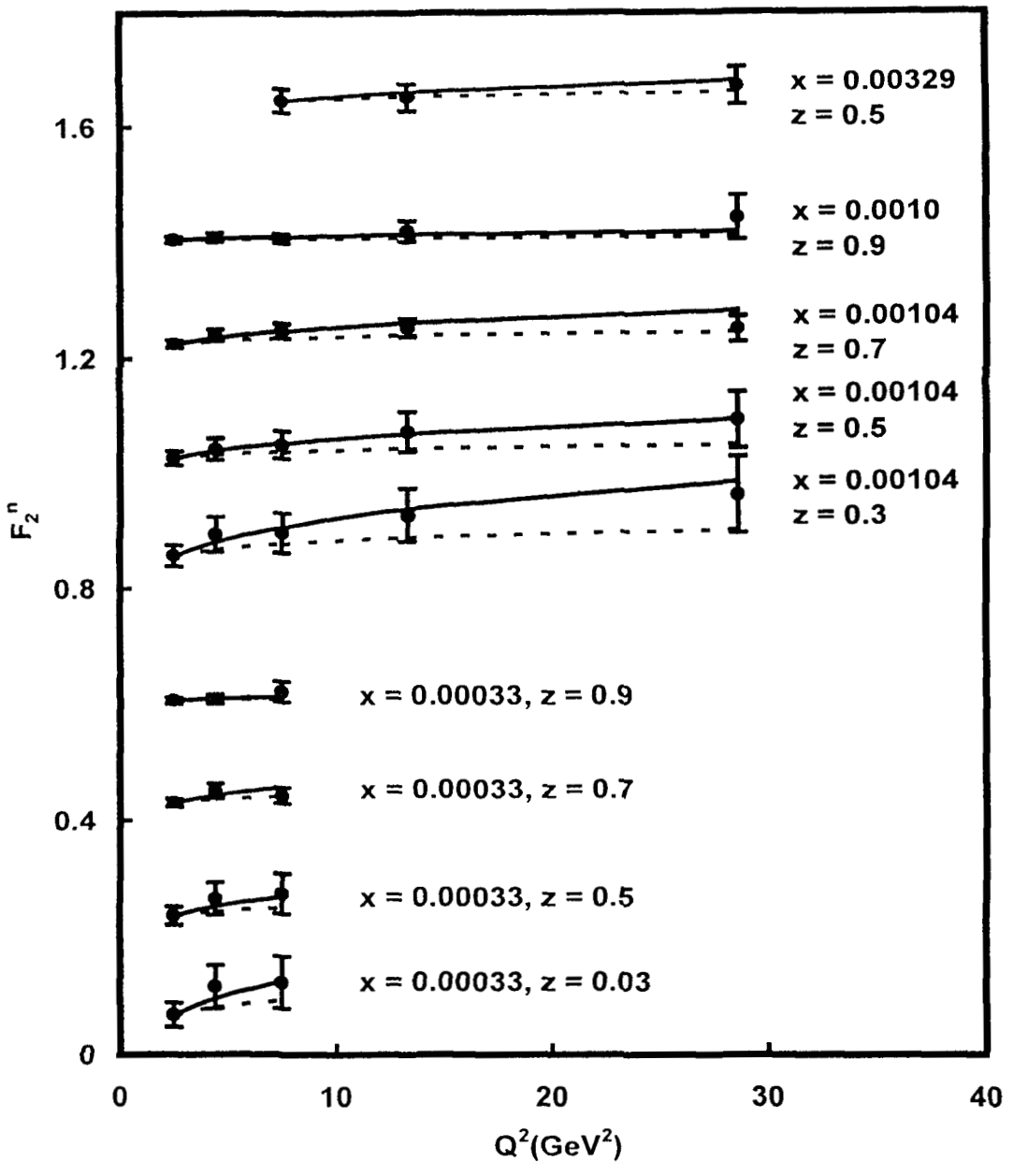

Fig.3.4: t-Evolution of neutron structure functions in leading order.

In figure 3.4, we present our results of t-evolutions of neutron structure functions F_2^n(solid lines) for the representative values of x given in the figure for $y = 2$. Data points at lowest-Q^2 values in the figure are taken as inputs to test the evolution equation (3.35). Agreement is found to be excellent. In the same figure, we also plot the results of t-evolutions of neutron structure functions F_2^n (dashed lines) for y maximum in the $\beta = \alpha^3$ relation. The results of approximate solution [86-88] of GLDAP evolution equations are similar to that of our LO results for y maximum in $\beta = \alpha^3$ relation. We observe that the LO results for $y = 2$ are of better agreement with experimental data in general. For

convenience, value of each data point is increased by adding $0.2i$, where i = 0, 1, 2, 3... are the numberings of curves counting from the bottom of the lowermost curve as the 0-th order.

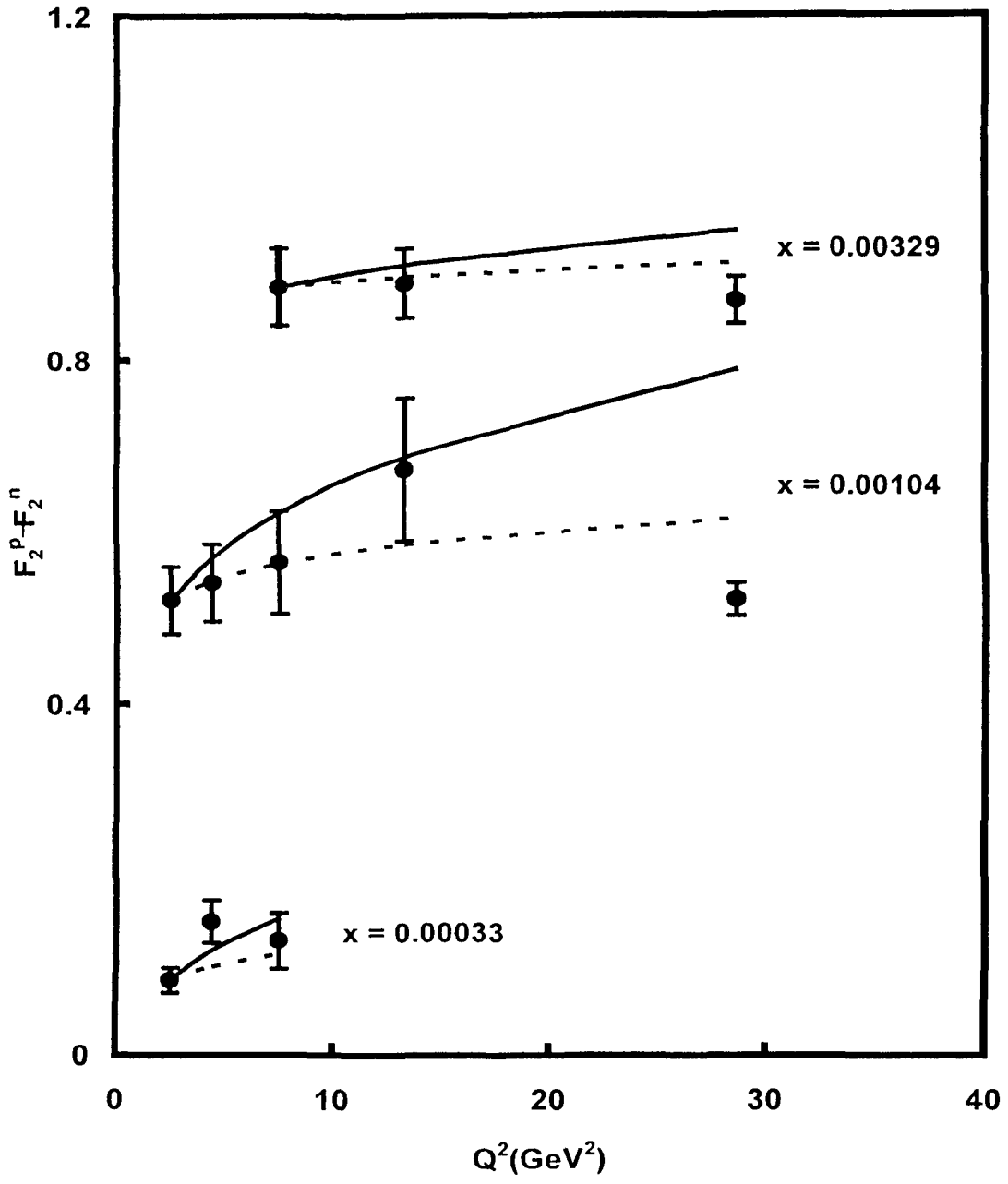

Fig. 3.5: t-Evolution of difference of proton and neutron structure functions in leading order.

In figure 3.5, we present our results of t-evolutions of difference of proton and neutron structure functions $F_2^p - F_2^n$ (solid lines) for the representative values of x given in the figure for $y = 2$. Data points at lowest-Q^2 values in the figure are taken as inputs to test the evolution equation (3.36). Agreement is found to be excellent. In the same figure, we also plot the results of t-evolutions of difference of proton and neutron structure functions F_2^p–

F_2^n (dashed lines) for y maximum in the $\beta = \alpha^v$ relation. The results of approximate solution [86-88] from equation (3.40) of GLDAP evolution equations are similar to that of our LO results for y maximum in the $\beta = \alpha^v$ relation. We observe that the LO results for $y = 2$ are of better agreement with experimental data in general. For convenience, value of each data point is increased by adding $0.4i$, where $i = 0, 1, 2, 3...$ are the numberings of curves counting from the bottom of the lowermost curve as the 0-th order.

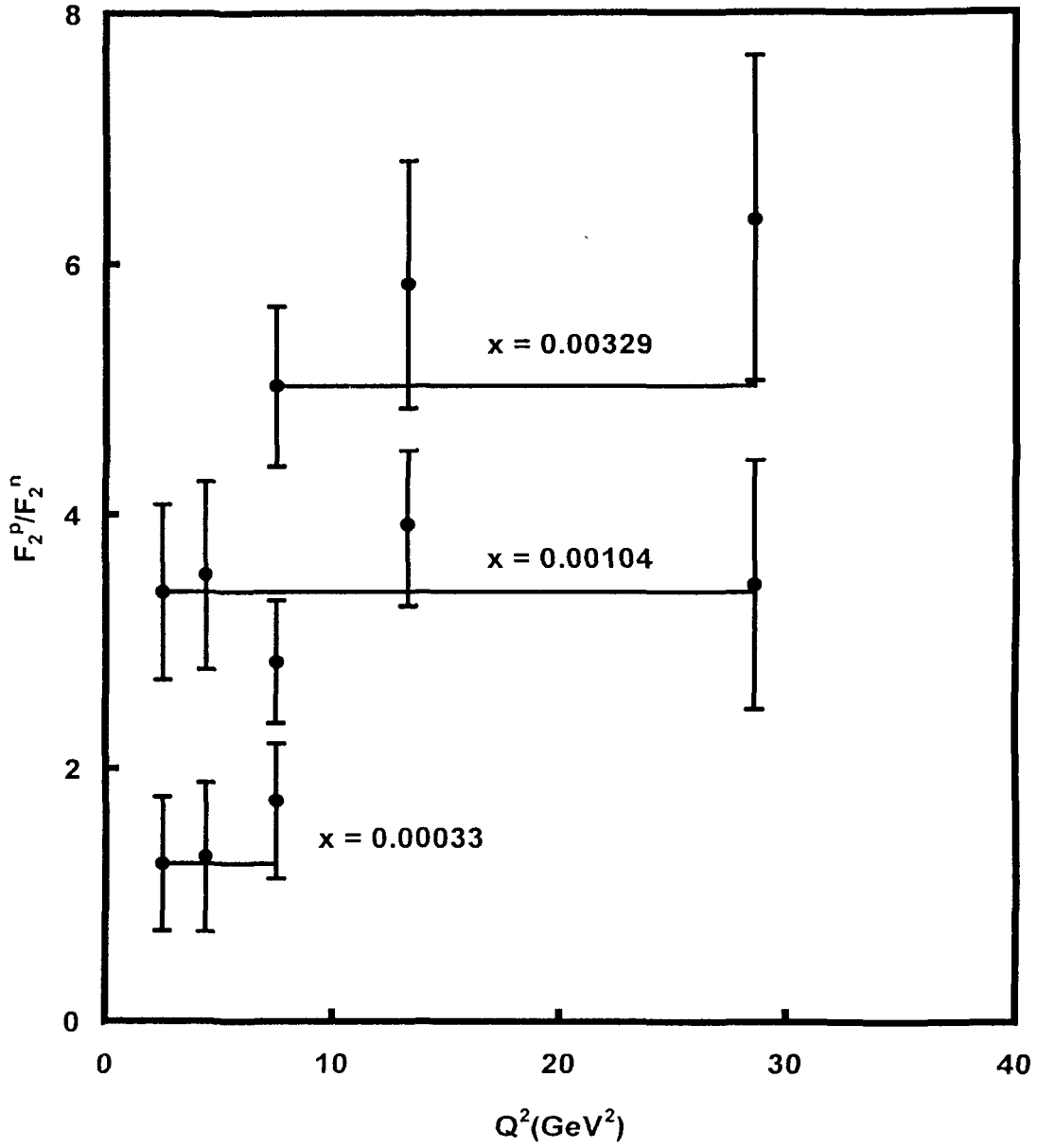

Fig.3.6: t-Evolution of ratio of proton and neutron structure functions in leading order.

In figure 3.6, we present our results of t-evolutions of ratio of proton and neutron structure functions F_2^p/F_2^n (solid lines) for the representative values of x given in the figures. Though according to our theory the ratio should be independent of t, due to the

lack of sufficient amount of data and due to large error bars, a clear cut conclusion can not be drawn.

For a quantitative analysis of x-distributions of structure functions, we calculate the integrals that occurred in equation (3.31) using Simpson's one – third rule for $N_f = 4$.

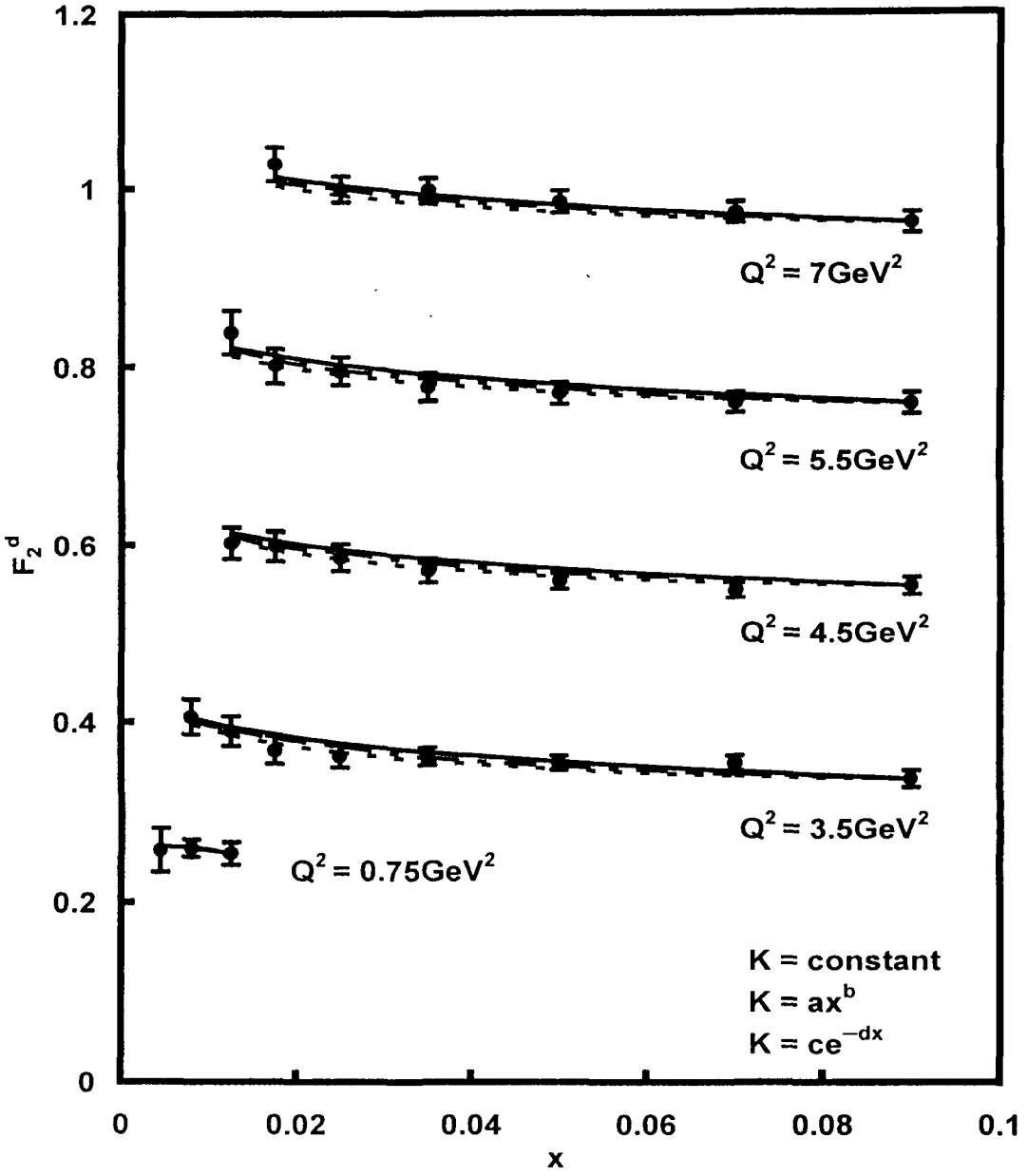

Fig.3.7: x-Evolution of deuteron neutron structure functions in leading order.

In figure 3.7, we present our results of x-distribution of deuteron structure functions F_2^d for $K(x)$ = constant (solid lines), $K(x) = ax^b$ (dashed lines) and for $K(x) = ce^{-dx}$ (dotted lines), where a, b, c and d are constants and for representative values of Q^2 given in each figure for $y = 2$ in $\beta = \alpha^y$ relation, and compare them with NMC deuteron low-x low- Q^2

data [95]. In each curve, the data point for x-value just below 0.1 has been taken as input $F_2^d(x_0, t)$. If we take $K(x) = 4.5$ in equation (3.31) then agreement of the result, with experimental data is found to be excellent. On the other hand, if we take $K(x) = ax^b$, then

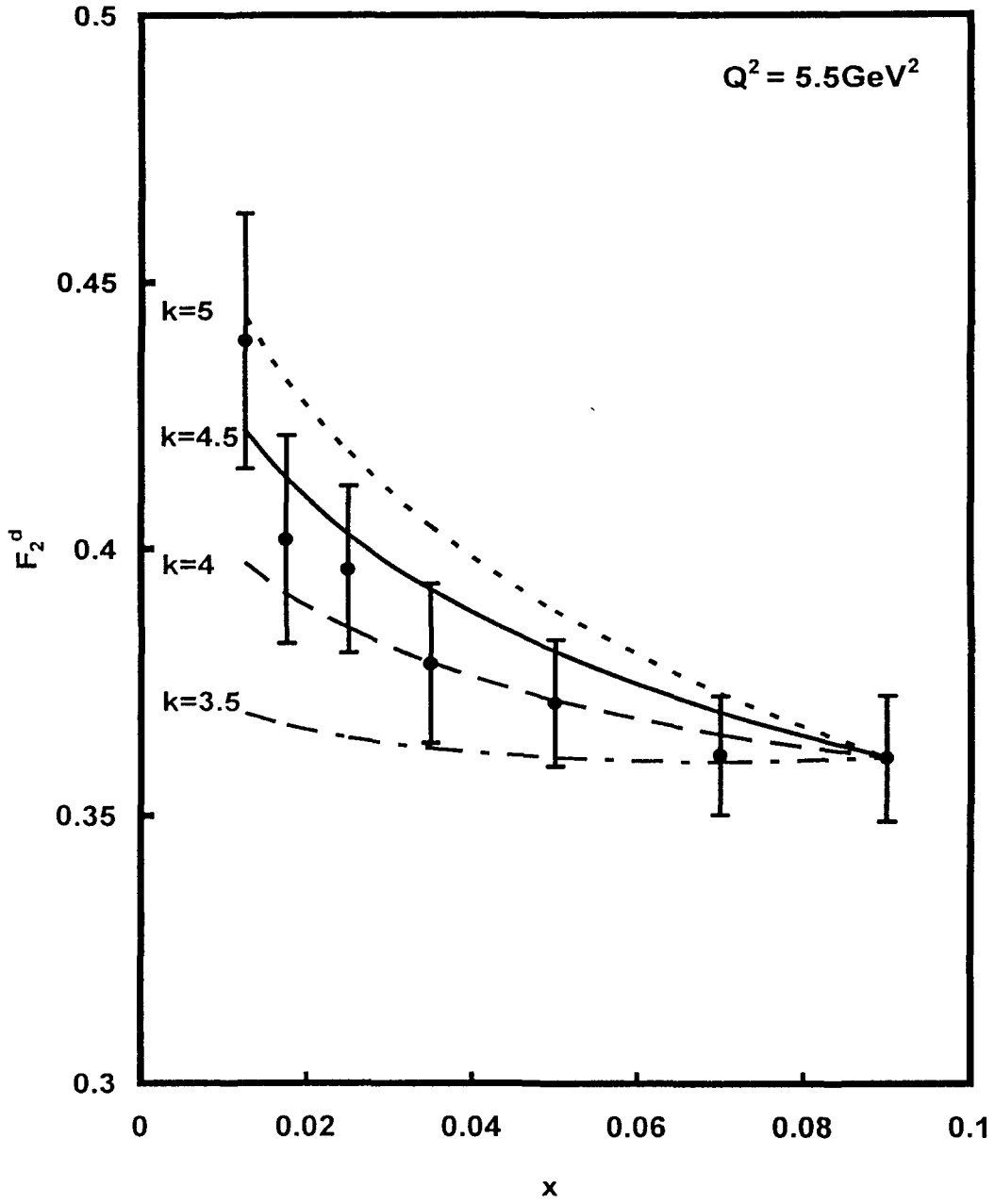

Fig.3.8: Sensitivity of our results for different values of 'k'.

agreement of the results with experimental data is found to be good at $a = 4.5$, $b = 0.01$. Again if we take $K(x) = ce^{-dx}$, then agreement of the results with experimental data is found to be good at $c = 5$, $b = 1$. We observe that there is no significant difference between the results for $y = 2$ and y maximum value in the $\beta = \alpha^y$ relation. For convenience, value of each data point is increased by adding $0.2i$, where $i = 0, 1, 2, 3, \ldots$

are the numberings of curves counting from the bottom of the lowermost curve as the 0-th order.

In figure 3.8, we present the sensitivity of our results for different constant values of $K(x)$. We observe that at $K(x) = 4.5$, agreement of the results with experimental data is found to be excellent. If value of $K(x)$ is increased, the curve goes upward direction and if value of $K(x)$ is decreased, the curve goes downward direction, but the nature of the curve is similar.

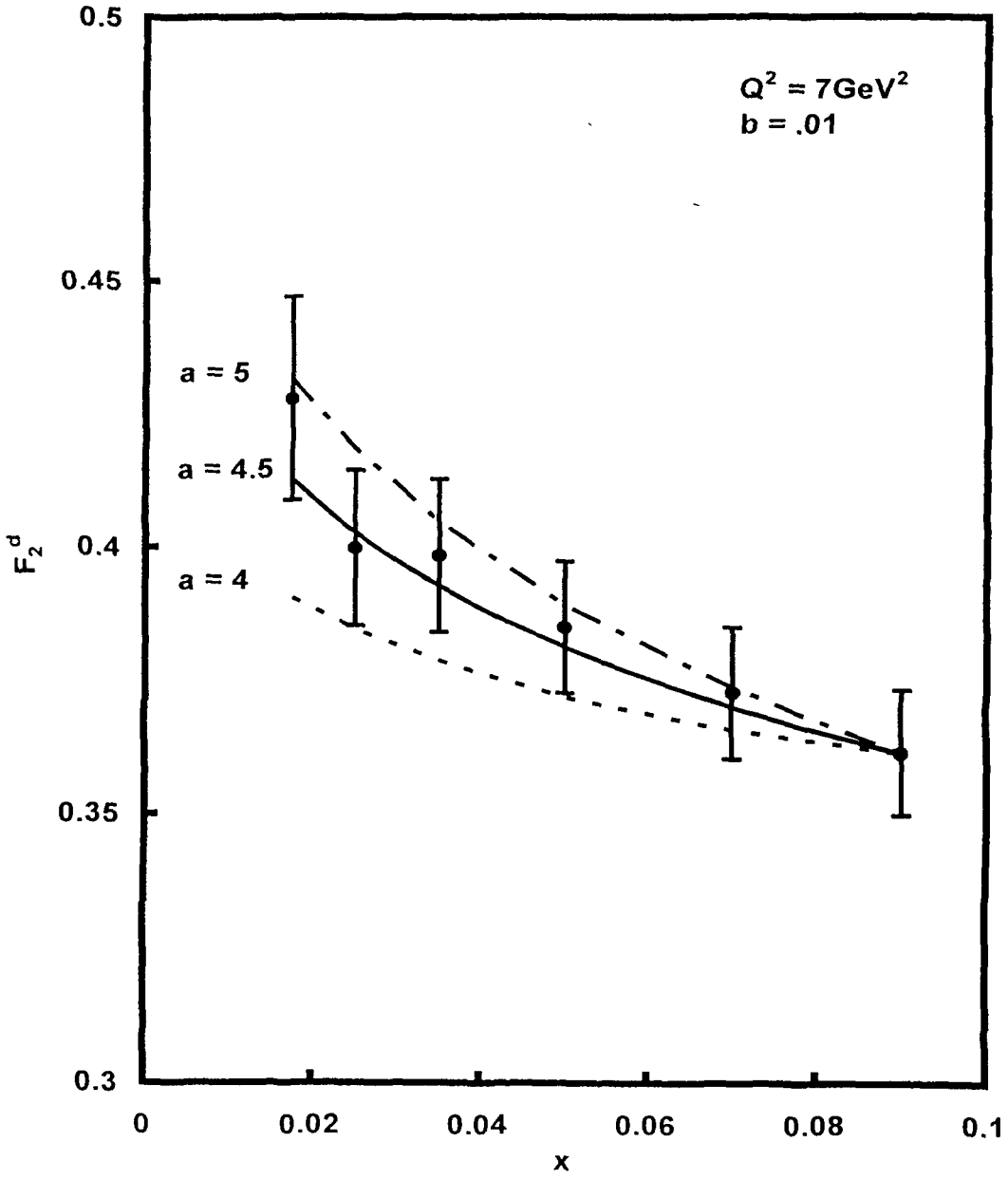

Fig.3.9: Sensitivity of our results for different values of 'a' at fixed value of 'b'.

In figure 3.9, we present the sensitivity of our results for different values of 'a' at fixed

value of 'b'. Here we take $b = 0.01$. We observe that at $a = 4.5$, agreement of the results with experimental data is found to be excellent. If value of 'a' is increased, the curve goes upward direction and if value of 'a' is decreased, the curve goes downward direction, but the nature of the curve is similar.

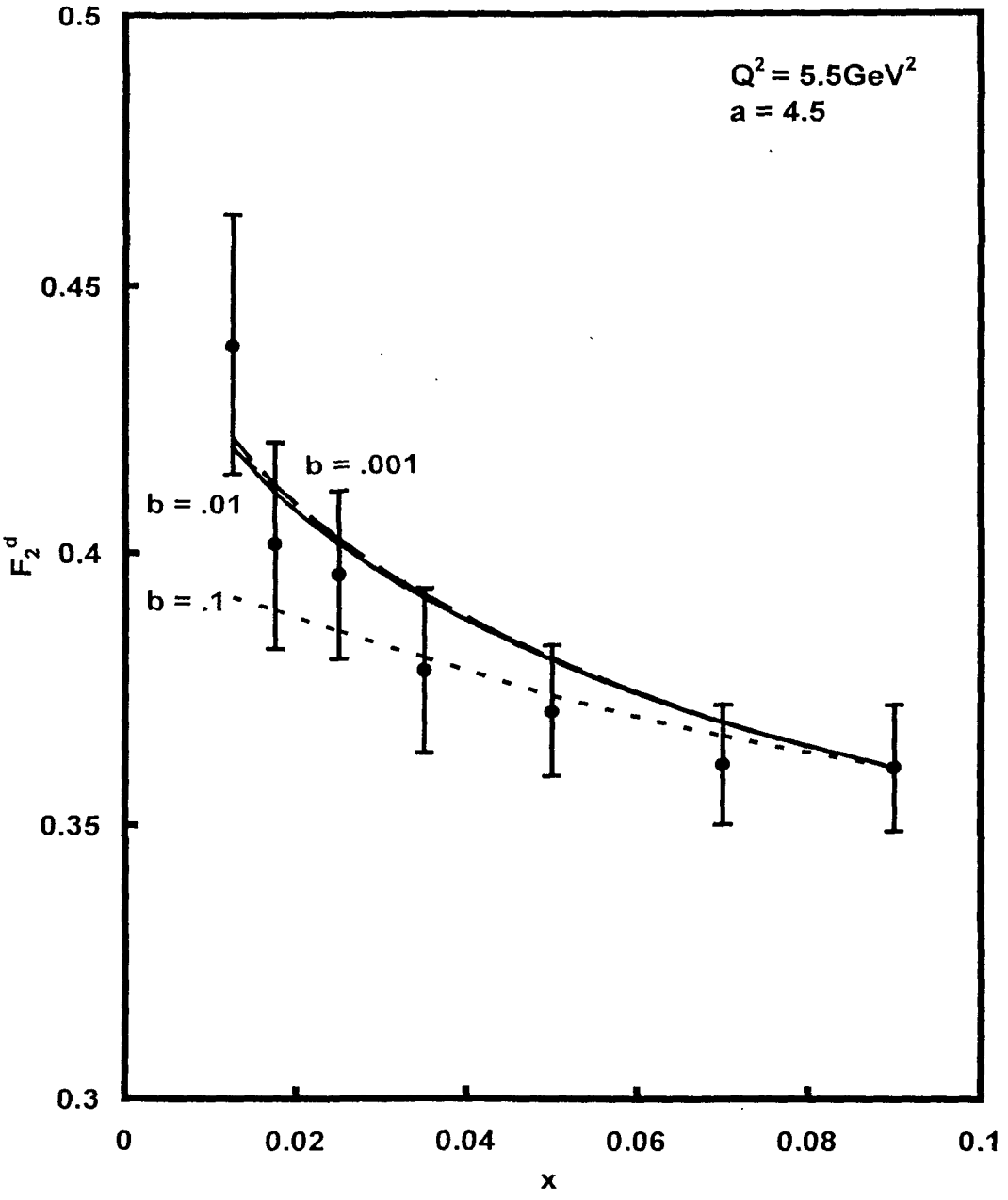

Fig.3.10: Sensitivity of our results for different values of 'b' at fixed value of 'a'.

In figure 3.10, we present the sensitivity of our results for different values of 'b' at fixed value of 'a'. Here we take $a = 4.5$. We observe that at $b = 0.01$, agreement of the results with experimental data is found to be excellent. If value of 'b' is increased then the curve goes downward direction and if value of 'b' is decreased the curve goes upward direction.

But we observe that differences of the curves for b = 0.01, 0.001 and lower values are very small and all these curves are almost overlapped. Here also the nature of the curve is similar.

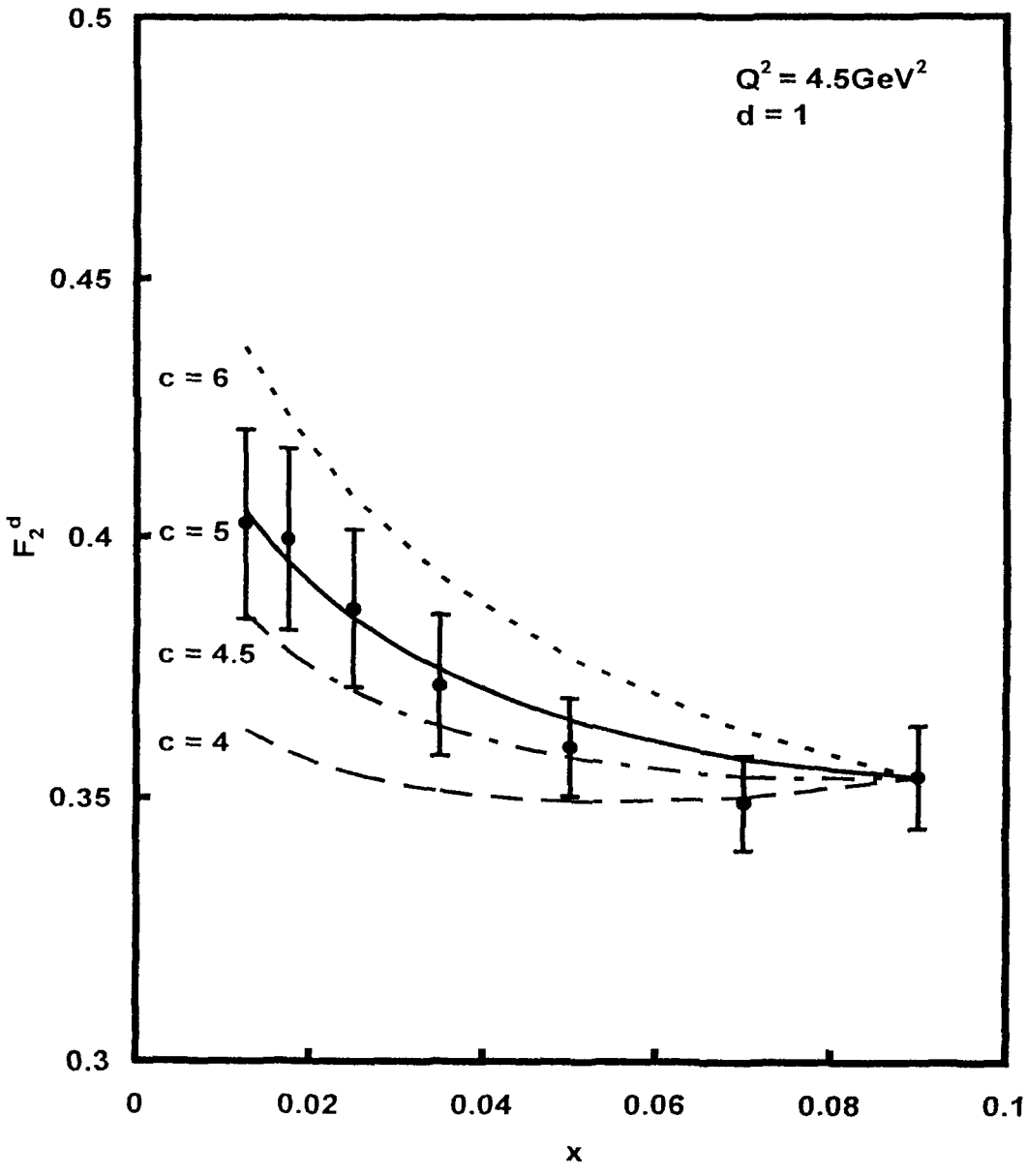

Fig.3.11: Sensitivity of our results for different values of 'c' at fixed value of 'd'.

In figure 3.11, we present the sensitivity of our results for different values of 'c' at fixed value of 'd'. Here we take d = 1. We observe that at c = 5, agreement of the results with experimental data is found to be excellent. If value of 'c' is increased the curve goes upward direction and if value of 'c' is decreased the curve goes downward direction. But the nature of the curve is similar.

In figure 3.12, we present sensitivity of our results for different values of '*d*' at fixed value of '*c*'. Here we take $c = 5$. We obsęrve that at $d = 1$, agreement of the results with

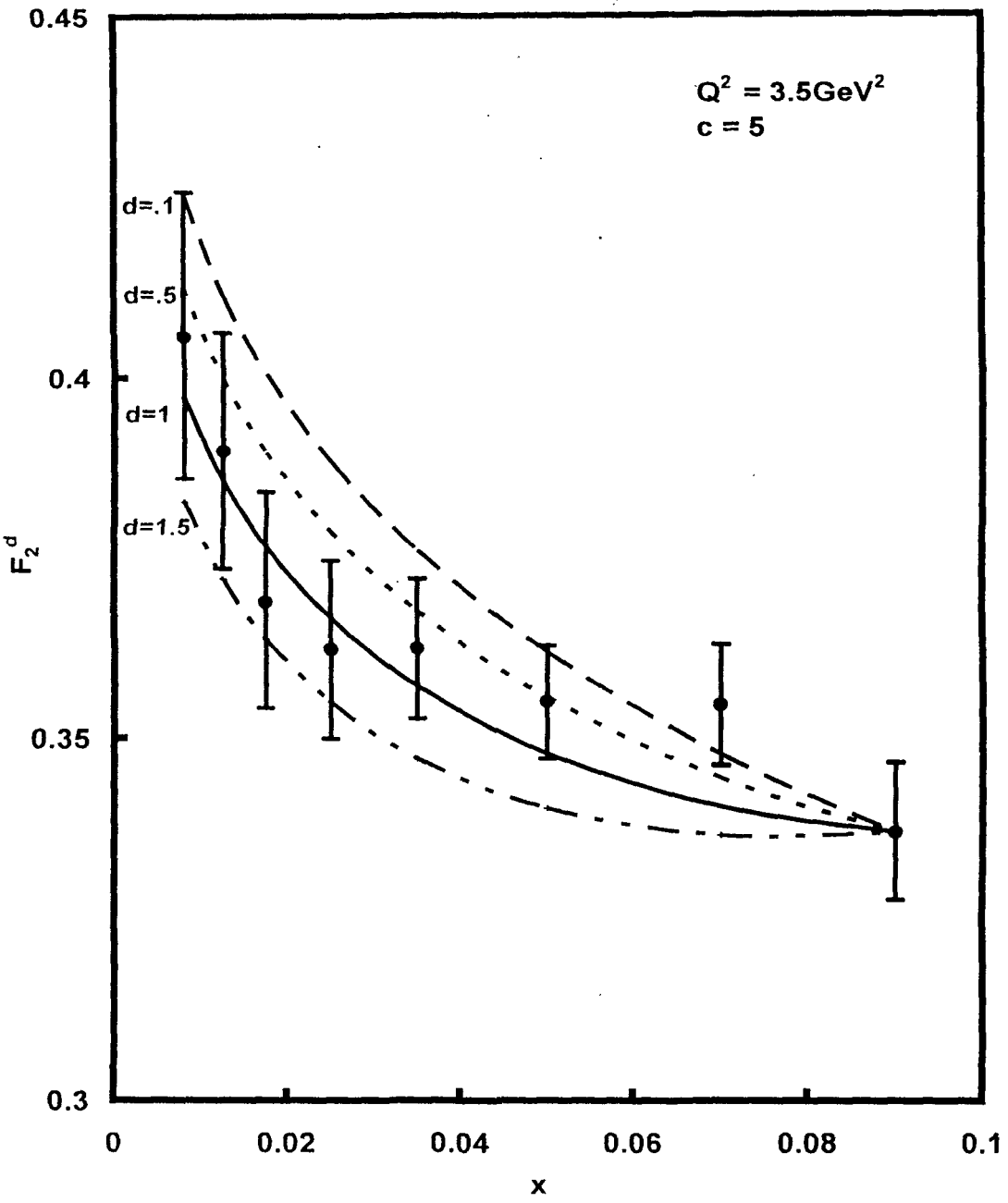

Fig.3.12: Sensitivity of our results for different values of 'd' at fixed value of 'c'.

experimental data is found to be excellent. If value of '*d*' is increased then the curve goes downward direction and if value of '*d*' is decreased the curve goes upward direction. Here also the nature of the curve is similar.

Traditionally the GLDAP evolution provide a means of calculating the manner in which

the parton distributions change at fixed-x as Q^2 varies. This change comes about because of the various types of parton branching emission processes and the x-distributions are modified as the initial momentum is shared among the various daughter partons. However, the exact rate of modifications of x-distributions at fixed-Q^2 can not be obtained from the GLDAP equations since it depends not only on the initial x, but also on the rate of change of parton distributions with respect to x, $d^nF(x)/dx^n$ ($n = 1$ to ∞), up to infinite order. Physically, this implies that at high-x, the parton has a large momentum fraction at its disposal and as a result it radiates partons including gluons in innumerable ways, some of them involving complicated QCD mechanisms. However for low-x, many of the radiation processes will cease to occur due to momentum constraints and the x-evolutions get simplified. It is then possible to visualize a situation in which the modification of the x-distribution simply depends on its initial value and its first derivative. In this simplified situation, the GLDAP equations give information on the shapes of the x-distribution. The clearer testing of our results of x-evolution is actually the equation (3.25) which is free from the additional assumption equation (3.15). But non-singlet data is not sufficiently available in low-x to test our result.

3.3. Conclusion

In this chapter, we obtain complete and particular solutions of singlet and non-singlet structure functions at low-x using by Taylor's expansion method from GLDAP evolution equations and t and x-evolution of singlet and non-singlet structure functions in LO. Hence t-evolutions of deuteron, proton, neutron and difference and ratio of proton and neutron structure functions and x-evolutions of deuteron structure functions in LO have been calculated. These evolutions are non-unique. We compare our results with HERA, NMC low-x low Q^2 data and a recent global parameterization. In all the result from experimental as well as global fits, it is seen that deuteron structure functions increases when x decreases and Q^2 increases for fixed values of Q^2 and x respectively, and proton, neutron, difference and ratio of proton and neutron structure functions increases when Q^2 increases for fixed value of x. It is clear from the figures that the LO results of t-evolutions for $y = 2$ in the relation $\beta = \alpha^y$, are of better agreement with experimental data and parameterization in general.

Chapter-4

t AND x-EVOLUTIONS OF GLDAP EVOLUTION EQUATIONS IN NEXT-TO-LEADING ORDER

In the previous chapter, particular solution of the Gribov-Lipatov-Dokshitzer-Altarelli-Parisi (GLDAP) evolution equations [29-32] for t and x-evolutions of singlet and non-singlet structure functions in leading order (LO) at low-x have been discussed. The same technique can be applied to the GLDAP evolution equations in next-to-leading order (NLO) for singlet and non-singlet structure functions to obtain t-evolutions of deuteron, proton, neutron, and difference and ratio of proton and neutron structure functions and x-evolution of deuteron structure functions at low-x. These NLO results are compared with the HERA H1 [94] and NMC [95] low-x, low-Q^2 data and with those of particular solution in LO and we also compare our results of t-evolution of proton structure functions with a recent global parameterization [96].

4.1. Theory

The GLDAP evolution equations with splitting functions [103-105] for singlet and non-singlet structure functions in NLO are in the standard forms [106-109]

$$\frac{\partial F_2^S(x,t)}{\partial t} - \frac{\alpha_S(t)}{2\pi}$$
$$\left[\frac{2}{3}\{3+4\ln(1-x)\}F_2^S(x,t)+\frac{4}{3}\int_x^1\frac{dw}{1-w}\left\{\left(1+w^2\right)F_2^S\left(\frac{x}{w},t\right)-2F_2^S(x,,t)\right\}+N_f\int_x^1\{w^2+(1-w)^2\}G\left(\frac{x}{w},t\right)\right]$$
$$-\left(\frac{\alpha_S(t)}{2\pi}\right)^2\left[(x-1)F_2^S(x,t)+\int_0^1 f(w)dw+\int_x^1 f(w)F_2^S\left(\frac{x}{w},t\right)dw+\int_x^1 F_{qq}^S(w)F_2^S\left(\frac{x}{w},t\right)dw\right]$$
$$+\left(\frac{\alpha_S(t)}{2\pi}\right)^2\int_x^1 F_{qg}^S(w)G\left(\frac{x}{w},t\right)dw=0 \qquad (4.1)$$

and

$$\frac{\partial F_2^{NS}(x,t)}{\partial t} = \frac{\alpha_S(t)}{2\pi}$$
$$\left[\frac{2}{3}\{3+4\ln(1-x)\}F_2^{NS}(x,t)+\frac{4}{3}\int_x^1 \frac{dw}{1-w}\left\{\left(1+w^2\right)F_2^{NS}\left(\frac{x}{w},t\right)-2F_2^{NS}(x,t)\right\}\right]$$
$$-\left(\frac{\alpha_S(t)}{2\pi}\right)^2\left[(x-1)F_2^{NS}(x,t)+\int_0^1 f(w)dw+\int_x^1 f(w)F_2^{NS}\left(\frac{x}{w},t\right)dw\right]=0, \qquad (4.2)$$

where

$$\alpha_S(t)=\frac{4\pi}{\beta_0 t}\left[1-\frac{\beta_1 \ln t}{\beta_0^2 t}\right],\ \beta_0=\frac{33-2N_f}{3} \text{ and } \beta_1=\frac{306-38N_f}{3},$$

N_f being the number of flavours. Here,

$$f(w)=C_F^2\left[P_F(w)-P_A(w)\right]+\frac{1}{2}C_F C_A\left[P_G(w)+P_A(w)\right]+C_F T_R N_f P_{N_F}(w),$$
$$F_{qq}^S(w)=2C_F T_R N_f F_{qq}(w)$$

and

$$F_{qg}^S(w)=C_F T_R N_f F_{qg}^1(w)+C_G T_R N_f F_{qg}^2(w).$$

The explicit forms of higher order kernels are [103-105]

$$P_F(w)=-2\left(\frac{1+w^2}{1-w}\right)\ln w\ln(1-w)-\left(\frac{3}{1-w}+2w\right)\ln w-\frac{1}{2}(1+w)\ln^2 w-5(1-w),$$
$$P_G(w)=\frac{1+w^2}{1-w}\left(\ln^2 w+\frac{11}{3}\ln w+\frac{67}{9}-\frac{\pi^2}{3}\right)+2(1+w)\ln w+\frac{40}{3}(1-w),$$
$$P_{N_F}(w)=\frac{2}{3}\left[\frac{1+w^2}{1-w}\left(-\ln w-\frac{5}{3}\right)-2(1-w)\right],$$
$$P_A(w)=2\left(\frac{1+w^2}{1-w}\right)\int_{w/(1+w)}^{1/(1+w)}\frac{dk}{k}\ln\frac{1-k}{k}+2(1+w)\ln w+4(1-w),$$
$$F_{qq}(w)=\frac{20}{9w}-2+6w-\frac{56}{9}w^2+\left(1+5w+\frac{8}{3}w^2\right)\ln w-(1+w)\ln^2 w,$$
$$F_{qg}^1(w)=4-9w-(1-4w)\ln w-(1-2w)\ln^2 w+4\ln(1-w)$$
$$+\left[2\ln^2\left(\frac{1-w}{w}\right)-4\ln\left(\frac{1-w}{w}\right)-\frac{2}{3}\pi^2+10\right]P_{qg}(w)$$

and

$$F_{qg}^{2}(w) = \frac{182}{9} + \frac{14}{9}w + \frac{40}{9w} + \left(\frac{136}{3}w - \frac{38}{3}\right)\ln w - 4\ln(1-w) - (2+8w)\ln^2 w$$

$$+\left[-\ln^2 w + \frac{44}{3}\ln w - 2\ln^2(1-w) + 4\ln(1-w) + \frac{\pi^2}{3} - \frac{218}{3}\right]P_{qg}(w)$$

$$+2P_{qg}(-w)\int_{w/(1+w)}^{1/(1+w)}\frac{dz}{z}\ln\frac{1-z}{z},$$

where $P_{qg}(w) = w^2 + (1-w)^2$, $C_A = C_G = N_C = 3$, $C_F = (N_C{}^2 - 1)/2N_C$ and $T_R = 1/2$.

Now, using Taylor expansion method [80] and neglecting higher order terms of x as discussed in the Chapter-3 we can write $F_2^S(x/w, t)$, $G(x/w, t)$ and $F_2^{NS}(x/w, t)$ as

$$F_2^S(x/w,t) \cong F_2^S(x,t) + x\sum_{k=1}^{\infty}u^k\frac{\partial F_2^S(x,t)}{\partial x}, \tag{4.3}$$

$$G(x/w,t) \cong G(x,t) + x\sum_{k=1}^{\infty}u^k\frac{\partial G(x,t)}{\partial x} \tag{4.4}$$

and

$$F_2^{NS}(x/w,t) \cong F_2^{NS}(x,t) + x\sum_{k=1}^{\infty}u^k\frac{\partial F_2^{NS}(x,t)}{\partial x}, \tag{4.5}$$

where $u = 1-w$.

Using equations (4.3) and (4.4) in equation (4.1) and performing u-integrations we get,

$$\frac{\partial F_2^S(x,t)}{\partial t} -$$

$$\left[\frac{\alpha_S(t)}{2\pi}A_1(x) + \left(\frac{\alpha_S(t)}{2\pi}\right)^2 B_1(x)\right]F_2^S(x,t) - \left[\frac{\alpha_S(t)}{2\pi}A_2(x) + \left(\frac{\alpha_S(t)}{2\pi}\right)^2 B_2(x)\right]G(x,t) -$$

$$\left[\frac{\alpha_S(t)}{2\pi}A_3(x) + \left(\frac{\alpha_S(t)}{2\pi}\right)^2 B_3(x)\right]\frac{\partial F_2^S(x,t)}{\partial x} - \left[\frac{\alpha_S(t)}{2\pi}A_4(x) + \left(\frac{\alpha_S(t)}{2\pi}\right)^2 B_4(x)\right]\frac{\partial G(x,t)}{\partial x} = 0, \tag{4.6}$$

where

$$A_1(x) = \frac{2}{3}\{3 + 4\ln(1-x) + (x-1)(x+3)\},$$

$$A_2(x) = N_f\left[\frac{1}{3}(1-x)\left(2 - x + 2x^2\right)\right],$$

$$A_3(x) = \frac{2}{3}\left\{x\left(1-x^2\right) + 2x\ln\left(\frac{1}{x}\right)\right\},$$

$$A_4(x) = N_f x\left\{\ln\frac{1}{x} - \frac{1}{3}(1-x)\left(5 - 4x + 2x^2\right)\right\},$$

$$B_1(x) = x\int_0^1 f(w)dw - \int_0^x f(w)dw + \frac{4}{3}N_f\left[\begin{array}{l} -\ln x\left(\frac{20}{9} + 3x + 3x^2 + \frac{8}{9}x^3\right) + \frac{1}{2}x(2+x)\ln^2 x \\ +5x - \frac{3}{2}x^2 + \frac{64}{27}x^3 - \frac{317}{54} \end{array}\right],$$

$$B_2(x) = \frac{2}{3}N_f\left[\begin{array}{l} -\left(9x - 5x^2 + \frac{32}{9}x^3\right)\ln x + \left(3x - 3x^2 + \frac{4}{3}x^3\right)\ln^2 x \\ +\left(\frac{32}{9}x^3 - \frac{14}{3}x^2 + \frac{8}{3}x - \frac{14}{9}\right)\ln(1-x) + \left(\frac{4}{3} - 2x + 2x^2 - \frac{4}{3}x^3\right)\ln^2(1-x) \\ +\left(\frac{2}{3} - \frac{4}{9}\pi^2\right) + \left(\frac{2}{3}\pi^2 - \frac{59}{9}\right)x + \left(\frac{113}{9} - \frac{2}{3}\pi^2\right)x^2 + \left(\frac{4}{9}\pi^2 - \frac{20}{3}\right)x^3 \end{array}\right]$$

$$+\frac{3}{2}N_f\left[\begin{array}{l} -\left(\frac{40}{9} + 8x + 11x^2 + \frac{92}{9}x^3\right)\ln x + \left(3x + 3x^2 + \frac{2}{3}x^3\right)\ln^2 x + \\ \left(\frac{14}{9} - \frac{8}{3}x + \frac{14}{3}x^2 - \frac{32}{9}x^3\right)\ln(1-x) + \left(-\frac{4}{3} + 2x - 2x^2 + \frac{4}{3}x^3\right)\ln^2(1-x) + \\ \left(\frac{2}{9}\pi^2 - \frac{769}{54}\right) + \left(\frac{122}{9} - \frac{1}{3}\pi^2\right)x + \left(\frac{1}{3}\pi^2 - \frac{361}{18}\right)x^2 + \left(\frac{560}{27} - \frac{2}{9}\pi^2\right)x^3 \end{array}\right]$$

$$+\frac{3}{2}N_f\int_x^1 2\left(w^2 + (1+w)^2\right)\left[-\ln\ln(1+w) - \ln w\ln(1+w) + \ln\ln\left(\frac{1+w}{w}\right) + \ln\frac{1}{w}\ln\left(1+\frac{1}{w}\right)\right]dw,$$

$$B_3(x) = x\int_x^1 \frac{1-w}{w}f(w)dw + \frac{4}{3}N_f x\left[\begin{array}{l} \left(\frac{38}{9} - 4x + \frac{5}{3}x^2 + \frac{8}{9}x^3\right)\ln x - \frac{1}{2}\left(1+x^2\right)\ln^2 x \\ +\frac{1}{3}\ln^3 x + \frac{20}{9x} - 4x + \frac{95}{18}x^2 - \frac{64}{27}x^3 - \frac{61}{54} \end{array}\right]$$

and

$$B_4(x) = x\int_x^1 \frac{1-w}{w} F_{qg}^S(w)dw .$$

Let us assume for simplicity [86-88, 106-110]

$$G(x, t) = K(x)\, F_2^S(x, t), \tag{4.7}$$

where $K(x)$ is a function of x. Now equation (4.6) becomes

$$\frac{\partial F_2^S(x,t)}{\partial t} - \left[\frac{\alpha_S(t)}{2\pi} L_1(x) + \left(\frac{\alpha_S(t)}{2\pi}\right)^2 M_1(x)\right] F_2^S(x,t) - \left[\frac{\alpha_S(t)}{2\pi} L_2(x) + \left(\frac{\alpha_S(t)}{2\pi}\right)^2 M_2(x)\right] \frac{\partial F_2^S(x,t)}{\partial x} = 0, \tag{4.8}$$

where

$$L_1(x) = A_1(x) + K(x)A_2(x) + A_4(x)\frac{\partial K(x)}{\partial x},$$

$$L_2(x) = A_3(x) + K(x)A_4(x)$$

and

$$M_1(x) = B_1(x) + K(x)B_2(x) + B_4(x)\frac{\partial K(x)}{\partial x},$$

$$M_2(x) = B_3(x) + K(x)B_4(x).$$

For a possible solution, we assume [106-109] that

$$\left(\frac{\alpha_S(t)}{2\pi}\right)^2 = T_0\left(\frac{\alpha_S(t)}{2\pi}\right), \tag{4.9}$$

where T_0 is a numerical parameter to be obtained from the particular Q^2-range under study. By a suitable choice of T_0 we can reduce the error to a minimum. Now equation (4.8) can be recast as

$$\frac{\partial F_2^S(x,t)}{\partial t} - P_S(x,t)\frac{\partial F_2^S(x,t)}{\partial x} - Q_S(x,t)F_2^S(x,t) = 0, \tag{4.10}$$

where

$$P_S(x,t) = \frac{\alpha_S(t)}{2\pi}\left[L_2(x) + T_0 M_2(x)\right]$$

and

$$Q_S(x,t) = \frac{\alpha_S(t)}{2\pi}\left[L_1(x) + T_0 M_1(x)\right].$$

Secondly, using equations (4.5) and (4.9) in equation (4.2) and performing u-integration we have

$$\frac{\partial F_2^{NS}(x,t)}{\partial t} - P_{NS}(x,t)\frac{\partial F_2^{NS}(x,t)}{\partial x} - Q_{NS}(x,t)F_2^{NS}(x,t) = 0, \tag{4.11}$$

where

$$P_{NS}(x,t) = \frac{\alpha_S(t)}{2\pi}\left[A_5(x) + T_0 B_5(x)\right]$$

and

$$Q_{NS}(x,t) = \frac{\alpha_S(t)}{2\pi}\left[A_6(x) + T_0 B_6(x)\right],$$

with

$$A_5(x) = \frac{2}{3}\left\{x\left(1 - x^2\right) + 2x\ln\left(\frac{1}{x}\right)\right\}, \quad B_5(x) = x\int_x^1 \frac{1-w}{w} f(w)dw,$$

$$A_6(x) = \frac{2}{3}\{3 + 4\ln(1-x) + (x-1)(x+3)\}, \text{ and } \quad B_6(x) = -\int_0^x f(w)dw + x\int_0^1 f(w)dw.$$

The general solutions [80-81] of equations (4.10) is $F(U, V) = 0$, where F is an arbitrary function and $U(x, t, F_2^S) = C_1$ and $V(x, t, F_2^S) = C_2$ where, C_1 and C_2 are constants and they form a solution of equations

$$\frac{dx}{P_S(x,t)} = \frac{dt}{-1} = \frac{dF_2^S(x,t)}{-Q_S(x,t)}. \tag{4.12}$$

We observe that the Lagrange's auxiliary system of ordinary differential equations [80-81] occurred in the formalism can not be solved without the additional assumption of linearization (equation 4.9) and introduction of an ad hoc parameter T_0. But this parameter does not effect in the results of t-evolutions of structure functions. Solving equation (4.12) we obtain,

$$U\left(x,t,F_2^S\right)=t^{(b/t+1)}\exp\left[\frac{b}{t}+\frac{N_S(x)}{a}\right] \text{ and } V\left(x,t,F_2^S\right)=F_2^S(x,t)\exp\left[M_S(x)\right]$$

where

$$a=\frac{2}{\beta_0},\quad b=\frac{\beta_1}{\beta_0^2},\quad N_S(x)=\int\frac{dx}{L_2(x)+T_0M_2(x)}dx, \text{ and } M_S(x)=\int\frac{L_1(x)+T_0M_1(x)}{L_2(x)+T_0M_2(x)}dx.$$

If U and V are two independent solutions of equation (4.12) and if α and β are arbitrary constants, then $V=\alpha U+\beta$ may be taken as a complete solution of equation (4.11). Then the complete solution [80-81]

$$F_2^S(x.t)\exp\left[M_S(x)\right]=\alpha\left[t^{(b/t+1)}\exp\left(\frac{b}{t}+\frac{N_S(x)}{a}\right)\right]+\beta \tag{4.13}$$

is a two-parameter family of planes. The one parameter family determined by taking $\beta=\alpha^2$ has equation

$$F_2^S(x,t)\exp\left[M_S(x)\right]=\alpha\left[t^{(b/t+1)}\exp\left(\frac{b}{t}+\frac{N_S(x)}{a}\right)\right]+\alpha^2. \tag{4.14}$$

Differentiating equation (4.14) with respect to α, we obtain

$$\alpha=-\frac{1}{2}t^{(b/t+1)}\exp\left[\frac{b}{t}+\frac{N_S(x)}{a}\right].$$

Putting the value of α again in equation (4.14), we obtain the envelope

$$F_2^S(x,t)\exp\left[M_S(x)\right]=-\frac{1}{4}\left[t^{(b/t+1)}\exp\left(\frac{b}{t}+\frac{N_S(x)}{a}\right)\right]^2.$$

Therefore,

$$F_2^S(x,t)=-\frac{1}{4}t^{2(b/t+1)}\exp\left[\frac{2b}{t}+\frac{2N_S(x)}{a}-M_S(x)\right], \tag{4.15}$$

which is merely a particular solution of the general solution. Now defining

$$F_2^S\left(x,t_0\right)=-\frac{1}{4}t_0^{2(b/t_0+1)}\exp\left[\frac{2b}{t_0}+\frac{2N_S(x)}{a}-M_S(x)\right],$$

at $t = t_0$, where, $t_0 = \ln (Q_0^2/\Lambda^2)$ at any lower value $Q = Q_0$, we get from equation (4.15)

$$F_2^S(x,t) = F_2^S(x,t_0)\left\{\frac{t^{(b/t+1)}}{t_0^{(b/t_0+1)}}\right\}^2 \exp\left[2b\left(\frac{1}{t}-\frac{1}{t_0}\right)\right], \tag{4.16}$$

which gives the t-evolution of singlet structure function $F_2^S(x, t)$ in NLO for $\beta = \alpha^2$. Proceeding exactly in the same way, and defining

$$F_2^{NS}(x,t_0) = -\frac{1}{4}t_0^{2(b/t_0+1)}\exp\left[\frac{2b}{t_0}+\frac{2N_{NS}(x)}{a}-M_{NS}(x)\right],$$

where

$$N_{NS}(x) = \int\frac{dx}{A_5(x)+T_0B_5(x)} \text{ and } M_{NS}(x) = \int\frac{A_5(x)+T_0B_5(x)}{A_6(x)+T_0B_6(x)}dx,$$

we get,

$$F_2^{NS}(x,t) = F_2^{NS}(x,t_0)\left\{\frac{t^{(b/t+1)}}{t_0^{(b/t_0+1)}}\right\}^2 \exp\left[2b\left(\frac{1}{t}-\frac{1}{t_0}\right)\right], \tag{4.17}$$

which gives the t-evolution of non-singlet structure function $F_2^{NS}(x, t)$ in NLO for $\beta = \alpha^2$.

In the previous chapter, we obtained that for low-x in LO for $\beta = \alpha^2$,

$$F_2^S(x,t) = F_2^S(x,t_0)\left\{\frac{t}{t_0}\right\}^2 \tag{4.18}$$

and

$$F_2^{NS}(x,t) = F_2^{NS}(x,t_0)\left\{\frac{t}{t_0}\right\}^2. \tag{4.19}$$

We observe that if b tends to zero, then equation (4.16) and (4.17) tends to equation (4.18) and (4.19) respectively, i.e., solution of NLO equations goes to that of LO equations. Physically b tends to zero means number of flavours is high.

Again defining,

$$F_2^S(x_0,t) = -\frac{1}{4}t^{(b/t+1)}\exp\left[\frac{2b}{t} + \frac{2N_S(x)}{a} - M_S(x)\right]_{x=x_0},$$

we obtain from equation (4.15)

$$F_2^S(x,t) = F_2^S(x_0,t)\exp\left[\int_{x_0}^{x}\left(\frac{2}{a}\cdot\frac{1}{L_2(x)+T_0M_2(x)} - \frac{L_1(x)+T_0M_1(x)}{L_2(x)+T_0M_2(x)}\right)dx\right], \tag{4.20}$$

which gives the x-evolution of singlet structure function $F_2^S(x, t)$ in NLO for $\beta = \alpha^2$. Similarly defining,

$$F_2^{NS}(x_0,t) = -\frac{1}{4}t^{(b/t+1)}\exp\left[\frac{2b}{t} + \frac{2N_{NS}(x)}{a} - M_{NS}(x)\right]_{x=x_0},$$

we get

$$F_2^{NS}(x,t) = F_2^{NS}(x_0,t)\exp\left[\int_{x_0}^{x}\left(\frac{2}{a}\cdot\frac{1}{A_5(x)+T_0B_5(x)} - \frac{A_6(x)+T_0B_6(x)}{A_5(x)+T_0B_5(x)}\right)dx\right], \tag{4.21}$$

which gives the x-evolution of non-singlet structure function $F_2^{NS}(x, t)$ in NLO for $\beta = \alpha^2$. In the previous chapter, we obtained that for low-x in LO for $\beta = \alpha^2$,

$$F_2^S(x,t) = F_2^S(x_0,t)\exp\left[\int_{x_0}^{x}\left(\frac{2}{A_f M(x)} - \frac{L(x)}{M(x)}\right)dx\right] \tag{4.22}$$

and

$$F_2^{NS}(x,t) = F_2^{NS}(x_0,t)\exp\left[\int_{x_0}^{x}\left(\frac{2}{A_f Q(x)} - \frac{P(x)}{Q(x)}\right)dx\right], \tag{4.23}$$

where

$A_f = 4/(33-2N_f)$, $P(x) = 3 + 4\ln(1-x) - (1-x)(x+3)$, $Q(x) = x(1-x^2) - 2x\ln x$,

$L(x) = P(x) + K(x)C(x) + D(x)\dfrac{\partial K(x)}{\partial x}$ and $M(x) = Q(x) + K(x)D(x)$,

where again,

$C(x) = (1/2)N_f(1-x)(2-x+2x^2)$ and $D(x) = N_f x[(-1/2)(1-x)(5-4x+2x^2) + (3/2)\ln(1/x)$.

Of course, unlike for the t-evolution equations, we could not have for the x-evolution equations in LO as some limiting case of NLO equations.

Deuteron, proton and neutron structure functions can be written in terms of singlet and non-singlet quark distribution functions [7] as

$$F_2^d(x,t) = (5/9)\, F_2^S(x,t), \tag{4.24}$$

$$F_2^p(x,t) = (5/18)\, F_2^S(x,t) + (3/18)\, F_2^{NS}(x,t), \tag{4.25}$$

$$F_2^n(x,t) = (5/18)\, F_2^S(x,t) - (3/18)\, F_2^{NS}(x,t), \tag{4.26}$$

$$F_2^p(x,t) - F_2^n(x,t) = (1/3)\, F_2^{NS}(x,t). \tag{4.27}$$

Now using equations (4.16) and (4.20) in equation (4.24) we will get t and x-evolution of deuteron structure function $F_2^d(x,t)$ at low-x in NLO for $\beta = \alpha^2$ as

$$F_2^d(x,t) = F_2^d(x,t_0)\left(\frac{t^{(b/t+1)}}{t_0^{(b/t_0+1)}}\right)^2 \exp\left[2b\left(\frac{1}{t}-\frac{1}{t_0}\right)\right] \tag{4.28}$$

and

$$F_2^d(x,t) = F_2^d(x_0,t)\exp\left[\int_{x_0}^{x}\left(\frac{2}{a}.\frac{1}{L_2(x)+T_0M_2(x)} - \frac{L_1(x)+T_0M_1(x)}{L_2(x)+T_0M_2(x)}\right)dx\right], \tag{4.29}$$

where the input functions are $F_2^d(x,t_0)=(5/9)F_2^S(x,t_0)$ and $F_2^d(x_0,t)=(5/9)F_2^S(x_0,t)$. The corresponding results for a particular solution of GLDAP evolution equations in LO for $\beta = \alpha^2$ obtained earlier [110] given in equations (3.30) and (3.31) in the Chapter-3.

Similarly using equations (4.16) and (4.17) in equations (4.25), (4.26) and (4.27) we get the t-evolutions of proton, neutron, and difference and ratio of proton and neutron structure functions at low-x in NLO as

$$F_2^p(x,t) = F_2^p(x,t_0)\left(\frac{t^{(b/t+1)}}{t_0^{(b/t_0+1)}}\right)^2 \exp\left[2b\left(\frac{1}{t}-\frac{1}{t_0}\right)\right], \tag{4.30}$$

$$F_2^n(x,t) = F_2^n(x,t_0)\left(\frac{t^{(b/t+1)}}{t_0^{(b/t_0+1)}}\right)^2 \exp\left[2b\left(\frac{1}{t}-\frac{1}{t_0}\right)\right], \tag{4.31}$$

$$F_2^p(x,t) - F_2^n(x,t) = [F_2^p(x,t_0) - F_2^n(x,t_0)]\left(\frac{t^{(b/t+1)}}{t_0^{(b/t_0+1)}}\right)^2 \exp\left[2b\left(\frac{1}{t}-\frac{1}{t_0}\right)\right] \tag{4.32}$$

and

$$\frac{F_2^p(x,t)}{F_2^n(x,t)} = \frac{F_2^p(x,t_0)}{F_2^n(x,t_0)} = R(x), \tag{4.33}$$

where $R(x)$ is a constant for fixed-x. And the input functions are

$$F_2^p(x,t_0) = (5/18)\,F_2^S(x,t_0) + (3/18)\,F_2^{NS}(x,t_0),$$

$$F_2^n(x,t_0) = (5/18)\,F_2^S(x,t_0) - (3/18)\,F_2^{NS}(x,t_0)$$

and

$$F_2^p(x,t_0) - F_2^n(x,t_0) = (1/3)F_2^{NS}(x,t_0).$$

The corresponding results for particular solutions of GLDAP evolution equations in LO for $\beta = \alpha^2$ have been given in equations (3.34), (3.35), (3.35), (3.36) and (3.37) in the Chapter-3. It is observed that ratio of proton and neutron is same for both NLO and LO and it is independent of t for fixed-x. But the determination of x-evolutions of proton and neutron structure functions like those of deuteron structure function is not possible by this method as is discussed in the Chapter-3.

For the particular solution of equation (4.10), we take $\beta = \alpha^2$ in equation (4.13). If we take $\beta = \alpha$ in equation (4.13) and differentiating with respect to α as before, we get $0 = t^{(b/t+1)} \exp\left(\frac{b}{t} + \frac{N_S(x)}{a}\right) + 1$ from which we can not determine the value of α. But if we take $\beta = \alpha^3$ in equation (4.14) and differentiating with respect to α, we get $\alpha = \sqrt{-\frac{1}{3}t^{(b/t+1)} \exp\left(\frac{b}{t} + \frac{N_S(x)}{a}\right)}$. Putting this value of α in equation (4.14) we get

$$F_2^S(x,t) = t^{(b/t+1)^{3/2}}\left\{\left(-\frac{1}{3}\right)^{1/2} + \left(-\frac{1}{3}\right)^{3/2}\right\}\exp\left[\left(\frac{b}{t} + \frac{N_S(x)}{a}\right)^{3/2} - M_S(x)\right].$$

Now, defining

$$F_2^S(x,t_0) = t_0^{(b/t_0+1)^{3/2}}\left\{\left(-\frac{1}{3}\right)^{1/2}+\left(-\frac{1}{3}\right)^{3/2}\right\}\exp\left[\left(\frac{b}{t_0}+\frac{N_S(x)}{a}\right)^{3/2}-M_S(x)\right],$$

we get

$$F_2^S(x,t) = F_2^S(x,t_0)\left(\frac{t^{(b/t+1)}}{t_0^{(b/t_0+1)}}\right)^{3/2}\exp\left[\frac{3}{2}b\left(\frac{1}{t}-\frac{1}{t_0}\right)\right].$$

Proceeding exactly in the same way we get for non-singlet structure function also

$$F_2^{NS}(x,t) = F_2^{NS}(x,t_0)\left(\frac{t^{(b/t+1)}}{t_0^{(b/t_0+1)}}\right)^{3/2}\exp\left[\frac{3}{2}b\left(\frac{1}{t}-\frac{1}{t_0}\right)\right].$$

Then using equations (4.24), (4.25) and (4.26) we get t-evolutions of deuteron, proton and difference of proton and neutron structure functions

$$F_2^{d,p,n,p-n}(x,t) = F_2^{d,p,n,p-n}(x,t_0)\left(\frac{t^{(b/t+1)}}{t_0^{(b/t_0+1)}}\right)^{3/2}\exp\left[\frac{3}{2}b\left(\frac{1}{t}-\frac{1}{t_0}\right)\right].$$

Proceeding in the same way, we get x-evolution of deuteron structure function as

$$F_2^d(x,t) = F_2^d(x_0,t)\exp\left[\int_{x_0}^{x}\left(\frac{3/2}{a}\cdot\frac{1}{L_2(x)+T_0M_2(x)}-\frac{L_1(x)+T_0M_1(x)}{L_2(x)+T_0M_2(x)}\right)dx\right].$$

Proceeding exactly in the same way we can show that if we take $\beta = \alpha^4$ we get

$$F_2^{d,p,n.p-n}(x,t) = F_2^{d,p,n,p-n}(x,t_0)\left(\frac{t^{(b/t+1)}}{t_0^{(b/t_0+1)}}\right)^{4/3}\exp\left[\frac{4}{3}b\left(\frac{1}{t}-\frac{1}{t_0}\right)\right]$$

and

$$F_2^d(x,t) = F_2^d(x_0,t)\exp\left[\int_{x_0}^{x}\left(\frac{4/3}{a}\cdot\frac{1}{L_2(x)+T_0M_2(x)}-\frac{L_1(x)+T_0M_1(x)}{L_2(x)+T_0M_2(x)}\right)dx\right],$$

and so on. So in general, if we take $\beta = \alpha^\nu$, we get

$$F_2^{d,p,n,p-n}(x,t) = F_2^{d,p,n,p-n}(x,t_0)\left(\frac{t^{(b/t+1)}}{t_0^{(b/t_0+1)}}\right)^{y/(y-1)} \exp\left[\frac{y}{y-1}b\left(\frac{1}{t}-\frac{1}{t_0}\right)\right]$$

and

$$F_2^d(x,t) = F_2^d(x_0,t)\exp\left[\int_{x_0}^{x}\left(\frac{y/(y-1)}{a}\cdot\frac{1}{L_2(x)+T_0M_2(x)} - \frac{L_1(x)+T_0M_1(x)}{L_2(x)+T_0M_2(x)}\right)dx\right],$$

which are t-evolutions of deuteron, proton, neutron, and difference of proton and neutron structure functions and x-evolution of deuteron structure function respectively for $\beta = \alpha^y$. We observe if $y \to \infty$ (very large), $y/(y-1) \to 1$.

Thus we observe that if we take $\beta = \alpha$ in equation (4.14) we can not obtain the value of α and also the required solution. But if we take $\beta = \alpha^2, \alpha^3, \alpha^4, \alpha^5$..... and so on, we see that the powers of $t^{b/t+1}/t_0^{b/t_0+1}$ and co-efficient of $b\{(1/t) - (1/t_0)\}$ of exponential part in t-evolutions of deuteron, proton, neutron, and difference of proton and neutron structure functions are 2, 3/2, 4/3, 5/4....and so on respectively as discussed above. Similarly, for x-evolutions of deuteron structure functions we see that the numerators of the first term inside the integral sign are 2, 3/2, 4/3, 5/4....and so on respectively for the same values of α. Thus we see that if in the relation $\beta = \alpha^y$, y varies between 2 to a maximum value, the powers of $t^{b/t+1}/t_0^{b/t_0+1}$, co-efficient of $t^{b/t+1}/t_0^{b/t_0+1}$ of exponential part in t-evolution and the numerator of the first term in the integral sign in x-evolution varies between 2 to 1. Then it is understood that the solutions of equations (4.10) and (4.11) obtained by this method are not unique and so the t- evolutions of deuteron, proton and neutron structure functions, and x-evolution of deuteron structure function obtained by this method are not unique.

4.2. Results and Discussion

We compare our results of t-evolution of deuteron, proton, neutron and difference and ratio of proton and neutron structure functions with the HERA [94] and NMC [95] low-x and low-Q^2 data. In case of HERA data [94] proton and neutron structure functions are measured in the range $2 \leq Q^2 \leq 50$ GeV^2. Moreover here $P_T \leq 200$ MeV, where P_T is the

transverse momentum of the final state baryon. In case of NMC data, proton and deuteron structure functions are measured in the range $0.75 \leq Q^2 \leq 27\text{GeV}^2$. We consider number of flavours $N_f = 4$. We also compare our results of t-evolution of proton structure

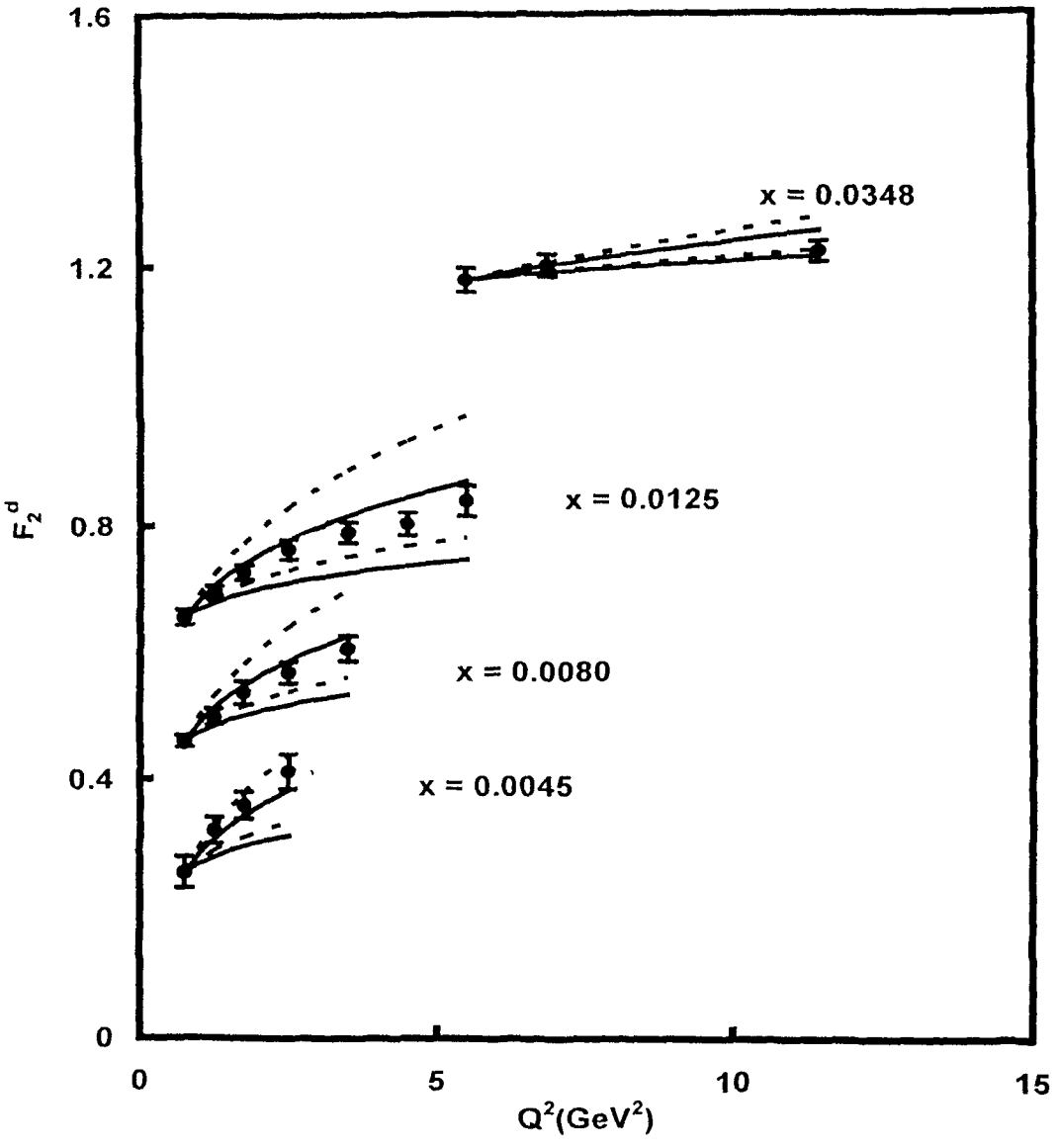

Fig.4.1: t-Evolution of deuteron structure functions in leading order (dashed lines) and next-to-leading order (solid lines).

functions with a recent global parameterization [96]. This parameterization includes data from H1, ZEUS, NMC and E665 experiment [95, 97-102]. The result of x-evolution of deuteron structure function has been compared with NMC low-x and low-Q^2 data, and also our results of x and t-evolutions have been compared with those of LO results.

In figure 4.1, we present our results of t-evolutions of deuteron structure functions F_2^d for

the representative values of x given in the figure for $y = 2$ (upper solid lines) and y maximum (lower solid lines) in the $\beta = \alpha^y$ relation. Data points at lowest-Q^2 values in the figures are taken as inputs to test the evolution equation. Agreement with the data [95] is found to be good. In the same figure we also plot the results of t-evolutions of deuteron

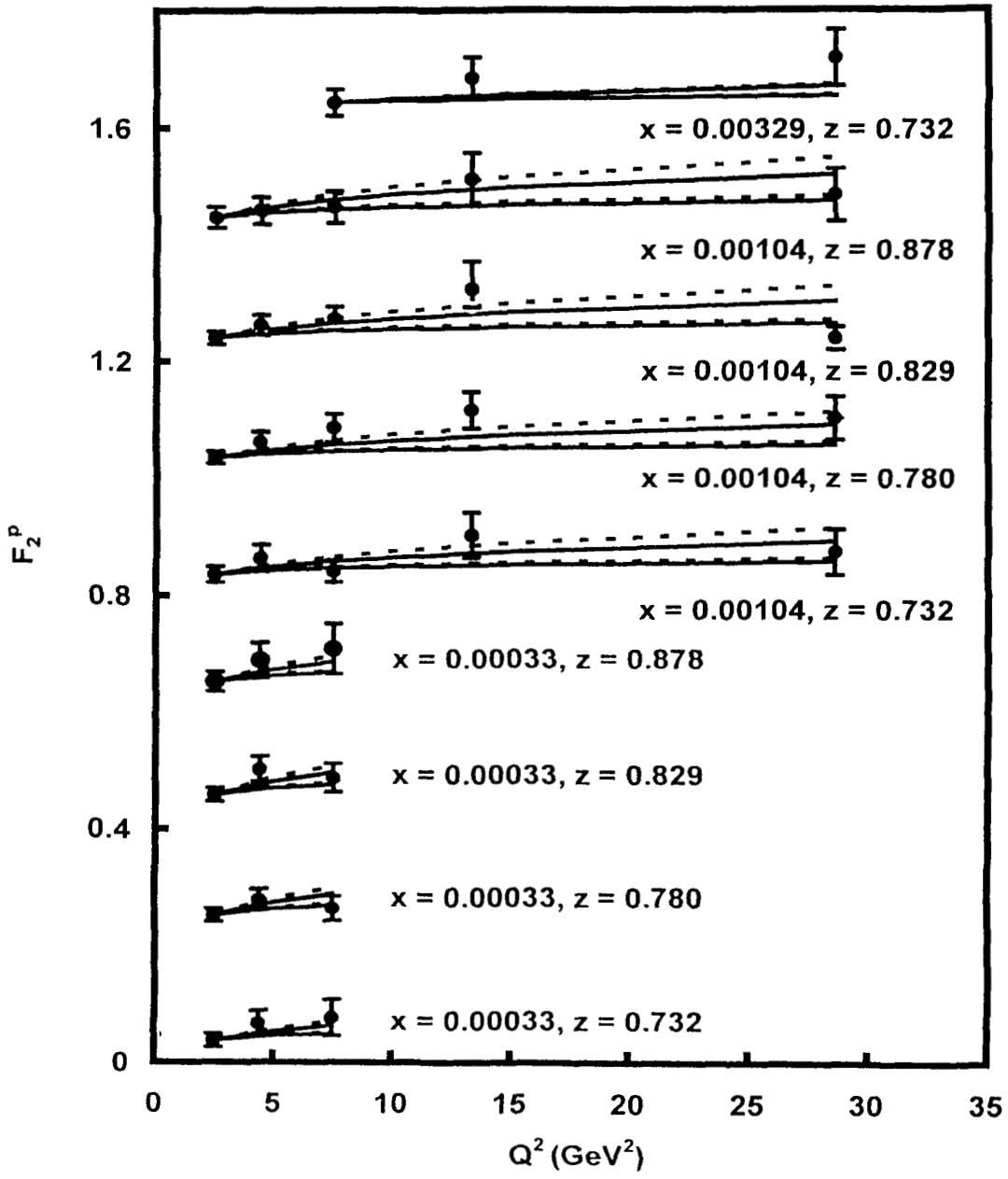

Fig.4.2: t-Evolution of proton structure functions in leading order (dashed lines) and next-to-leading order (solid lines).

structure functions F_2^d (dashed lines) for the particular solutions in LO. Here, upper dashed lines are for $y = 2$ and lower dashed lines for y maximum in the $\beta = \alpha^y$ relation. We observe that t-evolutions are slightly steeper in LO calculations than those of NLO. But NLO results for $y = 2$ are of better agreement with F_2^d experimental data in general.

For convenience, value of each data point is increased by adding $0.2i$, where i = 0, 1, 2, 3... are the numberings of curves counting from the bottom of the lowermost curve as the 0-th order.

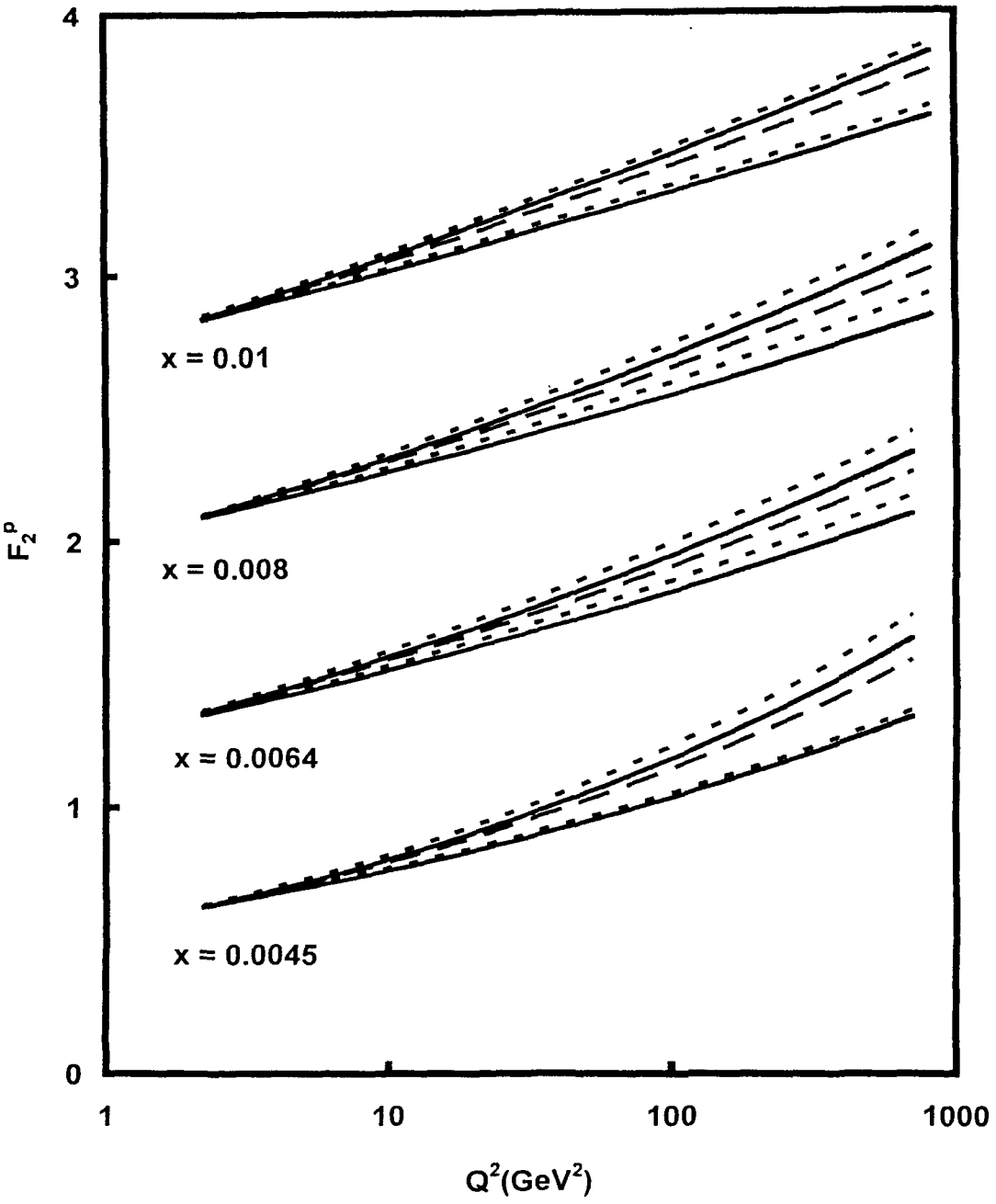

Fig.4.3: t-Evolution of proton structure functions in leading order (dashed lines) and next-to-leading order (solid lines).

In figure 4.2, we present our results of t-evolutions of proton structure functions F_2^p (solid lines) for the representative values of x given in the figure for $y = 2$ (upper solid lines) and y maximum (lower solid lines) in the $\beta = \alpha^y$ relation. Data points at lowest-Q^2 values in the figures are taken as inputs to test the evolution equation. Agreement with the data [94]

is found to be excellent. In the same figure, we also plot the results of t-evolutions of proton structure functions F_2^p (dashed lines) for the particular solutions in leading order. Here, upper dashed lines are for $y = 2$ and lower dashed lines for y maximum in the $\beta = \alpha^y$ relation. We observe that t-evolutions are slightly steeper in LO calculations than those of NLO. But differences in the results are small. For convenience, value of each data point is increased by adding $0.2i$, where i = 0, 1, 2, 3 ... are the numberings of curves counting from the bottom of the lowermost curve as the 0-th order.

In figure 4.3, we compare our results of t-evolutions of proton structure functions F_2^p with a recent global parameterization [96] (long dashed lines) for the representative values of x given in the figures for $y = 2$ (upper solid lines) and y maximum (lower solid lines) in the $\beta = \alpha^y$ relation. Data points at lowest-Q^2 values in the figures are taken as inputs to test the evolution equation. In the same figure, we also plot the results of t-evolutions of proton structure functions F_2^p (dashed lines) for the particular solutions in LO. Here, upper dashed lines are for $y = 2$ and lower dashed lines for y maximum in the $\beta = \alpha^y$ relation. We observe that t-evolutions are slightly steeper in LO calculations than those of NLO. Agreement with the NLO results is found to be better than with the LO results. For convenience, value of each data point is increased by adding $0.5i$, where i = 0, 1, 2, 3 ... are the numberings of curves counting from the bottom of the lowermost curve as the 0-th order.

In figure 4.4, we present our results of t-evolutions of neutron structure functions F_2^n forthe representative values of x given in the figure for $y = 2$ (upper solid lines) and y maximum (lower solid lines) in the $\beta = \alpha^y$ relation. Data points at lowest-Q^2 values in the figures are taken as inputs to test the evolution equation. Agreement with the data [94] is found to be excellent. In the same figure, we also plot the results of t-evolutions of neutron structure functions F_2^n (dashed lines) for the particular solutions in LO. Here, upper dashed lines are for $y = 2$ and lower dashed lines for y maximum in the $\beta = \alpha^y$ relation. We observe that t-evolutions are slightly steeper in LO calculations than those of NLO. But differences in the results are small. For convenience, value of each data point is increased by adding $0.2i$, where i = 0, 1, 2, 3 ... are the numberings of curves counting from the bottom of the lowermost curve as the 0-th order.

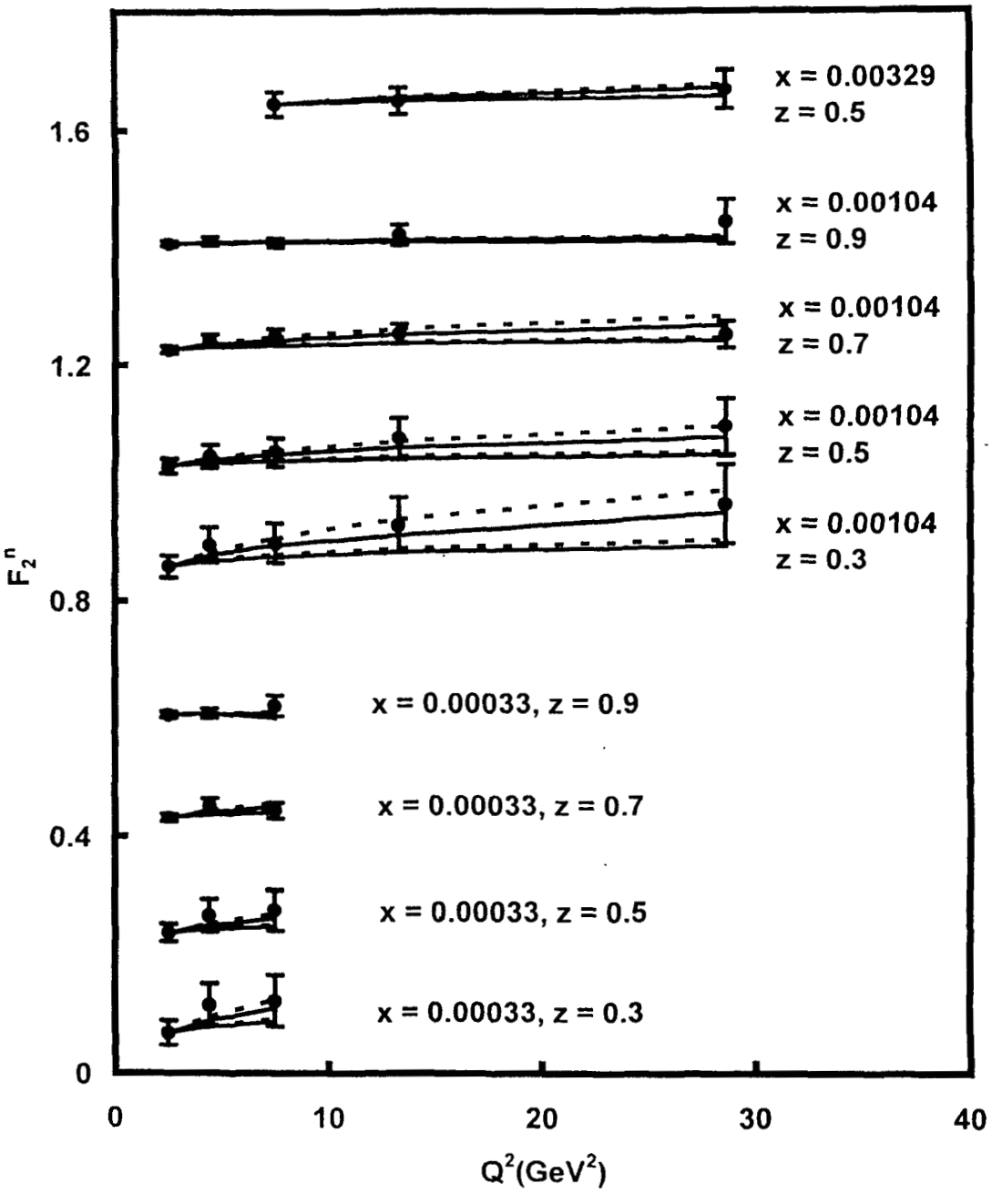

Fig.4.4: t-Evolution of neutron structure functions in leading order (dashed lines) and next-to-leading order (solid lines).

In figure 4.5, we present our results of t-evolutions of difference of proton and neutron structure functions $F_2^p - F_2^n$ which is a non-singlet combination, for the representative values of x given in the figures for $y = 2$ (upper solid lines) and y maximum (lower solid lines) in the $\beta = \alpha^y$ relation. Data points at lowest-Q^2 values in the figures are taken as inputs to test the evolution equation. Agreement with the data [94] is found to be excellent. In the same figure, we also plot the results of t-evolutions of difference of proton and neutron structure functions $F_2^p - F_2^n$ (dashed lines) for the particular solutions

in LO. Here, upper dashed lines for $y = 2$ and lower dashed lines for y maximum in the $\beta = \alpha^y$ relation. We observe that t-evolutions are slightly steeper in LO calculations than

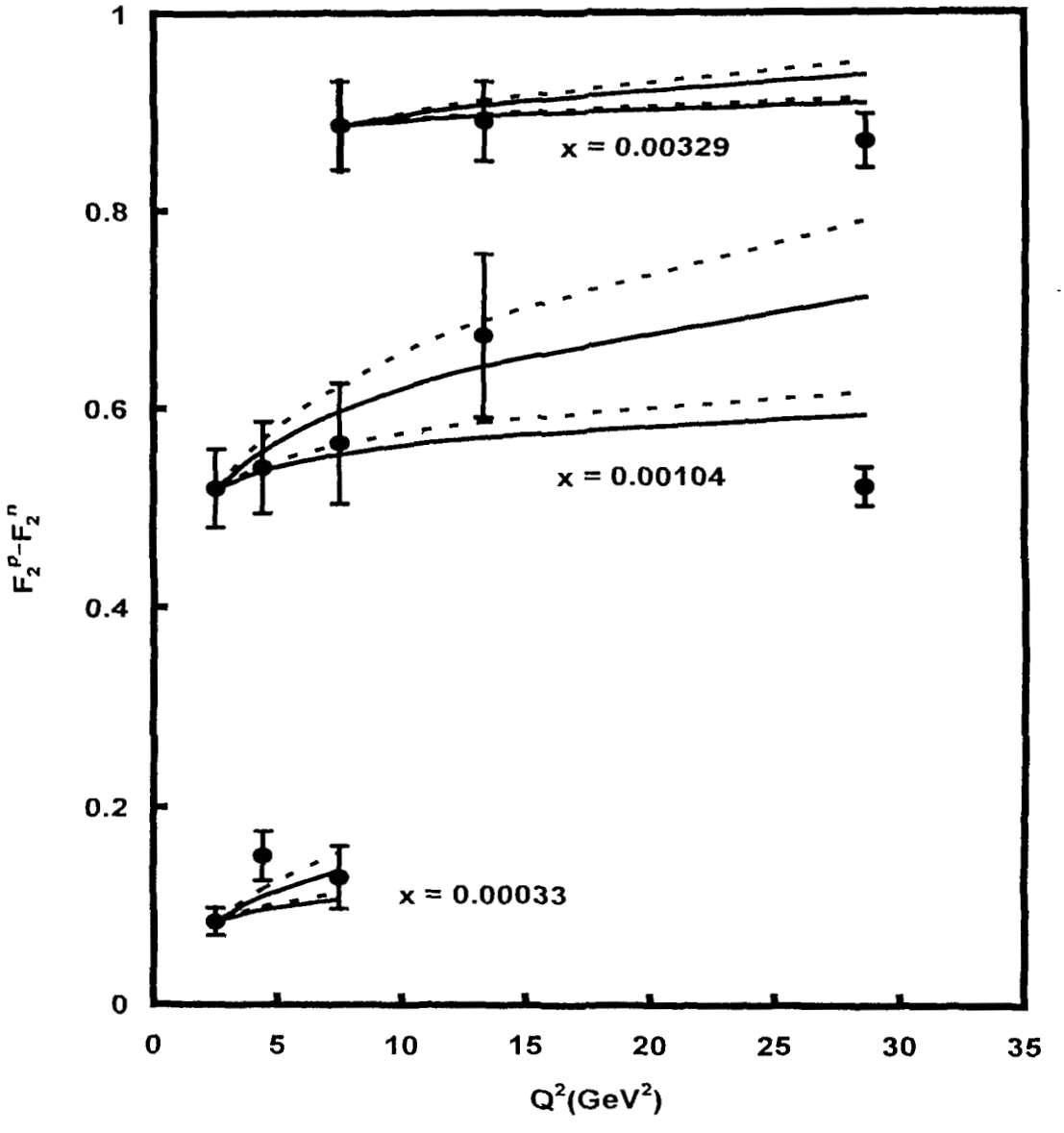

Fig.4.5: t-Evolution of difference of proton and neutron structure functions in leading order (dashed lines) and next-to-leading order (solid lines).

those of NLO. For convenience, value of each data point is increased by adding $0.4i$, where $i = 0, 1, 2, 3 \ldots$ are the numberings of curves counting from the bottom of the lowermost curve as the 0-th order.

In figure 4.6, we present our results of t-evolutions of ratio of proton and neutron structure functions F_2^p/F_2^n (solid lines) for the representative values of x given in the

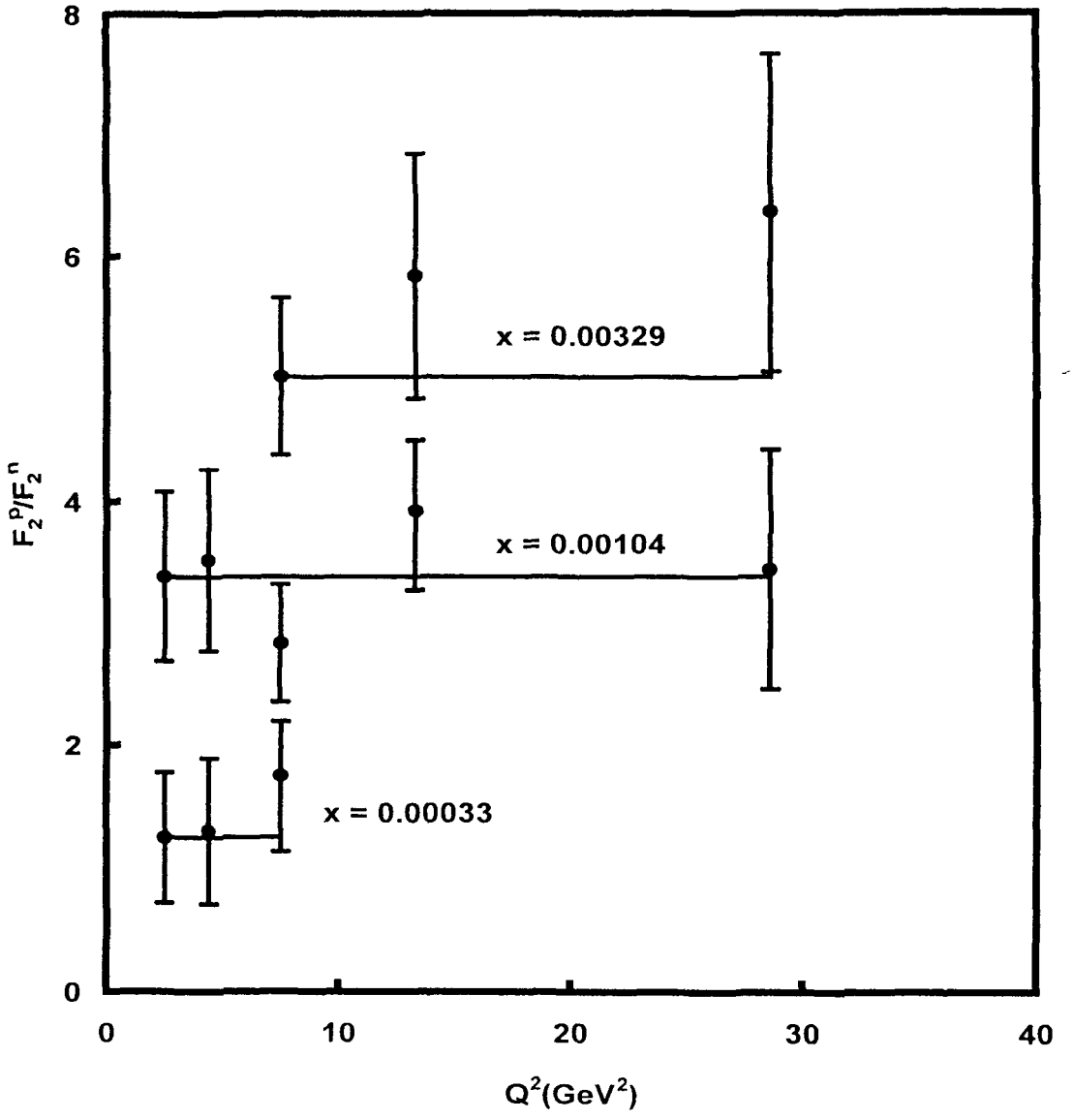

Fig.4.6: t-Evolution of ratio of proton and neutron structure functions in next-to-leading order.

figures. Though according to our theory the ratio should be independent of t, due to the lack of sufficient amount of data and due to large error bars, a clear cut conclusion can not be drawn.

Though we compare our results which $y = 2$ and y maximum in the $\beta = \alpha^y$ relation with data, agreement of the result with experimental data is found to be excellent with $y = 2$ for t- evolution in NLO.

For a quantitative analysis of x-distributions of structure functions, we calculate the integrals that occurred in equation (4.29) using Simpson's one- third rule for $N_f = 4$. In this case, we neglect first and second terms of the function $B_1(x)$ as x is small. In figure

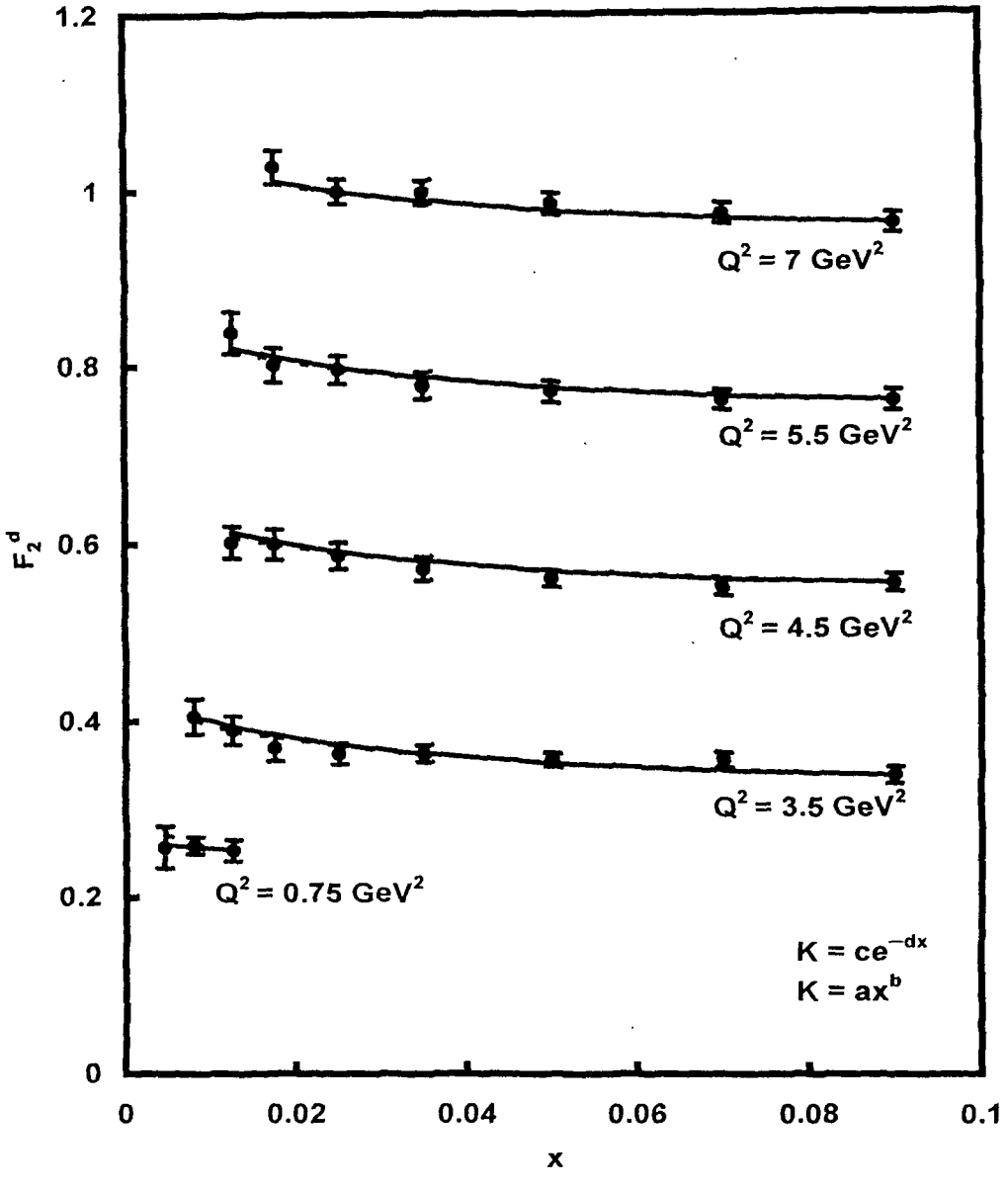

Fig.4.7: x-Evolution of deuteron structure functions in next-to-leading order for $K(x) = ax^b$ (dashed lines) and $K(x) = ce^{-dx}$ (solid lines).

4.7, we present our results of x-distribution of deuteron structure functions F_2^d for $K(x) = ax^b$ (dashed lines) and for $K(x) = ce^{-dx}$ (solid lines) in the relation $\beta = \alpha^y$ for y minimum (= 2), where a, b, c and d are constants and for representative values of Q^2 given in each figure, and compare them with NMC deuteron low-x low-Q^2 data [95]. Each data point for x-value just below 0.1 has been taken as input $F_2^d(x_0, t)$. If we take $K(x) = ax^b$ in

equation (4.29), then agreement of the result with experimental data is found to be excellent at $a = 10$, $b = 0.016$. On the other hand, if we take $K(x) = ce^{-dx}$ then agreement of the results with experimental data is found to be good at $c = 0.5$, $d = -3.8$. In this connection, earlier we observed [110] that agreement of the results with experimental data

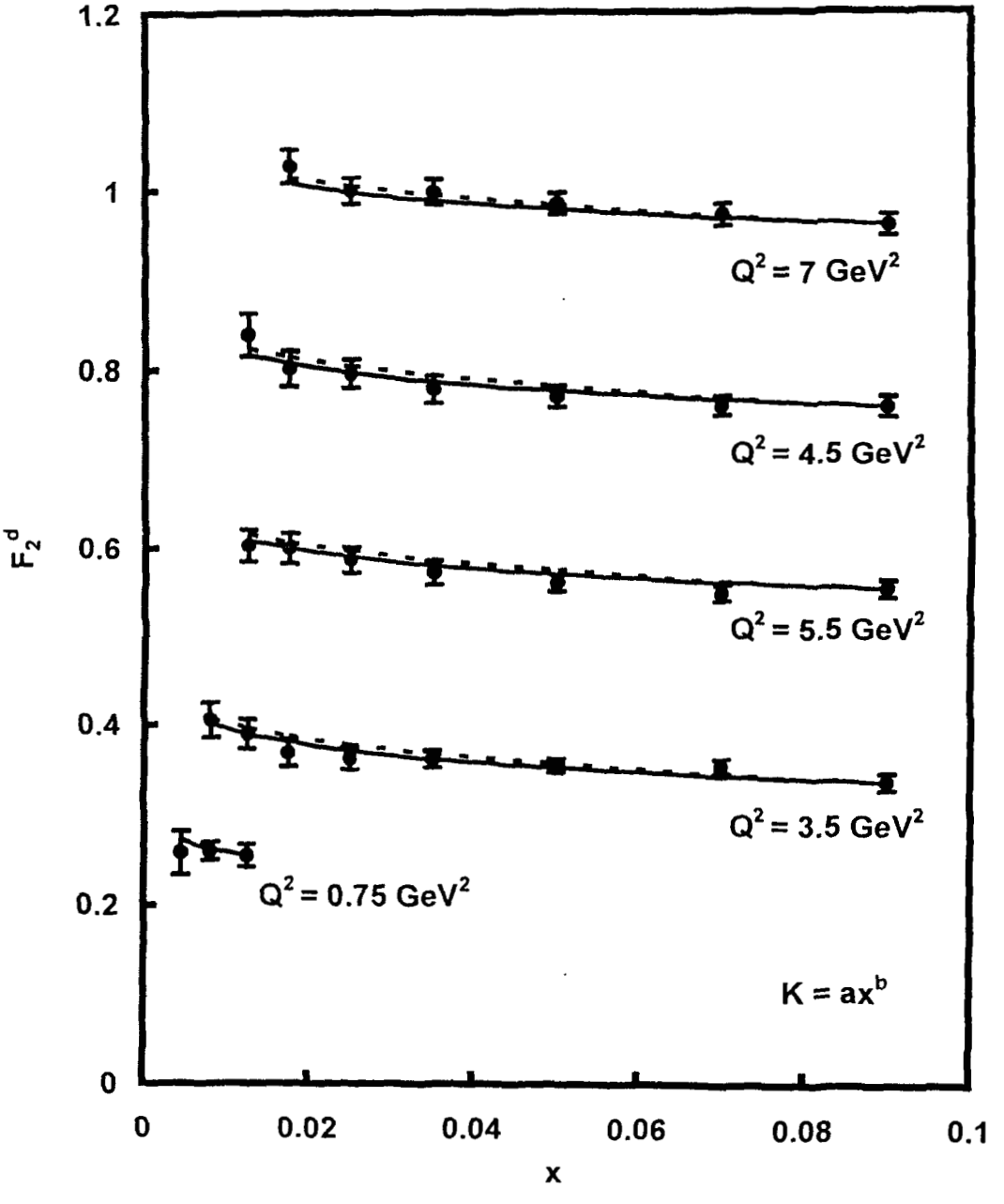

Fig.4.8: x-Evolution of deuteron structure function for $K(x) = ax^b$ in the relation $\beta=\alpha\gamma$, for y minimum (solid lines) and maximum (dashed lines).

is found to be excellent for $K(x) = 4.5$ (constant), $a = 4.5$, $b = 0.01$, $c = 5$, $d = 1$ for low-x in LO. But in the case of NLO, agreement of the results with experimental data is found to be very poor for any constant value of $K(x)$. Therefore we do not present our result of

x-distribution at $K(x)$ = constant in NLO. For convenience, value of each data point is increased by adding $0.2i$, where i = 0, 1, 2, 3 ... are the numberings of curves counting from the bottom of the lowermost curve as the 0-th order.

In figure 4.8, we compare our results of x-evolution of deuteron structure function for $K(x) = ax^b$ in the relation $\beta = \alpha^y$, for y = 2 (solid lines) and maximum (dashed lines) at

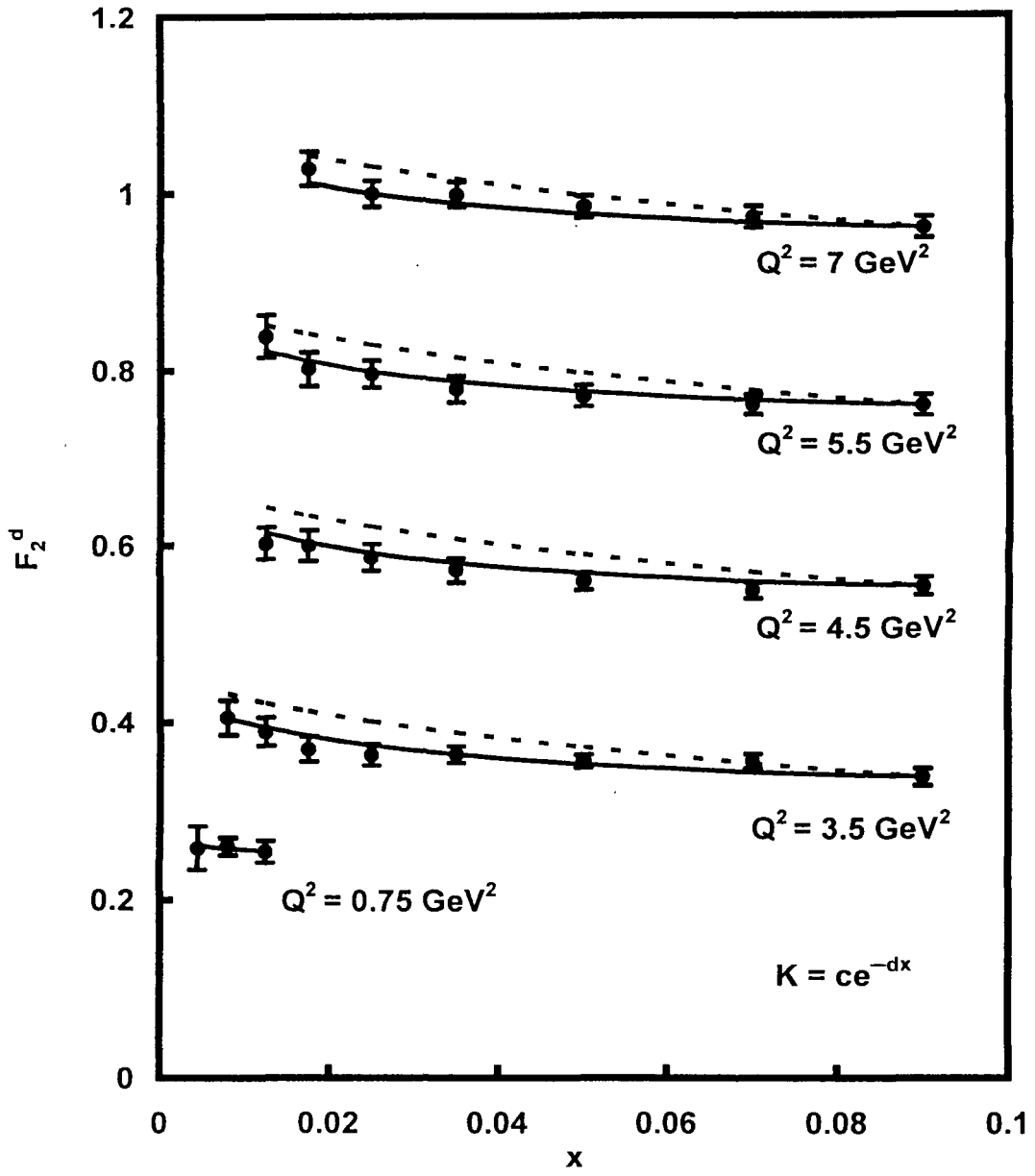

Fig.4.9: x-Evolution of deuteron structure function for $K(x) = ce^{-dx}$ in the relation $\beta=\alpha^y$, for y minimum (solid lines) and maximum (dashed lines).

same parameter values, a = 10, b = 0.016 and for representative values of Q^2 given in each figure, and compare them with NMC deuteron low-x low-Q^2 data [95]. Each data

point for x-value just below 0.1 has been taken as input $F_2^d(x_0, t)$. We observe that difference between the lines is very small. In this connection, earlier we observed that there is no any significant difference between the lines in LO [110]. For convenience, value of each data point is increased by adding $0.2i$, where i = 0, 1, 2, 3 ... are the numberings of curves counting from the bottom of the lowermost curve as the 0-th order.

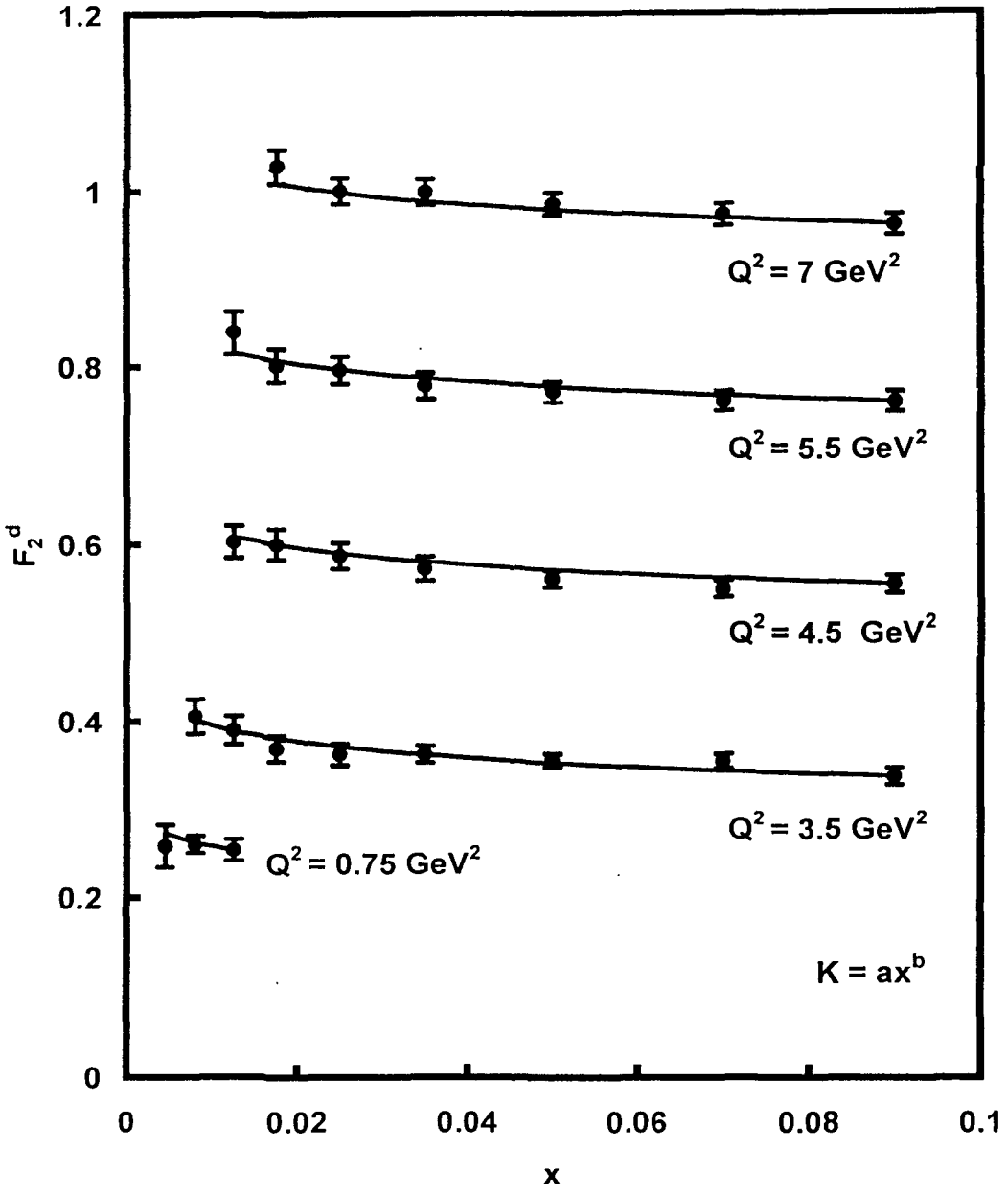

Fig.4.10: x-Evolution of deuteron structure function for $K(x) = ax^b$ in the relation $\beta=\alpha^y$, for y = 2 (solid lines) and maximum (dashed lines).

In figure 4.9, we compare our results of x-evolution of deuteron structure function for $K(x) = ce^{-dx}$ in the relation $\beta = \alpha^y$, for $y = 2$ (solid lines) and maximum (dashed lines) at same parameter values, $c = 0.5$, $d = -3.8$ and for representative values of Q^2 given in

each figure, and compare them with NMC deuteron low-x low- Q^2 data [95]. Each data point for x-value just below 0.1 has been taken as input $F_2^d(x_0, t)$. We observe that difference between the lines is small. In this connection, earlier we observed that there is no any significant difference between the lines in LO [110]. For convenience, value of each data point is increased by adding $0.2i$, where $i = 0, 1, 2, 3$ ... are the numberings of curves counting from the bottom of the lowermost curve as the 0-th order.

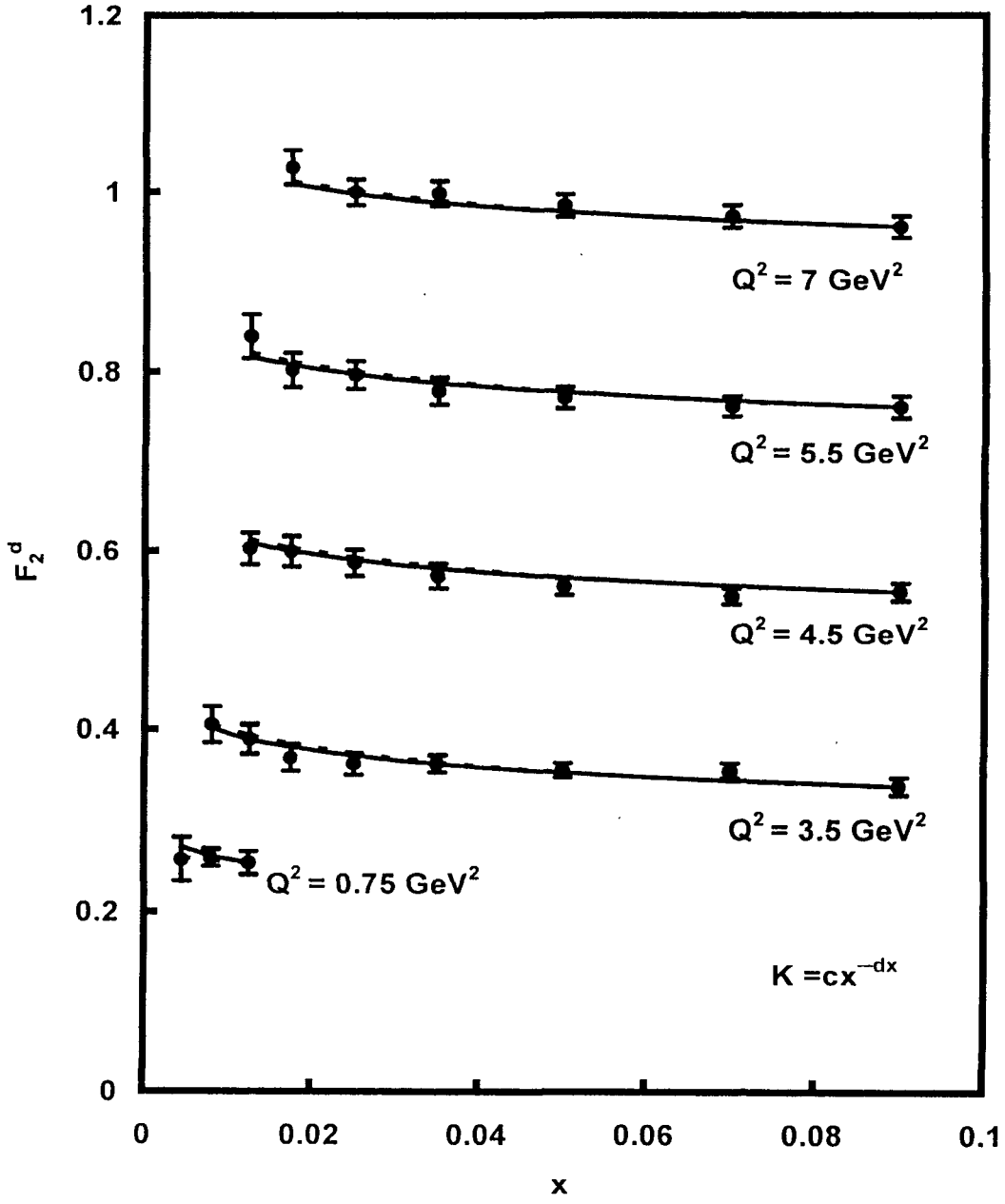

Fig.4.11: x-Evolution of deuteron structure function for $K(x) = cx^{-dx}$ in relation $\beta = \alpha^y$, for y = 2 (solid lines) and maximum (dashed lines).

In figure 4.10 and figure 4.11, we present our results of x-evolution of deuteron structure function for $K(x) = ax^b$ and $K(x) = ce^{-dx}$ in the relation $\beta = \alpha^y$, for $y = 2$ (solid lines) and

maximum (dashed lines) at different parameter values and for representative values of Q^2 given in each figure, and compare them with NMC deuteron low-x low-Q^2 data [95]. Each data point for x-value just below 0.1 has been taken as input $F_2^d(x_0, t)$. We observe that result of x-evolution of deuteron structure function in relation $\beta = \alpha^y$, for y maximum (dashed lines) coincide with result of x-evolution of deuteron structure function for $y = 2$ (solid lines) when $a = 5.5$, $b = 0.016$ and $c = 0.28$, $d = -3.8$. That means if y varies from

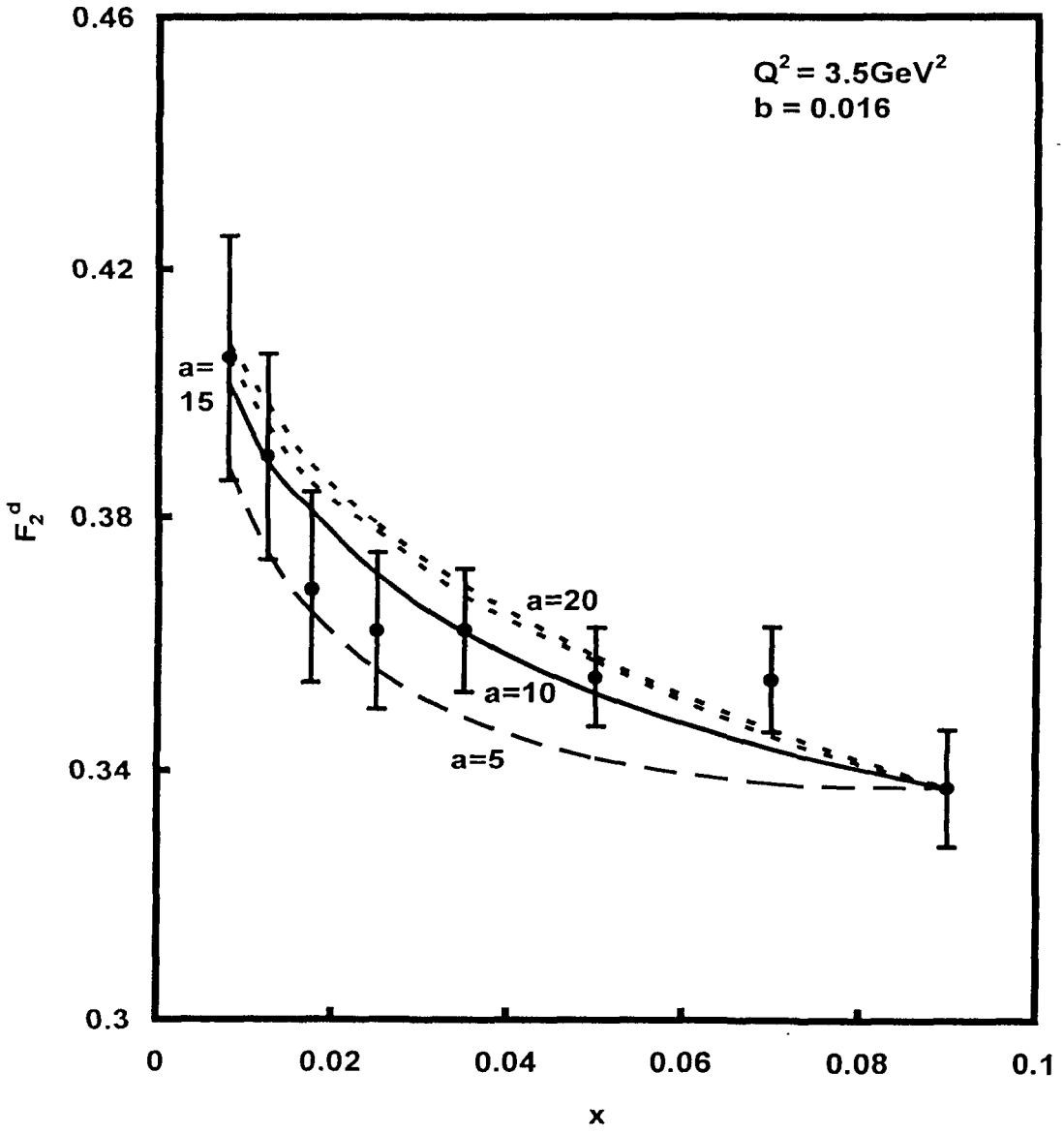

Fig.4.12: Sensitivity of our results in the relation $\beta=\alpha^y$ for y = 2 for different values of 'a' at fixed value of b = 0.016.

minimum to maximum, then value of parameter 'a' varies from 10 to 5.5 and 'c' varies from 0.5 to 0.28. In this case, values of parameters 'b' and 'd' remain constant. For convenience, value of each data point is increased by adding $0.2i$, where $i = 0, 1, 2, 3 \ldots$ are the numberings of curves counting from the bottom of the lowermost curve as the 0-th

order.

In figure 4.12, we present the sensitivity of our results for different values of '*a*' at fixed value of '*b*' in the relation $\beta = \alpha^{y}$, for y =2. Here we take b = 0.016. We observe that at a

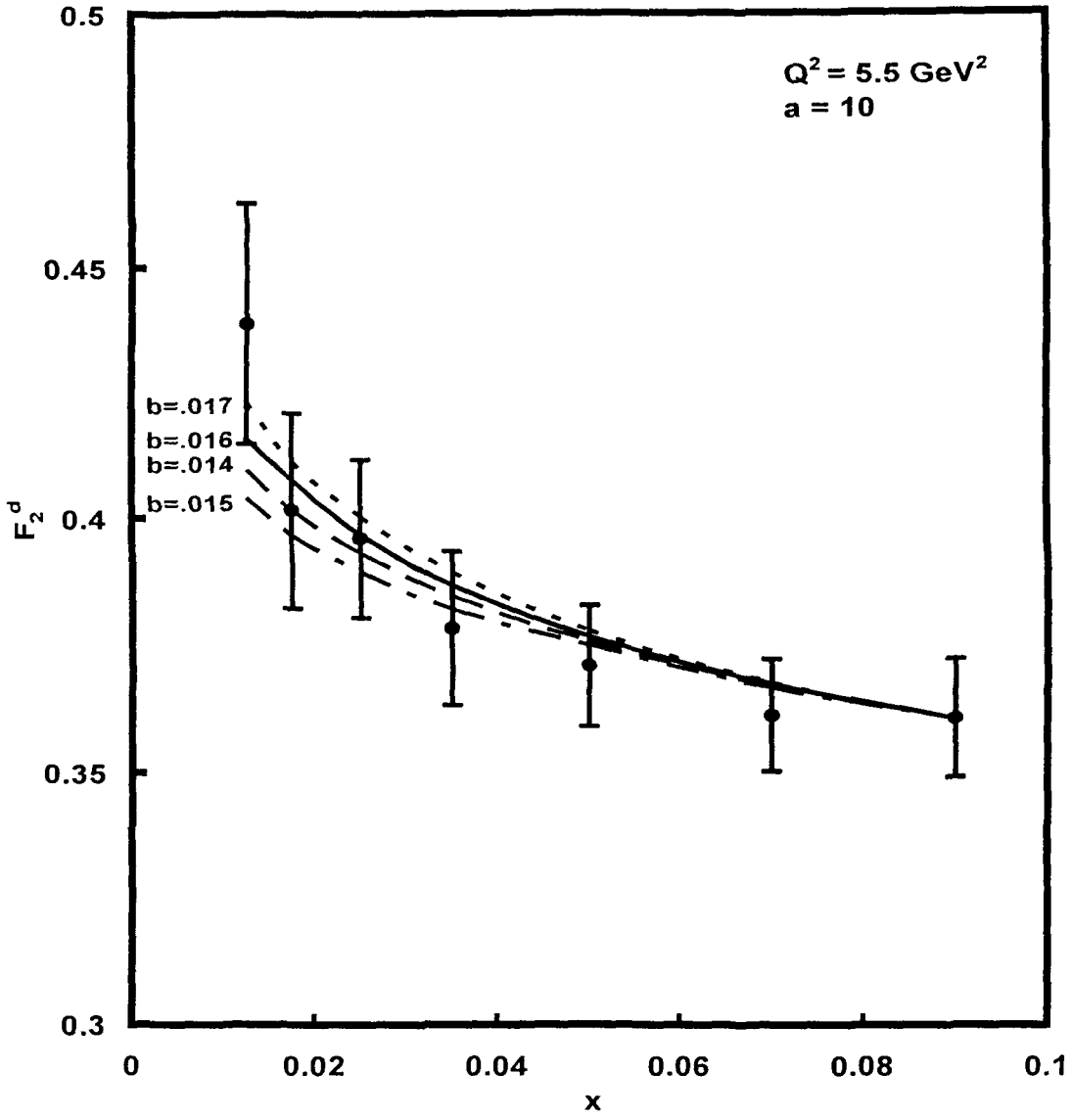

Fig.4.13: Sensitivity of our results in the relation $\beta=\alpha^{y}$ for y = 2 for different values of 'b' at fixed value of a = 10.

= 10, agreement of the results with experimental data is found to be excellent. If value of 'a' is increased, the curve goes upward direction and if value of '*a*' is decreased, the curve goes downward direction. Though the nature of the curve is similar, curvature of the curves is decreased and difference of the curves is small when value of '*a*' is increased.

In figure 4.13, we present the sensitivity of our results for different values of '*b*' at fixed value of '*a*' in the relation $\beta = \alpha^y$, for $y = 2$. Here we take $a = 10$. We observe that at $b = 0.016$, agreement of the results with experimental data is found to be excellent. If value of '*b*' is increased the curve goes upward direction and if value of '*b*' is decreased, the curve goes downward direction. But the nature of the curves is similar and difference of the curves is small.

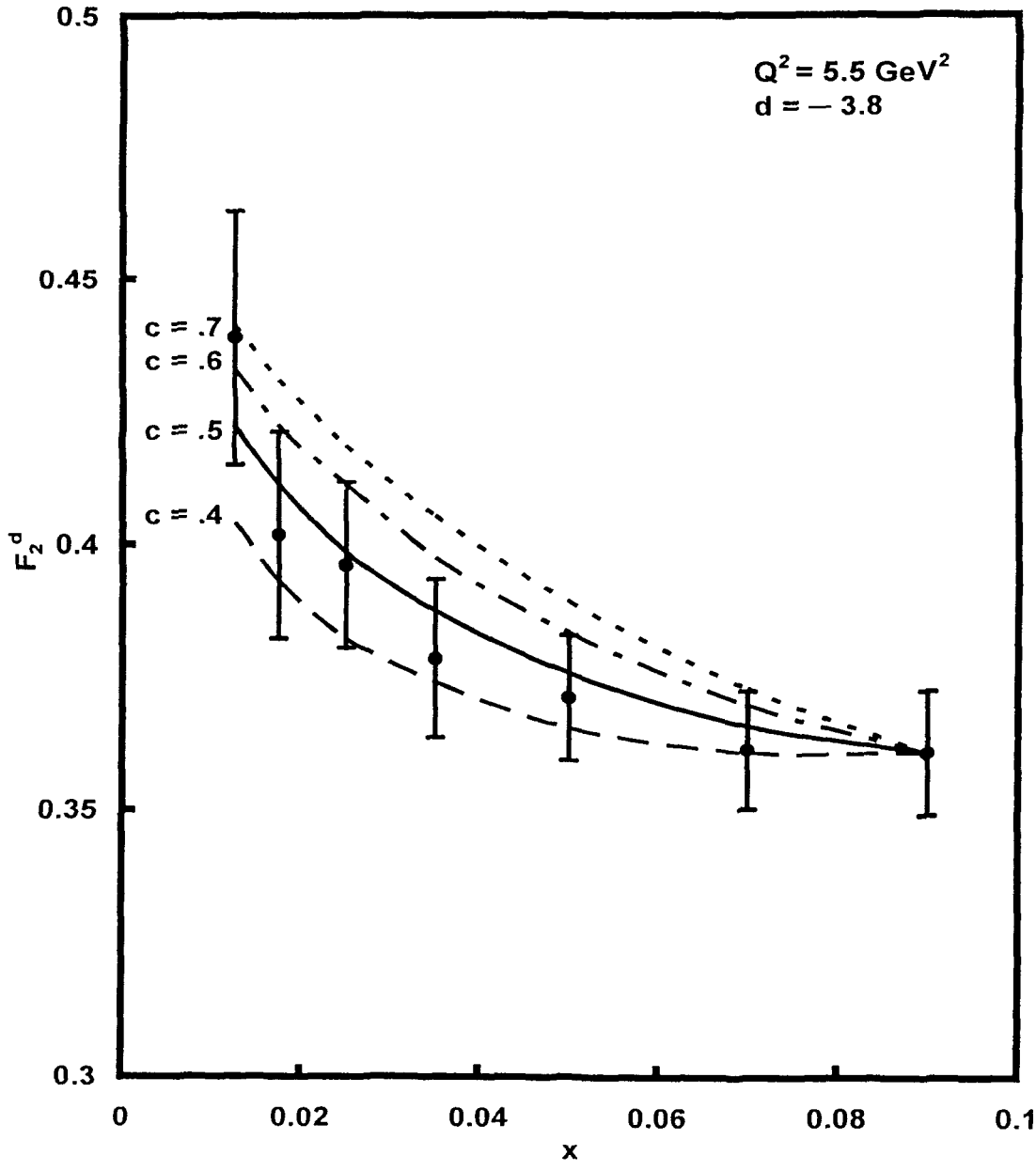

Fig.4.14: Sensitivity of our results in the relation $\beta=\alpha^y$ for y = 2 for different values of 'c' at fixed value of d = — 3.8.

In figure 4.14, we present the sensitivity of our results for different values of '*c*' at fixed value of '*d*' in the relation $\beta = \alpha^y$, for $y = 2$. Here we take $d = -3.8$. We observe that at $c =$

0.5, agreement of the results with experimental data is found to be excellent. If value of 'c' is increased, the curve goes upward direction and if value of 'c' is decreased, the curve goes downward direction. Though the nature of the curves is similar, curvature and difference of the curves are decreased when value of 'c' is increased.

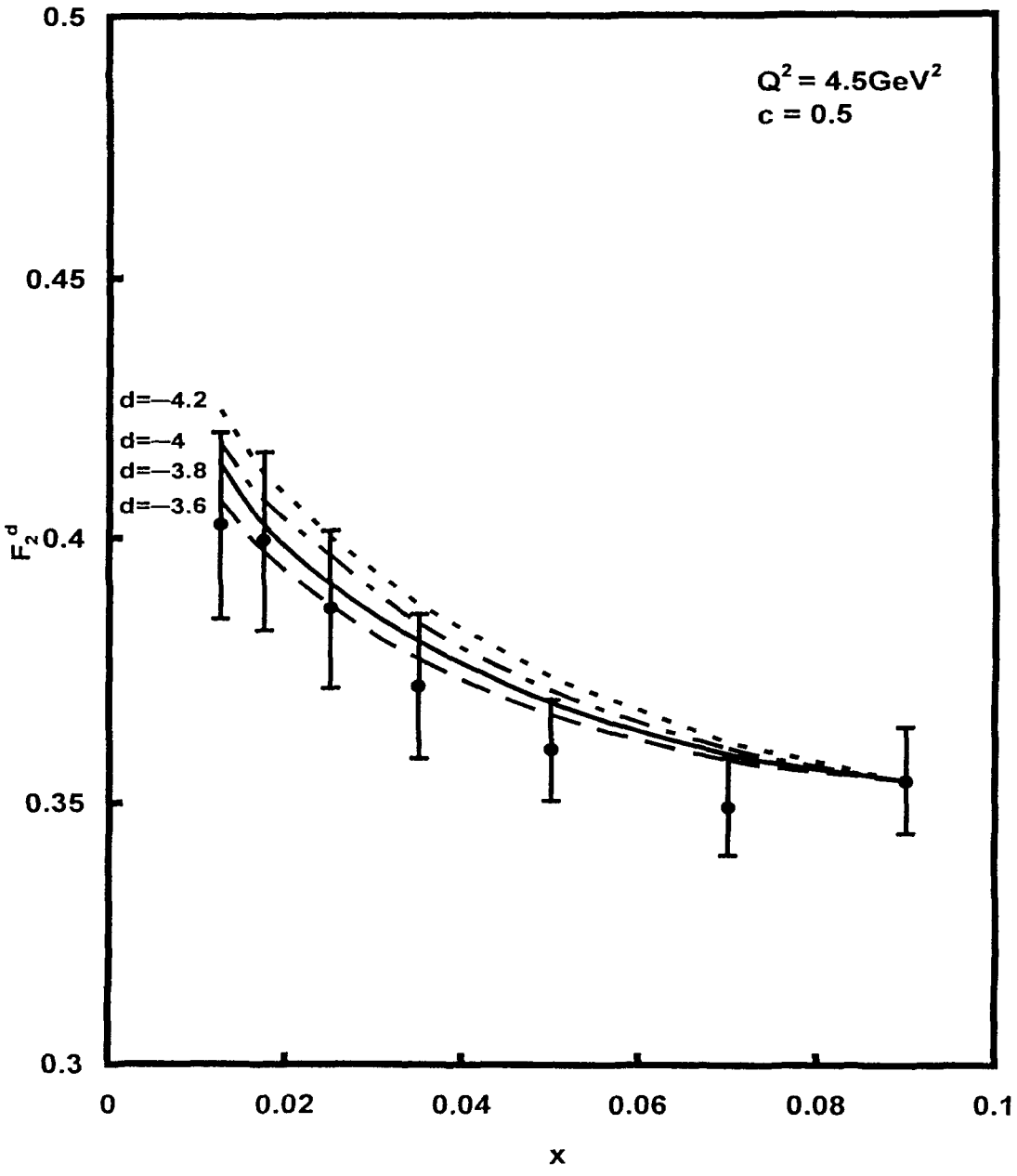

Fig.4.15: Sensitivity of our results in the relation $\beta=\alpha^y$ for y = 2 for different values of 'd' at fixed value of c = 0.5.

In figure 4.15, we present the sensitivity of our results for different values of 'd' at fixed value of 'c' in the relation $\beta = \alpha^y$, for $y = 2$. Here we take $c = 0.5$. We observe that at $d = -3.8$, agreement of the results with experimental data is found to be excellent. If value of

'd' is increased, the curve goes downward direction and if value of '*d*' is decreased, the curve goes upward direction. But the nature of the curves is similar and difference of the curves is small.

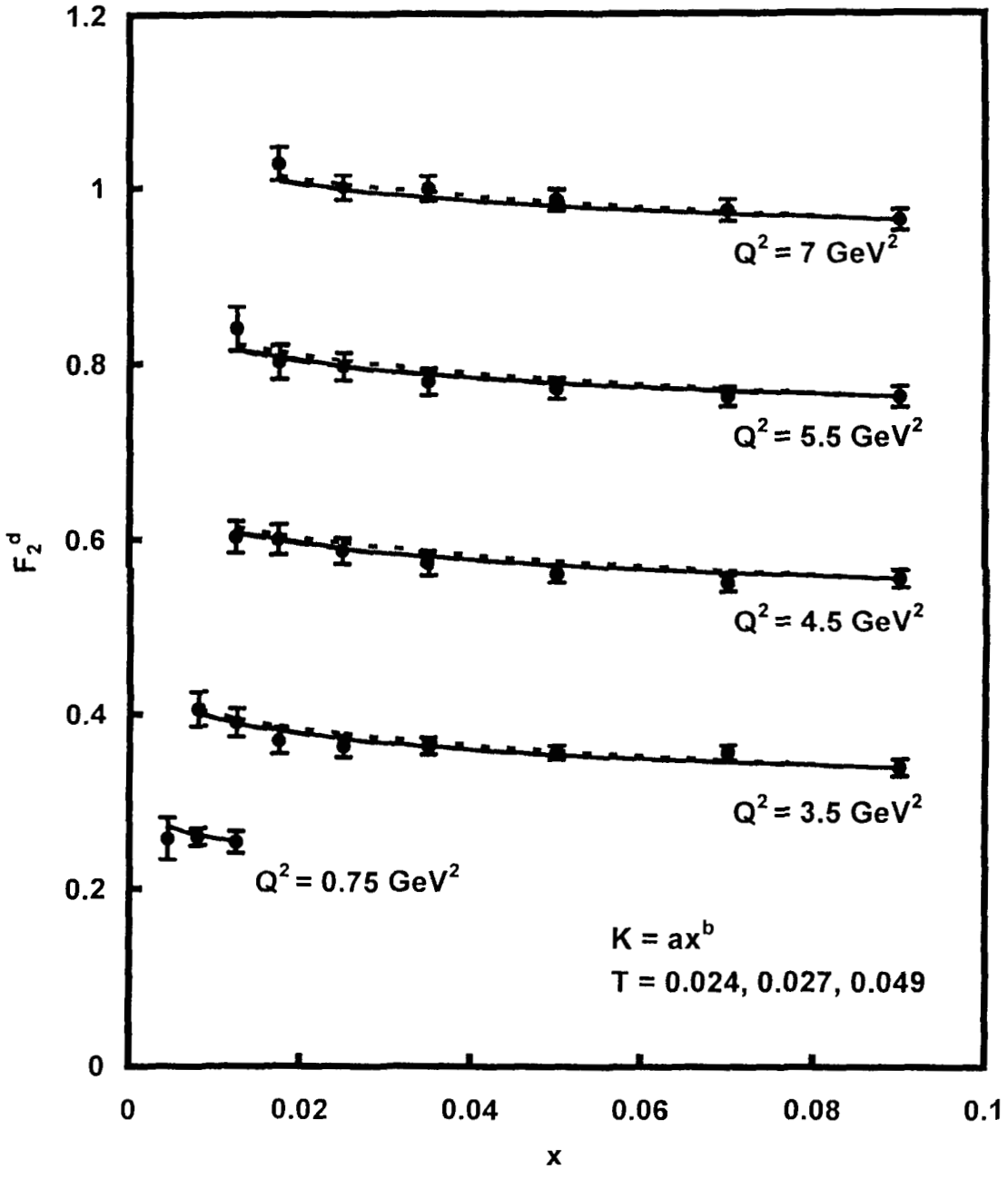

Fig.4.16: Sensitivity of our results of x-distribution of deuteron structure function for different values of T_0 at best fit of $K(x) = ax^b$ in the relation $\beta=\alpha^y$ for y = 2.

In figure 4.16 and figure 4.17, we present the sensitivity of our results for $T_0 = 0.024$ ($Q^2 = 50$ GeV^2), $T_0 = 0.027$ ($Q^2 = 15$ GeV^2) and $T_0 = 0.049$ ($Q^2 = 0.5$ GeV^2) at best fit of $K(x) = ax^b$ and $K(x) = ce^{-dx}$ in the relation $\beta = \alpha^y$, for $y = 2$. Here $a = 10$, $b = 0.016$, $c = 0.5$, $d = -3.8$. We observe that if the value of T_0 is increased, the curved goes slightly upward

direction and if the value of T_0 is decreased, the curve goes slightly downward direction. But the nature of the curves is similar and difference of curves is extremely small in both cases.

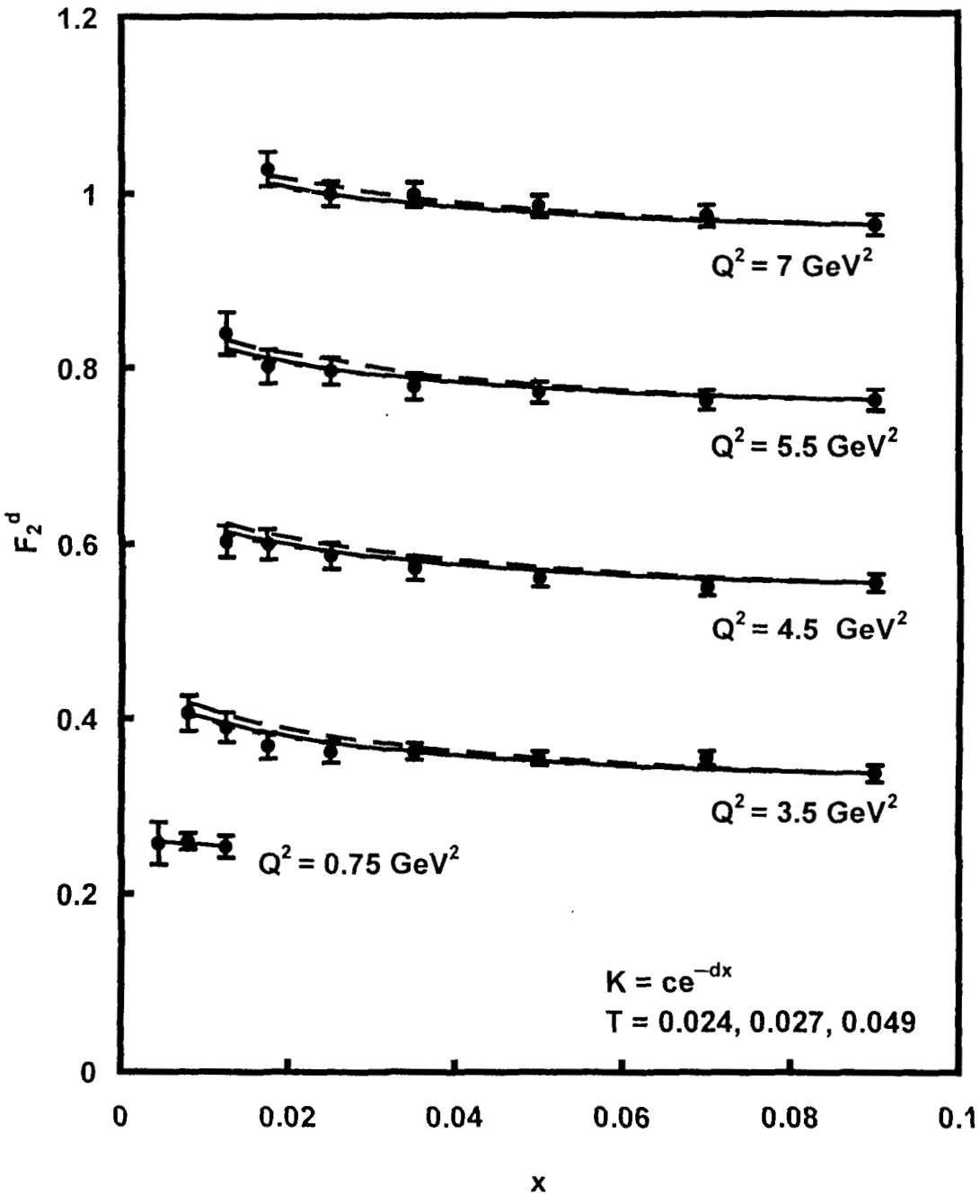

Fig.4.17: Sensitivity of our results of x-distribution of deuteron structure function for different values of T_0 at best fit of $K(x) = cx^{-dx}$ in the relation $\beta = \alpha^y$ for y = 2.

In figure 4.18 and figure 4.19, we present the results of x-evolution of deuteron structure function in the relation $\beta = \alpha^y$, for $y = 2$ in LO and NLO for $K(x) = ax^b$ and $K(x) = ce^{-dx}$ respectively for representative values of Q^2 given in each figure, and compare them with

NMC deuteron low-x low-Q^2 data [95]. Each data point for x-value just below 0.1 has been taken as input $F_2^d(x_0, t)$. We have already discussed that agreement of the result

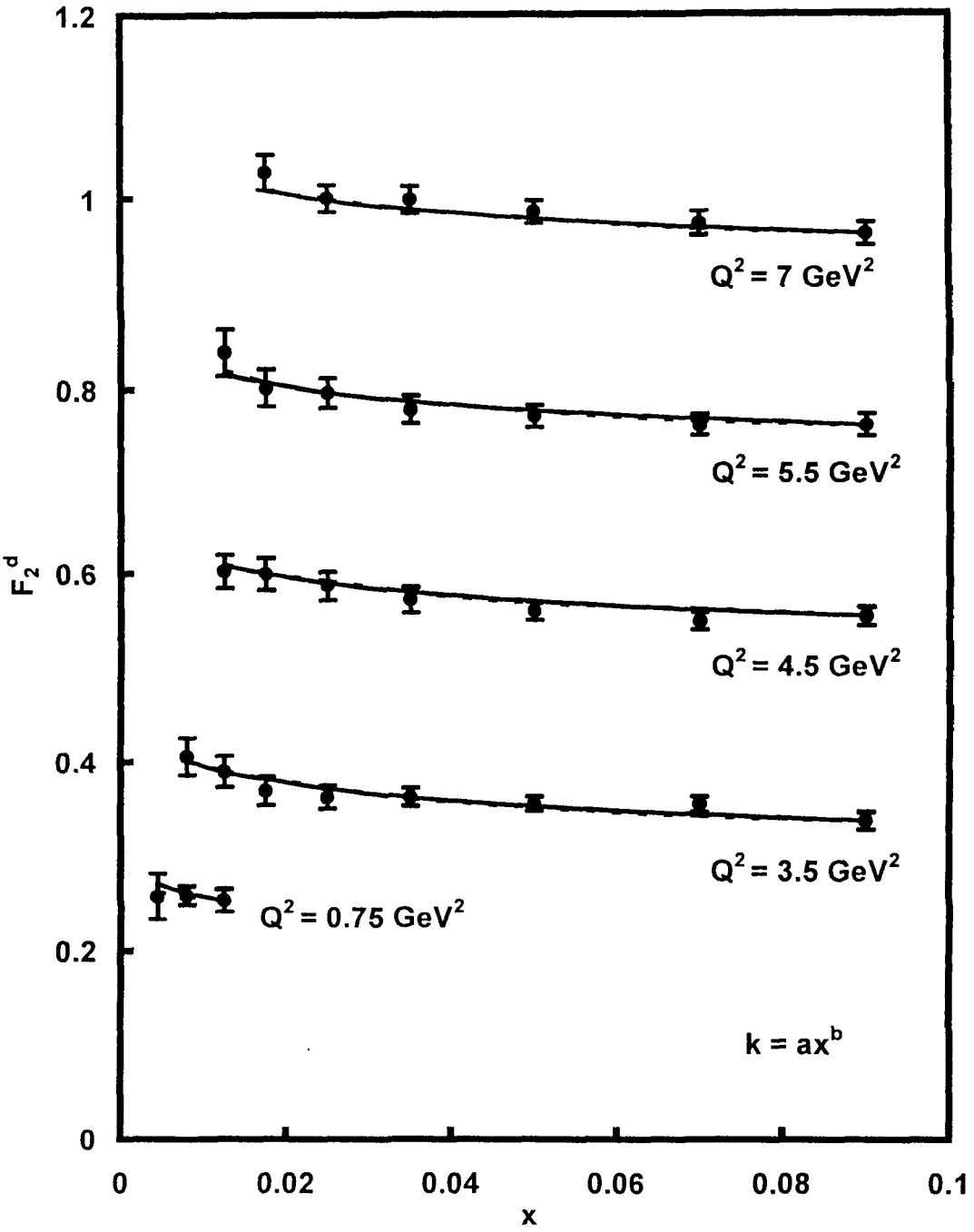

Fig.4.18: x-Distribution of deuteron structure functions for $K(x) = ax^b$ in the relation $\beta=\alpha^y$ for $y = 2$ in next-to-leading order (solid lines) and leading order (dotted lines).

with experimental data is found to be excellent for $a = 4.5$, $b \doteq 0.01$, $c = 5$, $d = 1$ in LO and $a = 10$, $b = 0.016$, $c = 0.5$, $d = -3.8$ in NLO. For convenience, value of each data

point is increased by adding $0.2i$, where i = 0, 1, 2, 3, ... are the numberings of curves counting from the bottom of the lowermost curve as the 0-th order.

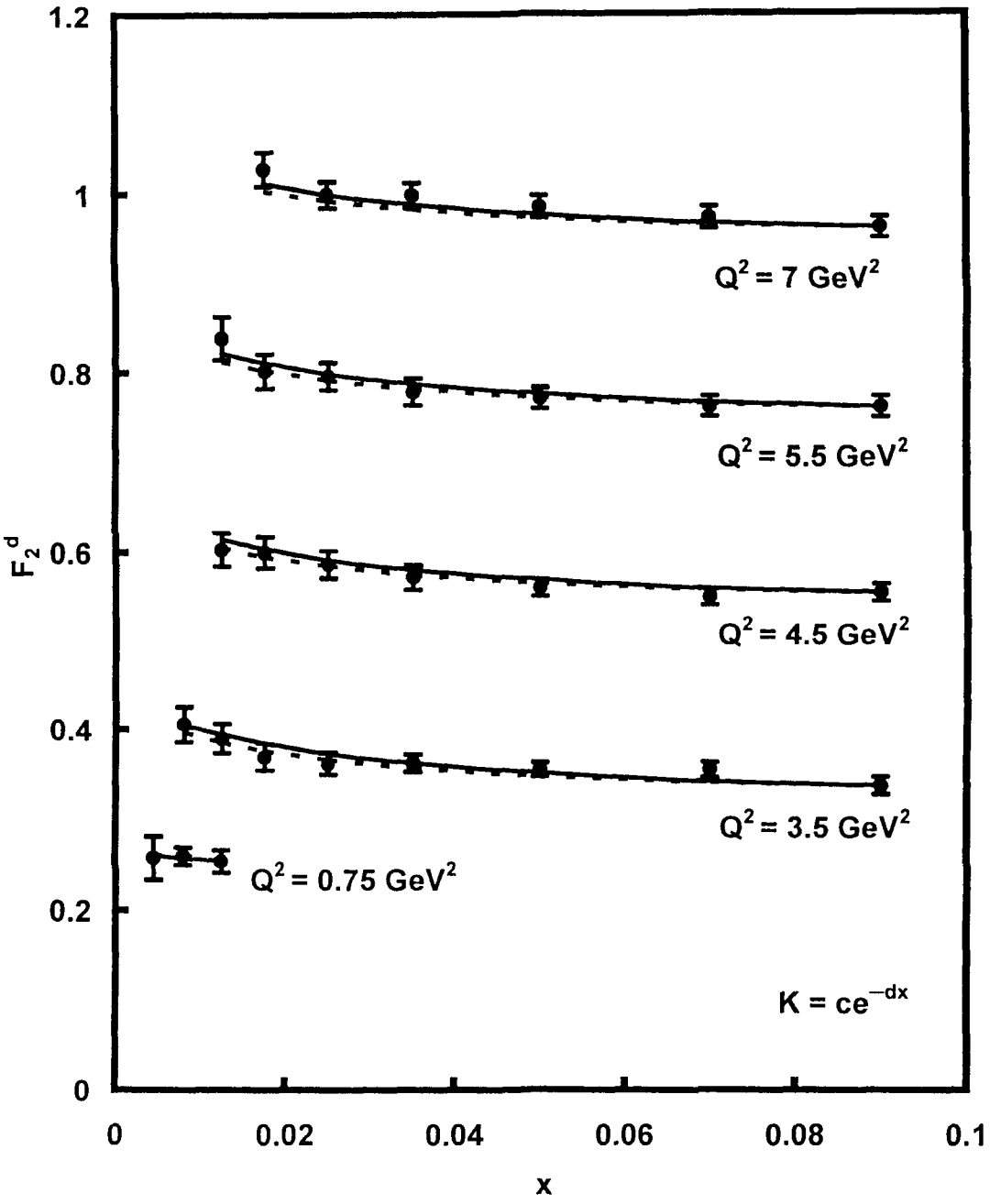

Fig.4.19: x-Distribution of deuteron structure functions K(x) = ce^{-dx} in the relation β=α^γ for y = 2 in next-to-leading order (solid lines) and leading order (dotted lines).

In figure 4.20, we plot $T(t)^2$ (solid line) and $T_0T(t)$ (dashed line), where $T(t) = \alpha_s / 2\pi$ against Q^2 in the Q^2-range $0 \leq Q^2 \leq 50$ GeV^2. We observe that for $T_0 = 0.027$, error becomes minimum in the Q^2-range $0 \leq Q^2 \leq 50$ GeV^2.

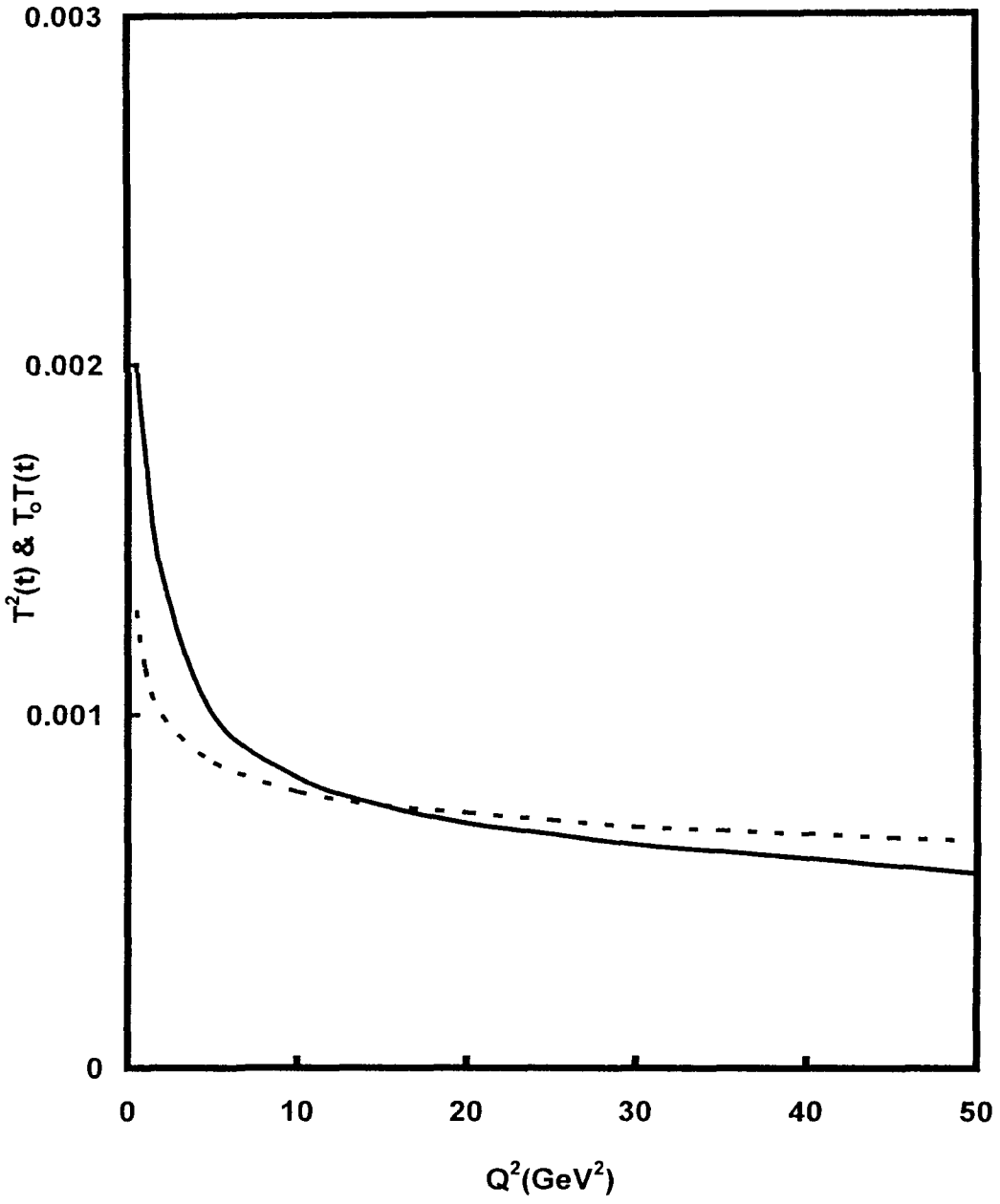

Fig.4.20: $T(t)^2$ (solid line) and $T_0T(t)$ (dotted line), where $T(t) = \alpha_s(t)/2\pi$ against Q^2 in the Q^2-range $0<Q^2<50$ GeV^2.

4.3. Conclusion

In this chapter, we obtain complete and particular solutions of singlet and non-singlet structure functions at low-x using Taylor's expansion method from GLDAP evolution equations and t and x-evolution of singlet and non-singlet structure functions in NLO and hence t-evolutions of deuteron, proton, neutron, and difference and ratio of proton and neutron structure functions and x-evolutions of deuteron structure functions in NLO.

These evolutions are non-unique. We compare our results with HERA and NMC low-x low-Q^2 data, and also compare our results with those of LO results. In all the results from experimental as well as global fits, it is seen that deuteron structure functions increases when x decreases and Q^2 increases for fixed values of Q^2 and x respectively, and proton, neutron, difference and ratio of proton and neutron structure functions increases when Q^2 increases for fixed value of x. It is clear from the figures that the NLO results of t-evolutions for $y = 2$ in the relation $\beta = \alpha^y$, are of better agreement with experimental data in general.□

Chapter-5

UNIQUE SOLUTIONS OF GLDAP EVOLUTION EQUATIONS IN LEADING AND NEXT-TO-LEADING ORDERS

In previous chapters, particular solutions of the Gribov-Lipatov-Dokshitzer-Altarelli-Parisi (GLDAP) evolution equations [29-32] for t and x-evolutions of singlet and non-singlet structure functions in leading order (LO) and next-to-leading order (NLO) at low-x have been presented. These are non unique solutions. In this chapter we report unique solutions of GLDAP evolution equations computed from complete solutions in LO and NLO at low-x and calculation of t and x-evolutions for singlet and non-singlet structure functions, and hence t-evolution of deuteron, proton, neutron, difference and ratio of proton and neutron structure functions and x-evolution of deuteron structure functions. These results are compared with NMC [95], HERA [94] low-x low Q^2 data and also compare our results of t-evolution of proton structure functions with a recent global parameterization [96].

5.1. Theory

The GLDAP evolution equations with splitting functions [103-105] for singlet and non-singlet structure functions are in the standard forms [89, 106-110]

$$\frac{\partial F_2^S(x,t)}{\partial t} - \frac{\alpha_{s1}(t)}{2\pi}\left[\frac{2}{3}\{3+4\ln(1-x)\}F_2^S(x,t)+\frac{4}{3}\int_x^1\frac{dw}{1-w}\left\{\left(1+w^2\right)F_2^S\left(\frac{x}{w},t\right)-2F_2^S(x,t)\right\}\right.$$
$$\left. N_f\int_x^1\left\{w^2+(1-w)^2\right\}G\left(\frac{x}{w},t\right)dw\right]=0, \qquad (5.1)$$

$$\frac{\partial F_2^{NS}(x,t)}{\partial t} - \frac{\alpha_{s1}(t)}{2\pi}\left[\frac{2}{3}\{3+4\ln(1-x)\}F_2^{NS}(x,t)+\frac{4}{3}\int_x^1\frac{dw}{1-w}\left\{\left(1+w^2\right)F_2^{NS}\left(\frac{x}{w},t\right)-2F_2^{NS}(x,t)\right\}\right], \qquad (5.2)$$

for LO, and

$$\frac{\partial F_2^S(x,t)}{\partial t} - \frac{\alpha_S(t)}{2\pi}$$

$$\left[\frac{2}{3}\{3+4\ln(1-x)\}F_2^S(x,t)+\frac{4}{3}\int_x^1\frac{dw}{1-w}\left\{\left(1+w^2\right)F_2^S\left(\frac{x}{w},t\right)-2F_2^S(x,t)\right\}+N_f\int_x^1\left\{w^2+(1-w)^2\right\}G\left(\frac{x}{w},t\right)\right]$$

$$-\left(\frac{\alpha_S(t)}{2\pi}\right)^2\left[(x-1)F_2^S(x,t)+\int_0^1 f(w)dw+\int_x^1 f(w)F_2^S\left(\frac{x}{w},t\right)dw+\int_x^1 F_{qq}^S(w)F_2^S\left(\frac{x}{w},t\right)dw\right]$$

$$+\left(\frac{\alpha_S(t)}{2\pi}\right)^2\int_x^1 F_{qg}^S(w)G\left(\frac{x}{w},t\right)dw=0, \qquad (5.3)$$

$$\frac{\partial F_2^{NS}(x,t)}{\partial t} - \frac{\alpha_S(t)}{2\pi}$$

$$\left[\frac{2}{3}\{3+4\ln(1-x)\}F_2^{NS}(x,t)+\frac{4}{3}\int_x^1\frac{dw}{1-w}\left\{\left(1+w^2\right)F_2^{NS}\left(\frac{x}{w},t\right)-2F_2^{NS}(x,t)\right\}\right]$$

$$-\left(\frac{\alpha_S(t)}{2\pi}\right)^2\left[(x-1)F_2^{NS}(x,t)+\int_0^1 f(w)dw+\int_x^1 f(w)F_2^{NS}\left(\frac{x}{w},t\right)dw\right]=0, \qquad (5.4)$$

for NLO, where

$$t=\ln\frac{Q^2}{\Lambda^2},\quad \alpha_{S1}(t)=\frac{4\pi}{\beta_0 t},\quad \alpha_S(t)=\frac{4\pi}{\beta_0 t}\left[1-\frac{\beta_1\ln t}{\beta_0^2 t}\right],$$

$$\beta_0=\frac{33-2N_f}{3}\quad\text{and}\quad\beta_1=\frac{306-38N_f}{3},$$

N_f being the number of flavours. Here,

$$f(w)=C_F^2[P_F(w)-P_A(w)]+\frac{1}{2}C_F C_A[P_G(w)+P_A(w)]+C_F T_R N_f P_{N_F}(w),$$

$$F_{qq}^S(w)=2C_F T_R N_f F_{qq}(w)\ \text{and}\ F_{qg}^S(w)=C_F T_R N_f F_{qg}^1(w)+C_G T_R N_f F_{qg}^2(w).$$

The explicit forms of higher order kernels [103-105] $P_F(w), P_G(w), P_{N_F}(w), P_A(w)$, $F_{qq}(w)$, $F_{qg}^1(w)$, $F_{qg}^2(w)$ are given in the Chapter-4.

Now, using Taylor expansion method [80] and neglecting higher order terms as discussed in the Chapter-3 we can write $F_2^S(x/w, t)$ as

$$F_2^S(x/w,t) \cong F_2^S(x,t) + x\sum_{k=1}^{\infty} u^k \frac{\partial F_2^S(x,t)}{\partial x}.$$

Similarly, $G(x/w, t)$ and $F_2^{NS}(x/w, t)$ can be approximated for small-x. Then putting these values of $F_2^S(x/w, t)$, $G(x/w, t)$ and $F_2^{NS}(x/w, t)$ in equation (5.1) and (5.3) and performing u-integrations we get,

$$\frac{\partial F_2^S(x,t)}{\partial t} - \frac{\alpha_{s_1}(t)}{2\pi}\left[A_1(x)F_2^S(x,t) + A_2(x)G(x,t) + A_3(x)\frac{\partial F_2^S(x,t)}{\partial x} + A_4(x)\frac{\partial G(x,t)}{\partial x}\right] = 0, \quad (5.5)$$

in LO and

$$\frac{\partial F_2^S(x,t)}{\partial t} - \left[\frac{\alpha_s(t)}{2\pi}A_1(x) + \left(\frac{\alpha_s(t)}{2\pi}\right)^2 B_1(x)\right]F_2^S(x,t) - \left[\frac{\alpha_s(t)}{2\pi}A_2(x) + \left(\frac{\alpha_s(t)}{2\pi}\right)^2 B_2(x)\right]G(x,t)$$
$$- \left[\frac{\alpha_s(t)}{2\pi}A_3(x) + \left(\frac{\alpha_s(t)}{2\pi}\right)^2 B_3(x)\right]\frac{\partial F_2^S(x,t)}{\partial x} - \left[\frac{\alpha_s(t)}{2\pi}A_4(x) + \left(\frac{\alpha_s(t)}{2\pi}\right)^2 B_4(x)\right]\frac{\partial G(x,t)}{\partial x} = 0, \quad (5.6)$$

in NLO, where

$$A_1(x) = \frac{2}{3}\{3 + 4\ln(1-x) + (x-1)(x+3)\},$$

$$A_2(x) = N_f[\frac{1}{3}(1-x)(2-x+2x^2)],$$

$$A_3(x) = \frac{2}{3}\{x(1-x^2) + 2x\ln(\frac{1}{x})\},$$

$$A_4(x) = N_f x\{\ln\frac{1}{x} - \frac{1}{3}(1-x)(5-4x+2x^2)\},$$

$$B_1(x) = x\int_0^1 f(w)dw - \int_0^x f(w)dw + \frac{4}{3}N_f\int_x^1 F_{qq}^S(w)dw,$$

$$B_2(x) = \int_x^1 F_{qg}^S(w)dw,$$

$$B_3(x) = x\int_x^1\left\{f(w) + \frac{4}{3}N_f F_{qq}(w)\right\}\frac{1-w}{w}\Big\}dw,$$

$$B_4(x) = x\int_x^1 \frac{1-w}{w}F_{qg}^S(w)dw.$$

Let us assume for simplicity [86-88, 106-110]

$$G(x,t) = K(x)\, F_2^S(x,t), \tag{5.7}$$

where $K(x)$ is a function of x. In this connection, earlier we considered [108-110] $K(x) = k, ax^b, ce^{-dx}$, where k, a, b, c, d are constants. Agreement of the results with experimental data is found to be excellent for $k = 4.5$, $a = 4.5$, $b = 0.01$, $c = 5$, $d = 1$ for low-x in LO and $a = 10$, $b = 0.016$, $c = 0.5$, $d = -3.8$ for low-x in NLO for $y = 2$ in the $\beta = \alpha^y$ relation. Therefore equation (5.5) and (5.6) becomes

$$\frac{\partial F_2^S(x,t)}{\partial t} - \frac{\alpha_{s_1}(t)}{2\pi}\left[L_1(x)F_2^S(x,t) + L_2(x)\frac{\partial F_2^S(x,t)}{\partial x}\right] = 0, \tag{5.8}$$

in LO and

$$\frac{\partial F_2^S(x,t)}{\partial t} - \left[\frac{\alpha_s(t)}{2\pi}L_1(x) + \left(\frac{\alpha_s(t)}{2\pi}\right)^2 M_1(x)\right]F_2^S(x,t) - \left[\frac{\alpha_s(t)}{2\pi}L_2(x) + \left(\frac{\alpha_s(t)}{2\pi}\right)^2 M_2(x)\right]\frac{\partial F_2^S(x,t)}{\partial x} = 0, \tag{5.9}$$

in NLO. For simplicity, we can write equation (5.8) as

$$\frac{\partial F_2^S(x,t)}{\partial t} - \left[L_1'(x,t)F_2^S(x,t) + L_2'(x,t)\frac{\partial F_2^S(x,t)}{\partial x}\right] = 0, \tag{5.10}$$

where

$$L_1(x) = A_1(x) + K(x)A_2(x) + A_4(x)\frac{\partial K(x)}{\partial x},$$

$$L_2(x) = A_3(x) + K(x)A_4(x),$$

$$M_1(x) = B_1(x) + K(x)B_2(x) + B_4(x)\frac{\partial K(x)}{\partial x},$$

$$M_2(x) = B_3(x) + K(x)B_4(x),$$

$$L_1'(x,t) = \frac{\alpha_{s_1}(t)}{2\pi}L_1(x),$$

$$L_2'(x,t) = \frac{\alpha_{s_1}(t)}{2\pi}L_2(x).$$

For a possible solution of equation (5.9), we assume [106-109] that

$$\left(\frac{\alpha_s(t)}{2\pi}\right)^2 = T_0\left(\frac{\alpha_s(t)}{2\pi}\right), \tag{5.11}$$

where, T_0 is a numerical parameter to be obtained from the particular Q^2-range under study. By a suitable choice of T_0 we can reduce the error to a minimum. Now equation (5.9) can be recast as

$$\frac{\partial F_2^S(x,t)}{\partial t} - \left[P(x,t)F_2^S(x,t) + Q(x,t)\frac{\partial F_2^S(x,t)}{\partial x} \right] = 0, \tag{5.12}$$

in NLO, where

$$P(x,t) = \frac{\alpha_S(t)}{2\pi}\left[L_1(x) + T_0 M_1(x)\right] \text{ and } Q(x,t) = \frac{\alpha_S(t)}{2\pi}\left[L_2(x) + T_0 M_2(x)\right]$$

The general solutions [80-81] of equation (5.10) is $F(U, V) = 0$, where F is an arbitrary function and $U(x, t, F_2^S) = C_1$ and $V(x, t, F_2^S) = C_2$ where, C_1 and C_2 are constants and they form a solutions of equations

$$\frac{dx}{L_2'(x,t)} = \frac{dt}{-1} = \frac{dF_2^S(x,t)}{-L_1'(x,t)F_2^S(x,t)}. \tag{5.13}$$

Solving equation (5.13) we obtain,

$$U\left(x,t,F_2^S\right) = t\exp\left[\frac{1}{A_f}\int\frac{1}{L_2(x)}dx\right], \text{ and } V\left(x,t,F_2^S\right) = F_2^S(x,t)\exp\left[\int\frac{L_1(x)}{L_2(x)}dx\right],$$

where $A_f = 4/(33-2N_f)$. Since U and V are two independent solutions of equation (5.13) and if α and β are arbitrary constants, then $V = \alpha U + \beta$ may be taken as a complete solution of equation (5.12). Then the complete solution [80-81]

$$F_2^S(x,t)\exp\left[\int\frac{L_1(x)}{L_2(x)}dx\right] = \alpha t\exp\left[\frac{1}{A_f}\int\frac{1}{L_2(x)}dx\right] + \beta \tag{5.14}$$

is a two-parameter family of planes.

Due to conservation of the electromagnetic current, F_2 must vanish as Q^2 goes to zero [7, 111]. Also $R \to 0$ in this limit. Here R indicates ratio of longitudinal and transverse cross-sections of virtual photon in DIS process. This implies that scaling should not be a valid concept in the region of very low–Q^2. The exchanged photon is then almost real and the close similarity of real photonic and hadronic interactions justifies the use of the Vector Meson Dominance (VMD) concept [112-113] for the description of F_2. In the language of

perturbation theory, this concept is equivalent to a statement that a physical photon spends part of its time as a 'bare', point-like photon and part as a virtual hadron (s) [111]. The power and beauty of explaining scaling violations with field theoretic methods (i.e., radiative corrections in QCD) remains, however, unchallenged in as much as they provide us with a framework for the whole x-region with essentially only one free parameter Λ [17]. For Q^2-values much larger than Λ^2, the effective coupling is small and a perturbative description in terms of quarks and gluons interacting weakly makes sense. For Q^2 of order Λ^2, the effective coupling is infinite and we cannot make such a picture, since quarks and gluons will arrange themselves into strongly bound clusters, namely, hadrons [7] and so, the perturbation series breaks down at small-Q^2 [7-8]. Thus, it can be thought of Λ as marking the boundary between a world of quasi-free quarks and gluons, and the world of pions, protons, and so on. The value of Λ is not predicted by the theory; it is a free parameter to be determined from experiment. It should expect that it is of the order of a typical hadronic mass [7]. Since the value of Λ is so small we can assume at $Q = \Lambda$, $F_2^S(x, t) = 0$ due to conservation of the electromagnetic current [7, 111]. This dynamical prediction agrees with most ad hoc parameterizations and with the data [17, 111]. Using this boundary condition in equation (5.14) we get $\beta = 0$ and

$$F_2^S(x,t) = \alpha t \exp\left[\int\left(\frac{1}{A_f L_2(x)} - \frac{L_1(x)}{L_2(x)}\right)dx\right]. \tag{5.15}$$

Now, defining

$$F_2^S(x,t_0) = \alpha t_0 \exp\left[\int\left(\frac{1}{A_f L_2(x)} - \frac{L_1(x)}{L_2(x)}\right)dx\right],$$

at $t = t_0$, where, $t_0 = \ln(Q_0^2/\Lambda^2)$ at any lower value $Q = Q_0$, we get from equation (5.15)

$$F_2^S(x,t) = F_2^S(x_0,t)\left(\frac{t}{t_0}\right), \tag{5.16}$$

which gives the t-evolution of singlet structure function $F_2^S(x, t)$ in LO. Proceeding in the same way we get from equation (5.15)

$$F_2^S(x,t) = F_2^S(x,t_0)\left(\frac{t^{(b/t+1)}}{t_0^{(b/t_0+1)}}\right)\exp\left[b\left(\frac{1}{t} - \frac{1}{t_0}\right)\right], \tag{5.17}$$

which gives the t-evolution of singlet structure function $F_2^S(x, t)$ in NLO, where $b = \beta_1/\beta_0^2$. We observe that the Lagrange's auxiliary system of ordinary differential equations (5.12) occurred in the formalism can not be solved without the additional assumption of linearization (equation 5.11) and introduction of an ad hoc parameter T_0 [106-109]. This parameter does not effect in the results of t-evolution of structure functions.

Proceeding exactly in the same way, we get

$$F_2^{NS}(x,t) = F_2^{NS}(x,t_0)\left(\frac{t}{t_0}\right) \tag{5.18}$$

and

$$F_2^{NS}(x,t) = F_2^{NS}(x,t_0)\left(\frac{t^{(b/t+1)}}{t_0^{(b/t_0+1)}}\right)\exp\left[b\left(\frac{1}{t}-\frac{1}{t_0}\right)\right], \tag{5.19}$$

which give the t-evolutions of non-singlet structure functions $F_2^{NS}(x, t)$ in LO and NLO respectively. We observe that if b tends to zero, then equations (5.17) and (5.19) tend to equations (5.16) and (5.18) respectively, i.e., solution of NLO equations goes to that of LO equations. Again defining,

$$F_2^S(x_0,t) = \alpha t \exp\left[\int\left(\frac{1}{A_f L_2(x)} - \frac{L_1(x)}{L_2(x)}\right)dx\right]_{x=x_0},$$

we obtain from equation (5.15)

$$F_2^S(x,t) = F_2^S(x_0,t)\exp\left[\int_{x_0}^{x}\left(\frac{1}{A_f L_2(x)} - \frac{L_1(x)}{L_2(x)}\right)dx\right], \tag{5.20}$$

which gives the x-evolution of singlet structure function $F_2^S(x, t)$ in LO. Similarly we get

$$F_2^S(x,t) = F_2^S(x_0,t)\exp\left[\int_{x_0}^{x}\left(\frac{1}{a}\cdot\frac{1}{L_2(x)+T_0M_2(x)} - \frac{L_1(x)+T_0M_1(x)}{L_2(x)+T_0M_2(x)}\right)dx\right], \tag{5.21}$$

which gives the x-evolutions of singlet structure function $F_2^S(x, t)$ in NLO, where $a = 2/\beta_0$.

Proceeding in the same way, we get

$$F_2^{NS}(x,t) = F_2^{NS}(x_0,t)\exp\left[\int_{x_0}^{x}\left(\frac{1}{A_f A_3(x)} - \frac{A_1(x)}{A_3(x)}\right)dx\right] \tag{5.22}$$

and

$$F_2^{NS}(x,t) = F_2^{NS}(x_0,t)\exp\left[\int_{x_0}^{x}\left(\frac{1}{a}.\frac{1}{A_5(x)+T_0B_5(x)} - \frac{A_6(x)+T_0B_6(x)}{A_5(x)+T_0B_5(x)}\right)dx\right], \tag{5.23}$$

which give the x-evolutions of non-singlet structure functions $F_2^{NS}(x, t)$ in LO and NLO respectively. Here,

$$A_5(x) = (2/3)\{x(1-x^2)+2x\ln(1/x)\}, \quad B_5(x) = x\int_x^1 \frac{1-w}{w} f(w)dw,$$

$$A_6(x) = (2/3)\{3+4\ln(1-x)+(x-1)(x+3)\}, \quad B_6(x) = -\int_0^x f(w)dw + x\int_0^1 f(w)dw.$$

In our particular solutions [108-110], we observed that in the relation $\beta = \alpha^y$, if y varies between minimum ($y = 2$) to a maximum value, the powers of (t/t_0) in LO, and powers of $t^{b/t+1}/t_0^{b/t_0+1}$ and co-efficient of $b(1/t - 1/t_0)$ of exponential part in NLO in t-evolutions and the numerator of the first term in the integral sign in x-evolution in both LO and NLO varies between 2 to 1. Then it is understood that the particular solutions of GLDAP evolution equations in LO and NLO obtained by that method were not unique and so the t-evolutions of deuteron, proton and neutron structure functions, and x-evolution of deuteron structure function obtained by that method were not unique. Thus by that method, instead of having a single solution we arrive a band of solutions, of course the range for these solutions is reasonably narrow.

Now deuteron, proton and neutron structure functions measured in deep inelastic electro-production can be written in terms of singlet and non-singlet quark distribution functions [7] as

$$F_2^d(x, t) = (5/9)\, F_2^S(x, t), \tag{5.24}$$

$$F_2^p(x,t) = (5/18)\,F_2^S(x,t) + (3/18)\,F_2^{NS}(x,t), \tag{5.25}$$

$$F_2^n(x,t) = (5/18)\,F_2^S(x,t) - (3/18)\,F_2^{NS}(x,t), \tag{5.26}$$

$$F_2^p(x,t) - F_2^n(x,t) = (1/3)\,F_2^{NS}(x,t). \tag{5.27}$$

Now using equations (5.16), (5.17) and (5.20) and (5.21) in equation (5.24) we will get t and x-evolutions of deuteron structure function $F_2^d(x,t)$ at low-x as

$$F_2^d(x,t) = F_2^d(x,t_0)\left(\frac{t}{t_0}\right), \tag{5.28}$$

$$F_2^d(x,t) = F_2^d(x,t_0)\left(\frac{t^{(b/t+1)}}{t_0^{(b/t_0+1)}}\right)\exp\left[b\left(\frac{1}{t}-\frac{1}{t_0}\right)\right] \tag{5.29}$$

in LO and NLO respectively. And

$$F_2^d(x,t) = F_2^d(x_0,t)\exp\left[\int_{x_0}^{x}\left(\frac{1}{A_f L_2(x)} - \frac{L_1(x)}{L_2(x)}\right)dx\right], \tag{5.30}$$

$$F_2^d(x,t) = F_2^d(x_0,t)\exp\left[\int_{x_0}^{x}\left(\frac{1}{a}\cdot\frac{1}{L_2(x)+T_0M_2(x)} - \frac{L_1(x)+T_0M_1(x)}{L_2(x)+T_0M_2(x)}\right)dx\right], \tag{5.31}$$

in LO and NLO respectively.

Similarly using equations (5.16), (5.18) and (5.17), (5.19) in equations (5.25), (5.26) and (5.27) we get the t-evolutions of proton, neutron, and difference and ratio of proton and neutron structure functions at low-x in LO and NLO as

$$F_2^p(x,t) = F_2^p(x,t_0)\left(\frac{t}{t_0}\right), \tag{5.32}$$

$$F_2^p(x,t) = F_2^p(x,t_0)\left(\frac{t^{(b/t+1)}}{t_0^{(b/t_0+1)}}\right)\exp\left[b\left(\frac{1}{t}-\frac{1}{t_0}\right)\right], \tag{5.33}$$

$$F_2^n(x,t) = F_2^n(x,t_0)\left(\frac{t}{t_0}\right), \tag{5.34}$$

$$F_2^n(x,t) = F_2^n(x,t_0)\left(\frac{t^{(b/t+1)}}{t_0^{(b/t_0+1)}}\right)\exp\left[b\left(\frac{1}{t}-\frac{1}{t_0}\right)\right], \tag{5.35}$$

$$F_2^p(x,t) - F_2^n(x,t) = [F_2^p(x,t_0) - F_2^n(x,t_0)]\left(\frac{t}{t_0}\right), \tag{5.36}$$

$$F_2^p(x,t) - F_2^n(x,t) = [F_2^p(x,t_0) - F_2^p(x,t_0)]\left(\frac{t^{(b/t+1)}}{t_0^{(b/t_0+1)}}\right)\exp\left[b\left(\frac{1}{t}-\frac{1}{t_0}\right)\right] \tag{5.37}$$

and

$$\frac{F_2^p(x,t)}{F_2^n(x,t)} = \frac{F_2^p(x,t_0)}{F_2^n(x,t_0)} = R(x). \tag{5.38}$$

where $R(x)$ is a constant for fixed-x. It is observed that ratio of proton and neutron is same for both NLO and LO and it is independent of t for fixed-x. We also observed that unique solutions of GLDAP evolution equations in LO and NLO are same with particular solutions in LO and NLO for y maximum in the $\beta = \alpha^y$ relation [108-110].

5.2. Results and Discussion

In the present chapter, we compare our results of t-evolutions of deuteron, proton, and neutron and difference and ratio of proton and neutron structure functions with the HERA [94] and NMC [95] low-x and low-Q^2 data and results of x-evolution of deuteron structure functions with NMC low-x and low-Q^2 data. In case of HERA data, proton and neutron structure functions are measured in the range $2 \leq Q^2 \leq 50$ GeV^2. Moreover here $P_T \leq 200$ MeV, where P_T is the transverse momentum of the final state baryon. In case of NMC data proton and neutron structure functions are measured in the range $0.75 \leq Q^2 \leq 27$ GeV^2. We consider number of flavours $N_f = 4$. We also compare our results of t-evolution of proton structure functions with a recent global parameterization [96]. This parameterization includes data from H1, ZEUS, NMC, E665 experiment [95, 97-102].

In figure 5.1(a), (b), (c), (d), we present our results of t-evolutions of deuteron, proton, neutron, and difference of proton and neutron structure functions (solid lines for NLO and

dashed lines for LO) for the representative values of x given in the figure. Data points at

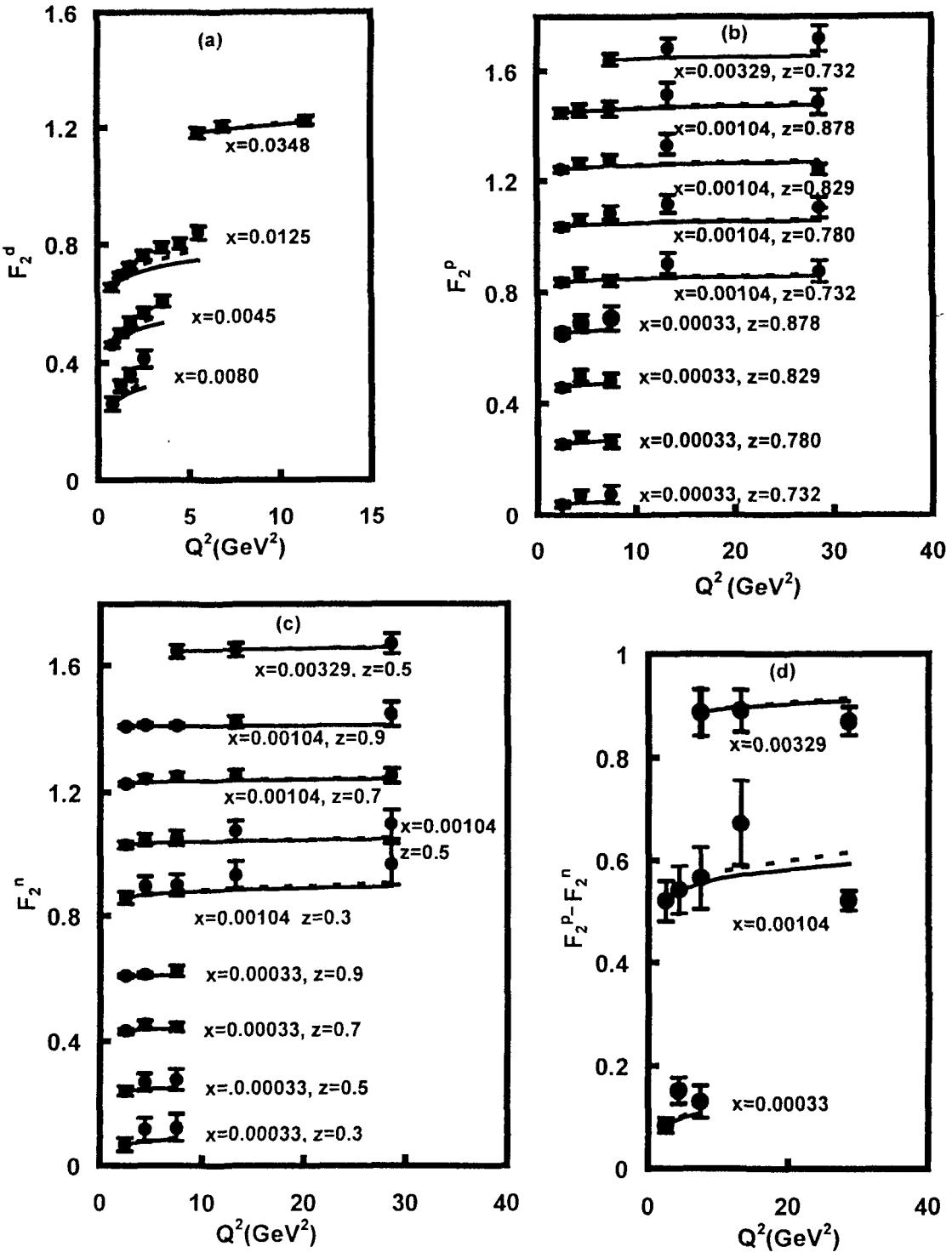

Fig.5.1 (a-d): t-Evolution of deuteron, proton, neutron, difference of proton and neutron structure functions.

lowest-Q^2 values in the figures are taken as inputs to test the evolution equations. Agreement with the data [94-95] is found to be good. We observe that t-evolutions are

slightly steeper in LO calculations than those of NLO. For convenience, value of each data point is increased by adding $0.2i$ for deuteron, proton, neutron and $0.4i$ for difference of proton and neutron structure functions, where i = 0, 1, 2, 3 ... are the numberings of curves counting from the bottom of the lowermost curve as the 0-th order. Data points at lowest-Q^2 values in the figures are taken as inputs.

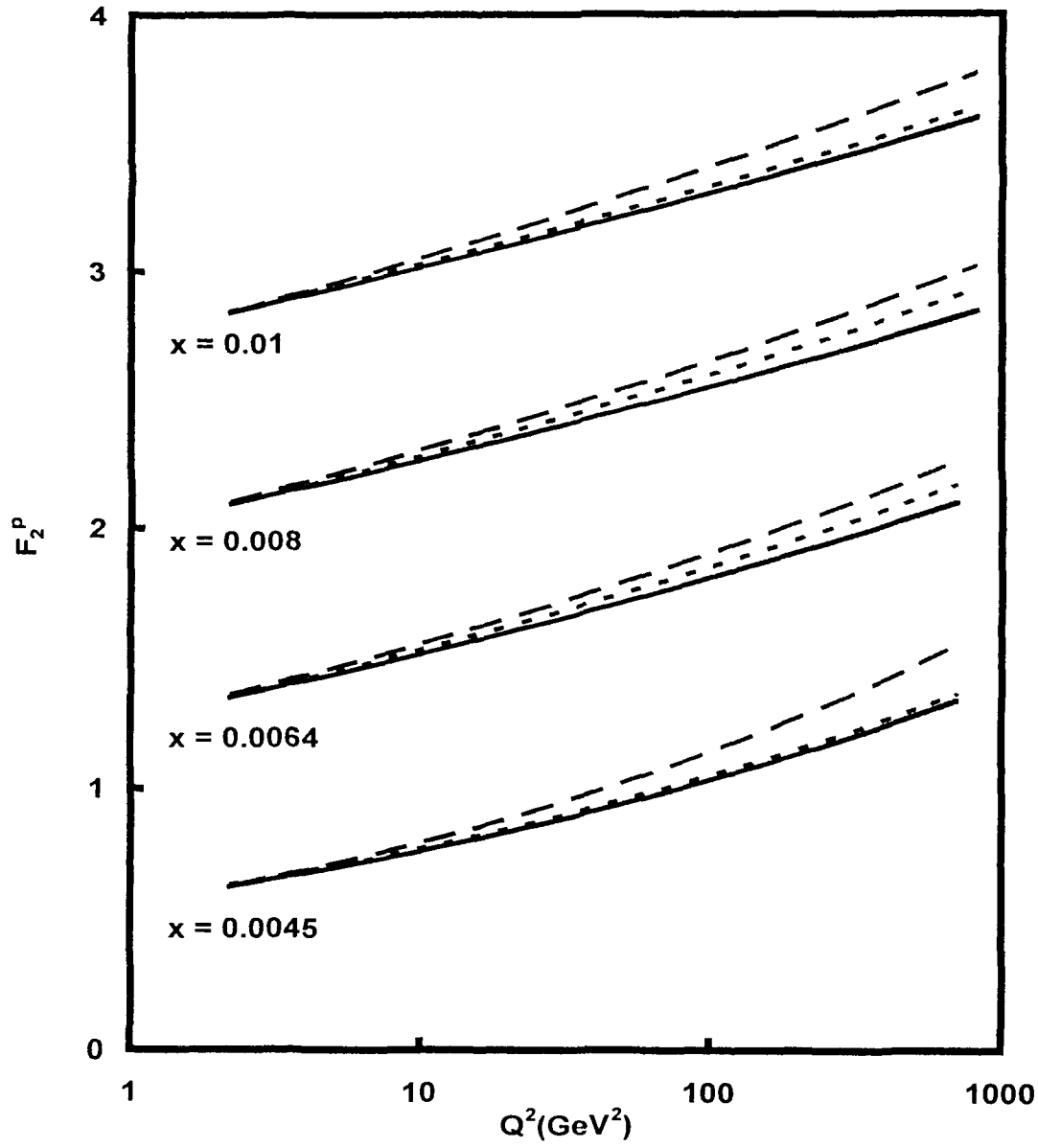

Fig.5.2: t-Evolution of proton structure functions.

In figure 5.2, we compare our results of t-evolutions of proton structure functions F_2^P (solid lines for NLO and dashed lines for LO) with a recent global parameterization [96] (long dashed lines) for the representative values of x given in the figure. Data points at lowest-Q^2 values in the figures are taken as input to test the evolution equation. We

observe that t-evolutions are slightly steeper in LO calculations than those of NLO. Agreement with the LO results is found to be better than with the NLO results. For convenience, value of each data point is increased by adding $0.5i$, where i = 0, 1, 2, 3 ... are the numberings of curves counting from the bottom of the lowermost curve as the 0-th order. Data points at lowest-Q^2 values in the figures are taken as inputs.

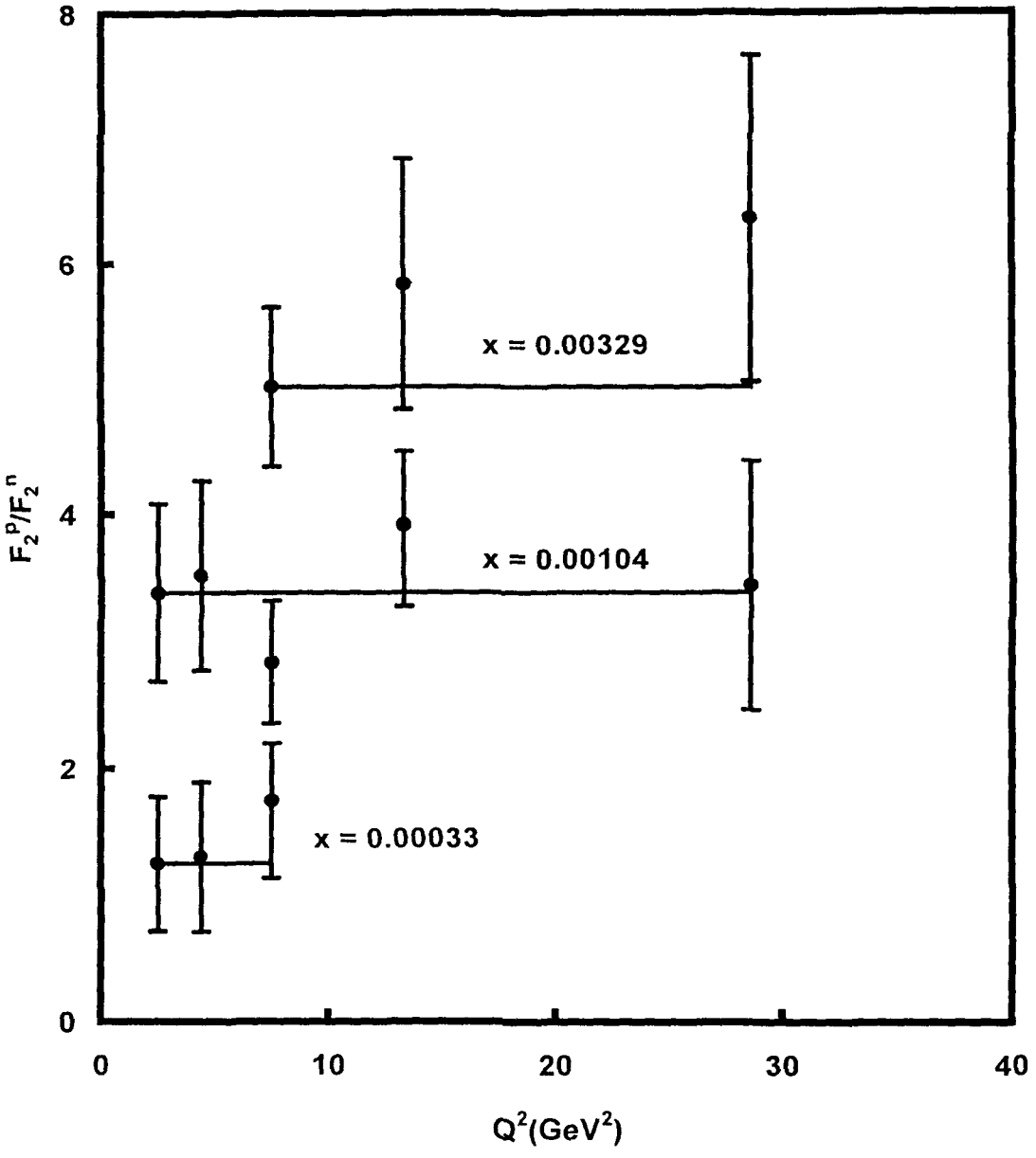

Fig.5.3: t-Evolution of ratio of proton and neutron structure functions.

In figure 5.3, we present our results of t-evolutions of ratio of proton and neutron structure functions F_2^p/ F_2^n (solid lines) for the representative values of x given in the figures. Though according to our theory the ratio should be independent of t, due to the

lack of sufficient amount of data and due to large error bars, a clear cut conclusion can not be drawn.

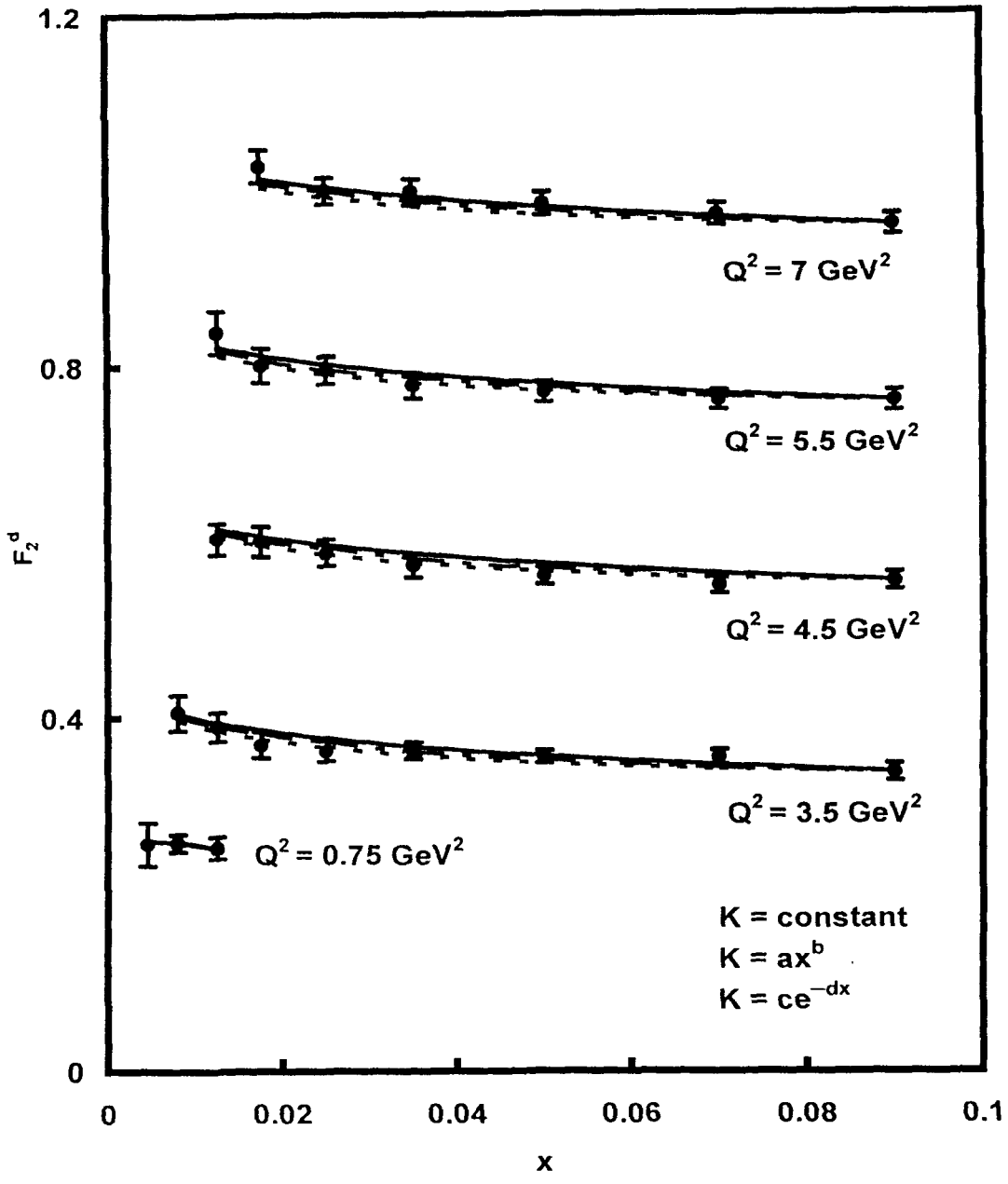

Fig.5.4: x-Evolution of deuteron structure function in leading order.

In figure 5.4, we present our results of x-distribution of deuteron structure functions F_2^d in LO for $K(x)$ = constant (solid lines), $K(x) = ax^b$ (dashed lines) and for $K(x) = ce^{-dx}$ (dotted lines), where a, b, c and d are constants and for representative values of Q^2 given in each figure, and compare them with NMC deuteron low-x low-Q^2 data [95]. Each data point for x-value just below 0.1 has been taken as input $F_2^d(x_0, t)$. If we take $K(x) = 4.5$, then agreement of the result with experimental data is found to be excellent. On the other

hand, if we take $K(x) = ax^b$, then agreement of the results with experimental data is found to be good at $a = 4.5$, $b = 0.01$. Again if we take $K(x) = ce^{-dx}$, then agreement of the results with experimental data is found to be good at $c = 5$, $b = 1$. For x-evolutions of deuteron structure function, results of unique solutions and results of particular solutions have not any significant difference in LO [110].

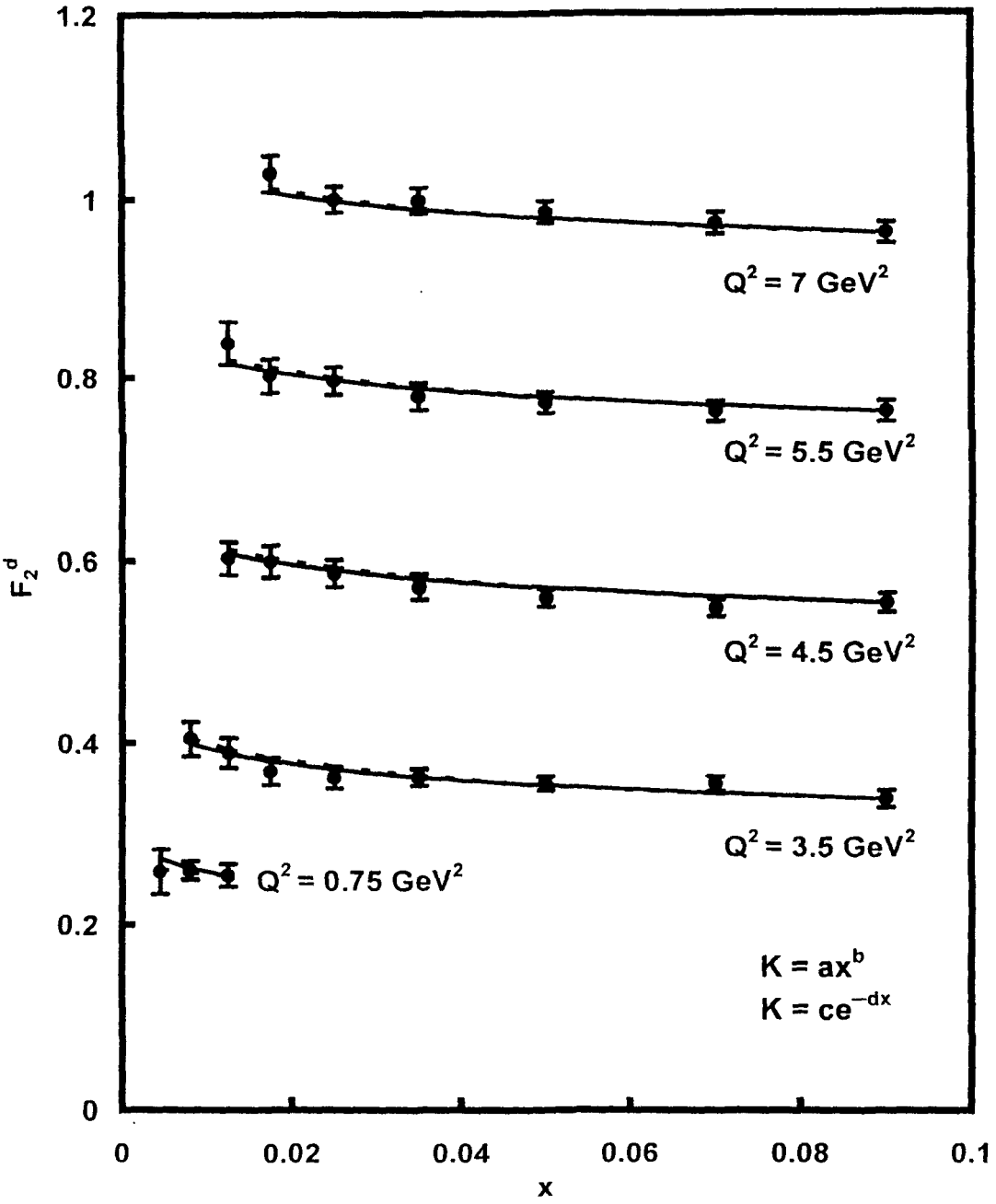

Fig.5.5: x-Evolution of deuteron structure function in next-to-leading order.

In figure 5.5, we compare our results of x-evolution of deuteron structure function in NLO for $K(x) = ax^b$ (solid lines) and for $K(x) = ce^{-dx}$ (dashed lines) with NMC [95] low-x

low-Q^2 data and for representative values of Q^2 given in each figure. Each data point for x-value just below 0.1 has been taken as input $F_2^d(x_0, t)$. If we take $K(x) = ax^b$, then agreement of the result with experimental data is found to be excellent at $a = 5.5$, $b = 0.016$. On the other hand, if we take $K(x) = ce^{-dx}$, then agreement of the results with experimental data is found to be good at $c = 0.28$, $d = -3.8$. But in the case of NLO, agreement of the results with experimental data is found to be very poor for any constant value of $K(x)$. Therefore we do not present our result of x-distribution at $K(x)$ = constant in NLO.

5.3. Conclusion

In this chapter, we obtain complete and unique solutions of singlet and non-singlet structure functions at low-x using by Taylor's expansion method from GLDAP evolution equations and t and x-evolution of singlet and non-singlet structure functions in leading and next-to-leading orders and hence t-evolutions of deuteron, proton, neutron and difference and ratio of proton and neutron structure functions and x-evolutions of deuteron structure functions. We compare our results with HERA, NMC low-x low-Q^2 data and a recent global parameterization. In all the result from experimental data as well as global fit, it is seen that deuteron structure functions increases when x decreases and Q^2 increases for fixed values of Q^2 and x respectively and proton, neutron, difference and ratio of proton and neutron structure functions increases when Q^2 increases for fixed value of x. It has been observed that, though we have derived a unique t-evolution for deuteron, proton, neutron, difference and ratio of proton and neutron structure functions in LO and NLO, yet we can not establish a completely unique x-evolution for deuteron structure function in LO and NLO due to the relation $K(x)$ between singlet and gluon structure functions. $K(x)$ may be in the forms of a constant, an exponential function or a power function and they can equally produce required x-distribution of deuteron or gluon structure functions. But unlike many parameter arbitrary input x-distribution functions generally used in the literature, our method requires only one or two such parameters. Explicit form of $K(x)$ can actually be obtained only by solving coupled GLDAP evolution equations for singlet and gluon structure functions, and works are going on in this regard.

Chapter-6

t AND x-EVOLUTIONS OF GLUON STRUCTURE FUNCTIONS

In the previous chapters, particular and unique solutions of the Gribov-Lipatov-Dokshitzer-Altarelli-Parisi (GLDAP) [29-32] evolution equations for t and x-evolutions of singlet and non-singlet structure functions in leading order (LO) and next-to-leading order (NLO) at low-x have been reported. The same technique can be applied to the GLDAP evolution equations for gluon structure functions in LO to obtain t and x-evolutions of gluon structure functions. These LO results are compared with a recent global parameterization [96, 114].

6.1. Theory

The GLDAP evolution equation for gluon structure function has the standard form in LO [89] as

$$\frac{\partial G(x,t)}{\partial t} - \frac{A_f}{t}\left\{\left(\frac{11}{12} - \frac{N_f}{18} + \ln(1-x)\right)G(x,t) + I_g\right\} = 0, \tag{6.1}$$

where

$$I_g = \int_x^1 dw\left[\frac{wG(x/w,t) - G(x,t)}{1-w} + \left(w(1-w) + \frac{1-w}{w}\right)G(x/w,t) + \frac{2}{9}\left(\frac{1+(1-w)^2}{w}\right)F_2^S(x/w,t)\right], \tag{6.2}$$

$t = \ln\left(Q^2/\Lambda^2\right)$ and $A_f = 36/(33 - N_f)$, N_f being the number of flavours.

Now, using Taylor expansion method [80] and neglecting higher order terms of x as discussed in the Chapter-3, we can write $G(x/w, t)$ as

$$G(x/w,t) \cong G(x,t) + x\sum_{k=1}^{\infty} u^k \frac{\partial G(x,t)}{\partial x}.$$

Similarly, $F_2^S(x/w, t)$ can be approximated for small-x. Putting these values of $G(x/w, t)$ and $F_2^S(x/w, t)$, in equation (6.2) and (6.1) and performing u-integrations we get

$$\frac{\partial G(x,t)}{\partial t} - \frac{A_f}{t}\left[A_1(x)F_2^S(x,t) + B_1(x)\frac{\partial F_2^S(x,t)}{\partial x} + C_1(x)G(x,t) + D_1(x)\frac{\partial G(x,t)}{\partial x}\right] = 0, \tag{6.3}$$

where

$$A_1(x) = -\left[\frac{2}{9}(1-x) + \frac{1}{9}(1-x)^2 + \frac{4}{9}\ln x\right],$$

$$B_1(x) = x\left[\frac{4}{9x} + \frac{4}{9}(1-x) + \frac{1}{9}(1-x)^2 + \frac{8}{9}\ln x - \frac{4}{9}\right],$$

$$C_1(x) = \left(\frac{11}{12} - \frac{N_f}{18}\right) + \ln(1-x) - \left[2(1-x) - \frac{1}{2}(1-x)^2 + \frac{1}{3}(1-x)^3 + \ln x\right],$$

$$D_1(x) = x\left[\frac{1}{x} + 2(1-x) + \frac{1}{3}(1-x)^3 + 2\ln x - 1\right].$$

For simplicity we assume [86-88, 106-110] $G(x, t) = K(x)\ F_2^S\ (x, t)$, where $K(x)$ is a function of x. Therefore

$$F_2^S(x,t) = K_1(x)G(x,t), \tag{6.4}$$

where $K_1(x) = 1/\ K(x)$.

Now equation (6.3) becomes

$$\frac{\partial G(x,t)}{\partial t} - \frac{A_f}{t}\left[P(x)G(x,t) + Q(x)\frac{\partial G(x,t)}{\partial x}\right] = 0, \tag{6.5}$$

where $P(x) = A_1(x)K_1(x) + B_1(x)\dfrac{\partial K_1(x)}{\partial x} + C_1(x)$ and $Q(x) = B_1(x)K_1(x) + D_1(x)$.

The general solution of equation (6.5) is [80-81] $F\ (U,\ V) = 0$, where F is an arbitrary function and $U(x, t, G) = C_1$ and $V(x, t, G) = C_2$ form a solution of equations

$$\frac{dx}{A_f Q(x)} = \frac{dt}{-t} = \frac{dG(x,t)}{-A_f P(x)G(x,t)}. \tag{6.6}$$

Solving equations (6.6) we obtain,

$$U\left(x,t,F_2^S\right) = t\exp\left[\frac{1}{A_f}\int\frac{1}{Q(x)}dx\right],$$

and

$$V\left(x,t,F_2^S\right)=F_2^S(x,t)\exp\left[\int\frac{P(x)}{Q(x)}dx\right].$$

If U and V are two independent solutions of equations (6.6) and if α and β are arbitrary constants, then $V = \alpha U + \beta$ may be taken as a complete solution of equation (6.5). Now the complete solution [80-81]

$$G(x,t)\exp\left[\int\frac{P(x)}{Q(x)}dx\right]=\alpha t\exp\left[\frac{1}{A_f}\int\frac{1}{Q(x)}dx\right]+\beta, \tag{6.7}$$

is a two-parameter family of surfaces, which does not have an envelope, since the arbitrary constants enter linearly [80]. Differentiating equation (6.7) with respect to β we get 0 = 1, which is absurd. Hence there is no singular solution. The one parameter family determined by taking $\beta = \alpha^2$ has equation

$$G(x,t)\exp\left[\int\frac{P(x)}{Q(x)}dx\right]=\alpha t\exp\left[\frac{1}{A_f}\int\frac{1}{Q(x)}dx\right]+\alpha^2. \tag{6.8}$$

Differentiating equation (6.8) with respect to α, we get

$$\alpha=-\frac{1}{2}t\exp\left[\frac{1}{A_f}\int\frac{1}{Q(x)}dx\right].$$

Putting the value of α in equation (6.8), we obtain the envelope

$$G(x,t)=-\frac{1}{4}t^2\exp\left[\int\left(\frac{2}{A_fQ(x)}-\frac{P(x)}{Q(x)}\right)dx\right], \tag{6.9}$$

which is merely a particular solution of the general solution. Now, defining

$$G(x,t_0)=-\frac{1}{4}t_0^2\exp\left[\int\left(\frac{2}{A_fQ(x)}-\frac{P(x)}{Q(x)}\right)dx\right],$$

at $t = t_0$, where $t_0 = \ln(Q_0^2/\Lambda^2)$ at any lower value $Q = Q_0$, we get from equation (6.9)

$$G(x,t)=G\left(x,t_0\right)\left(\frac{t}{t_0}\right)^2, \tag{6.10}$$

which gives the t-evolution of gluon structure function $G(x, t)$. Again defining,

$$G(x_0,t) = -\frac{1}{4}t^2 \exp\left[\int\left(\frac{2}{A_f Q(x)} - \frac{P(x)}{Q(x)}\right)dx\right]_{x=x_0},$$

we obtain from equation (6.9)

$$G(x,t) = G(x_0,t)\exp\left[\int_{x_0}^{x}\left(\frac{2}{A_f Q(x)} - \frac{P(x)}{Q(x)}\right)dx\right], \tag{6.11}$$

which gives the x-evolution of gluon structure function $G(x, t)$.

For the particular solution of equation (6.5), we take $\beta = \alpha^2$ in equation (6.7). If we take $\beta = \alpha$ in equation (6.7) and differentiating with respect to α as before, we get

$$0 = t\exp\left[\frac{1}{A_f}\int_{x_0}^{x}\frac{1}{Q(x)}dx\right] + 1$$

from which we can not determine the value of α. But if we take $\beta = \alpha^3$ in equation (6.7) and differentiating with respect to α, we get

$$\alpha = \sqrt{-\frac{1}{3}t\exp\left[\frac{1}{A_f}\int\frac{1}{Q(x)}dx\right]},$$

from which we get,

$$G(x,t) = G(x,t_0)\left(\frac{t}{t_0}\right)^{3/2}$$

and

$$G(x,t) = G(x_0,t)\exp\left[\int_{x_0}^{x}\left(\frac{3/2}{A_f Q(x)} - \frac{P(x)}{Q(x)}\right)\right],$$

as before which are t and x-evolutions respectively of gluon structure function for $\beta = \alpha^3$.

Proceeding exactly in the same way we can show that if we take $\beta = \alpha^4$ we get

$$G(x,t)=G(x,t_0)\left(\frac{t}{t_0}\right)^{4/3}$$

and

$$G(x,t)=G(x_0,t)\exp\left[\int_{x_0}^{x}\left(\frac{4/3}{A_f Q(x)}-\frac{P(x)}{Q(x)}\right)dx\right],$$

and so on. So in general, if we take $\beta = \alpha^{\gamma}$, we get

$$G(x,t)=G(x,t_0)\left(\frac{t}{t_0}\right)^{\gamma/(\gamma-1)}$$

and

$$G(x,t)=G(x_0,t)\exp\left[\int_{x_0}^{x}\left(\frac{\gamma/(\gamma-1)}{A_f Q(x)}-\frac{P(x)}{Q(x)}\right)dx\right],$$

which give t and x-evolutions respectively of gluon structure function for $\beta = \alpha^{\gamma}$. We observe if $\gamma\rightarrow\infty$ (very large), $\gamma/(\gamma-1) \rightarrow 1$.

Thus we observe that, if we take $\beta = \alpha$ in equation (6.7) we can not obtain the value of α and also the required solution. But if we take $\beta = \alpha^2$, α^3, α^4, α^5..... and so on, we see that the powers of (t/t_0) in t-evolutions of gluon structure functions are 2, 3/2, 4/3, 5/4....and so on respectively as discussed above. Similarly, for x-evolutions of gluon structure functions we see that the numerators of the first term inside the integral sign are 2, 3/2, 4/3, 5/4....and so on respectively for the same values of α. Thus we see that, in the relation $\beta = \alpha^{\gamma}$, if γ varies between 2 to a maximum value, the powers of (t/t_0) and the numerators of the first term in the integral sign vary between 2 to 1. Then it is understood that the solution of equation (6.5) obtained by this method is not unique and so the t and x-evolution of gluon structure function obtained by this method is not unique. Thus by this method, instead of having a single solution we arrive a band of solutions, of course the range for these solutions is reasonably narrow.

Again the value of Λ is so small that we can take at $Q = \Lambda$, $F_2^S(x, t) = 0$ due to conservation of the electromagnetic current [111] as discussed in the Chapter-5. Since the relation between gluon and singlet structure functions is $G(x, t) = K_1(x)F_2^S(x, t)$, therefore $G(x, t) = 0$ at $Q = \Lambda$. This dynamical prediction agrees with most ad hoc parameterizations and with the data [17, 111]. Using this boundary condition in equations (6.7) we get $\beta = 0$ and

$$G(x,t) = \alpha t \exp\left[\int\left(\frac{1}{A_f Q(x)} - \frac{P(x)}{Q(x)}\right)dx\right]. \tag{6.12}$$

Now, defining

$$G(x,t_0) = \alpha t_0 \exp\left[\int\left(\frac{1}{A_f Q(x)} - \frac{P(x)}{Q(x)}\right)dx\right],$$

at $t = t_0$, where $t_0 = \ln(Q_0^2/\Lambda^2)$ at any lower value $Q = Q_0$, we get from equation (6.12)

$$G(x,t) = G\left(x_0,t\right)\left(\frac{t}{t0}\right), \tag{6.13}$$

which gives the t-evolution of gluon structure function $G(x, t)$ in LO. Again defining,

$$G(x_0,t) = \alpha t \exp\left[\int\left(\frac{1}{A_f Q(x)} - \frac{P(x)}{Q(x)}\right)dx\right]_{x=x_0},$$

we obtain from equation (6.12)

$$G(x,t) = G(x_0,t)\exp\left[\int_{x_0}^{x}\left(\frac{1}{A_f Q(x)} - \frac{P(x)}{Q(x)}\right)dx\right], \tag{6.14}$$

which gives the x-evolution of gluon structure function $G(x, t)$ in LO. We observed that unique solutions (equations (6.13) and (6.14)) of GLDAP evolution equation for gluon structure function are same with particular solutions for y maximum in $\beta = \alpha^y$ relation in LO.

6.2. Results and Discussion

In this chapter, we present our result of t-evolution of gluon structure function qualitatively and compare result of x-evolution with the recent global parameterizations

[96, 114]. These parameterizations include data from H1, ZEUS, DO, CDF, NMC, BCDMS, SLAC, E665, CCFR, E605, CTEQ experiments [97-102, 115-130]. Though we compare our results with $y = 2$ and y maximum in the $\beta = \alpha^{y}$ relation with the parameterizations, our result with y maximum is equivalent to that of the unique solution.

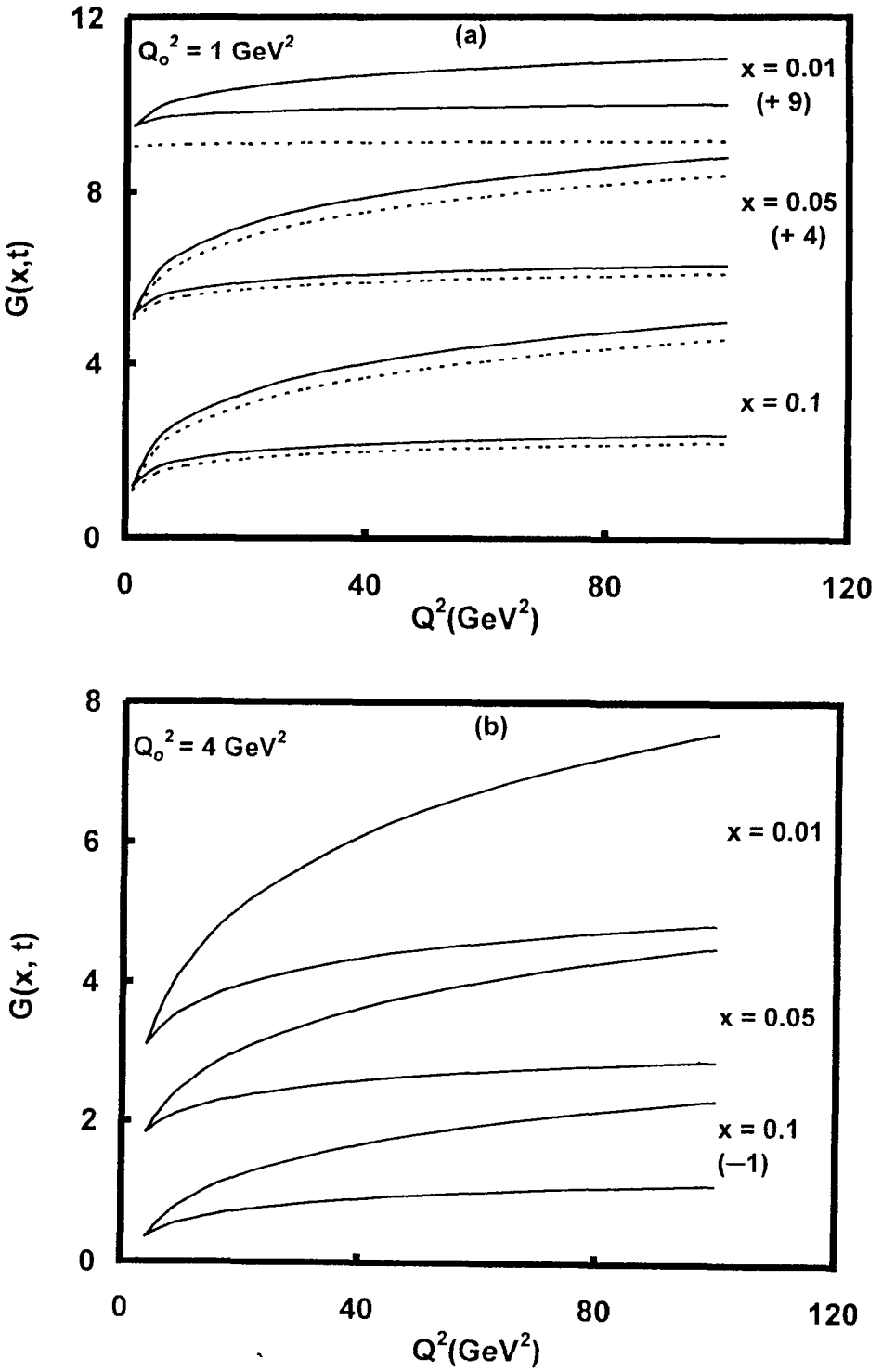

Fig.6.1 (a-b): t-Evolution of gluon structure functions.

In figure 6.1(a-b), we present our results of t-evolutions of gluon structure functions $G(x,$

t) qualitatively for the representative values of x given in the figures for y = 2 (upper solid and dashed lines) and y maximum (lower solid and dashed lines) in the $\beta = \alpha^{\gamma}$ relation.

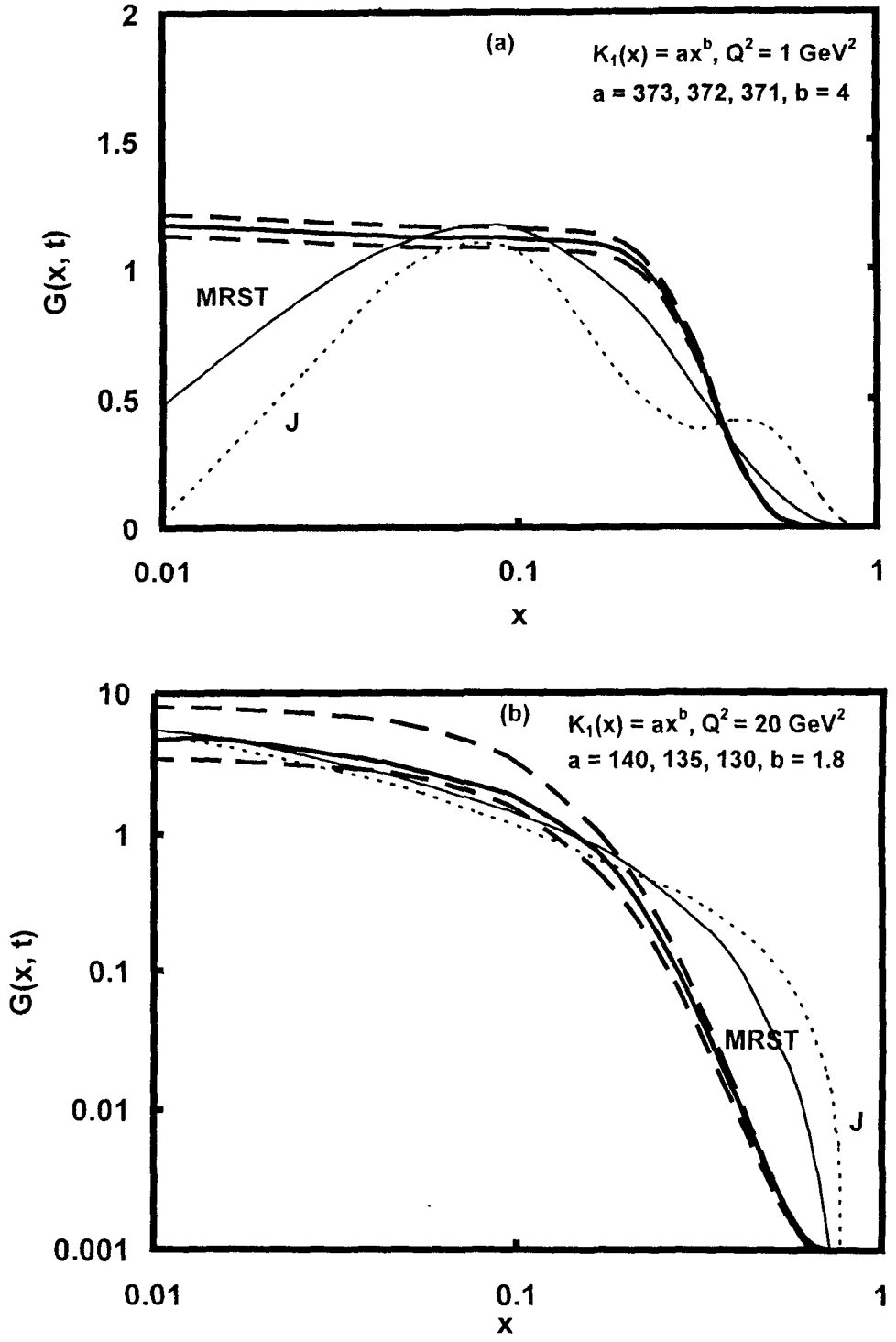

Fig.6.2 (a-b): x-Evolution of gluon structure functions and sensitivity of 'a'.

We have taken arbitrary inputs from recent global parameterizations MRST2001 (solid lines) and MRST2001J (dashed lines) in figure 6.1(a) at Q_0^2= 1 GeV^2 [96] and MRS data

in figure 6.1(b) at Q_0^2 = 4 GeV^2 [114]. It is clear from figures that t-evolutions of gluon structure functions depend upon input $G(x, t_0)$ values.

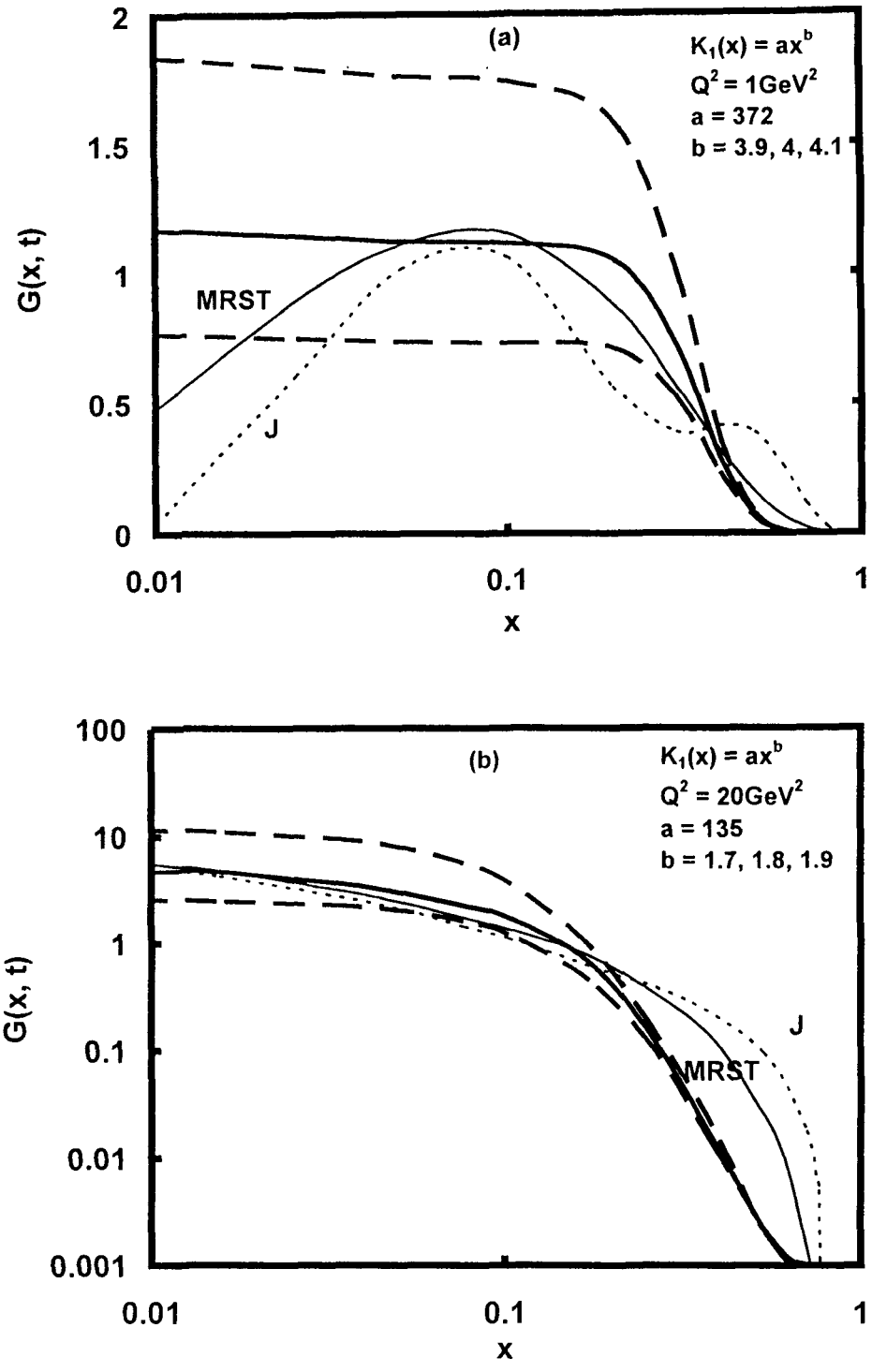

Fig.6.3 (a-b): x-Evolution of gluon structure functions and sensitivity of 'b'.

For a quantitative analysis of x distributions of gluon structure functions $G(x, t)$, we calculate the integrals that occurred in equation (6.14) for N_f= 4. In figure 6.2(a-b), we present our results of x-distribution of gluon structure functions for $K_1(x) = ax^b$, where 'a'

and 'b' are constants, for representative values of Q^2 given in each figure, and compare them with a recent global parameterization [96] for $y = 2$ in the relation $\beta = \alpha^y$. In figure 6.2 (a), we observe that agreement of the results with parameterization is found to be very poor for any values of 'a' and 'b' at low-x and agreement is found to be good at high-x at $a = 372$ and $b = 4$ (thick solid line). In figure 6.2(b), agreement of the results with parameterizations is found to be good at $a = 135$ and $b = 1.8$ (thick solid line) in the $\beta = \alpha^y$ relation. In the same figures, we present the sensitivity of our results for different values of 'a' (thick solid lines) at fixed value 'b'. Here we take $b = 4$ in figure 6.2(a) and $b = 1.8$ in figure 6.2(b). We observe that if value of 'a' is increased or decreased, the curve goes upward or downward direction respectively. But the nature of the curves is similar. Here thin solid and dotted lines are MRST2001 and MRST2001J [96] parameterizations.

In figure 6.3(a-b), we present the sensitivity of our results for different values of 'b' at fixed value of 'a'. Here we take $a = 372$ in figure 6.3(a) and $a = 135$ in figure 6.3(b). We observe that, agreement of the results (thick solid lines) with parameterizations is good in figure 6.3(a) at b = 4 and in figure 6.3(b) at $b = 1.8$. If value of 'b' is increased or decreased the curve goes downward or upward directions. But the nature of the curves is similar.

In figure 6.4(a-b), we present our results of x-evolution of gluon structure function $G(x, t)$ for $K_1(x) = ax^b$ for $y = 2$ (lower thick solid lines) and maximum (upper thick solid lines) in the relation $\beta = \alpha^y$ at same parameter values $a = 372$, $b = 4$ in figure 6.4(a) and $a = 135$, $b = 1.8$ in figure 6.4(b) and for representative values of Q^2 given in each figure, and compare them with a recent global parameterization [96]. We observe that result of x-evolution of gluon structure function for y maximum (long dashed lines) coincide with result of x-evolution of gluon structure function for $y = 2$ (lower thick solid lines) when $a = 375$, $b = 4.7$ in figure 6.4(a) and $a = 134$, $b = 2$ in figure 6.4(b). That means if y varies from minimum to maximum, then value of parameter 'a' varies from 372 to 375 and 'b' varies from 4 to 4.7 in figure 6.4(a) and 'a' varies from 135 to 134 and 'b' varies from 1.8 to 2 in figure 6.4(b).

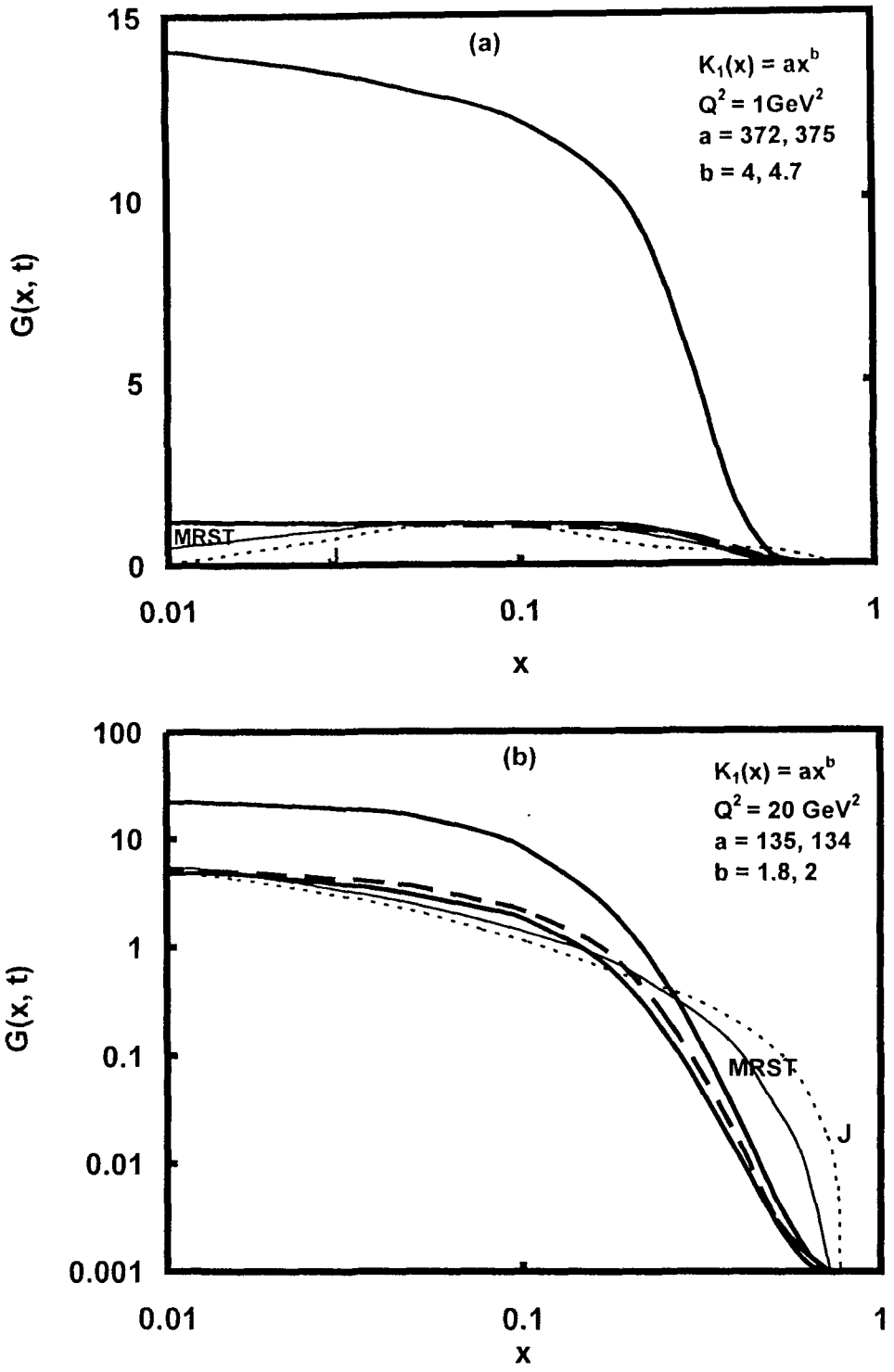

Fig.6.4 (a-b): x-Evolution of gluon structure functions at different parameter values of a, b.

In figure 6.5(a-b), we present our results of x-distribution of gluon structure functions $G(x, t)$ for $K_1(x) = ce^{-dx}$, where 'c' and 'd' are constants for representative values of Q^2 given in each figure, and compare them with a recent global parameterization [96] for $y = 2$ in the relation $\beta = \alpha^y$. In figure 6.5(a), we observe that agreement of the results with the parameterization is found to be very poor for any values of 'c' and 'd' at low-x and

agreement is found to be good at high-x at c = 300 and d = −3.8 (thick solid line). In figure 6.5(b), agreement of the results with parameterizations is found to be good at c = 5

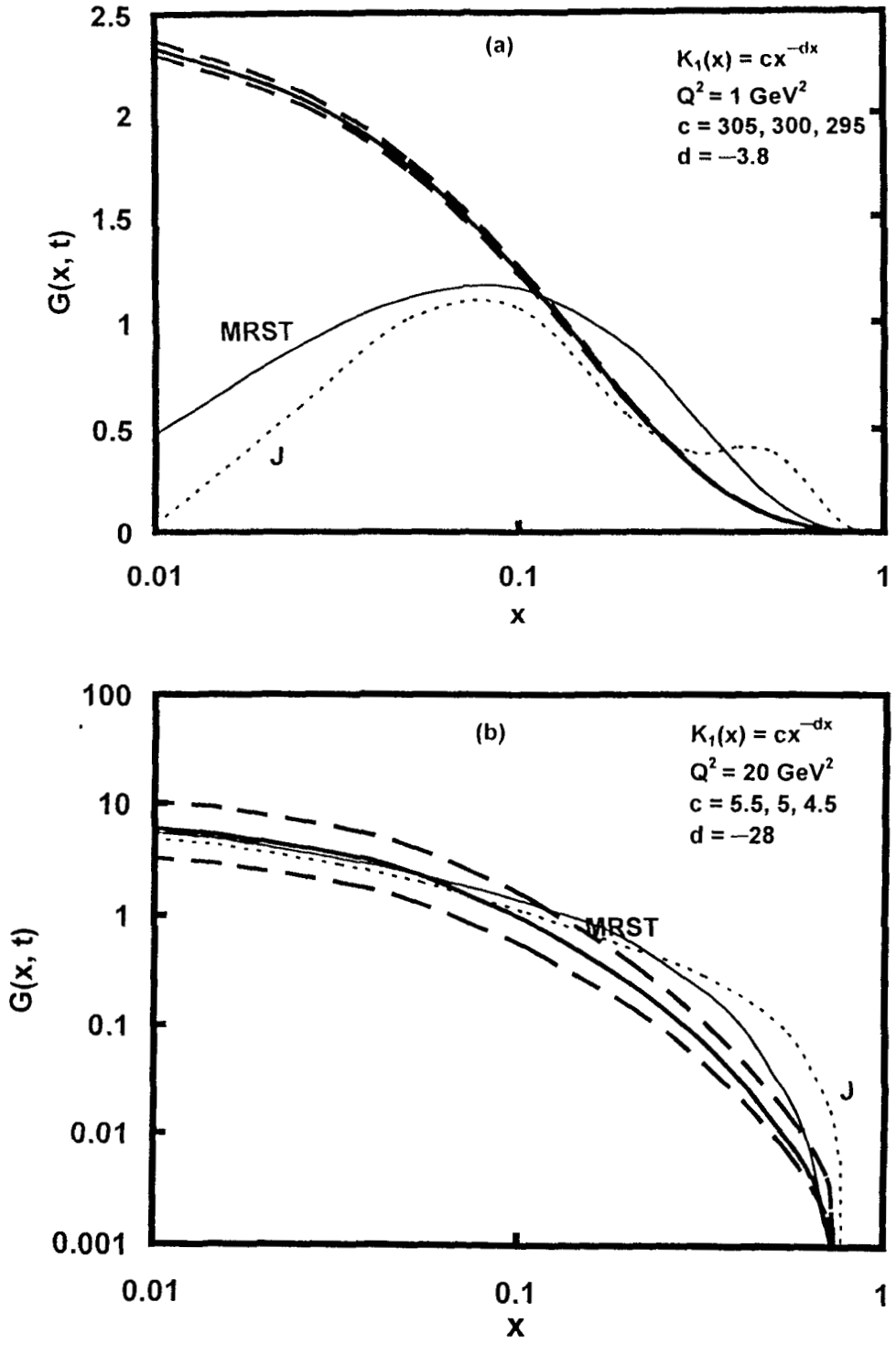

Fig.6.5 (a-b): x- Evolution of gluon structure functions and sensitivity of 'c'.

and d = −28 (thick solid line). In the same figures, we present the sensitivity of our results for different values of 'c' by thick dashed lines at fixed value 'd'. Here we take d = −3.8 in figure 6.5(a) and d = −28 in figure 6.5(b). We observe that, if value of 'c' is increased

or decreased, the curve goes upward or downward direction respectively. But the nature of the curve is similar.

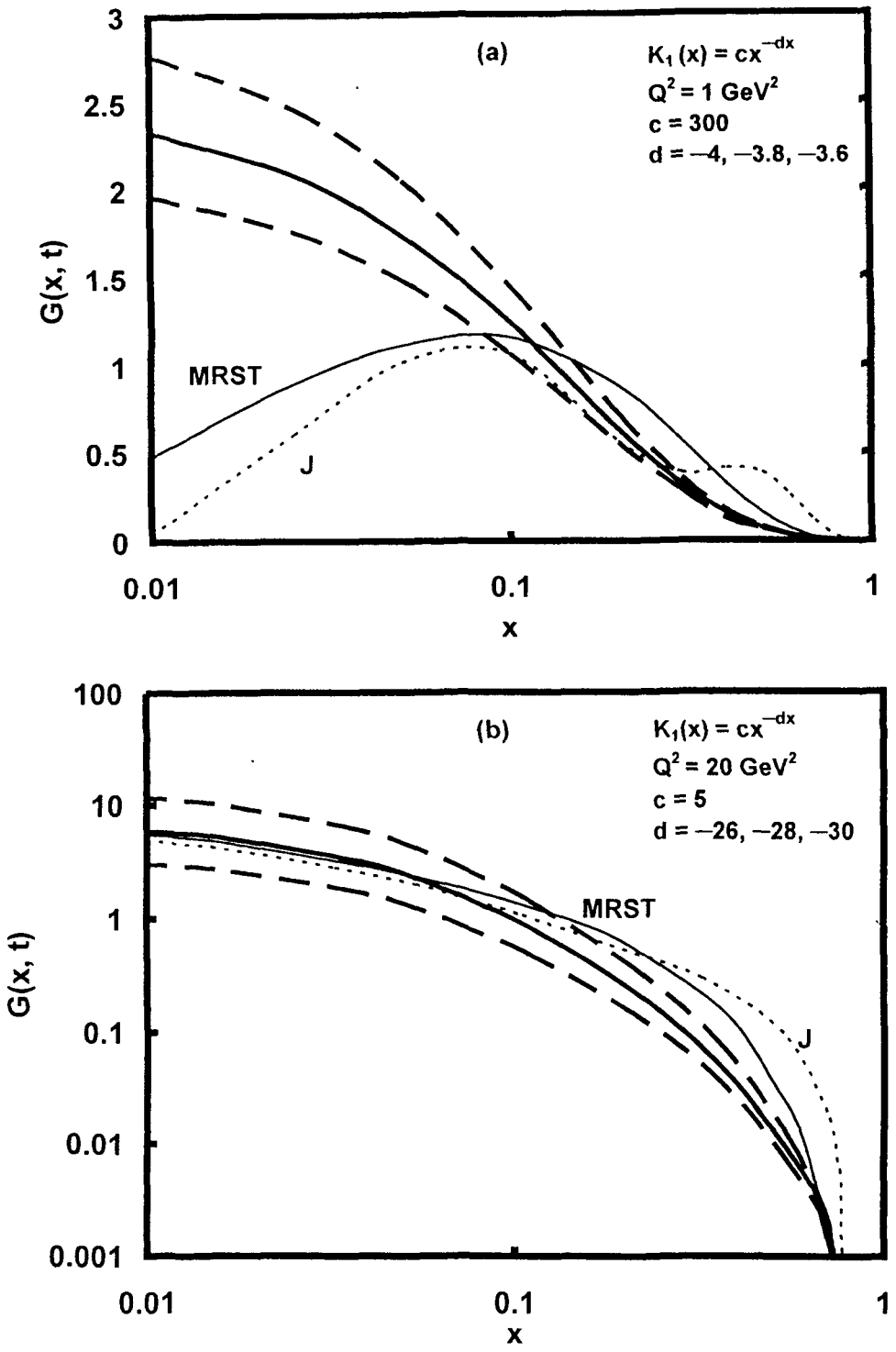

Fig.6.6 (a-b): x-Evolution of gluon structure functions and sensitivity of 'd'.

In figure 6.6(a-b), we present the sensitivity of our results for different values of '*d*' at fixed value of '*c*'. Here we take $c = 300$ in figure 6(a) and $c = 5$ in figure 6.6(b). We observe that, agreement of the results (thick solid lines) with the parameterization is good

in figure 6.6(a) at $d = -3.8$, and 6.6(b) at $d = -28$. If value of 'd' is increased or decreased, the curve goes downward or upward direction in figure 6.6(a), if value of 'd' is increased or decreased the curve goes upward or downward direction in figure 6.6(b) . But the nature of the curves is similar in both cases.

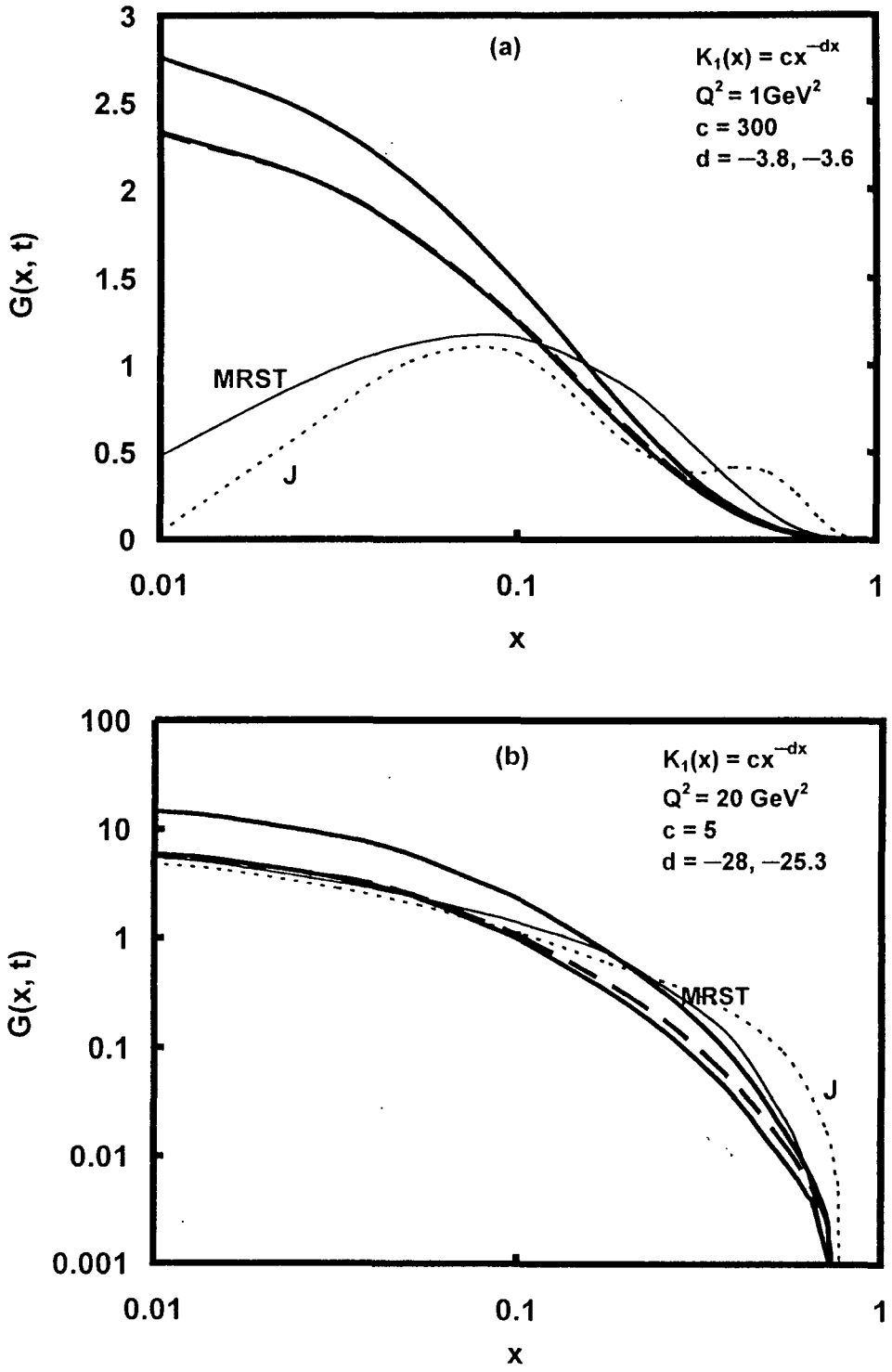

Fig.6.7 (a-b): x-Evolution of gluon structure functions at different parameter values of c, d.

In figure 6.7(a-b), we present our results of x-evolution of gluon structure function $G(x, t)$

for $K_1(x) = ce^{-dx}$ for $y = 2$ (lower thick solid lines) and maximum (upper thick solid lines) in the relation $\beta = \alpha^y$ at same parameter values $c = 300$, $d = -3.8$ in figure 6.7(a) and $c = 5$, $d = -28$ in figure 6.7(b) and for representative values of Q^2 given in each figure, and compare them with a recent global parameterization [96]. We observe that, result of x-evolution of gluon structure function, for y maximum (long dashed lines) coincide with result of x-evolution of gluon structure function for $y = 2$ (lower thick solid lines) when $c = 300$, $d = -3.6$ in figure 6.7(a) and $c = 5$, $d = -25.3$ in figure 6.7(b). That means if y varies from minimum to maximum, then value of parameter 'd' varies from -3.8 to -3.6 in figure 6.7(a) and from -28 to -25.3 in figure 6.7(b). In these cases, value of parameter 'c' remains constant. It is to be noted that, agreement of the results with the parameterization is found to be very poor for any constant value of $K_1(x)$. Therefore, we do not present our result of x-distribution at $K_1(x)$ = constant. Moreover, in general, the agreement of our results with the parameterization at small-x is poor for low-Q^2 value and excellent for high-Q^2 value which is quite expected.

It is to be noted that, agreement of the results with experimental data is found to be very poor for any constant value of $K_1(x)$. Therefore we do not present our result of x-distribution at $K_1(x)$ = constant in LO.

6.3. Conclusion

In this chapter, we obtain complete and unique solutions of gluon distribution function at low-x using Taylor's expansion method from GLDAP evolution equations and t and x-evolution of gluon structure functions in leading order. We compare our results with a global parameterization. In all the results from global fits, it is seen that, gluon structure functions increases when x decreases and Q^2 increases for fixed values of Q^2 and x respectively. It has been observed that, though we have derived a unique t-evolution for gluon in LO, yet we can not establish a completely unique x-evolution for gluon structure functions in LO due to the relation $K_1(x)$ between singlet and gluon structure functions. $K_1(x)$ may be in the forms of an exponential function or a power function and they can equally produce required x-distribution of gluon structure functions. But unlike many parameter arbitrary input x-distribution functions generally used in the literature, our method requires only one or two such parameters. □

Chapter-7

t AND x-EVOLUTIONS OF LIGHT SEA AND VALENCE QUARK STRUCTURE FUNCTIONS

In the previous chapters, particular and unique solutions of the Gribov-Lipatov-Dokshitzer-Altarelli-Parisi (GLDAP) [29-32] evolution equations for t and x-evolutions of singlet, non-singlet and gluon structure functions in leading order (LO) and next-to-leading order (NLO) at low-x have been reported. The same technique can be applied to the GLDAP evolution equations for light sea and valence quark structure functions in LO to obtain t and x-evolutions of light sea and valence quark structure functions. These LO results are compared with a recent global parameterization [96].

7.1. Theory

The GLDAP evolution equations for sea and valence quark structure functions in the standard forms are [131]

$$\frac{\partial F_2^S\left(x,Q^2\right)}{\partial \ln Q^2}-\frac{2\alpha_S(Q^2)}{3\pi}\left[\int_x^1\frac{dw}{1-w}\left\{\left(1+w^2\right)F_2^S\left(x/w,Q^2\right)-2F_2^S\left(x,Q^2\right)\right\}\right]+\frac{\alpha_S(Q^2)}{\pi} \tag{7.1}$$

$$\times\left[1+\frac{4\ln(1-x)}{3}\right]F_2^S(x,Q^2)+\frac{2\alpha_S(Q^2)}{3\pi}\left[\frac{3}{8}\left\{w^2+(1-w)^2\right\}\right]G(x/w,Q^2)=0$$

and

$$\frac{\partial F_2^v\left(x,Q^2\right)}{\partial \ln Q^2}-\frac{2\alpha_S(Q^2)}{3\pi}\left[\int_x^1\frac{dw}{1-w}\left\{\left(1+w^2\right)F_2^v\left(x/w,Q^2\right)-2F_2^v\left(x,Q^2\right)\right\}\right]+\frac{\alpha_S(Q^2)}{\pi} \tag{7.2}$$

$$\times\left[1+\frac{4\ln(1-x)}{3}\right]F_2^v(x,Q^2)=0,$$

where $F_2^s(x, Q^2) = xu_s, xd_s$ or $xs_s, F_2^v(x, Q^2) = xu_v$ or xd_v and

$$\frac{1}{\alpha_s(Q^2)} = \frac{33-2N_f}{12\pi}\ln\left(\frac{Q^2}{\Lambda^2}\right).$$

Taking $t = \ln(Q^2/\Lambda^2)$ and $A_f = 4/(33\text{-}2N_f)$, N_f being the number of flavours and Λ is the QCD cut off parameter, equations (7.1) and (7.2) become

$$\frac{\partial F_2^S(x,t)}{\partial t} - \frac{A_f}{t}\left[\{3+4\ln(1-x)\}F_2^S(x,t) + I_1^S(x,t) + I_2^S(x,t)\right] = 0 \tag{7.3}$$

and

$$\frac{\partial F_2^V(x,t)}{\partial t} - \frac{A_f}{t}\left[\{3+4\ln(1-x)\}F_2^V(x,t) + I^V(x,t)\right] = 0, \tag{7.4}$$

where

$$I_1^S(x,t) = 2\int_x^1 \frac{dw}{1\text{-}w}\left\{\left(1+w^2\right)F_2^S(x/w,t) - 2F_2^S(x,t)\right\}, \tag{7.5}$$

$$I_2^S(x,t) = \frac{3}{4}\int_x^1 \left\{w^2 + (1\text{-}w)^2\right\}G(x/w,t)dw \tag{7.6}$$

and

$$I^V(x,t) = 2\int_x^1 \frac{dw}{1\text{-}w}\left\{\left(1+w^2\right)F_2^V(x/w,t) - 2F_2^V(x,t)\right\}. \tag{7.7}$$

Now, using Taylor expansion method [80] and neglecting higher order terms of x as discussed in the Chapter-3, we can write $G(x/w, t)$ as

$$G(x/w,t) \cong G(x,t) + x\sum_{k=1}^{\infty} u^k \frac{\partial G(x,t)}{\partial x}.$$

Similarly, $F_2^S(x/w, t)$ and $F_2^V(x/w, t)$ can be approximated for small-x. Then putting these values of $F_2^S(x/w, t)$, $G(x/w, t)$ and $F_2^V(x/w, t)$ in equations (7.5), (7.6) and (7.7) and performing u-integrations we get

$$I_1^S = -\left[(1-x)(x+3)\right]F_2^S(x,t) + \left[2x\ln(1/x) + x\left(1-x^2\right)\right]\frac{\partial F_2^S(x,t)}{\partial x}, \tag{7.8}$$

$$I_2^S=\left[\frac{1}{4}(1-x)\left(2-x+2x^2\right)G(x,t)+\left\{-\frac{1}{4}x(1-x)\left(5-4x+2x^2\right)+\frac{3}{4}x\ln(1/x)\right\}\frac{\partial G(x,t)}{\partial x}\right] \tag{7.9}$$

and

$$I^V=-\left[(1-x)(x+3)F_2^V(x,t)\right]+\left[2x\ln(1/x)+x\left(1-x^2\right)\right]\frac{\partial F_2^V}{\partial x}. \tag{7.10}$$

Using equations (7.8) and (7.9) in equation (7.1) we have

$$\frac{\partial F_2^S(x,t)}{\partial t}-\frac{A_f}{t}\left[A(x)F_2^S(x,t)+B(x)\frac{\partial F_2^S(x,t)}{\partial x}+C(x)G(x,t)+D(x)\frac{\partial G(x,t)}{\partial x}\right]=0. \tag{7.11}$$

Let us assume for simplicity [86-88, 106-110]

$$G(x,t)=K(x)F_2^S(x,t), \tag{7.12}$$

where $K(x)$ is a function of x. Now equation (7.11) gives

$$\frac{\partial F_2^S(x,t)}{\partial t}-\frac{A_f}{t}[L(x)F_2^S(x,t)+M(x)\frac{\partial F_2^S(x,t)}{\partial x}]=0, \tag{7.13}$$

where

$A(x)=3+4\ln(1-x)-(1-x)(3+x)$, $B(x)=x(1-x^2)+2x\ln(1/x)$,

$C(x)=(1/4)(1-x)(2-x+2x^2)$, $D(x)=x[(-1/4)(1-x)(5-4x+2x^2)+(3/4)\ln(1/x)$,

$L(x)=A(x)+K(x)C(x)+D(x)\frac{\partial K(x)}{\partial x}$ and $M(x)=B(x)+K(x)D(x)$.

Secondly, using equation (7.10) in equation (7.2) we have

$$\frac{\partial F_2^V(x,t)}{\partial t}-\frac{A_f}{t}\left[P(x)F_2^V(x,t)+Q(x)\frac{\partial F_2^V(x,t)}{\partial x}\right]=0, \tag{7.14}$$

where

$P(x)=3+4\ln(1-x)-(1-x)(x+3)$ and

$Q(x)=x(1-x^2)-2x\ln x$.

The general solution of equation (7.13) is [80-81] $F(U, V)=0$, where F is an arbitrary function and $U(x, t, F_2)=C_1$ and $V(x, t, F_2)=C_2$ form a solution of equations

$$\frac{dx}{A_f M(x)} = \frac{dt}{-t} = \frac{dF_2^S(x,t)}{-A_f L(x) F_2^S(x,t)}. \tag{7.15}$$

Solving equations (7.15) we obtain

$$U\left(x,t,F_2^S\right) = t\exp\left[\frac{1}{A_f}\int\frac{1}{M(x)}dx\right] \quad \text{and} \quad V\left(x,t,F_2^S\right) = F_2^S(x,t)\exp\left[\int\frac{L(x)}{M(x)}dx\right].$$

If U and V are two independent solutions of equations (7.15), and if α and β are arbitrary constants, then $V = \alpha U + \beta$ may be taken as a complete solution of equation (7.14). Now the complete solution [80-81]

$$F_2^S(x,t)\exp\left[\int\frac{L(x)}{M(x)}dx\right] = \alpha t\exp\left[\frac{1}{A_f}\int\frac{1}{M(x)}dx\right] + \beta \tag{7.16}$$

is a two-parameter family of surfaces. The one parameter family determined by taking $\beta = \alpha^2$ has equation

$$F_2^S(x,t)\exp\left[\int\frac{L(x)}{M(x)}dx\right] = \alpha t\exp\left[\frac{1}{A_f}\int\frac{1}{M(x)}dx\right] + \alpha^2. \tag{7.17}$$

Differentiating equation (7.17) with respect to α, we get

$$\alpha = -\frac{1}{2}t\exp\left[\frac{1}{A_f}\int\frac{1}{M(x)}dx\right].$$

Putting the value of α in equation (7.17), we obtain the envelope

$$F_2^S(x,t) = -\frac{1}{4}t^2\exp\left[\int\left(\frac{2}{A_f M(x)} - \frac{L(x)}{M(x)}\right)dx\right], \tag{7.18}$$

which is merely a particular solution of the general solution. Now, defining

$$F_2^S(x,t_0) = -\frac{1}{4}t_0^2\exp\left[\int\left(\frac{2}{A_f M(x)} - \frac{L(x)}{M(x)}\right)dx\right],$$

at $t = t_0$, where $t_0 = \ln(Q_0^2/\Lambda^2)$ at any lower value $Q = Q_0$, we get from equation (7.18)

$$F_2^S(x,t) = F_2^S\left(x_0,t\left(\frac{t}{t0}\right)^2\right), \tag{7.19}$$

which gives the t-evolution of light sea quark structure function $F_2^s(x, t)$. Proceeding

exactly in the same way, and defining

$$F_2^v(x,t_0) = -\frac{1}{4}t_0^2 \exp\left[\int\left(\frac{2}{A_f Q(x)} - \frac{P(x)}{Q(x)}\right)dx\right],$$

we get

$$F_2^v(x,t) = F_2^v(x,t_0)\left(\frac{t}{t_0}\right)^2, \tag{7.20}$$

which gives the t-evolution of valence quark structure function $F_2^v(x, t)$. Again defining

$$F_2^S(x_0,t) = -\frac{1}{4}t^2 \exp\left[\int\left(\frac{2}{A_f M(x)} - \frac{L(x)}{M(x)}\right)dx\right]_{x=x_0},$$

we obtain from equation (7.18)

$$F_2^S(x,t) = F_2^S(x_0,t)\exp\left[\int_{x_0}^{x}\left(\frac{2}{A_f M(x)} - \frac{L(x)}{M(x)}\right)dx\right] \tag{7.21}$$

which gives the x-evolution of light sea quark function $F_2^s(x, t)$. Similarly defining

$$F_2^v(x_0,t) = -\frac{1}{4}t^2 \exp\left[\int\left(\frac{2}{A_f Q(x)} - \frac{P(x)}{Q(x)}\right)dx\right]_{x=x_0},$$

we get

$$F_2^v(x,t) = F_2^v(x_0,t)\exp\left[\int_{x_0}^{x}\left(\frac{2}{A_f Q(x)} - \frac{P(x)}{Q(x)}\right)dx\right]_{x=x_0}, \tag{7.22}$$

which gives the x-evolution of valence quark structure function $F_2^v(x, t)$.

For the particular solution of equation (7.13), we take $\beta = \alpha^2$ in equation (7.16). If we take $\beta = \alpha$ in equation (7.16) and differentiating with respect to α as before, we get

$$0 = t\exp\left[\frac{1}{A_f}\int\frac{1}{M(x)}dx\right] + 1$$

from which we can not determine the value of α. But if we take $\beta = \alpha^3$ in equation (7.16) and differentiating with respect to α, we get

$$\alpha = \sqrt{-\frac{1}{3} t \exp\left[\frac{1}{A_f}\int -\frac{1}{M(x)}dx\right]}.$$

Putting this value of α in equation (7.16), we get ultimately

$$F_2^S(x,t) = t^{3/2}\left\{\left(-\frac{1}{3}\right)^{1/2} + \left(-\frac{1}{3}\right)^{3/2}\right\}\exp\left[\int\left(\frac{3/2}{A_f M(x)} - \frac{L(x)}{M(x)}\right)dx\right].$$

Now, defining

$$F_2^S(x,t_0) = t_0^{3/2}\left\{\left(-\frac{1}{3}\right)^{1/2} + \left(-\frac{1}{3}\right)^{3/2}\right\}\exp\left[\int\left(\frac{3/2}{A_f M(x)} - \frac{L(x)}{M(x)}\right)dx\right],$$

we get

$$F_2^S(x,t) = F_2^S(x,t_0)\left(\frac{t}{t_0}\right)^{3/2},$$

which gives the t-evolution of light sea quark structure function $F_2^S(x, t)$. Proceeding exactly in the same way we get

$$F_2^V(x,t) = F_2^V(x,t_0)\left(\frac{t}{t_0}\right)^{3/2},$$

which gives the t-evolution of valence quark structure function $F_2^V(x, t)$.

Proceeding in the same way we get x-evolutions of light sea and valence quark structure functions as

$$F_2^S(x,t) = F_2^S(x_0,t)\exp\left[\int_{x_0}^{x}\left(\frac{3/2}{A_f M(x)} - \frac{L(x)}{M(x)}\right)dx\right]$$

and

$$F_2^V(x,t) = F_2^V(x_0,t)\exp\left[\int_{x_0}^{x}\left(\frac{3/2}{A_f Q(x)} - \frac{P(x)}{Q(x)}\right)dx\right]_{x=x_0}$$ respectively, and so on. So in

general, if we take $\beta = \alpha^3$, we get

$$F^{S,V}(x,t) = F^{S,V}(x,t_0)\left(\frac{t}{t_0}\right)^{y/(y-1)},$$

$$F_2^S(x,t) = F_2^S(x_0,t)\exp\left[\int_{x_0}^{x}\left(\frac{y/(y-1)}{A_f M(x)} - \frac{L(x)}{M(x)}\right)dx\right]$$

and

$$F_2^V(x,t) = F_2^V(x_0,t)\exp\left[\int_{x_0}^{x}\left(\frac{y/(y-1)}{A_f Q(x)} - \frac{P(x)}{Q(x)}\right)dx\right]_{x=x_0},$$

which are t and x-evolutions respectively of light sea and valence quark structure functions for $\beta = \alpha^y$ respectively. We observe, if $y \to \infty$ (very large), $y/(y-1) \to 1$.

Thus we observe that if we take $\beta = \alpha$ in equation (7.16), we can not obtain the value of α and also the required solution. But if we take $\beta = \alpha^2, \alpha^3, \alpha^4, \alpha^5$..... and so on, we see that the powers of (t/t_0) in t-evolutions and the numerators of the first term inside the integral for x-evolutions of valence and light sea quark structure functions are 2, 3/2, 4/3, 5/4....and so on respectively as discussed above. Thus we see that if in the relation $\beta = \alpha^y$, y varies between 2 to a maximum value, the powers of (t/t_0) varies between 2 to 1, and the numerator of the first term in the integral sign varies between 2 to 1. Then it is understood that the solutions of equations (7.13) and (7.14) obtained by this method are not unique and so the t-evolutions and x-evolutions of valence and light sea quark structure functions obtained by this methodology are not unique. Thus by this methodology, instead of having a single solution we arrive a band of solutions, of course the range for these solutions is reasonably narrow.

Since the value of Λ is so small that we can take at $Q = \Lambda$, $F_2^S(x, t)$ or $F_2^V(x, t) = 0$ due to conservation of the electromagnetic current [111] and at small-x valence quark structure function must vanish. This dynamical prediction agrees with most ad hoc parameterizations and with the data [17, 111]. Using this boundary condition in equation (7.16) we get $\beta = 0$ and

$$F_2^S(x,t) = \alpha t \exp\left[\int\left(\frac{1}{A_f M(x)} - \frac{L(x)}{M(x)}\right)dx\right]. \tag{7.23}$$

Now, defining

$$F_2^S(x,t_0) = \alpha t_0 \exp\left[\int\left(\frac{1}{A_f M(x)} - \frac{L(x)}{M(x)}\right)dx\right],$$

at $t = t_0$, where, $t_0 = \ln(Q_0^2/\Lambda^2)$ at any lower value $Q = Q_0$, we get from equation (7.23)

$$F_2^S(x,t) = F_2^S(x,t)\left(\frac{t}{t_0}\right), \tag{7.24}$$

which gives the t-evolutions of light sea quark structure function in LO.

Again defining,

$$F_2^S(x_0,t) = \alpha t \exp\left[\int\left(\frac{1}{A_f M(x)} - \frac{L(x)}{M(x)}\right)dx\right]_{x=x_0}$$

we obtain from equation (7.23)

$$F_2^S(x,t) = F_2^S(x_0,t)\exp\left[\int_{x_0}^{x}\left(\frac{1}{A_f M(x)} - \frac{L(x)}{M(x)}\right)dx\right], \tag{7.25}$$

which gives the x-evolutions of light sea quark structure functions in LO. Similarly we get for valence quark

$$F_2^V(x,t) = F_2^V(x,t_0)\left(\frac{t}{t_0}\right) \tag{7.26}$$

and

$$F_2^V(x,t) = F_2^V(x_0,t)\exp\left[\int_{x_0}^{x}\left(\frac{1}{A_f Q(x)} - \frac{P(x)}{Q(x)}\right)dx\right]. \tag{7.27}$$

We observed that unique solutions (equations (7.24), (7.25), (7.26) and (7.27)) of GLDAP evolution equations for valence and light sea quark structure functions are same with particular solutions for y maximum in the $\beta = \alpha^y$ relation in LO.

7.2. Results and Discussion

In this chapter, we present our result of t-evolution of light sea and valence quark structure functions qualitatively and compare result of x-evolution with a recent global

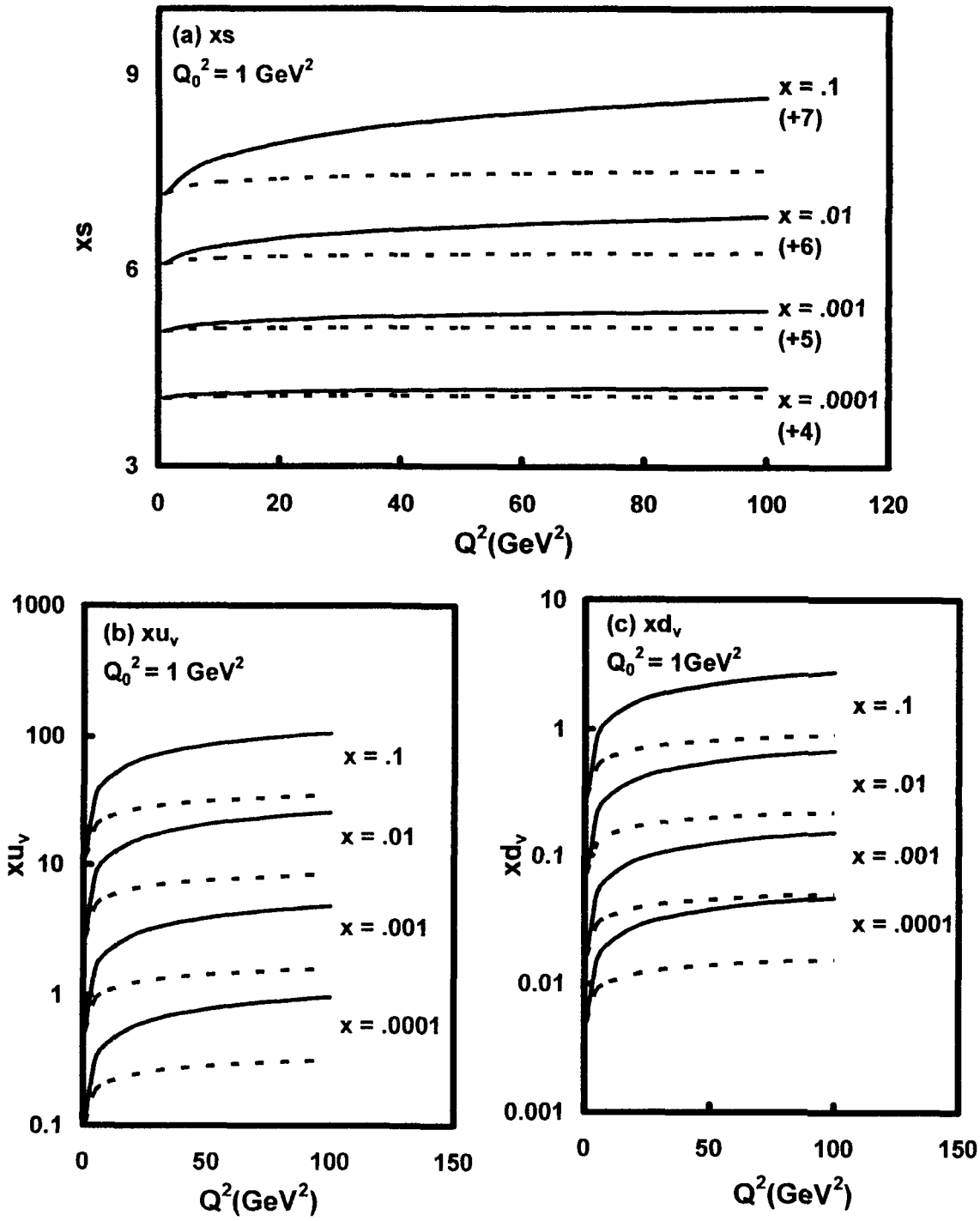

Fig.7.1 (a-c): t-Evolution of light sea and valence quark structure functions.

parameterization [96]. This parameterization includes data from H1, ZEUS, NMC, BCDMS, SLAC, E665, CCFR, E605, and CDF experiments [95, 97-102, 117-124].

Though we present our results of t-evolution with $y = 2$ and y = maximum in the $\beta - \alpha^y$ relation, our result with y = maximum is equivalent to that of unique solution and results of x-evolution for $y = 2$ and y maximum in the $\beta - \alpha^y$ relation have not any significant difference

In figure 7.1(a-c), we present our results of t-evolutions of light sea and valence quark structure functions qualitatively for the representative values of x given in the figures for $y = 2$ (solid lines) and y maximum (dashed lines) in the $\beta = \alpha^y$ relation. We have taken arbitrary inputs from a recent global parameterization MRST2001 [96] at $Q_0^2 = 1$ GeV^2. It is clear from figures that t-evolutions of light sea and valence quark structure functions depend upon input $F_2^s(x, t_0)$ and $F_2^v(x, t_0)$ values. Unique solutions of t-evolution for light sea and valence quark structure functions are same with particular solutions for y maximum in the $\beta = \alpha^y$ relation in LO.

For a quantitative analysis of x-distributions of light sea quark structure functions, we calculate the integrals that occurred in equation (7.21) for $N_f = 4$. In figure 7.2 (a-b), we present our results for $K(x)$ = constant for representative values of $Q^2 = 10$ GeV^2 (figure 7.2(a)) and $Q^2 = 10^4$ GeV^2 (figure 7.2(b)) and compare them with a recent global parameterization (thin solid lines) [96] in the relation $\beta = \alpha^y$ for $y = 2$ (thick solid lines). Since our theory is in small-x region and does not explain the peak portion for u & d, so a point for x-value just below 0.1 for s and 0.01 for u & d has been taken as input to test the evolution equation. We observe that agreement of the results (thick solid line) with parameterization is found to be good at $K(x) \approx 68, 590$ for u & d and $K(x) \approx 210, 520$ for s in figure 7.2(a) and figure 7.2(b) respectively. In the same figures we present the sensitivity of our results (dashed lines) for different constant values of $K(x)$. We observe that if value of $K(x)$ is increased or decreased, the curve goes upward or downward direction respectively. But the nature of the curve is similar.

In figures 7.3(a-b) and 7.4(a-b), we present our results of x-distribution of light sea quark structure functions for $K(x) = ax^b$, where 'a' and 'b' are constants for representative values of $Q^2 = 10$ GeV^2 (figure 7.3(a-b)) and $Q^2 = 10^4$ GeV^2 (figure 7.4(a-b)) and compare them with recent global parameterizations (thin solid lines) [96] in the relation

$\beta=\alpha^y$ for $y = 2$ (thick solid lines). Since our theory is in small-x region and does not explain the peak portion for u & d, so a point for x-value just below 0.1 for s and 0.01 for

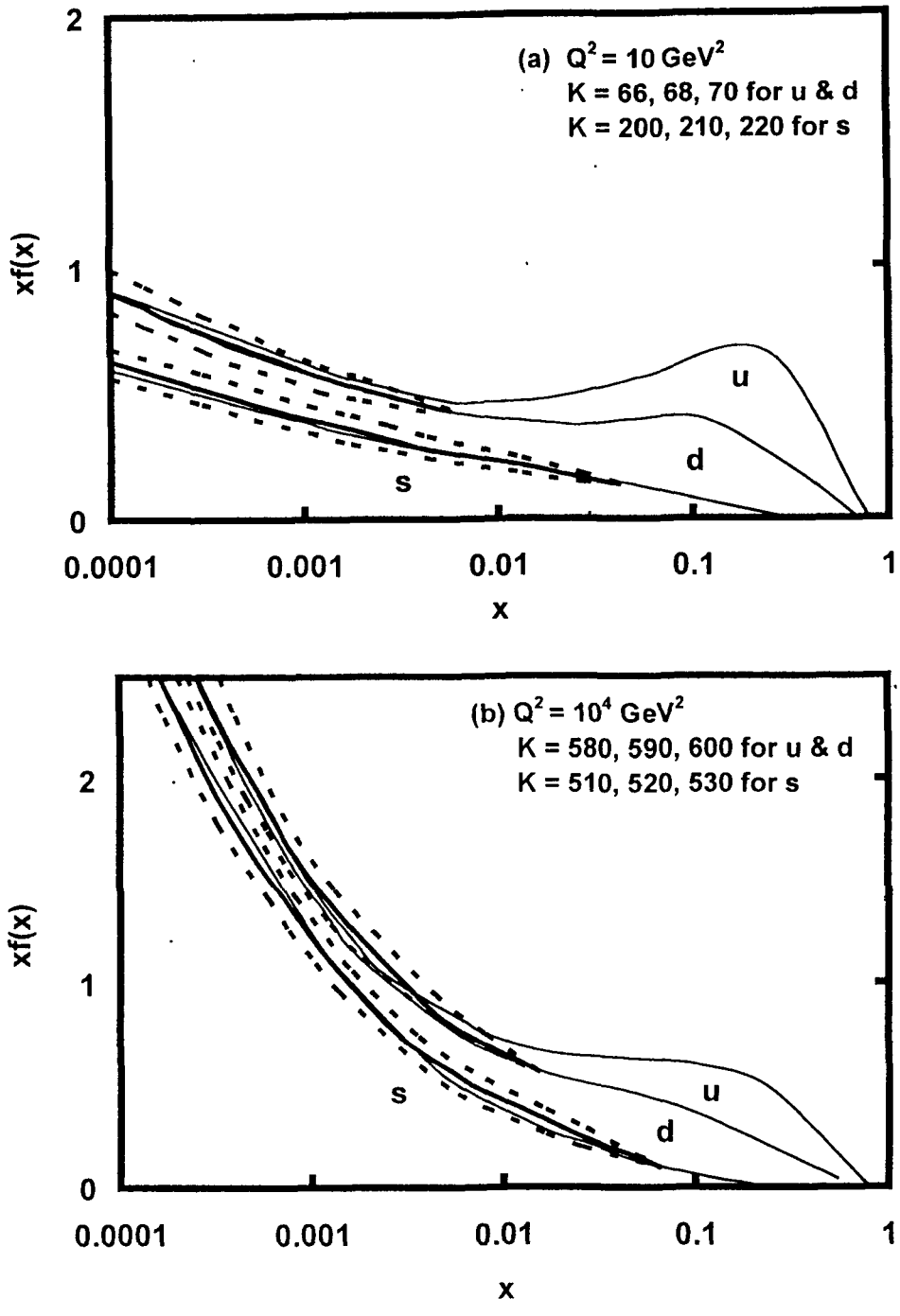

Fig.7.2 (a-b): x-Evolution of light sea quark structure functions and sensitivity of 'K'.

u & d has been taken as input to test the evolution equation (7.21). We observe that agreement of the results (thick solid line) with the parameterization is found to be good at

a =135 & b = 0.33 for u & d and a = 130 & b = 0.35 for s at Q^2 = 10 GeV^2 in figure 7.3(a-b) and a = 211 & b = 0.25 for u & d and a = 260 & b = 0.29 for s at Q^2 = 10^4 GeV^2 in figure 7.4(a-b). In the same figures, we present the sensitivity of our results (dashed lines) for different values of 'a' and 'b'. Here we take b = 0.33, 0.35 in figure 7.3(a) and b

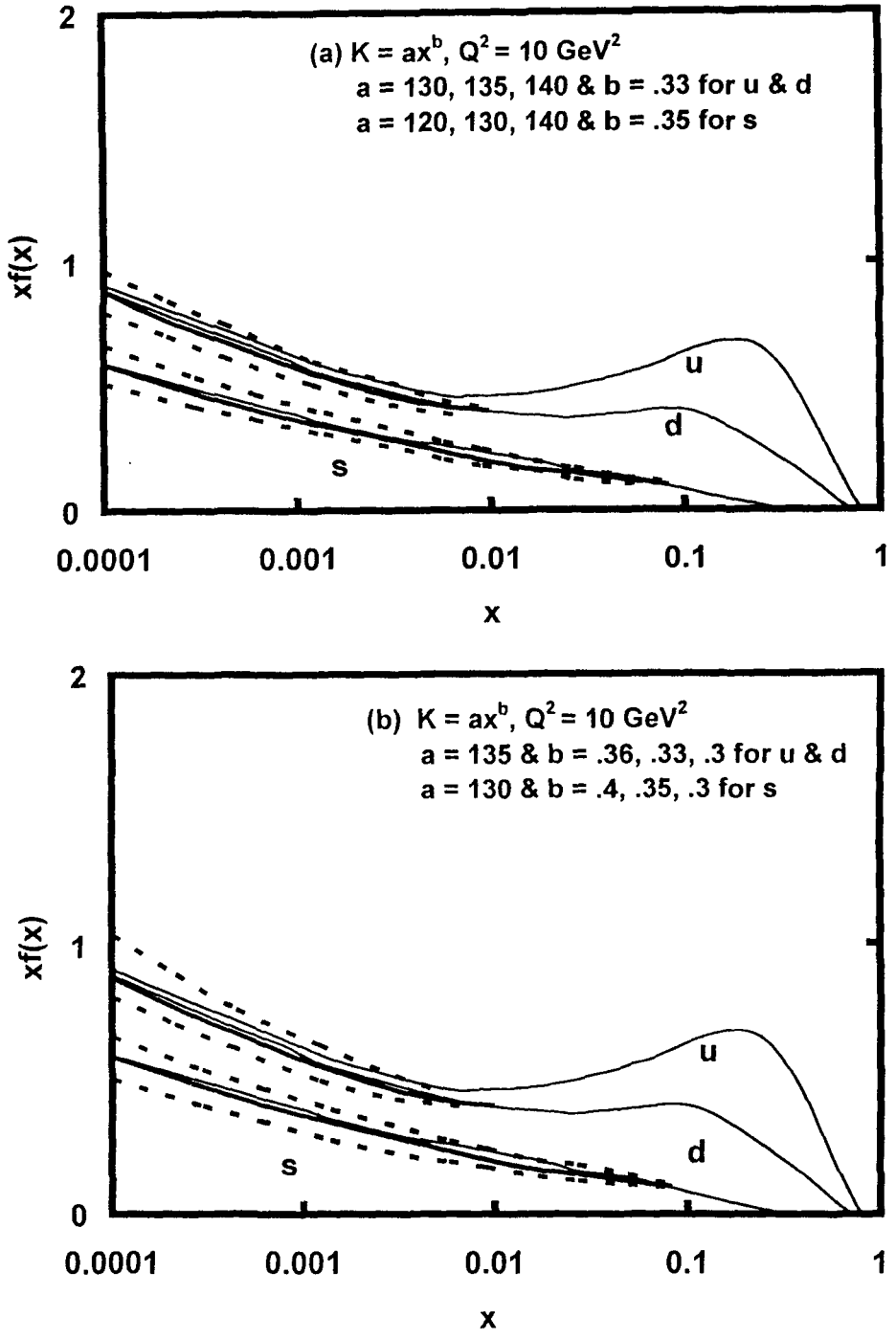

Fig.7.3 (a-b): x-Evolution of light sea quark structure functions and sensitivity of 'a' and 'b'.

= 0.25, 0.29 in figure 7.4(a). We observe that if value of 'a' is increased or decreased, the curve goes upward or downward direction. But the nature of the curve is similar. In

figure7.3 (b) and figure 7.4(b), we present the sensitivity of our results (dashed lines) for different values of '*b*' at fixed value of '*a*'. Here we take *a* = 135, 130 in figure 7.3(b) and *a* = 211, 260 in figure 7.4(b). We observe that at *b* = 0.33 & 0.35, agreement of the results

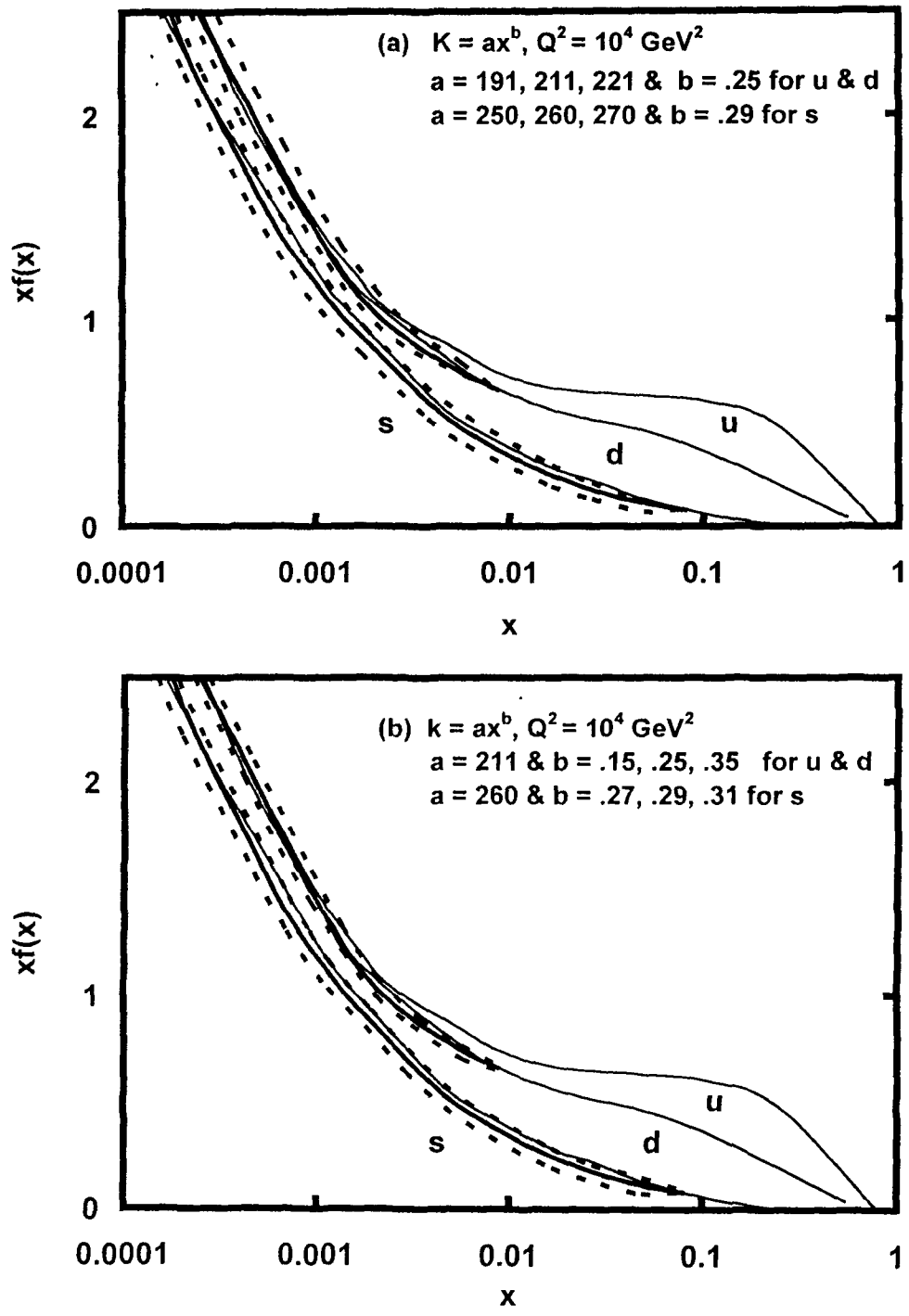

Fig.7.4 (a-b): x-Evolution of light sea quark structure functions and sensitivity of 'a' and 'b'.

(thick solid lines) with the parameterization is found to be good in figure 7.3(b) and at *b* = 0.25 & 0.29, agreement of the results (thick solid lines) with parameterizations data is

found to be excellent in figure 7.4(b). If value of '*b*' is increased or decreased the curve goes downward or upward direction. But the nature of the curve is similar.

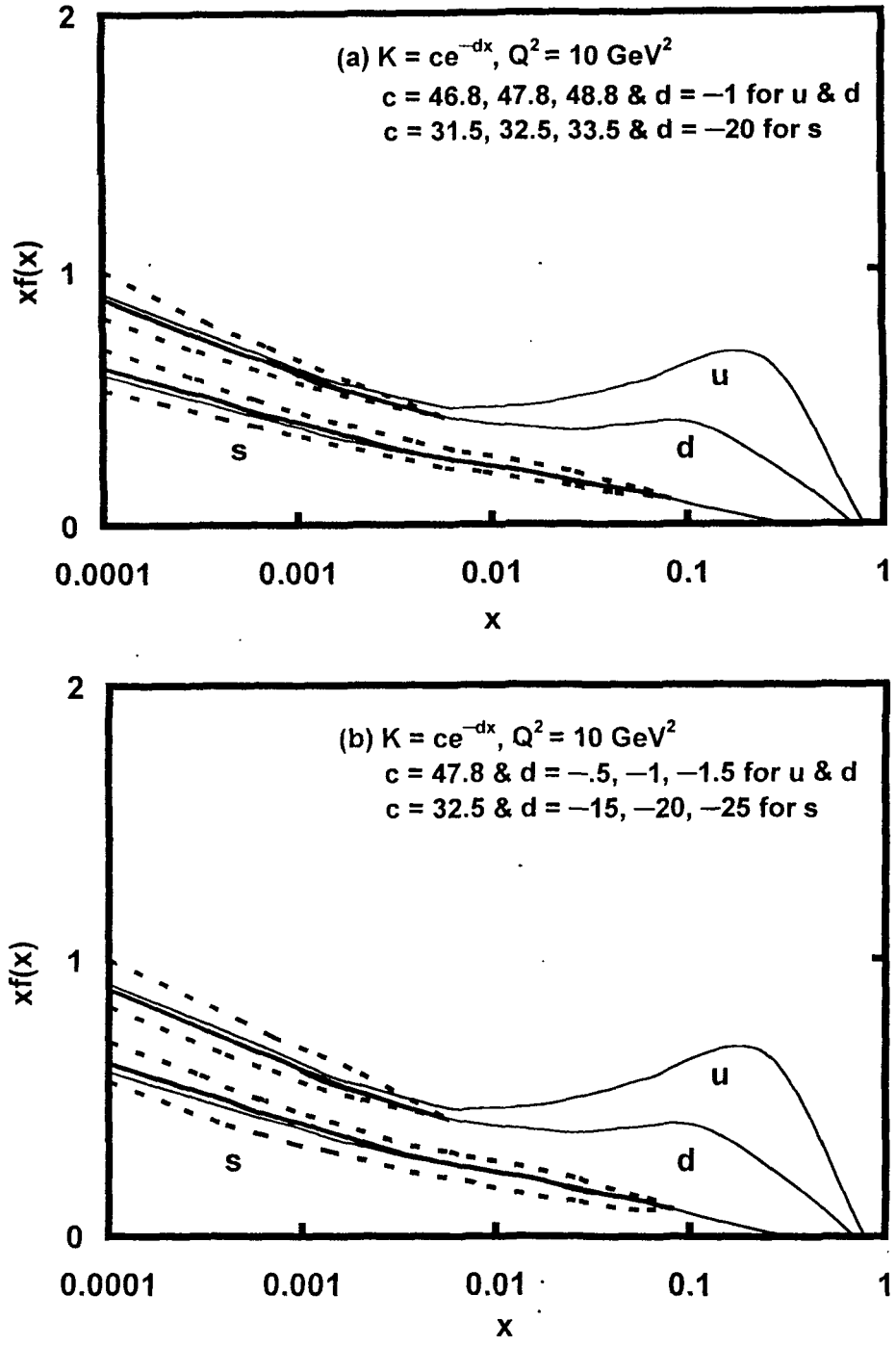

Fig.7.5 (a-b): x-Evolution of light sea quark structure functions and sensitivity of 'c' and 'd'.

In figures 7.5(a-b) and 7.6(a-b) we present our results of x-distribution of light sea quark structure functions for $K(x) = ce^{-dx}$, where 'c' and 'd' are constants for representative values of $Q^2 = 10$ GeV^2 (figure 7.5(a-b)) and $Q^2 = 10^4$ GeV^2 (figure 7.6(a-b)) and

compare them with a recent global parameterization (thin solid lines) [96] in the relation $\beta = \alpha^{y}$ for $y = 2$ (thick solid lines). Since our theory is in small-x region and does not explain the peak portion for u & d, so a point for x-value just below 0.1 for s and 0.01 for u & d has been taken as input to test the evolution equation (7.21). We observe that

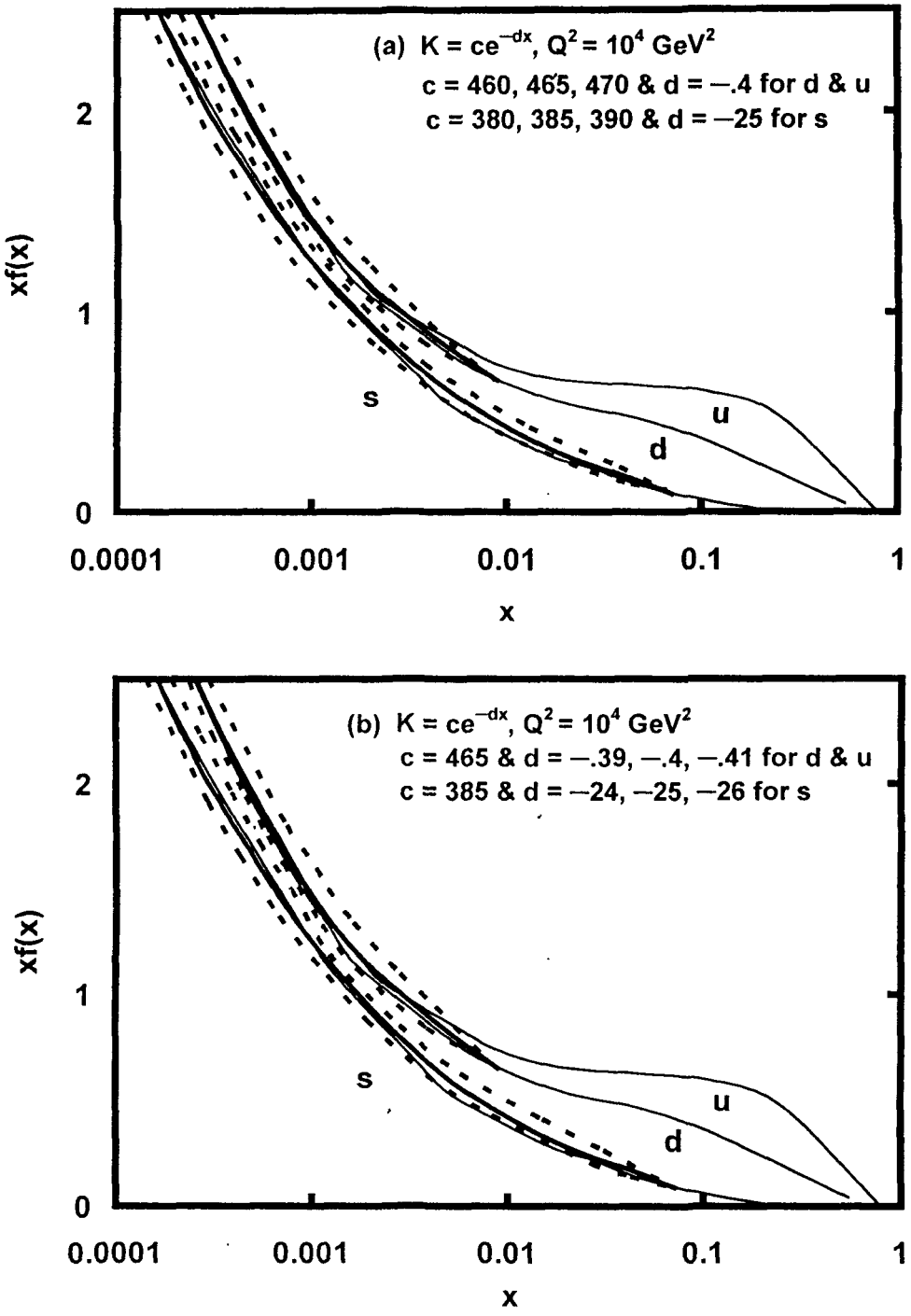

Fig.7.6 (a-b): x-Evolution of light sea quark structure functions and sensitivity of 'c' and 'd'.

agreement of the results (thick solid line) with parameterization is found to be good at $c = 47.8$ & $d = -1$ for u, d and $c = 32.5$ & $d = -20$ for s at $Q^2 = 10$ GeV^2 in figure 7.5(a-b)

and c = 465 & d = -.4 for u ,d and c = 385 & d = −25 for s at $Q^2 = 10^4$ GeV^2 in figure 7.6(a-b). In the same figures we present the sensitivity of our results (by dashed lines) for different values of 'c' and 'd'. Here we take d = −1, −20 in figure 7.5(a) and d = .4, -25 in figure 7.6(a). We observe that if value of 'c' is increased or decreased, the curve goes upward or downward direction. But the nature of the curve is similar. In figure 7.5(b) and figure 7.6 (b), we present the sensitivity of our results (dashed lines) for different values of 'd' at fixed value of 'c'. Here we take c = 47.8, 32.5 in figure 7.5(b) and c = 465, 385 in figure 7.4(b). We observe that at d = −1, & −20, agreement of the results (thick solid lines) with parameterizations data is found to be good in figure 7.5(b) and at d .4 & −25, agreement of the results (thick solid lines) with the parameterization is found to be excellent in figure 7.6(b). If value of 'd' is increased or decreased the curve goes upward or downward direction. But the nature of the curve is similar. We observe that for x-evolutions of light sea quark structure functions, results for $y = 2$ and maximum in the $\beta = \alpha^y$ relation in LO have not any significant difference. It is to be noted that unique solutions of evolution equations for light sea and valence quark structure functions are same with particular solutions for y maximum in $\beta = \alpha^y$ relation in LO.

From our above discussion, it has been observed that though we can derive a complete unique t-evolution for light sea and valence quark structure functions in LO, yet we can not establish a complete unique x-evolution for light sea quark structure function in LO due to the presence of $K(x)$. $K(x)$, the relation between light sea quark and gluon structure functions, may be in the forms of a constant, an exponential function of x or a power in x and they can equally produce required x-distribution of light sea quark. On the other hand, the explicit form of $K(x)$ can actually be obtained only by solving coupled GLDAP evolution equations for singlet and gluon structure functions, and works are going on in this regard.

7.3. Conclusion

In this chapter, we obtain complete, particular and unique solutions of light sea quark and valence quark distribution functions at low-x using Taylor's expansion method from GLDAP evolution equations and t-evolution of light sea and valence quark structure functions and x- evolution of light sea quark structure function in LO. We compare our

results with a global parameterization. In all the results from global fits, it is seen that light sea and valence quark structure functions increases when x decreases and Q^2 increases for fixed values of Q^2 and x respectively. It has been observed that, though we have derived a unique t-evolution for light sea and valence quark structure functions in LO, yet we can not establish a completely unique x-evolution for light sea quark structure functions in LO due to the relation $K(x)$ between singlet and gluon structure functions. $K(x)$ may be in the forms of a constant, an exponential function or a power function and they can equally produce required x-distribution of light sea quark structure functions. But unlike many parameter arbitrary input x-distribution functions generally used in the literature, our method requires only one or two such parameters. □

Chapter-8

CONCLUSION

This thesis deals with proton, neutron as well as deuteron structure functions determined from deep inelastic scattering experiments approximated for low-x region. Structure functions are calculated from complete, particular and unique solutions of GLDAP evolution equations which are deduced from pertubative quantum chromodynamics. t and x-evolutions of structure functions at low-x region are predicted. Theoretical predictions are compared with experimental data and recent global parameterizations.

In the Chapter-1, we present a brief introduction of the problem. Quark and gluon distribution functions at low-x are important for understanding of the inner structure of hadrons and for examination of quantum Chromodynamics, the underlying dynamics of quarks and gluons. Gluons are expected to be dominant in the low-x region. In addition to that, quark and gluon distributions are important inputs in many high energy processes. On the other hand, gluon distribution cannot be measured directly from experiment. It is therefore, important to measure gluon distribution function indirectly from quark structure function. In this chapter, we discuss about structure of matter, lepton-nucleon interactions, small-x physics, evolution equations and experimental overview of structure functions. In the Chapter-2, we discuss about the Taylor expansion method, complete and particular solutions of first order linear partial differential equation and several methods of numerical integrations which will be used in subsequent chapters. In the Chapter-3, we discuss briefly about the t-evolutions of deuteron, proton, neutron, difference and ratio of proton and neutron and x-evolution of deuteron structure functions at low-x. We consider the leading order GLDAP evolution equation for singlet and non-singlet structure functions and obtained complete and particular solution by solving it by applying Taylor expansion method. We compare our results with recent standard parametrizations and make predictions for the NMC and HERA data. And also we compare our results with those of earlier approximate solutions of GLDAP evolution equations. In the Chapter-4, we discuss briefly about the t evolutions of deuteron, proton, neutron, difference and ratio

of proton and neutron and x-evolution of deuteron structure functions at low-x as in the Chapter-3. But here we consider the next-to-leading order GLDAP evolution equation for singlet and non-singlet structure functions and obtained complete and particular solution by solving it applying Taylor expansion method. We compare our results with recent standard parametrizations and make predictions for the NMC and HERA data. And also we compare our results with those of leading order results. In the Chapter-5, we discuss briefly about the t-evolutions of deuteron, proton, neutron, difference and ratio of proton and neutron and x-evolution of deuteron structure functions at low-x as in the Chapter-3. But here we consider the leading order and next-to-leading order GLDAP evolution equation for singlet and non-singlet structure functions and obtained complete and unique solutions by solving it applying Taylor expansion method and applying boundary conditions. We compare our results with recent standard parametrizations and make predictions for the NMC and HERA data. In the Chapter-6, we discuss briefly about the t and x-evolutions of gluon structure function at low-x. We consider the leading order GLDAP evolution equation for gluon distribution function and obtained complete, particular and unique solutions by solving it applying Taylor expansion method and boundary conditions. We compare our results with recent standard parametrizations. In the Chapter-7, we discuss briefly about the t and x-evolutions of light sea and valence quark structure functions at low-x. We consider the leading order GLDAP evolution equation for light sea and valence quark structure functions and obtained complete, particular and unique solutions by solving it applying Taylor expansion method and boundary conditions. We compare our results with recent standard parametrizations.

In all the results from experiments as well as global fits, it is seen that all the mentioned structure functions increase when x decreases and Q^2 increases for fixed values of Q^2 and x respectively in general. It is observed that the results from our methods are also generally comparable with those of experiments as well as global fits. We observe that x-evolution results of deuteron and light sea quark structure functions for $y = 2$ and y maximum in the $\beta = \alpha^y$ relation in leading order have not any significant differences. It has been observed that though we have derived unique t-evolutions for deuteron, proton, neutron, and difference and ratio of proton and neutron structure functions in leading order and next-to-leading order and gluon, sea and valence quark structure functions in leading order , yet we can not establish completely unique x-evolutions for deuteron

structure function in leading order and next-to-leading order and gluon and sea quark structure functions in leading order due to the relation $K(x)$ between singlet and gluon structure functions. $K(x)$ may be in the forms of a constant, an exponential function or a power function and they can equally produce required x-distribution of deuteron or gluon structure functions. But unlike many parameter arbitrary input x-distribution functions generally used in the literature, our method requires only one or two such parameters. On the other hand, our methods are mathematically simpler with less number of approximations. Explicit form of $K(x)$ can actually be obtained only by solving coupled GLDAP evolution equations for singlet and gluon structure functions, and works are going on in this regard as mentioned in the Chapter-5.□

REFERENCES

[1] D Griffiths, 'Introduction to Elementary Particles', John Wiley & Sons, New York (1987).

[2] V E Levin, 'Nuclear Physics and Nuclear Reactors', MIR Publishers, Moscow (1981).

[3] R C Sharma, 'Nuclear Physics', K Nath & Co., Meerut-2. U. P. (1982).

[4] B N Srivastaba, 'Basic Nuclear Physics', Pragati Prakashan, Meerut, India (1990).

[5] G I Kopylov, 'Elementary Kinematics of Elementary Particles', Mir Publishers, Moscow (1983).

[6] B. Lal and N. Subrahmanyam, 'Atomic and Nuclear Physics', S. Chand & Company Ltd., India (1986).

[7] F Halzen and A D Martin, 'Quarks and Lepton, An Introductory Course in Modern Particle Physics', John Wiley and Sons, New York (1990).

[8] P D B Collins, A D Martin and R H Dalitz, 'Hadron Interactions', Adam Hilger Ltd., Bristol, (1984).

[9] C. Sutton, 'Elementary Particles', Encyclopedia Britannica, 1994-2001(2001).

[10] 'Elementary Particles', Encyclopedia, Microsoft® Encarta® 1993-2001(2001).

[11] Greiner and Schafer, 'Quantum Chromodynamics', Springer-Verlag, New York, Berlin, Heidlegberg (1995).

[12] Physics of Leptons, Proceedings of the XXV SLAC summer institute on Particle Physics, SLAC, California (1997).

[13] M Breidenbach et al., Phys. Rev. Lett. **23** (1969)935.

[14] W J Stirling in Proc. of the 1999 European School of High Energy Physics, Ed. A Olchevski, CERN, Geneva (2000)305.

[15] J Feltesse, Proceedings of the Lepton Photon Conference 1989, SLAC, ed. M Riordan (1989)13.

[16] P Amaudruz et al, NMC Collaboration, CERN PPE-**92-124**.

[17] E Reya, Phys. Rep. **69** (1981) 195.

[18] B Foster, International Journal of Modern Physics **A 13**, No. 10(1998)1543.

[19] G Wolf, 'First Results from HERA', DESY **92-190** (1992).

[20] V D Darger and R J N Philips, 'Collider Physics', West View Press, Oxford (1991).

[21] J F Douogue, E Golowich, B R Holstein, 'Dynamics of the Standard Model', Cambridge (1996).

[22] G Jariskog and D Rein, eds, Proc. 'Large Hardon Collider Workshop', CERN report, CERN **90-10**, (1990).

[23] Ya Ya Balitskij and L N Lipatov, Sov. J. Nucl. Phys. **28** (1978) 822.

[24] E A Kuraev, L N Lipatov and V S Fadin, Sov. Phys. JETP **44** (1976) 443.

[25] E A Kuraev, L N Lipatov and V S Fadin, Sov. Phys. JETP **45** (1977) 199.

[26] A D Martin, 'Small-x Physics', DTP/**92/70** (1992).

[27] B Andersson et al., 'Small-x Phenomenology Summary and Status', DESY **02-041**, hep-ph/0204115 (2002).

[28] A Ali and J Bartels, eds. Proc 'DESY-Topical Meeting on the Small-x Behaviour of Deep Inelastic Structure Functions in QCD', (1990), (North- Holland, Amsterdam, (1991).

[29] G Altarelli and G Parisi, Nucl. Phys **B 126** (1977) 298.

[30] G Altarelli, Phy. Rep. **81** (1981) 1.

[31] V Gribov and L Lipatov, Sov. J. Nucl. Phys. **15** (1972) 438 & 675.

[32] Y L Dokshitzer, Sov. Phys. JETP **46** (1977) 641.

[33] V S Fadin and L N Lipatov, Phys. Lett. **B 429** (1998) 127.

[34] M Ciafaloni, Nucl. Phys. **B 296** (1988) 49.

[35] S Catani, F Fiorani and G Marchesini, Phys. Lett. **B 234** (1990) 339.

[36] S Catani, F Fiorani and G Marchesini, Nucl. Phys. **B 336** (1990) 18.

[37] G Marchesini, Nucl. Phys. **B 445** (1995) 49.

[38] J R Forshaw, A SabioVera, Phys. Lett. **B 440** (1998)141.

[39] B R Webber, Phys. Lett. **B 444** (1998) 81.

[40] G Salam, JHEP **03** (1999) 009.

[41] S Catani, M Ciafaloni and F Hautmann, Nucl. Phys. **B366** (1991)135.

[42] J Collins and R Ellis, Nucl. Phys. **B366** (1991)3.

[43] L Gribov, E Levin and M Ryskin, Phys. Rep. **100** (1983)1.

[44] E M Levin, M G Ryskin, Y M Shabelski and A G Shuvaev, Sov. J. Nucl. Phys. **53** (1991)657.

[45] L V Gribov, E M Levin and M G Ryskin, Phys. Rep.**1009** (1983) 1.

[46] L V Gribov, E M Levin and M G Ryskin, Nucl. Phys. **B188** (1981) 555.

[47] L V Gribov, E M Levin and M G Ryskin, Zh. Eksp. Theo. Fiz. **80** (1981) 2132; Sov. Phys. JETP **53** (1981) 1113.

[48] J Kwiecinski, A Martin, P Sutton, Phys. Rev. **D 52** (1995) 1445.

[49] B A Gordon et al., CHIO, Phys. Rev. **D20** (1979) 2645.

[50] A Arvidson et al., Nucl. Instrum. Methods **A251** (1986)437; Uppsala Univ. preprint GWI-PH **7/86**.

[51] M Arneodo et al., EMC, NA28, Nucl Phys. **B333** (1990)1; Phys. Lett. **B211** (1988) 493.

[52] I G Brid, NMC, talk given at the Joint Int. Lepton-Photon Symposium and Europhysics Conf.on High Energy Physics, Geneva (1991).

[53] D Allasia et al., NMC, Phys. Lett. **B249** (1990) 366.

[54] P Amaudruz et al., NMC, NA37, Phys. Rev. Lett. **66** (1991) 2712.

[55] A Brull, NMC, talk given at the XXVI Rencontres de Moriond, Les Arcs 1991.

[56] D Allasia et al., NMC, CERN-PPE/**91-147**.

[57] P Amaudruz et al., NMC, Z. Phys. **C51** (1991)387.

[58] C Halliwell, FNAL, E665, talk given at the XXV Int. Conf. on High Energy Physics, Singapore (1990).

[59] D E Jaffe, FNAL, E665, talk given at the XXVI Rencontres de Moriond, Les Arcs (1991); Schellman, FNAL, E665, talk given at the Joint Int. Lepton-Photon Symposium and Europhysics Conf.on High Energy Physics, Geneva (1991).

[60] J Franz et al., Z. Phys. **C10** (1981)105.

[61] J S Poucher et al., SLAC, E49a, Phys. Rev. Lett. **32** (1974) 118 and SLAC-PUB- **1309** (1973).

[62] S Stein et al., SLAC, E61, Phys Rev. **D12** (1975) 1884.

[63] A Bodek et al., SLAC-MIT, E87, Phys. Rev. **D20** (1979) 1471; SLAC-MIT, E87; A Bodek et al., Phys. Rev. Lett. **50** (1983) 1431.

[64] R G Arnold et al., SLAC, E139, Phys Rev. Lett. **52** (1984)727 and SLAC-PUB-**3257** (1983).

[65] S Dasu et al., SLAC, E140, Phys. Rev. Lett. **32** (1988)2591; S Dasu et al., SLAC, E140, Phys. Rev. Lett. **61** (1988) 1061.

[66] L W Whitlow, SLAC, Ph.D. Thesis, Standford Univ (1990) Slac-Report-**357** (1990); L W Whitlow et al., SLAC, Phys. Lett. **B250** (1990) 193; A Bodek, SLAC, talk given at the Joint Int. Lepton-Photon Symposium and Europhysics Conf.on High Energy Physics, Geneva (1991).

[67] D B MacFarlane et al., CCFRR, Z. Phys. **C26** (1994)1.

[68] S Mishara, CCFR, talk given at the Joint Int. Lepton-Photon Symposium and Europhysics Conf.on High Energy Physics, Geneva (1991).

[69] P Berge et al., CDHSW, Z. Phys. **C49** (1991) 187.

[70] K Varvell et al., BEBC, Z. Phys. **C36** (1987)1; J. Guy et al., BEBC, Z. Phys. **C36** (1987) 337.

[71] Y M Ado, F C Shoemaker and C Sutton, 'Particle Accelerator', Encyclopedia Britannica, 1994-2001(2001).

[72] C H Llewellyn Smith, 'European Laboratory for particle physics', Encyclopedia, Microsoft® Encarta® 1993-2001(2001).

[73] 'Particle Accelerator', Encyclopedia, Microsoft® Encarta® 1993-2001(2001).

[74] From the official website of Koh-Ene-Ken (KEK) http: // www.kek.jp.

[75] From the official website of Variable Energy Cyclotron Centre (VECC) http: // www.veccal.ernet.in.

[76] S Narayan, 'A Course of Mathematical Analysis', S. Chand & Company (Pvt) Ltd., New Delhi (1987).

[77] J N Sharma and A R Vasishtha, 'Mathematical Analysis-II', Krishna Prakashan Mandir, Meerut (1990-1991).

[78] M R Spiegel, 'Advanced Calculus', Schaum's Outline Series, McGraw-Hill (1962).

[79] M D Raisnghania, 'Advanced Differential Equations', S Chand & Company Ltd, New Delhi (1991).

[80] F Ayres Jr, 'Differential Equations', Schaum's Outline Series, McGraw-Hill (1988).

[81] F H Miller, 'Partial Differential Equation', John and Willey (1960).

[82] I Sneddon, 'Elements of Partial Differential Equations', Mc. Graw Hill, New York (1957).

[83] P P Gupta, G S Malik and S Gupta, 'Calculus of Finite Differences and Numerical Integration' Krishana Prakashan Media Ltd., Meerut (1994).

[84] H C Saxena, 'Finite Differences and Numerical Analysis', S. Chand & Company ltd., New Delhi (2001).

[85] J B Scarborough, 'Numerical Mathematical Analysis', Oxford & IBH Publishing Co. Pvt. Ltd. (1966).

[86] J K Sarma and B Das, Phy. Lett. **B304** (1993) 323.

[87] J K Sarma, D K Choudhury, G K Medhi, Phys. Lett. **B403** (1997) 139.

[88] D K Choudhury and J K Sarma, Pramana--J.Physics. **38** (1992) 481.

[89] L F Abbott, W B Atwood and R M Barnett, Phys. Rev. **D22** (1980) 582.

[90] I S Granshteyn and I M Ryzhik, 'Tables of Integrals, Series and Products', ed. Alen Jeffrey, Academic Press, New York (1965).

[91] D K Choudhury , J K Sarma and B P Sarma, Z. Phys. **71** (1996) 469.

[92] D K Choudhury and A Saikia, Pramana J. Phys. **33** (1989) 359.

[93] J K Sarma and G A Ahmed, Indian Journal of Pure & Applied Physics, **40** (2002) 235.

[94] C Adloff, H1 Collaboration, DESY **98--169**, hep-ex/9811013,(1998).

[95] M Arneodo, hep/961031,NMC, Nucl. Phys. **B483** (1997) 3.

[96] A D Martin et. al, hep-ph / 0110215 (2001).

[97] C Adloff et al., H1 Collaboration, Eur. Phys. J. **C13** (2000) 609.

[98] C Adloff et al., H1 Collaboration, Eur. Phys. J. **C19** (2001) 269.

[99] C Adloff et al., H1 Collaboration, Eur. Phys. J. **C21** (2001) 33.

[100] S Chekanov et al., ZEUS Collaboration, Eur. Phys. J. **C21** (2001) 443.

[101] M Arneodo et al., NMC Collaboration, Nucl. Phys. **B487** (1997) 3.

[102] M R Adams et al., Phys. Rev. **D54** (1996) 3006.

[103] W Furmanski and R Petronzio, Nucl. Phys. **B 195** (1982) 237.

[104] W Furmanski and R Petronzio, Z. Phys. **C11** (1982) 293.

[105] W Furmanski and R Petronzio, Phys. Lett **B 97** (1980) 437.

[106] A Deshamukhya and D K Choudhury, Proc. 2nd Regional Conf. Phys. Research in North-East, Guwahati, India, October, 2001 (2001)34.

[107] A Deshamukhya and D K Choudhury, Indian J. Phys. **75A** (5) (2001) 573.

[108] R Rajkhowa and J K Sarma, Indian J. Phys. **79(1)** (2005) 55.

[109] R Rajkhowa and J K Sarma, Indian J. Phys. **78(9)** (2004) 979.

[110] R Rajkhowa and J K Sarma, Indian J. Phys. **78A (3)** (2004) 367.

[111] B Badelek et. al, 'Small x physics' DESY **91-124**, October 1991.

[112] G Grammer and J D Sullivan, in Electromagnetic Interactions of Hadrons, eds A Donnachie and G Shaw, Plenum Press (1978).

[113] T H Bauer ey al., Rev. Mod. Phys. **50** (1978) 261 and references therein.

[114] A D Martin et. al, RAL Report. RAL-**94-055** (1994).

[115] B Abbott et al., D0 Collaboration, Phys. Rev. Lett. **86** (2001) 1707.

[116] T Aolder et al., CDF Collaboration, Phys. Rev. **D64** (2001) 032001.

[117] A C Benvenuti et al., BCDMS Collaboration, Phys. Lett. **B223** (1989) 485.

[118] L W Whitlow et al., Phys. Lett. **B282** (1992) 475; L W Whitlow, preprint SLAC-(1990) 357.

[119] W G Seligman et al., CCFR Collaboration, Phys. Rev. Lett. **79** (1997) 1213.

[120] G Moreno et al., E605 Collaboration, Phys. Rev. **D43** (1991) 2815.

[121] F Abe et al., CDF Collaboration , Phys. Rev. Lett. **81** (1998) 5744.

[122] A C Benvenuti et al., BCDMS Collaboration, Phys. Lett. **B236** (1989) 592.

[123] B Badelek and J Kwiecinski, Phys. Rev. **D50** (1994) R4.

[124] J Breitweg et al., ZEUS collaboration, Eur. Phys. J. **C7** (1999) 609.

[125] I Abt et al., H1 Collaboration, Nucl. Phys. **B407** (1993)515.

[126] M Derrick et al., ZEUS Collaboration, Phys. Lett. **B316** (1993) 412.

[127] K Muller, H1 Collaboration, Proc. Of 29th Rencontre de Moriond, March 1994.

[128] P Amaudruz et al., NMC Collaboration, Phys. Lett. **B295** (1992) 159.

[129] J Botts et al., CTEQ Collaboration, Phys. Lett. **B304** (1993)159.

[130] P Amaudruz et al., NMC Collaboration, Phys. Rev. Lett. **66** (1991) 2712.

[131] E Eichten et al., 'Supercollider physics', Rev. Mod. Phys, **56** (1984) 585.□

APPENDIX

Programme-1: Integration programme to obtain x distribution of deuteron structure function in leading order

```
#include<math.h>
#include<stdio.h>
#include<conio.h>
#define a(x) (3+(4*log(1-x))-((1-x)*(3+x)))
#define b(x) ((x*(1-(x*x)))+(2*x*log(1/x)))
#define Nf 4
#define c(x) ((.5)*(Nf)*(1-x)*(2-x+(2*x*x)))
#define d(x) (Nf*x*(((-.5)*(1-x)*(5-(4*x)+(2*x*x)))+((1.5)*log(1/x))))
#define Af .16
#define t 100
#define w 1
#define j 5
#define k j*exp(-w*x)
#define l(x) (a(x)+(k*(c(x)))-(w*k*d(x)))
#define m(x) (b(x)+(k*d(x)))
#define f(x) (2/(Af*m(x))-(l(x)/m(x)))
main()
{
int i;
float h,ul,lm,s,sa,sb,u,e,x;
clrscr();
printf("\n upper limit: ");
scanf("%f", &ul);
printf("\n lower limit: ");
scanf("%f", &lm);
h=(ul-lm)/t;
s=f(ul)+f(lm);
for(i=1;i<=t-1;i=i+1)
{
sa=(lm+(i*h));
s=s+(2*(f(sa)));
```

```
}
for(i=1;i<=t-1;i=i+2)
{
sb=(lm+(i*h));
s=s+(2*(f(sb)));
}
u=(s*h)/3.0;
printf("\n integral=%f", u);
e=exp(u);
printf("\n  exponential=%f", e);
getch();
return(0);
}
```

*It is to be noted that in case of constant and power value of k, following few lines

```
#define w  1
#define j  5
#define k  j*exp(-w*x)
#define l(x)  (a(x)+(k*(c(x)))-(w*k*d(x)))   replaced by
#define k  4.5
#define l(x)  (a(x)+(k*(c(x))))
```

for constant value of k and

```
#define w  -.01
#define j  1.8
#define k  j*pow(x,w)
#define l(x)  (a(x)+(k*(c(x)))+(w*j*d(x)*pow(x,w-1)))
```

for power value of k.

Programme-2: Integration programme to obtain x distribution of deuteron structure function in next-to-leading order

```
#include<math.h>
#include<stdio.h>
#include<conio.h>
```

```
#define A1(x) (.666667*(3+(4*log(1-x))-((1-x)*(3+x))))
#define A2(x) (1.33333*(1-x)*(2-x+(2*x*x)))
#define A3(x) (.666667*((x*(1-(x*x)))+(2*x*log(1/x))))
#define A4(x) (4*x*(((-.33333)*(1-x)*(5-(4*x)+(2*x*x)))+(log(1/x))))
#define Fqq1(x) ((-log(x)*((2.222222) +(3*x)+(3*x*x)+ (.8888888*x*x*x))) +(.5*x*
                (log(x)*log(x))*(2+x))+(5*x)-(1.5*x*x)+(2.37037037*x*x*x)-
                5.87037037)
#define Fqq2(x) ((log(x)*((4.222222)-(4*x)+(1.66666*x*x)+(.8888888*x*x*x)))-(.5*
                (log(x)*log(x))*(1+(x*x)))+((.333333)*pow(log(x),3))+(2.2222222/x)-
                (4*x)+(5.277777778*x*x)-(2.37037037*pow(x,3))-1.12962963)
#define Fqg1(w) 4-(9*w)-((1-(4*w))*log(w))-((1-(2*w))*log(w)*log(w))+(4*log(1-w))
                +((2*log((1-w)/w)*log((1-w)/w))-(4*log((1-w)/w))+ 3.414367333)*(w
                *w+((1-w)*(1-w)))
#define y(w)    (-log(log(1+w))-(log(w)*log(1+w))+(log(log((1/w)+1))) +(log(1/w)*
                log(1+(1/w))))
#define F1(w) 20.222222+(1.555556*w)+(4.444444/w)+(((45.333333*w)-12.666667) *
                log(w))-4*log(1-w)-((2+(8*w))*log(w)*log(w))
#define F2(w) (-(log(w)*log(w))+(14.666667*log(w))-(2*log(1-w)*log(1-w))+ (4* log
                (1-w))+(3.292813)-72.666667)*((w*w)+((1-w)*(1-w)))
#define F3(w) 2*((w*w)+((1+w)*(1+w)))*y(w)
#define Fqg2(w) (F1(w)+F2(w)+F3(w))
#define Fqg(w)  ((2.66666666*(Fqg1(w)))+(6*Fqg2(w)))
#define Fqg11(x) (-log(x)*((9*x)-(5*x*x)+(3.5555556*x*x*x))+(((3*x)-(3*x*x) +
                (1.33333333*x*x*x))*log(x)*log(x))-3.7153777778+ (.017511111*x)
                +(5.982488889*x*x))
#define Fqg22(x) ((-2.284622222*x*x*x)+(((3.5555555*x*x*x)-(4.66666666*x*x)+
                (2.66666667*x)-1.55555556)*log(1-x))+((1.33333333-(2*x)+ (2* x*
                x)-(1.33333333*x*x*x))*log(1-x)*log(1-x)))
#define Fqg9(x)  Fqg11(x)+Fqg22(x)
#define F11(x)  -12.04971852+(10.26902222*x)-(16.7690222*x*x) + (18.549718 *x*
                x*x)+((-4.4444444-(8*x)-(11*x*x)-(10.2222222*x*x*x))*log(x))
#define F22(x)  (((3*x)+(3*x*x)+(.6666666*x*x*x))*log(x)*log(x))+((1.555555-
                (2.6666666*x)+(4.66666667*x*x)-(3.555555*x*x*x))*log(1-x))+
                ((-1.333333+(2*x)-(2*x*x)+(1.333333*x*x*x))*log(1-x)*log(1-x))
```

```
#define Fqg8(x) (F11(x)+F22(x))
#define Pf(w)   (((-2*(1+(w*w))/(1-w))*log(w)*log(1-w))-(((3/(1-w))+(2*w))*log(w))-
                (.5*(1+w)*log(w)*log(w))-(5*(1-w)))
#define Pg(w)  ((((1+(w*w))/(1-w))*((log(w)*log(w)) +((3.666667) *log(w))+
                (19.0468)))+ (2*(1+w)*log(w))+((13.333333)*(1-w)))
#define Pnf(w) ((.666666)*((((1+(w*w))/(1-w))*(-log(w)-1.666666))-(2*(1-w))))
#define Pa(w)  ((2*((1+(w*w))/(1+w))*y(w))+(2*(1+w)*log(w))+(4*(1-w)))
#define f(w)    (((1.777778)*Pf(w))+(2*Pg(w))+(2.66667*Pnf(w))+((.222222)*Pa(w)))
#define f1(w)  (((1-w)/w)*f(w))
#define f2(w)  (((1-w)/w)*Fqg(w))
#define n       10000
#define ul2     1
#define ul3     1
#define ul4     1
#define p     -170
#define q       2
#define k     p*exp(-x*q)
#define L1(x)    (A1(x)+(k*A2(x))-(k*q*(A4(x))))
#define L2(x)   (A3(x)+(k*A4(x)))
#define B1(x)   (5.333333*Fqq1(x))
#define B2(x)   ((2.66666666*(Fqg9(x)))+(6*(Fqg8(x)+u2)))
#define B3(x)  (x*(u3)+(5.333333*x*Fqq2(x)))
#define B4(x)  (x*(u4))
#define M1(x)  (B1(x)+(k*B2(x))-(k*q*(B4(x))))
#define M2(x)  (B3(x)+(k*B4(x)))
#define f3(x)  (1/(L2(x)+(.026*M2(x)))*(8.333333-(L1(x)+(.026*M1(x)))))
 main()
{
int i;
float  h2,h3,h4,h5,s2,s3,s4,s5,sa2,sa3,sa4,sa5,u2,u3,u4,u;
float  sb2,y,sb3,sb4,sb5,ul5,lm2,lm3,lm4,lm5,x,w,e ;
clrscr();
printf("\n value of upper limit5: ");
scanf("%f",  &ul5);
```

```
printf("\n value of lower limit2: ");
scanf("%f", &lm2);
printf("\n value of lower limit3: ");
scanf("%f", &lm3);
printf("\n value of lower limit4: ");
scanf("%f", &lm4);
printf("\n value of lower limit5: ");
scanf("%f", &lm5);
h2=(ul2-lm2)/n;
h3=(ul3-lm3)/n;
h4=(ul4-lm4)/n;
h5=(ul5-lm5)/n;
s2=F3(ul2)+F3(lm2);
s3=f1(ul3)+f1(lm3);
s4=f2(ul4)+f2(lm4);
for(i=1; i<=n-1; i++)
{
sa2=(lm2+(i*h2));
s2=s2+(2*F3(sa2));
}
for(i=1; i<=n-1; i+=2)
{
sb2=(lm2+(i*h2));
s2=s2+(2*F3(sb2));
}
u2=s2*h2/3;
printf("\n integral=%f", u2);
for(i=1; i<=n-1; i++)
{
sa3=(lm3+(i*h3));
s3=s3+(2*f1(sa3));
}
for(i=1; i<=n-1; i+=2)
{
```

```
sb3=(lm3+(i*h3));
s3=s3+(2*f1(sb3));
}
u3=s3*h3/3;
printf("\n integral=%f", u3);
for(i=1; i<=n-1; i++)
{
sa4=(lm4+(i*h4));
s4=s4+(2*f2(sa4));
}
for(i=1; i<=n-1; i+=2)
{
sb4=(lm4+(i*h4));
s4=s4+(2*f2(sb4));
}
u4=s4*h4/3;
printf("\n integral=%f", u4);
s5=f3(ul5)+f3(lm5);
for(i=1; i<=n-1; i++)
{
sa5=(lm5+(i*h5));
s5=s5+(2*f3(sa5));
}
for(i=1; i<=n-1; i+=2)
{
sb5=(lm5+(i*h5));
s5=s5+(2*f3(sb5));
}
u=s5*h5/3;
printf("\n integral=%f", u);
e=exp(u);
printf("\n exponential=%f", e);
getch();
return(0);
```

```
}

*In case of power value of k, following few lines
#define p  -170
#define q  2
#define k  p*exp(-x*q)
#define L1(x)  (A1(x)+(k*A2(x))-(k*q*(A4(x))))   replaced by
#define p  30
#define q  .014
#define k  p*pow(x,q)
#define L1(x)  (A1(x)+(k*(A2(x)))+(p*q*pow(x,q-1))*A4(x))
```

Programme-3: Integration programme to obtain x distribution of gluon structure function in leading order

```
#include<math.h>
#include<stdio.h>
#include<conio.h>
#define a(x)  (.694+(log(1-x))-(2*(1-x))+(.5*(1-x)*(1-x))-(.3333*(1-x)*(1-x)*(1-x))-
              log (x))
#define b(x)  ((-.2222222)*((1-x)+(.5*(1-x)*(1-x))+(2*log(x))))
#define c(x)  (x*(2*(1-x)+((.33333)*(1-x)*(1-x)*(1-x))+(2*log(x))+(1/x)-1))
#define d(x)  (x*(.222222)*(((.5)*(1-x)*(1-x))+(2*(1-x))+(4*log(x))+(2/x)-2))
#define Af  1.24
#define w  -4
#define j  300
#define k  j*exp(-w*x)
#define lm  .9
#define t 100
#define p(x)  (a(x)+(k*(b(x)))-(w*k*d(x)))
#define q(x)  (c(x)+(d(x)*k))
#define f(x)  (2/(Af*q(x))-(p(x)/q(x)))
main()
{
```

```
int i;
float h,ul,s,sa,sb,u,e,x;
clrscr();
printf("\n upper limit: ");
scanf("%f",  &ul);
h=(ul-lm)/t;
s=f(ul)+f(lm);
for(i=1;i<=t-1;i=i+1)
{
sa=(lm+(i*h));
s=s+(2*(f(sa)));
}
for(i=1;i<=t-1;i=i+2)
{
sb=(lm+(i*h));
s=s+(2*(f(sb)));
}
u=(s*h)/3.0;
printf("\n integral=%f", u);
e=exp(u);
printf("\n  exponential=%f", e);
getch();
return(0);
}
```

*It is to be noted that in case of power value of k, following few lines

```
#define w  -4
#define j  300
#define k  j*exp(-w*x)
#define p(x)  (a(x)+(k*(b(x)))-(w*k*d(x)))  replaced by
#define w  1.8
#define j  135
#define k  j*pow(x,w)
#define p(x)  (a(x)+(k*(b(x)))+(w*j*d(x)*pow(x,w-1)))
```

Programme-4: Integration programme to obtain x distribution of light sea quark structure function in leading order

```
#include<math.h>
#include<stdio.h>
#include<conio.h>
#define a(x) (3+(4*log(1-x))-((1-x)*(3+x)))
#define b(x) ((x*(1-(x*x)))+(2*x*log(1/x)))
#define Nf 4
#define c(x) ((.25)*(1-x)*(2-x+(2*x*x)))
#define d(x) (x*(((-2.5)*(1-x)*(5-(4*x)+(2*x*x)))+((.75)*log(1/x))))
#define Af .16
#define t 100
#define w 1
#define j 5
#define k j*exp(-w*x)
#define l(x) (a(x)+(k*(c(x)))-(w*k*d(x)))
#define m(x) (b(x)+(k*d(x)))
#define f(x) (2/(Af*m(x))-(l(x)/m(x)))
main()
{
int i;
float h,ul,lm,s,sa,sb,u,e,x;
clrscr();
printf("\n upper limit: ");
scanf("%f", &ul);
printf("\n lower limit: ");
scanf("%f", &lm);
h=(ul-lm)/t;
s=f(ul)+f(lm);
for(i=1;i<=t-1;i=i+1)
{
sa=(lm+(i*h));
s=s+(2*(f(sa)));
```

```
}
for(i=1;i<=t-1;i=i+2)
{
sb=(lm+(i*h));
s=s+(2*(f(sb)));
}
u=(s*h)/3.0;
printf("\n integral=%f", u);
e=exp(u);
printf("\n  exponential=%f", e);
getch();
return(0);
}
```

*It is to be noted that in case of constant and power value of k, following few lines

```
#define w   1
#define  j  5
#define k   j*exp(-w*x)
#define l(x)  (a(x)+(k*(c(x)))-(w*k*d(x)))     replaced by
#define k     210
#define l(x)  (a(x)+(k*(c(x))))
```

for constant value of k and

```
#define w   .25
#define  j  221
#define k   j*pow(x,w)
#define l(x)  (a(x)+(k*(c(x)))+(w*j*d(x)*pow(x,w-1)))
```

for power value of k. □

PUBLICATIONS

1. Particular solutions of GLDAP evolution equations in leading order and structure functions at low-x, Indian J. Phys. 78A (3), 367-375 (2004), hep-ph/0201263.
2. Particular solution of DGLAP evolution equation in next-to-leading order and structure functions at low-x, Indian J. Phys. 78 (9), 979-987 (2004), hep-ph/0203070.
3. Particular solution of DGLAP evolution equation in next-to-leading order and x-distributions of deuteron structure functions at low-x, Indian J. Phys. 79 (1), 55-64 (2005).
4. Unique solutions of DGLAP evolution equations in leading order and next-to-leading order and structure functions at low-x, communicate to Indian J. Phys.
5. Particular and Unique solutions of DGLAP evolution equation in leading order and gluon structure function at small-x, communicate to Indian J. Phys.
6. Taylor expansion method and hadron structure functions in leading and next-to-leading orders at small-x, communicated to Phys. Rev. D
7. Method of characteristics and solution of DGLAP evolution equation in leading order at small-x, communicated to Pramana J. Phys. □

ADDENDA

Indian J Phys **78A** (3), 367-375 (2004)

AN INTERNATIONAL JOURNAL
IJP A

Particular solutions of GLDAP evolution equations in leading order and structure functions at low-x

R Rajkhowa and J K Sarma*

Department of Physics Tezpur University Napaam
Tezpur 784 028 Assam India

E mail jks@tezu ernet in

Received 26 June 2003 accepted 3 November 2003

Abstract We present particular solutions of singlet and non singlet Gribov Lipatov Dokshitzer Altarelli Parisi (GLDAP) evolution equations in leading order (LO) at low x We obtain t evolutions of proton and neutron structure functions and x evolutions of deuteron structure functions at low x from GLDAP evolution equations The results of t evolutions are compared with HERA low x and low Q^2 data and those of x evolutions are compared with NMC low x and low Q^2 data

Keywords Particular solution complete solution Alterelli Parisi equation structure function

PACS Nos 12 38 Bx 12 39 x 13 60 Hb

1. Introduction

The Gribov-Lipatov-Dokshitzer-Altarelli-Parisi (GLDAP) evolution equations[1-4] are fundamental tools to study the $t\left(=\ln(Q^2/\Lambda^2)\right)$ and x evolutions of structure functions, where x and Q^2 are Bjorken scaling and four momenta transfer in a deep inelastic scattering (DIS) Process [5] respectively and Λ is the QCD cut off parameter On the other hand, the study of structure functions at low-x has become topical in view [6] of high energy collider and supercollider experiments [7] Solutions of GLDAP evolution equations give quark and gluon structure functions which produce ultimately proton, neutron and deuteron structure functions Though numerical solutions are available in the literature [8], the explorations of the possibility of obtaining analytical solutions of GLDAP evolution equations are always interesting In this connection, some particular solutions computed from general solutions of GLDAP evolution equations at low-x in leading order have already been obtained by applying Taylor expansion method [9] and t-evolutions [10] and x- evolutions [11] of structure functions have been presented

The present paper reports particular solutions of GLDAP evolution equations computed from complete solutions in leading order at low-x and calculation of t and x-evolutions for singlet and non-singlet structure functions and hence t-evolutions of proton and neutron structure functions and x-evolutions of deuteron structure functions In some instance, we can deal with particular solutions more conveniently than with the general solutions [12] In calculating structure functions, input data points have been taken from the experimental data directly, unlike the usual practice of using an input distribution function introduced arbitrarily Results of proton and neutron structure functions are compared with the HERA low-x low-Q^2 data and those of deuteron structure functions are compared with the NMC low-x low-Q^2 data Comparisons are also made with the results of earlier solutions [10, 11, 13] of GLDAP evolution equations In Section 2, necessary theory has been discussed Section 3 gives results and discussion

2. Theory

Though the basic theory has been discussed elsewhere [10, 11, 13], the essential steps of the theory have been presented here for clarity The GLDAP evolution equations for singlet and non-singlet structure functions in the standard forms are [14]

$$\frac{\partial F_2^S(x,t)}{\partial t} - \frac{A_f}{t}\left[\{3+4\ln(1-x)\}\, F_2^S(x,t) + I_1^S(x,t) + I_2^S(x,t)\right] = 0 \quad (1)$$

* Corresponding Author

and

$$\frac{\partial F_2^{NS}(x,t)}{\partial t} - \frac{A_f}{t}\left[\{3+4\ln(1-x)\}F_2^{NS}(x,t) + I^{NS}(x,t)\right] = 0, \quad (2)$$

where,

$$I_1^S(x,t) = 2\int_x^1 \frac{dw}{1-w}\left\{\left(1+w^2\right)F_2^S(x/w,t) - 2F_2^S(x,t)\right\}, \quad (3)$$

$$I_2^S(x,t) = \frac{3}{2}N_f\int_x^1 \left\{w^2+(1-w)^2\right\}G(x/w,t)\,dw, \quad (4)$$

and

$$I^{NS}(x,t) = 2\int_x^1 \frac{dw}{1-w}\left\{\left(1+w^2\right)F_2^{NS}(x/w,t) - 2F_2^{NS}(x,t)\right\} \quad (5)$$

Here, $t = \ln\left\{Q^2/\Lambda^2\right\}$ and $A_f = 4/(33-2N_f)$, N_f being the number of flavours and Λ is the QCD cut off parameter

Let us introduce the variable $u = 1-w$ and note that [15]

$$\frac{x}{w} = \frac{x}{1-u} = x\sum_{k=0}^{\infty} u^k \quad (6)$$

The series (6) is convergent for $|u| < 1$ Since $x < w < 1$ so $0 < u < 1-x$ and hence the convergence criterion is satisfied Now, using Taylor expansion method [9], we can rewrite $G(x/w, t)$ as

$$G(x/w,t) = G\left(x + x\sum_{k=1}^{\infty} u^k, t\right)$$

$$= G(x,t) + x\sum_{k=1}^{\infty} u^k \frac{\partial G(x,t)}{\partial x} + \frac{1}{2}x^2\left(\sum_{k=1}^{\infty} u^k\right)^2 \frac{\delta^2 G(x,t)}{\partial x^2} + \quad (7)$$

which covers the whole range of u, $0 < u < 1-x$ Since x is small in our region of discussion, the terms containing x^2 and higher powers of x can be neglected as the first approximation as discussed in our earlier works [11, 12, 14] and $G(x/w, t)$ can be approximated for small-x as

$$G(x/w,t) \equiv G(x,t) + x\sum_{k=1}^{\infty} u^k \frac{\partial G(x,t)}{\partial x} \quad (8)$$

Similarly, $F_2^S(x/w,t)$ and $F_2^{NS}(x/w,t)$ can be approximated for small x as

$$F_2^S(x/w,t) \equiv F_2^S(x,t) + x\sum_{k=1}^{\infty} u^k \frac{\partial F_2^S(x,t)}{\partial x}, \quad (9)$$

and

$$F_2^{NS}(x/w,t) \equiv F_2^{NS}(x,t) + x\sum_{k=1}^{\infty} u^k \frac{\partial F_2^{NS}(x,t)}{\partial x} \quad (10)$$

Using eqs (8) (10) in eqs (3)-(5) and performing u-integrations, we get

$$I_1^S = -\left[(1-x)(x+3)\right]F_2^S(x,t) + \left[2x\ln(1/x) + x\left(1-x^2\right)\right] \times \frac{\partial F_2^S(x,t)}{\partial x}, \quad (11)$$

$$I_2^S = N_f\left[\frac{1}{2}(1-x)\left(2-x+2x^2\right)G(x,t) + \left\{-\frac{1}{2}x(1-x)\left(5-4x+2x^2\right) + \frac{3}{2}x\ln(1/x)\right\}\frac{\partial G(x,t)}{\partial x}\right] \quad (12)$$

and

$$I^{NS} = -\left[(1-x)(x+3)\right]F_2^{NS}(x,t) + \left[2x\ln(1/x) + x\left(1-x^2\right)\right]\frac{\partial F_2^{NS}(x,t)}{\partial x} \quad (13)$$

Now using eqs (11) and (12) in eq (1), we have

$$\frac{\partial F_2^S(x,t)}{\partial t} - \frac{A_f}{t}\left[A(x)F_2^S(x,t) + B(x)\frac{\partial F_2^S(x,t)}{\partial x} + C(x)\,G(x,t) + D(x)\frac{\partial G(x,t)}{\partial x}\right] = 0 \quad (14)$$

Let us assume for simplicity

$$G(x,t) = K(x)\,F_2^S(x,t), \quad (15)$$

where $K(x)$ is a function of x Now, eq (14) gives

$$\frac{\partial F_2^S(x,t)}{\partial t} - \frac{A_f}{t}\left[L(x)\,F_2^S(x,T) + M(x)\frac{\partial F_2^S(x,t)}{\partial x}\right] = 0, \quad (16)$$

where

$$A(x) = 3 + 4\ln(1-x) - (1-x)(3+x),$$

$$B(x) = x(1-x^2) + 2x\ln(1/x),$$

$$C(x) = 1/2N_f(1-x)(2-x+2x^2),$$

$$D(x) = N_f x\left[-\frac{1}{2}(1-x)\left(5-4x+2x^2\right) + \left(\frac{3}{2}\right)\ln\left(\frac{1}{x}\right)\right],$$

$$L(x) = A(x) + K(x)C(x) + D(x)\frac{\partial K(x)}{\partial x}$$

and $M(x) = B(x) + K(x)\,D(x)$

Secondly, using eq (13) in eq (2), we have

$$\frac{\partial F_2^{NS}(x,t)}{\partial t} - \frac{A_f}{t}\left[P(x)\,F_2^{NS}(x,t) + Q(x)\frac{\partial F_2^{NS}(x,t)}{\partial x}\right] = 0, \quad (17)$$

where

$$P(x) = 3 + 4\ln(1-\text{ı}) - (1-x)(x+3),$$

and

$$Q(\text{ı}) = \text{ı}\left(1-\text{ı}^2\right) \quad 2\,\text{ı}\ln\text{ı}$$

The general solutions of eqs (16) is [9, 12] $F(U\ V) = 0$, where F is an arbitrary function and

$$U\left(\text{ı}, t, F_2^S\right) = C_1$$

and

$$V\left(\text{ı}, t, F_2^S\right) = C_2$$

form a solution of equation

$$\frac{d\text{ı}}{A_f M(\text{ı})} = \frac{dt}{-t} = \frac{dF_2^S(\text{ı}, t)}{-A_f L(\text{ı}) F_2^S(x,t)} \tag{18}$$

Solving eq (18) we obtain,

$$U\left(\text{ı}, t, F_2^S\right) = t\exp\left[\frac{1}{A_f}\int\frac{1}{M(x)}d\text{ı}\right]$$

and

$$V\left(\text{ı}, t, F_2^S\right) = F_2^S(x,t)\exp\left[\int\frac{L(\text{ı})}{M(x)}d\text{ı}\right]$$

If U and V are two independent solutions of eq (18) and if α and β are arbitrary constants, then $V = \alpha U + \beta$ may be taken as a complete solution of eq (18) We take this form as this is the simplest form of a complete solution which contains both the arbitrary constants α and β Earlier [10, 11, 13], we considered a solution $AU + BV = 0$, where A and B are arbitrary constants But that is not a complete solution having both the arbitrary constants as this equation can be transformed to the form $V = CU$, where $C = -A/B$, i e the equation contains only one arbitrary constant

Now, the complete solution [9, 12]

$$F_2^S(\text{ı}, t)\exp\left[\int\frac{L(\text{ı})}{M(\text{ı})}d\text{ı}\right] = \alpha t\exp\left[\frac{1}{A_f}\int\frac{1}{M(\text{ı})}d\text{ı}\right] + \beta \tag{19}$$

is a two-parameter family of surfaces, which does not have an envelope, since the arbitrary constants enter linearly [9] Differentiating eq (19) with respect to β, we get $0 = 1$ which is absurd Hence, there is no singular solution The one-parameter family determined by taking $\beta = \alpha^2$ has equation

$$F_2^S(\text{ı}, t)\exp\left[\int\frac{L(\text{ı})}{M(\text{ı})}d\text{ı}\right] = \alpha t\exp\left[\frac{1}{A_f}\int\frac{1}{M(\text{ı})}d\text{ı}\right] + \alpha^2 \tag{20}$$

Differentiating eq (20) with respect to α, we get

$$\alpha = -\frac{1}{2}t\exp\left[\frac{1}{A_f}\int\frac{1}{M(x)}dx\right]$$

Putting the value of α in eq (20), we obtain the envelope

$$F_2^S(\text{ı}, t) = -\frac{1}{4}t^2\exp\left[\int\left(\frac{1}{A_f M(\text{ı})} - \frac{L(\text{ı})}{M(\text{ı})}\right)d\text{ı}\right], \tag{21}$$

which is merely a particular solution of the general solution Unlike the case of ordinary differential equations, the envelope is not a new locus It is to be noted that when β is an arbitrary function of α, then the elimination of α in eq (20) is not possible Thus, the general solution can not be obtained from the complete solution [9] Actually, the general solution of a linear partial differential equation of order one is the totality of envelopes of all one-parameter families (21) obtained from a complete solution

Now, defining

$$F_2^S(\text{ı}_0, t) = -\frac{1}{4}t_0^2\exp\left[\int\left(\frac{2}{A_f M(\lambda)} - \frac{L(\text{ı})}{M(x)}\right)d\text{ı}\right],$$

at $t = t_0$, where $t_0 = \ln\left(Q_0^2/\Lambda^2\right)$ at any lower value $Q = Q_0$, we get from eq (21)

$$F_2^S(\text{ı}, t) = F_2^S(\text{ı}_0, t)\left(\frac{t}{t_0}\right)^2, \tag{22}$$

which gives the t evolution of singlet structure function $F_2^S(\text{ı}, t)$

Proceeding exactly in the same way, and defining

$$F_2^{NS}(\text{ı}, t_0) = -\frac{1}{4}t_0^2\exp\left[\int\left(\frac{2}{A_f Q(\text{ı})} - \frac{P(\text{ı})}{Q(\text{ı})}\right)d\text{ı}\right],$$

we get for non-singlet structure function

$$F_2^{NS}(\text{ı}, t) = F_2^{NS}(\text{ı}, t_0)\left(\frac{t}{t_0}\right)^2, \tag{23}$$

which gives the t-evolution of non-singlet structure function $F_2^{NS}(\text{ı}, t)$

Again defining

$$F_2^S(\text{ı}_0, t) = -\frac{1}{4}t^2\exp\left[\int\left(\frac{2}{A_f M(\text{ı})} - \frac{L(\text{ı})}{M(x)}\right)d\text{ı}\right]_{\text{ı}=\text{ı}_0},$$

we obtain from eq (21)

$$F_2^S(\text{ı}, t) = F_2^S(\text{ı}_0, t)\exp\left[\int_{\text{ı}_0}^{\text{ı}}\left(\frac{2}{A_f M(\text{ı})} - \frac{L(\text{ı})}{M(\text{ı})}\right)d\text{ı}\right] \tag{24}$$

which gives the x-evolution of singlet structure function $F_2^S(x,t)$ Similarly defining,

$$F_2^{NS}(x_0,t) = -\frac{1}{4}t^2 \exp\left[\int\left(\frac{2}{A_f Q(x)} - \frac{P(x)}{Q(x)}\right)dx\right]_{x=x}$$

we get

$$F_2^{NS}(x,t) = F_2^{NS}(x_0,t)\exp\left[\int_{x_0}^{x}\left(\frac{2}{A_f Q(x)} - \frac{P(x)}{Q(x)}\right)\right]dx, \quad (25)$$

which gives the x-evolution of non-singlet structure function $F_2^{NS}(x,t)$ Deuteron, proton and neutron structure functions measured in deep inelastic electro-production, can be written in terms of singlet and non-singlet quark distribution functions in leading order as

$$F_2^d(x,t) = 5/9\ F_2^S(x,t), \quad (26)$$

$$F_2^p(x,t) = 5/18\ F_2^S(x,t) + 3/18\ F_2^{NS}(x,t) \quad (27)$$

and $$F_2^n(x,t) = 5/18\ F_2^S(x,t) - 3/18\ F_2^{NS}(x,t) \quad (28)$$

Now using eqs (22) and (24) in eq (26), we will get t and x evolution of deuteron structure function $F_2^d(x,t)$ at low-x as

$$F_2^d(x,t) = F_2^d(x,t_0)\left(\frac{t}{t_0}\right)^2 \quad (29)$$

and

$$F_2^d(x,t) = F_2^d(x_0,t)\exp\left[\int_{x_0}^{x}\left(\frac{2}{A_f M(x)} - \frac{L(x)}{M(x)}\right)dx\right], \quad (30)$$

where the input functions are

$$F_2^d(x,t_0) = \frac{5}{9}F_2^S(x,t_0)$$

and

$$F_2^d(x_0,t) = \frac{5}{9}F_2^S(x_0,t)$$

The corresponding results for a particular solutions from the linear combination of U and V of general solutions $F(U, V) = 0$ of GLDAP evolution equations obtained earlier [10, 11, 13] are

$$F_2^d(x,t) = F_2^d(x,t_0)\left(\frac{t}{t_0}\right) \quad (31)$$

and

$$F_2^d(x,t) = F_2^d(x_0,t)\exp\left[\int_{x_1}^{x}\left(\frac{1}{A_f M(x)} - \frac{L(x)}{M(x)}\right)dx\right] \quad (32)$$

These were obtained by taking arbitrary linear combination $AU + BV = 0$ of general solution $F(U, V) = 0$, where A and B are two arbitrary constants as discussed earlier

Similarly using eqs (22) and (23) in eqs (27) and (28), we get the t- evolutions of proton and neutron structure functions at low x as

$$F_2^p(x,t) = F_2^p(x,t_0)\left(\frac{t}{t_0}\right)^2 \quad (33)$$

and

$$F_2^n(x,t) = F_2^n(x,t_0)\left(\frac{t}{t_0}\right)^2 \quad (34)$$

where the input functions are

$$F_2^p(x,t_0) = \frac{5}{18}F_2^S(x,t_0) + \frac{3}{18}F_2^{NS}(x,t_0)$$

and

$$F_2^n(x,t_0) = \frac{5}{18}F_2^S(x,t_0) - \frac{3}{18}F_2^{NS}(x,t_0)$$

The corresponding results for earlier solutions of GLDAP evolution equations [10, 11, 13] are

$$F_2^p(x,t) = F_2^p(x,t_0)\left(\frac{t}{t_0}\right) \quad (35)$$

and

$$F_2^n(x,t) = F_2^n(x,t_0)\left(\frac{t}{t_0}\right) \quad (36)$$

But the x evolutions of proton and neutron structure functions like those of deuteron structure function is not possible by this methodology, because to extract the x-evolution of proton and neutron structure functions, we are to put eqs (24) and (25) in eqs (27) and (28) But as the functions inside the integral sign of eqs (24) and (25) are different, we need to separate the input functions $F_2^S(x_0,t)$ and $F_2^{NS}(x_0,t)$ from the data points to extract the x-evolutions of the proton and neutron structure functions, which will contain large errors

For the complete solution of eq (16), we take $\beta = \alpha^2$ in eq (19) If we take $\beta = \alpha$ in eq (19) and differentiate with respect to α as before, we get

$$0 = t\exp\left[\frac{1}{A_f}\int\frac{1}{M(x)}dx\right] + 1,$$

from which we can not determine the value of α

But if we take $\beta = \alpha^2$ in eq (19) and differentiate with respect to α, we get

$$\alpha = \sqrt{-\frac{1}{3} t \exp\left[\frac{1}{A_f}\int \frac{1}{M(x)}\,dx\right]}$$

which is imaginary Putting this value of α in eq (19) we get ultimately

$$F_2^S(x,t) = t^{\frac{3}{2}}\left\{\left(-\frac{1}{3}\right)^{\frac{1}{2}} + \left(-\frac{1}{3}\right)^{\frac{3}{2}}\right\}\exp\left[\int\left(\frac{\frac{3}{2}}{A_f M(x)} - \frac{L(x)}{M(x)}\right)dx\right]$$

Now, defining

$$F_2^S(x,t_0) = t_0^{\frac{3}{2}}\left\{\left(-\frac{1}{3}\right)^{\frac{1}{2}} + \left(-\frac{1}{3}\right)^{\frac{3}{2}}\right\} \times \exp\left[\int\left(\frac{\frac{3}{2}}{A_f M(x)} - \frac{L(x)}{M(x)}\right)dx\right],$$

we get

$$F_2^S(x,t) = F_2^S(x,t_0)\left(\frac{t}{t_0}\right)^{\frac{3}{2}}$$

Proceeding exactly in the same way, we get for non singlet structure function also

$$F_2^{NS}(x,t) = F_2^{NS}(x,t_0)\left(\frac{t}{t_0}\right)^{\frac{3}{2}}$$

Then using eqs (26)–(28) we get t- evolutions of deuteron, proton and neutron structure functions

$$F_2^{d\,p\,n}(x,t) = F_2^{d\,p\,n}(x,t_0)\left(\frac{t}{t_0}\right)^{\frac{3}{2}}$$

Proceeding in the same way we get x- evolutions of deuteron structure function

$$F_2^d(x,t) = F_2^d(x,t_0)\exp\left[\int_{x_0}^{x}\left(\frac{\frac{3}{2}}{A_f M(x)} - \frac{L(x)}{M(x)}\right)dx\right]$$

But the determination of x- evolutions of proton and neutron structure functions like those of deuteron structure function is not possible by this methodology as discussed earlier

Proceeding exactly in the same way, we can show that if we take $\beta = \alpha^4$, we get

$$F_2^{d\,p\,n}(x,t) = F_2^{d\,p\,n}(x,t_0)\left(\frac{t}{t_0}\right)^{\frac{4}{3}}$$

and

$$F_2^d(x,t) = F_2^d(x_0,t)\exp\left[\int_{x_0}^{x}\left(\frac{\frac{4}{3}}{A_f M(x)} - \frac{L(x)}{M(x)}\right)dx\right]$$

Similarly, if we take $\beta = \alpha^5$, we get

$$F_2^{d\,p\,n}(x,t) = F_2^{d\,p\,n}(x,t_0)\left(\frac{t}{t_0}\right)^{\frac{4}{5}}$$

and

$$F_2^d(x,t) = F_2^d(x_0,t)\exp\left[\int_{x_0}^{x}\left(\frac{\frac{5}{4}}{A_f M(x)} - \frac{L(x)}{M(x)}\right)dx\right],$$

and so on

Thus, we observe that if we take $\beta = \alpha$ in eq (19), we can not obtain the value of α and also the required solution But if we take $\beta = \alpha^2, \alpha^3, \alpha^4, \alpha^5$ and so on, we see that the powers of (t/t_0) in t-evolutions of deuteron, proton and neutron structure functions are 2, 3/2, 4/3, 5/4 and so on respectively, as discussed above Similarly, for x- evolutions of deuteron structure functions, we see that the numerators of the first term inside the integral sign are 2, 3/2, 4/3, 5/4 and so on respectively, for the same values of α Thus, we see that if in the relation $\beta = \alpha^y$, y varies between 2 to a maximum value, the powers of (t/t_0) varies between 2 to 1, and the numerator of the first term in the integral sign varies between 2 to 1 Then it is understood that the solutions of eqs (16) and (17) obtained by this methodology are not unique and so the t-evolutions of deuteron, proton and neutron structure functions, and x- evolution of deuteron structure function obtained by this methodology are not unique They become eqs (29), (30), (33), (34) for $y = 2$, but they reduce to eqs (31), (32), (35) and (36) respectively, which are our earlier results for a maximum value of y

Thus by this methodology, instead of having a single solution, we arrive at a band of solutions, of course the range for these solutions is reasonably narrow

3. Results and discussion

In the present paper, we compare our results of t-evolutions of proton and neutron structure functions from eqs (33) and (34)

respectively, with the HERA low-x, low Q^2 data[16] Here, proton structure functions $F_2^p(x, Q^2, z)$ measured in the range $2 \le Q^2 \le 50$ GeV^2, $0.73 \le z \le 0.88$ and neutron structure functions $F_2^n(x, Q^2, z)$ measured in the range $2 \le Q^2 \le 50$ GeV^2, $0.3 \le z \le 0.9$ have been used Moreover, here $P_T \le$ 200MeV, where P_T is the transverse momentum of the final state baryon and $z = 1-q\,(p-p')/(q\ p)$, where p, q are the four momenta of the incident proton and the exchanged vector boson coupling to the positron and p' is the four-momentum of the final state baryon Though we compare our results with $y = 2$ in $\beta = \alpha^3$ relation with data, our results with y maximum, which are equivalent to our earlier results are equally valid For t-evolutions of deuteron, proton and neutron structure functions, the results will be the range-bounded by our new and old results But for x evolutions of deuteron structure function, new and old results have not any significance difference

In Figure 1, we present our results of t-evolutions of proton structure functions F_2^p (solid lines) for the representative values of x given in the figure Data points at lowest-Q^2 values in the figure are taken as input to test the evolution equation (33) Agreement is found to be excellent In the same figure, we also plot the results of t-evolutions of proton structure functions Γ_2^p (dashed lines) for our earlier solutions from eq (35) of GLDAP evolution equations We observe that our new results are in better agreement with data than the old ones

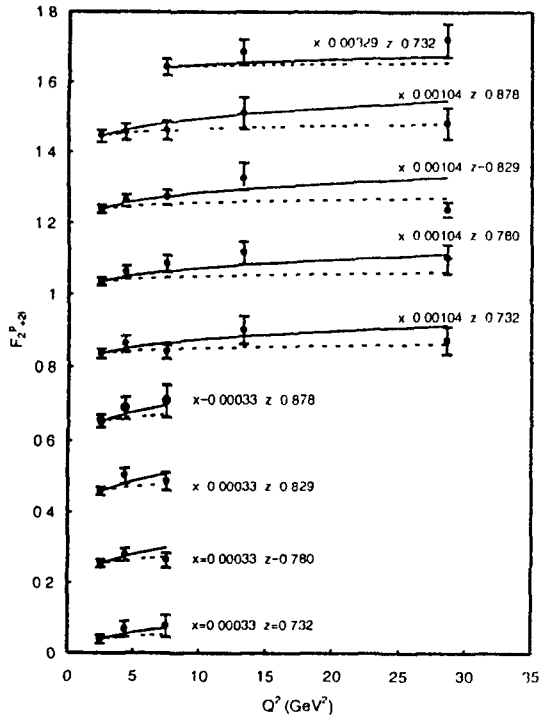

Figure 1. t evolutions of proton structure functions Γ_2^p (solid lines) for the representative values of x Data points at lowest Q^2 values are taken as input to test the evolution equation (33) We also plot the results of t evolutions of proton structure functions Γ_2^p (dashed lines) for our earlier solutions from eq (35) of GLDAP evolution equations For convenience value of each data point is increased by adding $0.2i$ where $i = 0\ 1\ 2\ 3$, are the numberings of curves counting from the bottom of the lowermost curve as the 0 th order

In Figure 2, we present our results of t-evolutions of neutron structure functions Γ_2^n (solid lines) for the representative values of x given in the figure Data points at lowest- Q^2 values in the figure are taken as input to test the evolution eq (34) Agreement is found to be excellent In the same figure, we also plot the results of t-evolutions of neutron structure functions F_2^n (dashed lines) for our earlier solutions from eq (36) of GLDAP evolution equations We observe that in this case also, our new results are in better agreement with data than the old ones

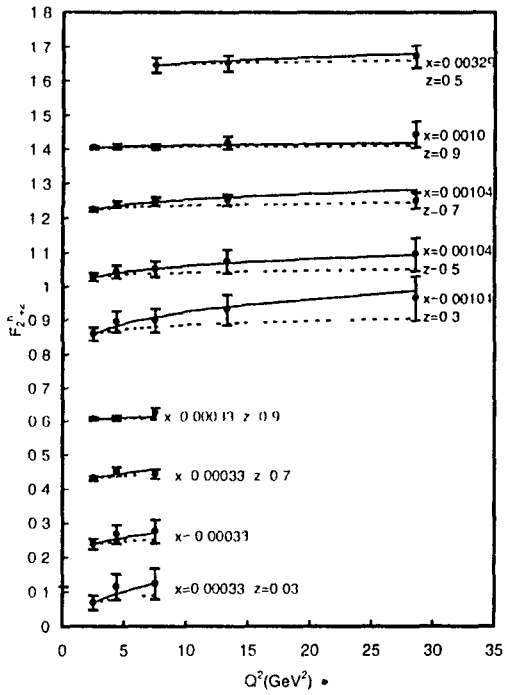

Figure 2. t evolutions of proton structure functions Γ_2^n (solid lines) for the representative values of x Data points at lowest Q^2 values are taken as input to test the evolution equation (34) We also plot the results of t evolutions of neutron structure functions Γ_2^n (dashed lines) for our earlier solutions from eq (36) of GLDAP evolution equations For convenience value of each data point is increased by adding $0.2i$ where $i = 0\ 1\ 2\ 3$ are the numberings of curves counting from the bottom of the lowermost curve as the 0 th order

For a quantitative analysis of x-distributions of structure functions, we calculate the integrals that occurred in eq (30) for $N_f = 4$ In Figure 3, we present our results of x distribution of deuteron structure functions F_2^d for $K(x) =$ constant (solid lines), $K(x) = ax^b$ (dashed lines) and for $K(x) = ce^{-dx}$ (dotted lines), where a, b, c and d are constants and for representative values of Q^2 given in each figure, and compare them with NMC deuteron low-x low- Q^2 data[17] In each, the data point for x value just below 0.1 has been taken as input $\Gamma_2^d(x_0, t)$

If we take $K(x) = 4\,5$ in eq (30), then agreement of the result with experimental data is found to be excellent On the other hand, if we take $K(x) = ax^b$, then agreement of the results with experimental data is found to be good at $a = 4\,5, b = 0\,01$ Again if we take $K(x) = ce^{-dx}$, then agreement of the results with experimental data is found to be good at $c = 5, b = 1$

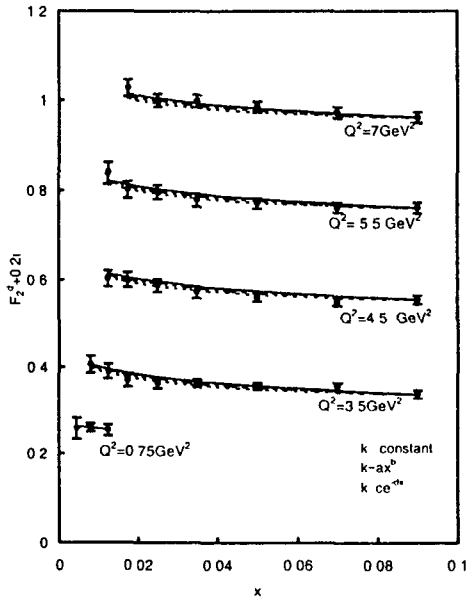

Figure 3 x distributions of deuteron structure functions F_2^d for $K(x)$ = constant (solid lines) $K(x) = ax^b$ (dashed lines) and for $K(x) = ce^{-dx}$ (dotted lines) where a b c and d are constants, and compare them with NMC deuteron low x low Q^2 data In each, the data point for x value just below 0 1 has been taken as input $F_2^d(x_0, t)$ For convenience value of each data point is increased by adding $0\,2t$ where $t = 0\ 1\ 2, 3$ are the numberings of curves counting from the bottom of the lowermost curve as the 0 th order

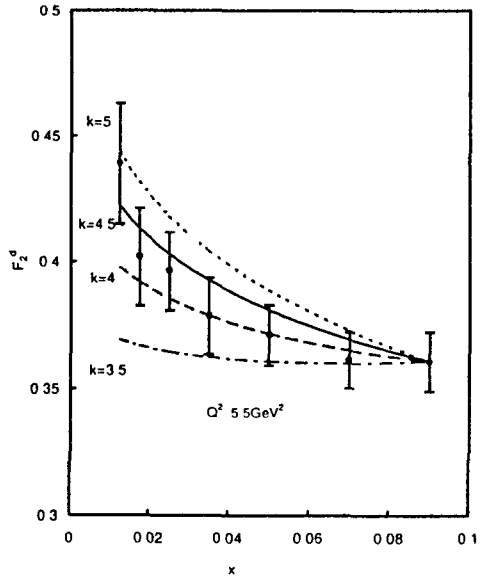

Figure 4 Sensitivity of our results for different constant values of $K(x)$

In Figure 4, we present the sensitivity of our results for different constant values of $K(x)$, we observe that at $K(x) = 4\,5$, agreement of the results with experimental data is found to be excellent If value of $K(x)$ is increased, the curve goes upward direction and if value of $K(x)$ is decreased, the curve goes downward direction But the nature of the curve is similar

In Figure 5, we present the sensitivity of our results for different values of a at fixed value of b Here, we take $b = 0\,01$ We observe that at $a = 4\,5$, agreement of the results with experimental data is found to be excellent If value of a is increased, the curve moves upward and if value of a is decreased, the curve goes downward But the nature of the curve is similar

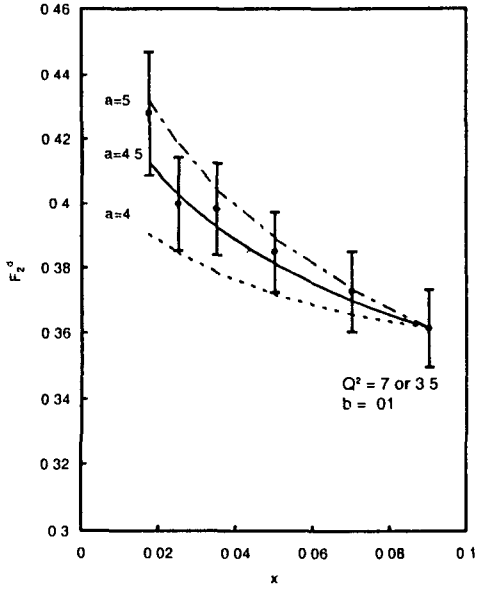

Figure 5 Sensitivity of our results for different values of a at fixed value of $b = 0\,01$

In Figure 6, we present the sensitivity of our results for different values of b at fixed value of a Here, we take $a = 4\,5$, we observe that at $b = 0\,01$, agreement of the results with experimental data is excellent If value of b is increased, then the curve goes downward and if value of b is decreased, the curve goes upward But we observe that difference of the curves for $b = 0\,01$, $0\,001$, $0\,0001$ is very small and all these curves are overlapped Here also the nature of the curves is similar

In Figure 7, we present the sensitivity of our results for different values of 'c' at fixed value of 'd' Here, we take $d = 1$ We observe that at $c = 5$, agreement of the results with experimental data is excellent If value of 'c' is increased, the curve goes upward and if value of 'c' is decreased, the curve goes downward direction But the nature of the curves is similar

In Figure 8, we present sensitivity of our results for different values of d at fixed value of c Here, we take $c = 5$, we observe that at $d = 1$, agreement of the results with experimental data is excellent If value of 'd' is increased, then the curve goes

downward and if value of d is decreased the curve goes upward Here also the nature of the curves is similar

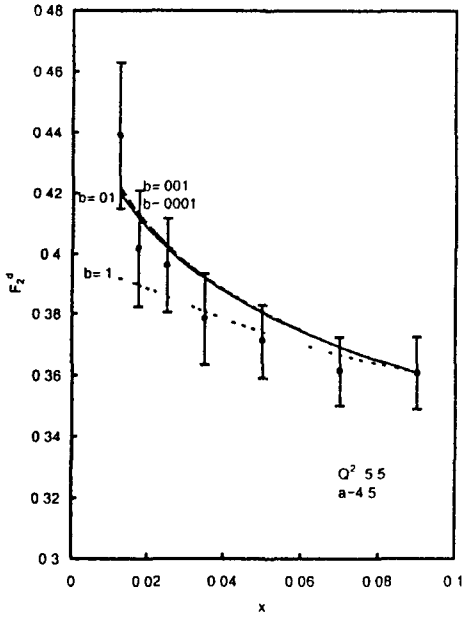

Figure 6 Sensitivity of our results for different values of b at fixed value of a =4 5

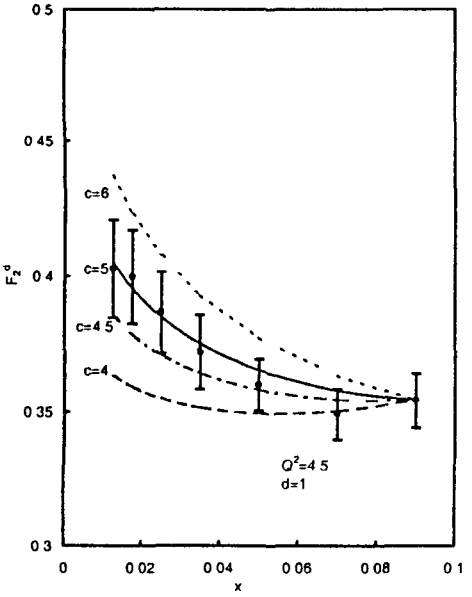

Figure 7. Sensitivity of our results for different values of c at fixed value of d =1

From our above discussion, it has been observed that we can not establish a unique relation between singlet and gluon structure functions *i e* a unique expression for $K(x)$ in eq (15) by this method, $K(x)$ in the forms of a constant, an exponential function of x or a power in x can equally produce required x distribution of deuteron structure functions But unlike many parameter input x distribution functions generally used in the literature, our method required only one or two such parameters The explicit form of $K(x)$ can actually be obtained only by solving coupled GLDAP evolution equations for singlet and gluon structure functions and works are going on in this direction

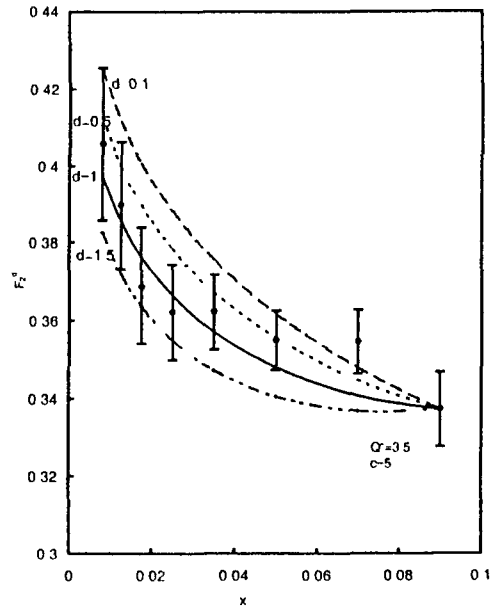

Figure 8 Sensitivity of our results for different values of d at fixed value of c = 5

Traditionally, the GLDAP equations provide a means of calculating the manner in which the parton distributions change at fixed x, as Q^2 varies This change occurs because of the various types of parton branching emission processes and the x distributions are modified due to sharing of initial momentum among the various daughter partons However, the exact rate of modifications of x-distributions at fixed Q^2 can not be obtained from the GLDAP equations since it depends not only on the initial x but also on the rate of change of parton distributions with respect to x, $d^n F(x)/dx^n$ (n = 1 to ∞), up to infinite order Physically, this implies that at high x, the parton has a large momentum fraction at its disposal and as a result, it radiates partons including gluons in innumerable ways, some of them involving complicated QCD mechanisms However for low-x, many of the radiation processes will cease to occur due to momentum constraints and the x-evolutions get simplified It is then possible to visualize a situation in which the modification of the x distribution simply depends on its initial value and its first derivative In this simplified situation, the GLDAP equations give information on the shapes of the x distribution as demonstrated in this paper The clearer testing of our results of x evolution is actually the eq (25) which is free from the additional assumption [eq (15)] But non singlet data is not sufficiently available in low-x to test our result It is observed in general that the results of particular solutions of GL DAP evolution equations

have improved over those of our earlier solutions, especially in t-evolution calculations. Of course, this is a leading order calculation. Its natural improvement will be the calculation considering next to leading order terms and our preliminary work [18] shows some improvement in this regard.

Acknowledgments

We are grateful to G. A. Ahmed of Physics Department, B. Gogoi and D. Sarma of Computer Science Department, and A. K. Bhattacharya of Mathematical Science Department of Tezpur University for the help in numerical part of this work. One of us (JKS) is grateful to the University Grants Commission, New Delhi for the financial assistance to this work in the form of a major research project.

References

[1] G. Altarelli and G. Parisi *Nucl. Phys.* **B126** p298 (1977)

[2] G. Altarelli *Phy. Rep.* **81** 1 (1981)

[3] V. N. Gribov and L. N. Lipatov *Sov. J. Nucl. Phys.* **20** 94 (1975)

[4] Y. L. Dokshitzer *Sov. Phy. JETP* **46** 641 (1977)

[5] F. Halzen and A. D. Martin *Quarks and Leptons: An Introductory Course in Modern Particle Physics* (New York: John Wiley) (1984)

[6] A. Ali and J. Bartels (eds.) *Proc. DESY Topical Meeting on the Small x Behaviour of Deep Inelastic Structure Functions in QCD* (1990) (Amsterdam: North Holland) (1991)

[7] G. Jarlskog and D. Rein (eds) *Proc. Large Hardon Collider Workshop* (CERN 90-10) (1990)

[8] D. K. Choudhury and J. K. Sarma *Pramana J. Phys.* **39** 273 (1992)

[9] F. Ayres (Jr) *Differential Equations* (Schaum's Outline Series) (New York: McGraw Hill) (1952)

[10] J. K. Sarma and B. Das *Phys. Lett.* **B304** 323 (1993)

[11] J. K. Sarma, D. K. Choudhury and G. K. Medhi *Phys. Lett.* **B403** 139 (1997)

[12] F. H. Miller *Partial Differential Equation* (New York: John Willey) (1960)

[13] D. K. Choudhury and J. K. Sarma *Pramana J. Phys.* **38** 481 (1992)

[14] L. F. Abbott, W. B. Atwood and R. M. Barnett *Phys. Rev.* **D22** 582 (1980)

[15] I. S. Gradshteyn and I. M. Ryzhik *Tables of Integrals, Series and Products* (ed) Alen Jeffrey (New York: Academic) (1965)

[16] C. Adloff H1 Collaboration **DESY 98-169** *hep ex/9811013* (1998)

[17] M. Arneodo hep/961031 New Muon Collaborators (NMC) *Nucl. Phys.* **B483** 3 (1997)

[18] R. Rajkhowa and J. K. Sarma hep ph/0203070 *Indian J. Phys. A* (submitted)

Indian J Phys 78 (9), 979-987 (2004)

AN INTERNATIONAL JOURNAL
IJP

Particular solution of DGLAP evolution equation in next-to-leading order and structure functions at low-x

R Rajkhowa and J K Sarma*

Department of Physics, Tezpur University, Napaam, Tezpur-784 028, Assam, India

E mail jks@tezu ernet in

Received 17 October 2003 accepted 9 June 2004

Abstract We present particular solutions of singlet and non singlet Dokshitzer-Gribov Lipatov Altarelli Parisi (DGLAP) evolution equations in next to leading order (NLO) at low x We obtain t evolutions of deuteron, proton neutron and difference and ratio of proton and neutron structure functions at low x from DGLAP evolution equations The results of t evolutions are compared with HERA and NMC low x and low Q^2 data and with those of leading order (LO) solutions of DGLAP evolution equations We also compare our result of t-evolution of proton structure function with a recent global parameterization

Keywords Particular solution, complete solution, Altarelli Parisi equation, structure function, low x physics

PACS Nos. 12 38 Bx, 12 39 x, 13 60Hb

1. Introduction

In a recent paper [1], particular solution of the Dokshitzer-Gribov-Lipatov-Altarelli-Parisi (DGLAP) evolution equations [2-5] for t and x-evolutions of singlet and non singlet structure functions in leading order at low-x have been reported The same technique can be applied to the DGLAP evolution equations in next-to-leading order (NLO) for singlet and non-singlet structure functions to obtain t-evolutions of deuteron, proton, neutron, difference and ratio of proton and neutron structure functions These NLO results are compared with the HERA H1 [6] and NMC [7] low-x, low Q^2 data and with those of particular solution in LO and we also compare our results of t-evolution of proton structure functions with recent global parameterization [8]

2. Theory

Though the necessary theory has been discussed elsewhere [9], here we mention some essential steps for clarity The DGLAP evolution equations with splitting functions [10, 11] for singlet and non-singlet structure functions in NLO are in the standard forms [12]

$$\frac{\partial F_2^S(x,t)}{\partial t} - \frac{\alpha_s(t)}{2\pi}\left[\frac{2}{3}\{3+4\ln(1-x)\}F_2^S(x,t)+\frac{4}{3}\int_x^1 \frac{dw}{1-w}\right.$$

$$\times\left\{(1+w^2)F_2^S\left(\frac{x}{w},t\right)-2F_2^S(x,t)\right\}+N_f\int_x^1\{w^2+(1-w)^2\}$$

$$\left.\times G\left(\frac{x}{w},t\right)dw\right]-\left(\frac{\alpha_s(t)}{2\pi}\right)^2\left[(x-1)F_2^S(x,t)\int_0^1 f(w)dw\right.$$

$$+\int_x^1 f(w)\,F_2^S\left(\frac{x}{w},t\right)dw+\int_x^1 F_{qq}^S(w)\,F_2^S\left(\frac{x}{w},t\right)dw$$

$$\left.+\int_x^1 F_{qk}^S(w)\,G\left(\frac{x}{w},t\right)dw\right]=0 \qquad (1)$$

and

$$\frac{\partial F_2^{NS}(x,t)}{\partial t} - \frac{\alpha_s(t)}{2\pi}\left[\frac{2}{3}\{3+4\ln(1-x)\}F_2^{NS}(x,t)+\frac{4}{3}\int_x^1 \frac{dw}{1-w}\right.$$

$$\left.\times\left\{(1+w^2)F_2^{NS}\left(\frac{x}{w},t\right)-2F_2^{NS}(x,t)\right\}\right]-\left(\frac{\alpha_s(t)}{2\pi}\right)^2$$

$$\times\left[(x-1)F_2^{NS}(x,t)\int_0^1 f(w)dw+\int_x^1 f(w)F_2^{NS}\left(\frac{x}{w},t\right)dw\right]=0, \qquad (2)$$

* Corresponding Author

where

$$\alpha_s(t)=\frac{4\pi}{\beta_0 t}\left[1-\frac{\beta_1 \ln t}{\beta_0^2 t}\right],\quad \beta_0=\frac{33-2n_f}{3}$$

and $$\beta_1=\frac{306-38n_f}{3},$$

N_f being the number of flavours

Here, $$f(w)=C_F^2\left[P_F(w)-P_A(w)\right]+\frac{1}{2}C_F C_A\left[P_G(w)+P_A(w)\right]$$
$$+C_F T_R N_f P_{N_f}(w)$$

and

$$F_{qq}^S(w)=2C_F T_R N_f F_{qq}(w)$$

and $$F_{qg}^S(w)=C_F T_R N_f F_{qg}^1(w)+C_G T_R N_f F_{qg}^2(w)$$

The explicit forms of higher order kernels are [10, 11]

$$P_F(w)=-\frac{2(1+w^2)}{1-w}\ln w\ln(1-w)-\left(\frac{3}{1-w}+2w\right)\ln w$$
$$-\frac{1}{2}(1+w)\ln^2 w-5(1-w)$$

$$P_G(w)=\frac{1+w^2}{1-w}\left(\ln^2 w+\frac{11}{3}\ln w+\frac{67}{9}-\frac{\pi^2}{3}\right)$$
$$+2(1+w)\ln w+\frac{40}{3}(1-w)$$

$$P_{N_f}(w)=\frac{2}{3}\left[\frac{1+w^2}{1-w}\left(-\ln w-\frac{5}{3}\right)-2(1-w)\right],$$

$$P_A(w)=\frac{2(1+w^2)}{1+w}\int_{w/(1+w)}^{1/(1+w)}\frac{dk}{k}\ln\frac{1-k}{k}+2(1+w)\ln w+4(1-w),$$

$$F_{qq}(w)=\frac{20}{9w}-2+6w-\frac{56}{9}w^2+\left(1+5w+\frac{8}{3}w^2\right)\ln w$$
$$-(1+w)\ln^2 w,$$

$$F_{qg}^1(w)=4-9w-(1-4w)\ln w-(1-2w)\ln^2 w+4\ln(1-w)$$
$$+\left[2\ln^2\left(\frac{1-w}{w}\right)-4\ln\left(\frac{1-w}{w}\right)-\frac{2}{3}\pi^2+10\right]P_{qg}(w)$$

and

$$F_{qg}^2(w)=\frac{182}{9}+\frac{14}{9}w+\frac{40}{9w}+\left(\frac{136}{3}w-\frac{38}{3}\right)\ln w-4\ln(1-w)$$
$$-(2+8w)\ln^2 w+\left[-\ln^2 w+\frac{44}{3}\ln w-2\ln^2(1-w)+4\ln(1-w)\right.$$
$$\left.+\frac{\pi^2}{3}-\frac{218}{3}\right]P_{qg}(w)+2P_{qg}(w)\int_{w/(1+w)}^{1/(1+w)}\frac{dz}{z}\ln\frac{1-z}{z},$$

where $P_{qg}(w)=w^2+(1-w)^2$, $C_A=C_G=N_C=3$,

$$C_F=\left(N_C^2-1\right)/2N_C \quad \text{and} \quad T_R=1/2$$

Let us introduce the variable $u=1-w$ and note that [13]

$$\frac{x}{w}=\frac{x}{1-u}=x\sum_{k=0}^{\infty}u^k$$

The above series is convergent for $|u|<1$. Since $x<w<1$, so $0<u<1-x$ and hence the convergence criterion is satisfied. Now using Taylor expansion method we can rewrite $F_2^S(x/w,t)$ as

$$F_2^S(x/w,t)-F_2^S\left(x+x\sum_{k=1}^{\infty}u^k,t\right)$$
$$=F_2^S(x,t)+x\sum_{k=1}^{\infty}u^k\frac{\partial F_2^S(x,t)}{\partial x}+\frac{1}{2}x^2\left(\sum_{k=1}^{\infty}u^k\right)^2\frac{\partial^2 F_2^S(x,t)}{\partial x^2}+$$

which covers the whole range of u, $0<u<1-x$. Since x is small in our region of discussion, the terms containing x^2 and higher powers of x can be neglected in the first approximation as discussed in our earlier works [1, 14-16]. $F_2^S(x/w,t)$ can be approximated for small x as

$$F_2^S(x/w,t)\cong F_2^S(x,t)+x\sum_{k=1}^{\infty}u^k\frac{\partial F_2^S(x,t)}{\partial x} \tag{3}$$

Similarly, $G(x/w,t)$ and $F_2^{NS}(x/w,t)$ can be approximated for small x as

$$G(x/w,t)\cong G(x,t)+x\sum_{k=1}^{\infty}u^k\frac{\partial G(x,t)}{\partial x} \tag{4}$$

and $$F_2^{NS}(x/w,t)\cong F_2^{NS}(x,t)+x\sum_{k=1}^{\infty}u^k\frac{\partial F_2^{NS}(x,t)}{\partial x} \tag{5}$$

Using eqs (3) and (4) in eq (1) and performing u integrations, we get

$$\frac{\partial F_2^S(x,t)}{\partial t}-\left[\frac{\alpha_s(t)}{2\pi}A_1(x)+\left(\frac{\alpha_s(t)}{2\pi}\right)^2 B_1(x)\right]F_2^S(x,t)$$
$$-\left[\frac{\alpha_s(t)}{2\pi}A_2(x)+\left(\frac{\alpha_s(t)}{2\pi}\right)^2 B_2(x)\right]G(x,t)$$

$$-\left[\frac{\alpha_s(t)}{2\pi}A_1(x)+\left(\frac{\alpha_s(t)}{2\pi}\right)^2 B_1(x)\right]\frac{\partial F_2^S(x,t)}{\partial x}$$

$$-\left[\frac{\alpha_s(t)}{2\pi}A_4(x)+\left(\frac{\alpha_s(t)}{2\pi}\right)^2 B_4(x)\right]\frac{\partial G(x,t)}{\partial x}=0, \quad (6)$$

where

$$A_1(x)=\frac{2}{3}\{3+4\ln(1-x)+(x-1)(x+3)\},$$

$$B_1(x)=x\int_0^1 f(w)dw-\int_0^x f(w)dw+\frac{4}{3}N_f\int_x^1 F_{qq}(w)dw,$$

$$A_2(x)=N_f\left[\frac{1}{3}(1-x)(2-x+2x^2)\right],$$

$$B_2(x)=\int_x^1 I_{qk}^S(w)\,dw,$$

$$A_3(x)=\frac{2}{3}\left\{x(1-x^2)+2x\ln\left(\frac{1}{x}\right)\right\},$$

$$B_3(x)=x\int_x^1\left\{f(w)+\frac{4}{3}N_f F_{qq}(w)\right\}\frac{1-w}{w}dw,$$

$$A_4(x)=N_f x\left\{\ln\frac{1}{x}-\frac{1}{3}(1-x)(5-4x+2x^2)\right\}$$

and

$$B_4(x)=x\int_x^1\frac{1-w}{w}I_{qx}^S(w)\,dw$$

Let us assume for simplicity [14 16]

$$G(x,t)=K(x)F_2^S(x,t), \quad (7)$$

where $K(x)$ is a function of x In this connection, earlier we considered [1] $K(x)=k, ax^b, ce^{-dx}$, where k, a b, c, d are constants Agreement of the results with experimental data is found to be excellent for $k=4\,5, a=4\,5, b=0\,01, c=5, d=1$ for low-x in leading order But correct form of $K(x)$ can actually be obtained only by solving coupled DGLAP evolution equations for singlet and gluon structure functions, and works are going on in this regard Therefore, eq (6) becomes

$$\frac{\partial F_2^S(x,t)}{\partial t}-\left[\frac{\alpha_s(t)}{2\pi}L_1(x)+\left(\frac{\alpha_s(t)}{2\pi}\right)^2 M_1(x)\right]F_2^S(x,t)$$

$$-\left[\frac{\alpha_s(t)}{2\pi}L_2(x)+\left(\frac{\alpha_s(t)}{2\pi}\right)^2 M_2(x)\right]\frac{\partial F_2^S(x,t)}{\partial x}=0, \quad (8)$$

where

$$L_1(x)=A_1(x)+K(x)A_2(x)+A_4(x)\frac{\partial K(x)}{\partial x},$$

$$M_1(x)=B_1(x)+K(x)B_2(x)+B_4(x)\frac{\partial K(x)}{\partial x},$$

$$L_2(x)=A_3(x)+K(x)A_4(x),$$

$$M_2(x)=B_3(x)+K(x)B_4(x)$$

For a possible solution, we assume [9, 12]

$$\left(\frac{\alpha_s(t)}{2\pi}\right)^2=T_0\left(\frac{\alpha_s(t)}{2\pi}\right), \quad (9)$$

where T_0 is a numerical parameter to be obtained from the particular Q^2-range under study By a suitable choice of T_0 we can reduce the error to a minimum Now, eq (8) can be recast as

$$\frac{\partial F_2^S(x,t)}{\partial t}-P_S(x,t)\frac{\partial F_2^S(x,t)}{\partial x}-Q_S(x,t)F_2^S(x,t)=0, \quad (10)$$

where

$$P_S(x,t)=\frac{\alpha_s(t)}{2\pi}\left[L_2(x)+T_0M_2(x)\right]$$

and $$Q_S(x,t)=\frac{\alpha_s(t)}{2\pi}\left[L_1(x)+T_0M_1(x)\right]$$

Secondly, using eqs (5) and (9) in eq (2) and performing u-integration, we have

$$\frac{\partial F_2^{NS}(x,t)}{\partial t}-P_{NS}(x,t)\frac{\partial F_2^{NS}(x,t)}{\partial x}-Q_{NS}(x,t)F_2^{NS}(x,t)=0, \quad (11)$$

where

$$P_{NS}(x,t)=\frac{\alpha_s(t)}{2\pi}\left[A_5(x)+T_0B_5(x)\right]$$

and

$$Q_{NS}(x,t)=\frac{\alpha_s(t)}{2\pi}\left[A_6(x)+T_0B_6(x)\right]$$

with

$$A_5(x)=\frac{2}{3}\left\{x(1-x^2)+2x\ln\left(\frac{1}{x}\right)\right\},$$

$$B_5(x)=x\int_x^1\frac{1-w}{w}f(w)\,dw,$$

$$A_6(x)=\frac{2}{3}\{3+4\ln(1-x)+(x-1)(x+3)\},$$

$$B_6(x)=-\int_0^x f(w)dw+x\int_0^1 f(w)dw$$

The general solutions [17, 18] of eq (10) is $F(U\ V)=0$ where F is an arbitrary function and $U\left(x,t,F_2^S\right)=C_1$ and $V\left(x,t,F_2^S\right)=C_2$, where C_1 and C_2 are constant and they form a solution of equations

$$\frac{dx}{P_S(x,t)}=\frac{dt}{-1}=\frac{dF_2^S(x,t)}{-Q_S(x,t)} \tag{12}$$

We observed that the Lagrange's auxiliary system of ordinary differential equations [17, 18] occurring in the formalism, can not be solved without the additional assumption of linearization (eq (9)) and introduction of an ad hoc parameter T_0. This parameter does not affect the results of t-evolution of structure functions. Solving eq (12), we obtain

$$U\left(x,t,F_2^S\right)=t^{(b/t+1)}\exp\left[\frac{b}{t}+\frac{N_S(x)}{a}\right]$$

and $$V\left(x,t,F_2^S\right)=F_2^S(x,t)\exp\left[M_S(x)\right],$$

where

$$a=\frac{2}{\beta_0},\ b=\frac{\beta_1}{\beta_0^2},\ N_S(x)=\int\frac{dx}{L_2(x)+T_0M_2(x)}$$

and $$M_S(x)=\int\frac{L_1(x)+T_0M_1(x)}{L_2(x)+T_0M_2(x)}\,dx$$

If U and V are two independent solutions of eq (12) and if α and β are arbitrary constants, then $V=\alpha U+\beta$ may be taken as a complete solution of eq (12). Then the complete solution [17, 18]

$$F_2^S(x,t)\exp\left[M_S(x)\right]=\alpha\left[t^{(b/t+1)}\exp\left(\frac{b}{t}+\frac{N_S(x)}{a}\right)\right]+\beta \tag{13}$$

is a two-parameter family of planes. The one parameter family determined by taking $\beta=\alpha^2$ has equation

$$F_2^S(x,t)\exp\left[M_S(x)\right]=\alpha\left[t^{(b/t+1)}\exp\left(\frac{b}{t}+\frac{N_S(x)}{a}\right)\right]+\alpha^2 \tag{14}$$

Differentiating eq (14) with respect to a, we obtain

$$\alpha=-\frac{1}{2}t^{(b/t+1)}\exp\left[\frac{b}{t}+\frac{N_S(x)}{a}\right]$$

Putting the value of α again in eq (14), we obtain envelope

$$F_2^S(x,t)\exp\left[M_S(x)\right]=-\frac{1}{4}\left[t^{(b/t+1)}\exp\left(\frac{b}{t}+\frac{N_S(x)}{a}\right)\right]^2$$

Therefore,

$$F_2^S(x,t)=-\frac{1}{4}t^{2(b/t+1)}\exp\left[\frac{2b}{t}+\frac{2N_S(x)}{a}-M_S(x)\right], \tag{15}$$

which is merely a particular solution of the general solution.

Now, defining

$$F_2^S(x,t_0)=-\frac{1}{4}t_0^{2(b/t_0+1)}\exp\left[\frac{2b}{t_0}+\frac{2N_S(x)}{a}-M_S(x)\right]$$

at $t=t_0$, where $t_0=\ln\left(Q_0^2/\Lambda^2\right)$ at any lower value $Q=Q_0$ we get from eq (15)

$$F_2^S(x,t)=F_2^S(x,t_0)\left(\frac{t^{(b/t+1)}}{t_0^{(b/t_0+1)}}\right)^2\exp\left[2b\left(\frac{1}{t}-\frac{1}{t_0}\right)\right], \tag{16}$$

which gives the t evolution of the singlet structure function $F_2^S(x,t)$ in NLO.

Proceeding exactly in the same way and defining

$$F_2^{NS}(x,t_0)=-\frac{1}{4}t_0^{2(b/t_0+1)}\exp\left[\frac{2b}{t_0}+\frac{2N_{NS}(x)}{a}-M_{NS}(x)\right],$$

where $$N_{NS}(x)=\int\frac{dx}{A_S(x)+T_0B_S(x)}$$

and $$N_{NS}(x)=\int\frac{A_6(x)+T_0B_6(x)}{A_S(x)+T_0B_S(x)}\,dx$$

we get for non singlet structure function in NLO

$$F_2^{NS}(x,t)=F_2^{NS}(x,t_0)\left(\frac{t^{(b/t+1)}}{t_0^{(b/t_0+1)}}\right)^2\exp\left[2b\left(\frac{1}{t}-\frac{1}{t_0}\right)\right], \tag{17}$$

which gives the t evolution of the singlet structure function $F_2^{NS}(x,t)$ in NLO for $\beta=\alpha^2$.

In an earlier communication [1], we suggested that for low-x in LO $\beta=\alpha^2$

$$F_2^S(x,t)=F_2^S(x,t_0)\left(\frac{t}{t_0}\right)^2 \tag{18}$$

and

$$F_2^{NS}(x,t)=F_2^{NS}(x,t_0)\left(\frac{t}{t_0}\right)^2 \tag{19}$$

We observe that if b tends to zero then eqs (16) and (17) tend to eqs (18) and (19) respectively i.e., solution of NLO equations goes to that of LO equations. Physically, b tends to zero means that the number of flavours is high.

Again defining,

$$F_2^S(x_0,t)=-\frac{1}{4}t^{(b/t+1)}\exp\left[\frac{2b}{t}+\frac{2N_S(x)}{a}-M_S(x)\right]_{x=x_0}.$$

we obtain from eq (15)

$$F_2^S(x,t) = F_2^S(x_0,t)\exp\int_{x_0}^{x}\left[\frac{2}{a}\frac{1}{L_2(x)+T_0M_2(x)} - \frac{L_1(x)+T_0M_1(x)}{L_2(x)+T_0M_2(x)}\right]dx, \quad (20)$$

which gives the x-evolution of singlet structure function $F_2^S(x,t)$ in NLO

Similarly, defining

$$F_2^{NS}(x_0,t) = -\frac{1}{4}t^{(b/t+1)}\exp\left[\frac{2b}{t}+\frac{2N_{NS}(x)}{a}-M_{NS}(x)\right]_{x_0},$$

we get

$$F_2^{NS}(x,t) = F_2^{NS}(x_0,t)\exp\int_{x_0}^{x}\left[\frac{2}{a}\frac{1}{A_S(x)+T_0B_S(x)} - \frac{A_6(x)+T_0B_6(x)}{A_S(x)+T_0B_S(x)}\right]dx, \quad (21)$$

which gives the x evolution of non-singlet structure function $F_2^{NS}(x,t)$ in NLO

In an earlier communication [1], we suggested that for low-x in LO for $\beta = \alpha^2$

$$F_2^S(x,t) = F_2^S(x_0,t)\exp\left[\int_{x_0}^{x}\left(\frac{2}{A_f M(x)} - \frac{L(x)}{M(x)}\right)dx\right], \quad (22)$$

and

$$F_2^{NS}(x,t) = F_2^{NS}(x_0,t)\exp\left[\int_{x_0}^{x}\left(\frac{2}{A_f Q(x)} - \frac{P(x)}{Q(x)}\right)dx\right], \quad (23)$$

where

$$A_f = 4/(33-2N_f),\quad P(x) = 3+4\ln(1-x)-(1-x)(x+3),$$

$$Q(x) = x(1-x^2)-2x\ln x,$$

$$L(x) = P(x)+K(x)C(x)+D(x)\frac{\partial K(x)}{\partial x}$$

and $M(x) = Q(x)+K(x)D(x)$,

where again,

$$C(x) = 1/2N_f(1-x)(2-x+2x^2)$$

and $D(x) = N_f x\left[-1/2(1-x)(5-4x+2x^2)+(3/2)\ln(1/x)\right]$

Of course, unlike for the t-evolution equations, we could not have for the x-evolution equations in LO as some limiting case of NLO equations

Deuteron, proton and neutron structure functions measured in deep inelastic electro-production, can be written in terms of singlet and non-singlet quark distribution functions [19] as

$$F_2^d(x,t) = 5/9F_2^S(x,t), \quad (24)$$

$$F_2^p(x,t) = 5/18F_2^S(x,t)+3/18F_2^{NS}(x,t), \quad (25)$$

$$F_2^n(x,t) = 5/18F_2^S(x,t)-3/18F_2^{NS}(x,t) \quad (26)$$

and $F_2^p(x,t)-F_2^n(x,t) = 1/3F_2^{NS}(x,t)$ (27)

Now using eqs (16) and (20) in eq (24), we will get t and x-evolution of deuteron structure function $F_2^d(x,t)$ at low-x in NLO as

$$F_2^d(x,t) = F_2^d(x,t_0)\left(\frac{t^{(b/t+1)}}{t_0^{(b/t_0+1)}}\right)^2\exp\left[2b\left(\frac{1}{t}-\frac{1}{t_0}\right)\right] \quad (28)$$

and $F_2^d(x,t) = F_2^d(x_0,t)\exp\int_{x_0}^{x}\left[\frac{2}{a}\frac{1}{L_2(x)+T_0M_2(x)} - \frac{L_1(x)+T_0M_1(x)}{L_2(x)+T_0M_2(x)}\right]dx,$ (29)

where the input functions are

$$F_2^d(x,t_0) = \frac{5}{9}F_2^S(x,t_0) \text{ and } F_2^d(x_0,t) = \frac{5}{9}F_2^S(x_0,t)$$

The corresponding results for particular solutions of DGLAP evolution equations in LO for $\beta = \alpha^2$ obtained earlier [1] are

$$F_2^d(x,t) = F_2^d(x_0,t)\left(\frac{t}{t_0}\right)^2 \quad (30)$$

and

$$F_2^d(x,t) = F_2^d(x_0,t)\exp\left[\int_{x_0}^{x}\left(\frac{1}{A_f M(x)} - \frac{L(x)}{M(x)}\right)dx\right] \quad (31)$$

Similarly, using eqs (16) and (17) in eqs (25), (26) and (27), we get the t – evolutions of proton, neutron, and difference and ratio of proton and neutron structure functions at low-x in NLO as

$$F_2^p(x,t) = F_2^p(x,t_0)\left(\frac{t^{(b/t+1)}}{t_0^{(b/t_0+1)}}\right)^2\exp\left[2b\left(\frac{1}{t}-\frac{1}{t_0}\right)\right], \quad (32)$$

$$F_2^n(x,t) = F_2^n(x,t_0)\left(\frac{t^{(b/t+1)}}{t_0^{(b/t_0+1)}}\right)^2\exp\left[2b\left(\frac{1}{t}-\frac{1}{t_0}\right)\right], \quad (33)$$

$$F_2^p(x,t)-F_2^n(x,t)=\left[F_2^p(x,t_0)-F_2^n(x,t_0)\right]\times\left(\frac{t^{(b/t+1)}}{t_0^{(b/t_0+1)}}\right)^2\exp\left[2b\left(\frac{1}{t}-\frac{1}{t_0}\right)\right], \quad (34)$$

and

$$\frac{F_2^p(x,t)}{F_2^n(x,t)}=\frac{F_2^p(x,t_0)}{F_2^n(x,t_0)}=R(x), \quad (35)$$

where $R(x)$ is a constant for fixed x. The input functions are

$$F_2^p(x,t_0)=\frac{5}{18}F_2^S(x,t_0)+\frac{3}{18}F_2^{NS}(x,t_0),$$

$$F_2^n(x,t_0)=\frac{5}{18}F_2^S(x,t_0)-\frac{3}{18}F_2^{NS}(x,t_0),$$

and $$F_2^p(x,t_0)-F_2^n(x,t_0)=\frac{1}{3}F_2^{NS}(x,t_0)$$

The corresponding results for particular solutions of DGLAP evolution equations in LO for $\beta=\alpha^2$ are

$$F_2^p(x,t)=F_2^p(x,t_0)\left(\frac{1}{t_0}\right)^2 \quad (36)$$

$$F_2^n(x,t)=F_2^n(x,t_0)\left(\frac{1}{t_0}\right)^2, \quad (37)$$

$$F_2^p(x,t)-F_2^n(x,t)=\left[F_2^p(x,t_0)-F_2^n(x,t_0)\right]\left(\frac{1}{t_0}\right)^2, \quad (38)$$

and $$\frac{F_2^p(x,t)}{F_2^n(x,t)}=\frac{F_2^p(x,t_0)}{F_2^n(x,t_0)}=R(x), \quad (39)$$

where $R(x)$ is a constant for fixed-x.

It is observed that the ratio of proton and neutron is same for both NLO and LO and it is independent of t for fixed x.

For the complete solution of eq (10), we take $\beta=\alpha^2$ in eq (13). If we take $\beta=\alpha$ in eq (13) and differentiate with respect to α as before, we get

$$0=t^{(b/t+1)}\exp\left(\frac{b}{t}+\frac{N_s(x)}{a}\right)+1,$$

from which we can not determine the value of α.

But taking $\beta=\alpha^3$ in eq (13) and differentiating with respect to α, we get

$$\alpha=\sqrt{-\frac{1}{3}t^{(b/t+1)}\exp\left(\frac{b}{t}+\frac{N_s(x)}{a}\right)}$$

which is imaginary. Putting this value of α in eq (13), we get ultimately

$$F_2^S(x,t)=t^{(b/t+1)^{3/2}}\left\{\left(-\frac{1}{3}\right)^{1/2}+\left(-\frac{1}{3}\right)^{3/2}\right\}\times\exp\left[\left(\frac{b}{t}+\frac{N_s(x)}{a}\right)^{3/2}-M_S(x)\right]$$

Now, defining

$$F_2^S(x,t_0)=t_0^{(b/t_0+1)^{3/2}}\left\{\left(-\frac{1}{3}\right)^{3/2}+\left(-\frac{1}{3}\right)^{3/2}\right\}\times\exp\left[\left(\frac{b}{t_0}+\frac{N_s(x)}{a}\right)^{3/2}-M_S(x)\right],$$

we get

$$F_2^S(x,t)=F_2^S(x,t_0)\left(\frac{t^{(b/t+1)}}{t_0^{(b/t_0+1)^{3/2}}}\right)^{3/2}\exp\left[\frac{3}{2}b\left(\frac{1}{t}-\frac{1}{t_0}\right)\right]$$

Proceeding exactly in the same way we get for non-singlet structure function also

$$F_2^{NS}(x,t)=F_2^{NS}(x,t_0)\left(\frac{t^{(b/t+1)}}{t_0^{(b/t_0+1)}}\right)^{3/2}\exp\left[\frac{3}{2}b\left(\frac{1}{t}-\frac{1}{t_0}\right)\right]$$

Then using eqs (24), (25) (26) and (27) we get t-evolutions of deuteron, proton, neutron and difference of proton and neutron structure functions

$$F_2^{d\,p\,n\,p-n}(x,t)=F_2^{d\,p\,n\,p-n}(x,t_0)\left(\frac{t^{(b/t+1)}}{t_0^{(b/t_0+1)}}\right)^{3/2}\times\exp\left[\frac{3}{2}b\left(\frac{1}{t}-\frac{1}{t_0}\right)\right]$$

Proceeding in the same way, we get x evolutions of deuteron structure function

$$F_2^d(x,t)=F_2^d(x,t_0)\exp\int_{x_0}^{x}\left(\frac{3/2}{a}\right.\quad\left.\frac{1}{L_2(x)+T_0M_2(x)}\right.\left.-\frac{L_1(x)+T_0M_1(x)}{L_2(x)+T_0M_2(x)}\right)dx$$

But the x-evolutions of proton and neutron structure functions like those of deuteron structure function can not be obtained by this methodology as discussed earlier.

Proceeding exactly in the same way, we can show that if we take $\beta = \alpha^4$, we get

$$F_2^{d\,p\,n\,p-n}(x,t) = F_2^{d\,p\,n\,p-n}(x,t_0)\left(\frac{t^{(b/t+1)}}{t_0^{(b/t_0+1)}}\right)^{4/3} \times \exp\left[\frac{4}{3}b\left(\frac{1}{t}-\frac{1}{t_0}\right)\right]$$

and

$$F_2^d(x,t) = F_2^d(x,t_0)\exp\int_{t_0}^{t}\left(\frac{4/3}{a}\frac{1}{L_2(x)+T_0M_2(x)} - \frac{L_1(x)+T_0M_1(x)}{L_2(x)+T_0M_2(x)}\right)dx$$

Similarly, if we take $\beta = \alpha^5$, we get

$$F_2^{d\,p\,n\,p-n}(x,t) = F_2^{d\,p\,n\,p\,\,n}(x,t_0)\left(\frac{t^{(b/t+1)}}{t_0^{(b/t_0+1)}}\right)^{5/4} \times \exp\left[\frac{5}{4}b\left(\frac{1}{t}-\frac{1}{t_0}\right)\right]$$

and $F_2^d(x,t) = F_2^d(x_0,t)\exp\int_{x_0}^{x}\left(\frac{5/4}{a}\frac{1}{L_2(x)+T_0M_2(x)} - \frac{L_1(x)+T_0M_1(x)}{L_2(x)+T_0M_2(x)}\right)dx$ and so on

Thus we observe that if we take $\beta = \alpha$ in eq (13), we can not obtain the value of α and also the required solution But if we take $\beta = \alpha^2, \alpha^3, \alpha^4, \alpha^5$ and so on, we see that the powers of $t^{b/t+1}/t_0^{b/t_0+1}$ and coefficient of $b(1/t-1/t_0)$ of the exponential part in t-evolutions of deuteron, proton and neutron structure functions are 2, 3/2, 4/3, 5/4 and so on respectively, as discussed above Similarly, for x evolutions of deuteron structure functions we see that the numerators of the first term inside the integral sign are 2, 3/2, 4/3, 5/4 and so on respectively, for the same values of α Thus we see that if in the relation $\beta = \alpha^\nu$, ν varies between 2 and a maximum value, the powers of $t^{b/t+1}/t_0^{b/t_0+1}$ and coefficient of $b(1/t-1/t_0)$ of the exponential part in t- evolution varies between 2 and 1, and the numerator of the first term in the integral sign in x-evolution varies between 2 and 1 Then it is understood that the solutions of eqs (10) and (11) obtained by this methodology are not unique and so the *t*-evolutions of deuteron, proton, neutron and difference of proton and neutron structure functions, and x-evolution of deuteron structure function obtained by this methodology are also not unique They become eqs (28), (29), (32), (33), (34) for $\nu = 2$, but they reduce to equations

$$F_2^{d\,p\,n\,p-n}(x,t) = F_2^{d\,p\,n\,p-n}(x,t_0)\left(\frac{t^{(b/t+1)}}{t_0^{(b/t_0+1)}}\right)\exp\left[b\left(\frac{1}{t}-\frac{1}{t_0}\right)\right]$$

and

$$F_2^d(x,t) = F_2^d(x_0,t)\exp\int_{x_0}^{x}\left(\frac{1}{a}\frac{1}{L_2(x)+T_0M_2(x)} - \frac{L_1(x)+T_0M_1(x)}{L_2(x)+T_0M_2(x)}\right)dx$$

for a maximum value of ν

Thus by this methodology, instead of having a single solution, we arrive at a band of solutions, of course the range for these solutions is reasonably narrow

3. Results and discussion

In the present paper, we compare our results of *t*-evolution of deuteron, proton, neutron and difference and ratio of proton and neutron structure functions with the HERA [6] and NMC [7] low-x and low-Q^2 data In case of HERA data [6], proton and neutron structure functions are measured in the range of $2 \le Q^2 \le 50$ GeV^2 Moreover, here $P_t \le 200$ MeV, where P_t is the transverse momentum of the final state baryon In case of NMC data, proton and deuteron structure functions are measured in the range of $0.75 \le Q_2 \le 27$ GeV^2 We consider number of flavours $N_f = 4$ We also compare our results of *t* evolution of proton structure functions with recent global parameterization [8] This parameterization includes data from H1-96\99, ZEUS-96/97(X0 98), NMC, E665 data

In Figures 1(a-d), we present our results of *t*-evolutions of deuteron, proton, neutron and difference of proton and neutron structure functions (solid lines) respectively, for the representative values of x given in the figures for $\nu = 2$ (upper solid lines) and ν = maximum (lower solid lines) in $\beta = \alpha^\nu$ relation Data points at lowest Q^2 values in the figures are taken as input to test the evolution equation Agreement with the data [7, 6] is found to be good In the same figures, we also plot the results of *t* evolutions of deuteron, proton, neutron and difference of proton and neutron structure functions (dashed lines) for the particular solutions in leading order Here, the upper dashed lines are for $\nu = 2$ and lower dashed lines, for ν = maximum in $\beta = \alpha^\nu$ relation We observe that *t*-evolutions are slightly steeper in LO calculations than those of NLO But differences in results for proton and neutron structure functions are smaller and NLO results for $\nu = 2$ are in better agreement with experimental data, in general

In Figure 2, we compare our results of t evolutions of proton structure functions F_2^p (solid lines) with recent global parameterization [8] (long dashed lines) for the representative

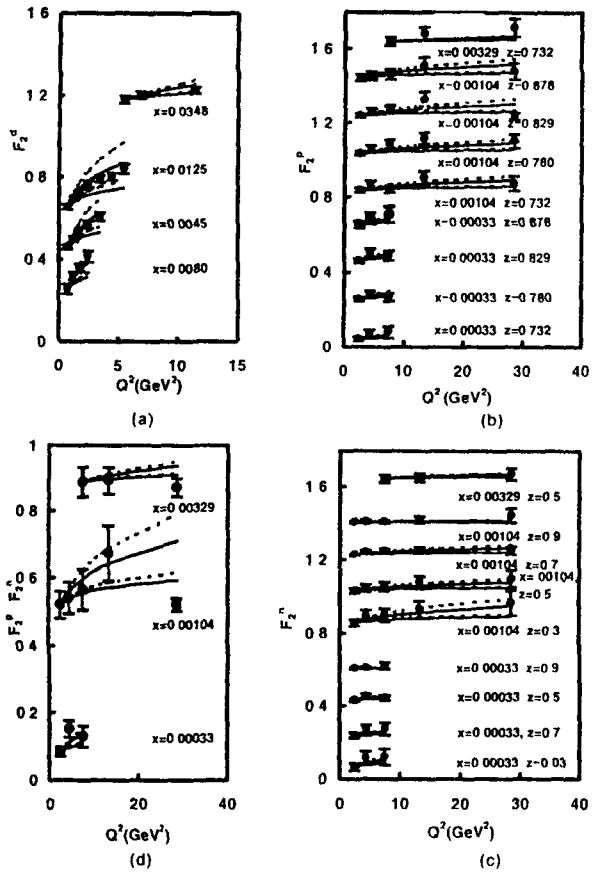

Figure 1(a-d) Results of t evolutions of deuteron proton neutron and difference of proton and neutron structure functions (solid lines) for the representative values of x in next to leading order for NMC and HERA data For convenience value of each data point is increased by adding $0.2i$ (a c) and $0.4i$ (d) where $i = 0, 1, 2, 3$ are the numberings of curves counting from the bottom of the lowermost curve as the 0 th order In the same figures we also plot the results of t evolutions of deuteron proton neutron and difference of proton and neutron structure functions (dashed lines) for the particular solutions in leading order Data points at lowest Q^2 values in the figures are taken as input

values of x given in the figures for $y = 2$ (upper solid lines) and $y =$ maximum (lower solid lines) in $\beta = \alpha'$ relation Data points at lowest-Q^2 values in the figures are taken as input to test the evolution equation In the same figure, we also plot the results of t-evolutions of proton structure functions F_2^p (dashed lines) for the particular solutions in leading order Here, the upper dashed lines are for $y = 2$ and the lower dashed lines are for $y =$ maximum in $\beta = \alpha'$ relation We observe that the t-evolutions are slightly steeper in LO calculations than those of NLO Agreement with the NLO results is found to be better than with the LO results

In Figure 3, we present our results of t evolutions of ratio of proton and neutron structure functions F_2^p/F_2^n (solid lines) for the representative values of x given in the figures Though according to our theory, the ratio should be independent of t,

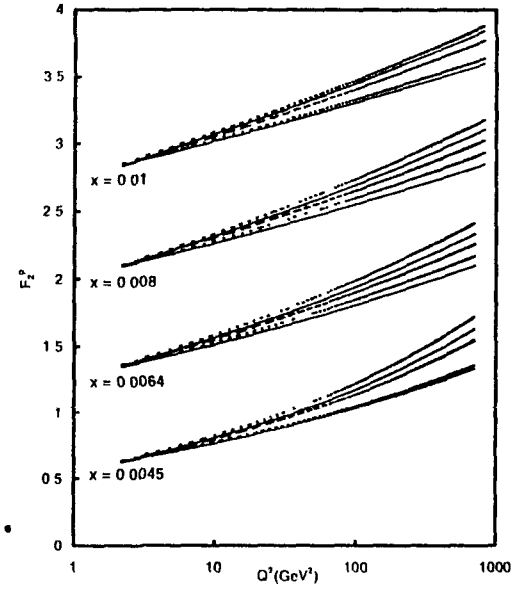

Figure 2 Results of t evolutions of proton structure functions F_2^p (solid lines) with recent global parameterization (long dashed lines) for the representative values of x given in the figures Data points at lowest Q^2 values in the figures are taken as input In the same figure we also plot the results of t evolutions of proton structure functions F_2^p (dashed lines) for the particular solutions in leading order For convenience value of each data point is increased by adding $0.5i$ where $i = 0, 1, 2, 3$ are the numberings of curves counting from the bottom of the lowermost curve as the 0 th order

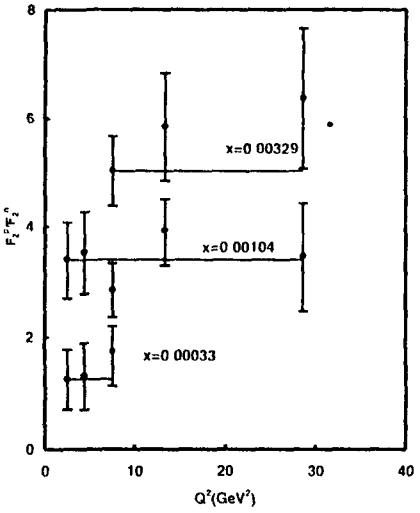

Figure 3 Results of t evolutions of the ratio of proton and neutron structure functions F_2^p/F_2^n (solid lines) for the representative values of x given in the figures Data points at lowest Q^2 values in the figures are taken as input

due to the lack of sufficient amount of data and due to large error bars a clear cut conclusion can not be drawn

In Figure 4, we plot $T(t)^2$ and $I_0 T(t)$ where $T(t) = \alpha_s(t)/2\pi$ against Q^2 in the Q^2 range of $0.5 \le Q^2 < 1000\ \text{GeV}^2$ as required by the data used by us Though the explicit value of T0 is not necessary in calculating t evolution yet we observe that for $T_0 = 0.027$ errors become minimum in the Q^2 range of $0.5 \le Q^2 \le 1000\ \text{GeV}^2$

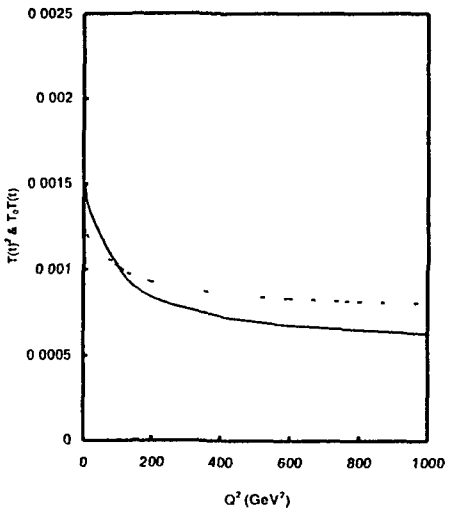

Figure 4 $T(t)^2$ and $I_0 I(t)$ where $I(t) = \alpha_s(t)/2\pi$ against Q^2 in the Q^2 range of $0.5 < Q^2 \le 1000\ \text{GeV}^2$

Though we compare our results for $\nu = 2$ and y = maximum in $\beta = \alpha^{\nu}$ relation with data, agreement of the result with experimental data is found to be excellent with $\nu = 2$ for t evolution in next to leading order

We can also calculate x evolution of non singlet and singlet structure function at low x from eqs (22) and (23) But it involves complicated integrals as eqs (22) and (23) involve $L_1(x)$ $L_2(x)$, $M_1(x)$, and $M_2(x)$ which are again functions of $A_1(x)$ $A_2(x)$ $A_3(x)$, $A_4(x)$ $B_1(x)$ $B_2(x)$, $B_3(x)$ and $B_4(x)$ But these functions involve many integrals making the calculation of x distribution complicated We keep it as our subsequent work

Acknowledgment

We are grateful to G A Ahmed of Department of Physics of Tezpur University for the help in the computational part of this work One of us (JKS) is grateful to the University Grants Commission, New Delhi for the financial assistance to this work in the form of a major research project

References

[1] R Rajkhowa and J K Sarma *Indian J Phys* **78A(3)** 365 (2004)
[2] G Altarelli and G Parisi *Nucl Phys* **B126** 298 (1977)
[3] G Altarelli *Phys Rep* **81** 1 (1981)
[4] V N Gribov and L N Lipatov *Sov J Nucl Phys* **20** 94 (1975)
[5] Y L Dokshitzer *Sov Phys JETP* **46** 641 (1977)
[6] C Adloff III Collaboration DESY 98-169 hep-ex/9811013 (1998)
[7] M Arneodo hep/961031 NMC *Nucl Phys* **B483** 3 (1997)
[8] A D Martin *et al* hep ph / 0110215 (2001)
[9] R Rajkhowa and J K Sarma hep ph/0203070 (2002)
[10] W Furmanski and R Petronzio *Nucl Phys* **B195** 237 (1982)
[11] W Furmanski and R Petronzio *Z Phys* **C11** 293 (1982) *Phys Lett* **B97** 437 (1980)
[12] A Deshamukhya and D K Choudhury *Proc 2nd Regional Conf Phys Research* (in North East Guwahati India October 2001) 34 (2001)
[13] I S Gradshteyn and I M Ryzhik *Tables of Integrals Series and Products* (ed) Alen Jeffrey (New York Academic) (1965)
[14] D K Choudhury and J K Sarma *Pramana J Phys* **39** 273 (1992)
[15] J K Sarma D K Choudhury G K Medhi *Phys Lett* **B403** 139 (1997)
[16] J K Sarma and B Das *Phys Lett* **B304** 323 (1993)
[17] F Ayres (Jr) *Differential Equations* (Schaums Outline Series) (New York McGraw Hill) (1952)
[18] F H Miller *Partial Differential Equation* John and Wiley (1960)
[19] F Halzen A D Martin *Quarks and Leptons An Introductory Course in Modern Particle Physics* (New York John Wiley) (1984)

Indian J Phys **79** (1), 55-64 (2005)

AN INTERNATIONAL JOURNAL
IJP

Particular solution of DGLAP evolution equation in next-to leading order and x-distributions of deuteron structure functions at low-x

R Rajkhowa and J K Sarma*
Department of Physics Tezpur University
Napaam Tezpur 784 028 Assam India

E mail jks@tezu ernet in

Received 13 February 2004 accepted 29 November 2004

Abstract We present particular solutions of singlet and non singlet Dokshitzer Gribov Lipatov Altarelli Parisi (DGLAP) evolution equations in next to leading order (NLO) at low x We obtain x evolutions of deuteron structure functions at low x from DGLAP evolution equations The results of x evolutions are compared with NMC low x and low Q^2 data and with those of leading order (LO) solutions of DGLAP evolution equations

Keywords Dokshitzer Gribov Lipatov Altarelli Parisi evolution equations particular solution deuteron structure functions

PACS Nos 21 30 x 21 45 +v

1. Introduction

The Dokshitzer-Gribov-Lipatov-Altarelli Parisi (DGLAP) evolution equations [1-4] are fundamental tools to study the $t\left(=\ln\left(Q^2/\Lambda^2\right)\right)$ and x evolutions of structure functions, where x and Q^2 are Bjorken variable and four momenta transfer respectively in a deep inelastic scattering (DIS) process [5] and Λ is the QCD cut off parameter On the other hand, the study of structure functions at low x has become topical in view [6] of high energy collider and super collider experiments [7] Solutions of DGLAP evolution equations give quark and gluon structure functions which ultimately produce, proton, neutron and deuteron structure functions Those structure functions are important inputs in many high energy processes Moreover the determination of their t and x evolutions is a test for QCD the underlying dynamics of quarks and gluons inside hadrons Though some numerical solutions are available in the literature [8, 9], the explorations of the possibility of obtaining analytical solutions of DGLAP evolution equations are always interesting In this connection particular solutions of DGLAP evolution equations at low x in leading order (LO) have already been obtained by applying Taylor expansion method [10] and t and x evolutions [11-15] of structure functions for intermediate and low-x have been presented Here, the particular solutions have been obtained either by a linear combination of U and V of the general solution $f(U, V) = 0$ [11-13] or from the complete solution [14, 15] of the equation We also have obtained particular solution of DGLAP evolution equation from the complete solution in next to-leading order (NLO) for non-singlet and singlet structure functions [15, 16] and compared our results with HERA H1 [17] and NMC [18] data

The present paper reports particular solutions of DGLAP evolution equations computed from complete solutions in NLO at low x and calculation of t and x-evolutions for singlet and non-singlet structure functions, and hence x-evolutions of deuteron structure functions In some instance we can deal with particular solutions more conveniently than with the general solutions [19] In calculating structure functions input data points have been taken from experimental data directly unlike the usual practice of using an input distribution function introduced by hand These NLO results are compared with the NMC low-x, low-Q^2 data and with those of particular solution in LO Here, Section 1, Section 2, and Section 3 present the introduction, the relevant theory and the results and discussion, respectively

2. Theory

Though the basic theory has been discussed elsewhere [15,

* Corresponding Author

16], here we have mentioned some essential steps for clarity The DGLAP evolution equations with splitting functions [20, 21] for singlet and non-singlet structure functions in NLO are in the standard forms [22]

$$\frac{\partial F_2^S(x,t)}{\partial t} = \frac{\alpha_s(t)}{2\pi} \times \left[\frac{2}{3}\{3+4\ln(1-x)\}F_2^S(x,t) + \frac{4}{3}\int_x^1 \frac{dw}{1-w}\left\{\left(1+w^2\right)F_2^S\left(\frac{x}{w},t\right) - 2F_2^S(x,t)\right\} + N_f\int_x^1 \left\{w^2+(1-w)^2\right\}G\left(\frac{x}{w},t\right)\right] + \left(\frac{\alpha_s(t)}{2\pi}\right)^2 \times \left[(x-1)F_2^S(x,t)\int_0^1 f(w)dw + \int_x^1 f(w)F_2^S\left(\frac{x}{w},t\right)dw + \int_x^1 \Gamma_{qq}^S(w)F_2^S\left(\frac{x}{w},t\right)dw\right] + \left(\frac{\alpha_s(t)}{2\pi}\right)^2 \int_x^1 I_{qs}^S(w)G\left(\frac{x}{w},t\right)dw = 0 \tag{1}$$

and

$$\frac{\partial F_2^{NS}(x,t)}{\partial t} = \frac{\alpha_s(t)}{2\pi} \times \left[\frac{2}{3}\{3+4\ln(1-x)\}F_2^{NS}(x,t) + \frac{4}{3}\int_x^1 \frac{dw}{1-w}\left\{\left(1+w^2\right)F_2^{NS}\left(\frac{x}{w},t\right) - 2F_2^{NS}(x,t)\right\}\right] - \left(\frac{\alpha_s(t)}{2\pi}\right)^2 \left[(x-1)F_2^{NS}(x,t)\int_0^1 f(w)dw + \int_x^1 f(w)F_2^{NS}\left(\frac{x}{w},t\right)dw\right] = 0, \tag{2}$$

where $\beta_0 = \frac{33-2N_f}{3}$ and $\beta_1 = \frac{306-38N_f}{3}$, N_f being the number of flavours

Here, $f(w) = C_F^2\left[P_F(w) - P_A(w)\right] + \frac{1}{2}C_F C_A\left[P_G(w) + P_A(w)\right] + C_F T_R N_f P_{N_f}(w)$,

$$F_{qq}^S(w) = 2C_F T_R N_f F_{qq}(w)$$

and $F_{qg}^S(w) = C_F T_R N_f \Gamma_{qg}^1(w) + C_G T_R N_f \Gamma_{qg}^2(w)$

The explicit forms of higher order kernels are [20–21]

$$P_F(w) = -2\left(\frac{1+w^2}{1-w}\right)\ln w \ln(1-w) - \left(\frac{3}{1-w}+2w\right)\ln w - \frac{1}{2}(1+w)\ln^2 w - 5(1-w),$$

$$P_G(w) = \frac{1+w^2}{1-w}\left(\ln^2 w + \frac{11}{3}\ln w + \frac{67}{9} - \frac{\pi^2}{3}\right) + 2(1+w)\ln w + \frac{40}{3}(1-w),$$

$$P_{N_f}(w) = \frac{2}{3}\left[\frac{1+w^2}{1-w}\left(-\ln w - \frac{5}{3}\right) - 2(1-w)\right],$$

$$P_A(w) = 2\left(\frac{1+w^2}{1-w}\right)\int_{w/(1+w)}^{1/(1+w)} \frac{dk}{k}\ln\frac{1-k}{k} + 2(1+w)\ln w + 4(1-w),$$

$$I_{qq}(w) = \frac{20}{9w} - 2 + 6w - \frac{56}{9}w^2 + \left(1+5w+\frac{8}{3}w^2\right)\ln w - (1+w)\ln^2 w,$$

$$I_{qs}^1(w) = 4 - 9w - (1-4w)\ln w - (1-2w)\ln^2 w + 4\ln(1-w) + \left[2\ln^2\left(\frac{1-w}{w}\right) - 4\ln\left(\frac{1-w}{w}\right) - \frac{2}{3}\pi^2 + 10\right]P_{qg}(w)$$

and

$$F_{qg}^2(w) = \frac{182}{9} + \frac{14}{9}w + \frac{40}{9w} + \left(\frac{136}{3}w - \frac{38}{3}\right)\ln w - 4\ln(1-w) - (2+8w)\ln^2 w + \left[-\ln^2 w + \frac{44}{3}\ln w - 2\ln^2(1-w) + 4\ln(1-w) + \frac{\pi^2}{3} - \frac{218}{3}\right]P_{qg}(w) + 2P_{qg}(-w)\int_{w/(1+w)}^{1/(1+w)} \frac{dz}{z}\ln\frac{1-z}{z},$$

where $P_{qg}(w) = w^2 + (1-w)^2$, $C_1 = C_G = N_C = 3$,

$C_F = (N_C^2 - 1)/2N_C$ and $T_R = 1/2$

Let us introduce the variable $u = 1-w$ and note that [23]

$$\frac{x}{w} = \frac{x}{1-u} = x\sum_{k=0}^{\infty} u^k \tag{3}$$

The series (3) is convergent for $|u| < 1$ Since $x < w < 1$, so $0 < u < 1 - x$ and hence the convergence criterion is satisfied Now, using Taylor expansion method [10], we can rewrite $F_2^S(x/w, t)$ as

$$F_2^S(x/w,t) = F_2^S\left(x + x\sum_{k=1}^{\infty} u^k, t\right)$$

$$= F_2^S(x,t) + x\sum_{k=1}^{\infty} u^k \frac{\partial F_2^S(x,t)}{\partial x} + \frac{1}{2}x^2\left(\sum_{k=1} u^k\right)^2 \frac{\partial^2 F_2^S(x,t)}{\partial x^2} + \quad (4)$$

which covers the whole range of u $0 < u < 1-x$. Since x is small in our region of discussion the terms containing x^2 and higher powers of x can be neglected as our first approximation as discussed in our earlier works [11, 12, 14–16]. $F_2^S(x/u,t)$ can be approximated for small x as

$$F_2^S(x/u,t) \cong F_2^S(x,t) + x\sum_{k=1}^{\infty} u^k \frac{\partial F_2^S(x,t)}{\partial x} \quad (5)$$

Similarly, $G(x/u,t)$ and $F_2^{NS}(x/u,t)$ can be approximated for small-x as

$$G(x/u,t) \cong G(x,t) + x\sum_{k=1}^{\infty} u^k \frac{\partial G(x,t)}{\partial x} \quad (6)$$

and

$$F_2^{NS}(x/u,t) \cong F_2^{NS}(x,t) + x\sum_{k=1}^{\infty} u^k \frac{\partial F_2^{NS}(x,t)}{\partial x} \quad (7)$$

Using eq (3), (5) and (6) in eq (1) and performing u integrations, we get

$$\frac{\partial F_2^S(x,t)}{\partial x} - \left[\frac{\alpha_s(t)}{2\pi}A_1(x) + \left(\frac{\alpha_s(t)}{2\pi}\right)^2 B_1(x)\right] F_2^S(x,t)$$

$$- \left[\frac{\alpha_s(t)}{2\pi}A_2(x) + \left(\frac{\alpha_s(t)}{2\pi}\right)^2 B_2(x)\right] G(x,t)$$

$$- \left[\frac{\alpha_s(t)}{2\pi}A_3(x) + \left(\frac{\alpha_s(t)}{2\pi}\right)^2 B_3(x)\right] \frac{\delta F_2^S(x,t)}{\partial x}$$

$$- \left[\frac{\alpha_s(t)}{2\pi}A_3(x) + \left(\frac{\alpha_s(t)}{2\pi}\right)^2 B_3(x)\right] 4$$

$$- \left[\frac{\alpha_s(t)}{2\pi}A_4(x) + \left(\frac{\alpha_s(t)}{2\pi}\right)^2 B_4(x)\right] \frac{\partial G(x,t)}{\partial x} = 0, \quad (8)$$

where

$$A_1(x) = \frac{2}{3}\left\{3 + 4\ln(1-x) + (x-1)(x+3)\right\},$$

$$A_2(x) = N_f\left[\frac{1}{3}(1-x)\left(2 - x + 2x^2\right)\right]$$

$$A_3(x) = \frac{2}{3}\left\{x\left(1-x^2\right) + 2x\ln\left(\frac{1}{x}\right)\right\}$$

$$A_4(x) = N_f x\left\{\ln\frac{1}{x} - \frac{1}{3}(1-x)\left(5 - 4x + 2x^2\right)\right\}$$

$$B_1(x) = x\int_0^1 f(u)du - \int_0^x f(u)du + \frac{4}{3}N_f\left[-\ln x\left(\frac{20}{9} + 3x + 3x^2 + \frac{8}{9}x^3\right) + \frac{1}{2}x(2+x)\ln^2 x + 5x - \frac{3}{2}x^2 + \frac{64}{27}x^3 - \frac{317}{54}\right].$$

$$B_2(x) = \frac{2}{3}N_f\left[-\left(9x - 5x^2 + \frac{32}{9}x^3\right)\ln x + \left(3x - 3x^2 + \frac{4}{3}x^3\right)\ln^2 x + \left(\frac{32}{9}x^3 - \frac{14}{3}x^2 + \frac{8}{3}x - \frac{14}{9}\right)\ln(1-x) + \left(\frac{4}{3} - 2x + 2x^2 - \frac{4}{3}x^3\right)\ln^2(1-x) + \left(\frac{2}{3} - \frac{4}{9}\pi^2\right) + \left(\frac{2}{3}\pi^2 - \frac{59}{9}\right)x + \left(\frac{113}{9} - \frac{2}{3}\pi^2\right)x^2 + \left(\frac{4}{9}\pi^2 - \frac{20}{3}\right)x^3\right]$$

$$+ \frac{3}{2}N_f\left[-\left(\frac{40}{9} + 8x + 11x^2 + \frac{92}{9}x^2\right)\ln x + \left(3x + 3x^2 + \frac{2}{9}x^3\right)\ln^2 x + \left(\frac{14}{9} - \frac{8}{3}x + \frac{14}{3}x^2 - \frac{32}{9}x^3\right)\ln(1-x) + \left(-\frac{4}{3} + 2x - 2x^2 + \frac{4}{3}x^3\right)\ln^2(1-x) + \left(\frac{2}{9}\pi^2 - \frac{769}{54}\right) + \left(\frac{122}{9} - \frac{1}{3}\pi^2\right)x + \left(\frac{1}{3}\pi^2 - \frac{361}{18}\right)x^2 + \left(\frac{560}{27} - \frac{2}{9}\pi^2\right)x^3\right]$$

$$+ \frac{3}{2}N_f\int_x^1 2\left(w^2 + (1+w)^2\right)\left[-\ln\ln(1+w) - \ln w\ln(1+w) + \ln\ln\left(\frac{1+w}{w}\right) + \ln\frac{1}{w}\ln\left(1+\frac{1}{w}\right)\right].$$

$$B_3(x) = x\int_x^1 \frac{1-w}{w}f(w)dw + \frac{4}{3}N_f x\left[\left(\frac{38}{9} - 4x + \frac{5}{3}x^2 + \frac{8}{9}x^3\right)\ln x - \frac{1}{2}\left(1+x^2\right)\ln^2 x + \frac{1}{3}\ln^3 x + \frac{38}{9x} - 4x + \frac{95}{18}x^2 - \frac{64}{27}x^3 - \frac{61}{54}\right]$$

and

$$B_4(x) = x\int_x^1 \frac{1-w}{w}F_{qs}^S(w)dw$$

Let us assume for simplicity [11-14]

$$G(x,t) = K(x)\,F_2^S(x,t), \tag{9}$$

where $K(x)$ is a function of x. Now eq (8) becomes

$$\frac{\partial F_2^S(x,t)}{\partial t} - \left[\frac{\alpha_s(t)}{2\pi}L_1(x) + \left(\frac{\alpha_s(t)}{2\pi}\right)^2 M_1(x)\right]F_2^S(x,t)$$

$$-\left[\frac{\alpha_s(t)}{2\pi}L_2(x) + \left(\frac{\alpha_s(t)}{2\pi}\right)^2 M_2(x)\right]\frac{\partial F_2^S(x,t)}{\partial x} = 0 \tag{10}$$

where

$$L_1(x) = A_1(x) + K(x)A_2(x) + A_4(x)\frac{\partial K(x)}{\partial x}$$

$$M_1(x) = B_1(x) + K(x)B_2(x) + B_4(x)\frac{\partial K(x)}{\partial x},$$

$$L_2(x) = A_3(x) + K(x)A_4(x)$$

and $$M_2(x) = B_3(x) + K(x)B_4(x)$$

For a possible solution, we assume [15, 22] that

$$\left(\frac{\alpha_s(t)}{2\pi}\right)^2 = T_0\left(\frac{\alpha_s(t)}{2\pi}\right), \tag{11}$$

where T_0 is a numerical parameter to be obtained from the particular Q^2-range under study. By a suitable choice of T_0 we can reduce the error to a minimum. Now eq (10) can be recast as

$$\frac{\partial F_2^S(x,t)}{\partial t} - P_S(x,t)\frac{\partial F_2^S(x,t)}{\partial x} - Q_S(x,t)F_2^S(x,t) = 0, \tag{12}$$

where $$P_S(x,t) = \frac{\alpha_s(t)}{2\pi}\left[L_2(x) + T_0 M_2(x)\right]$$

and $$Q_S(x,t) = \frac{\alpha_s(t)}{2\pi}\left[L_1(x) + T_0 M_1(x)\right]$$

Secondly using eqs (3), (7) and (11) in eq (2) and performing u-integration, we have

$$\frac{\partial F_2^{NS}(x,t)}{\partial t} - P_{NS}(x,t)\frac{\partial F_2^{NS}(x,t)}{\partial x} - Q_{NS}(x,t)F_2^{NS}(x,t) = 0 \tag{13}$$

where $$P_{NS}(x,t) = \frac{\alpha_s(t)}{2\pi}\left[A_5(x) + T_0 B_5(x)\right]$$

and $$Q_{NS}(x,t) = \frac{\alpha_s(t)}{2\pi}\left[A_6(x) + T_0 B_6(x)\right]$$

with $$A_5(x) = \frac{2}{3}\left\{x(1-x^2) + 2x\ln\left(\frac{1}{x}\right)\right\}$$

$$B_5(x) = x\int_x^1 \frac{1-u}{u} f(u)\,du$$

$$A_6(x) = \frac{2}{3}\{3 + 4\ln(1-x) + (x-1)(x+3)\}$$

and $$B_6(x) = \int_0^x f(u)\,du + x\int_0^1 f(u)\,du$$

The general solutions [10, 19] of eqs (12) is $F(U, V) = 0$, where F is an arbitrary function and $U\left(x, t, F_2^S\right) = C_1$ and $V\left(x, t, F_2^S\right) = C_2$ where C_1 and C_2 are constants and they form a solution of equations

$$\frac{dx}{P_S(x,t)} = \frac{dt}{-1} = \frac{dF_2^S(x,t)}{-Q_S(x,t)} \tag{14}$$

We observed that the Lagrange's auxiliary system of ordinary differential equations [10, 19] occurred in the formalism can not be solved without the additional assumption of linearization (eq (11)) and introduction of an *ad hoc* parameter T_0. Which does not affect the results of t evolution of structure functions. Solving eq (14), we obtain

$$U\left(x, t, F_2^S\right) = t^{(b/a+1)}\exp\left[\frac{b}{t} + \frac{N_S(x)}{a}\right]$$

and $$V\left(x, t, F_2^S\right) = F_2^S(x,t)\exp\left[M_S(x)\right],$$

where $a = \frac{2}{\beta_0}$, $b = \frac{\beta_1}{\beta_0^2}$, $N_S(x) = \int \frac{dx}{L_2(x) + T_0 M_2(x)}$

and $M_S(x) = \int \frac{L_1(x) + T_0 M_1(x)}{L_2(x) + T_0 M_2(x)}dx$. If U and V are two independent solutions of eq (14) and if α and β are arbitrary constants, then $V = \alpha U + \beta$ may be taken as a complete solution of eq (14). We take this form as this is the simplest form of a complete solution which contains both the arbitrary constants α and β. Further [11, 12] we considered an equation $AU + BV = 0$ where A and B are arbitrary constants. But that is not a complete solution having both the arbitrary constants as this equation can be transformed to the form $V = CU$ where $C = -A/B$, i.e. the equation contains only one arbitrary constant. Then the complete solution [10, 19]

$$F_2^S(x,t)\exp\left[M_S(x)\right] = \alpha\left[t^{(b/a+1)}\exp\left(\frac{b}{t} + \frac{N_S(x)}{a}\right)\right] + \beta \tag{15}$$

is a two parameter family of planes which does not have an envelope since the arbitrary constants enter linearly [10]. Again differentiating eq (15) with respect to β we get $0 = 1$ which is absurd. Hence, there is no singular solution. The one parameter family determined by taking $\beta = \alpha^2$ has equation

$$F_2^S(x,t)\exp\left[M_S(x)\right] = \alpha\left[t^{(b/a+1)}\exp\left(\frac{b}{t} + \frac{N_S(x)}{a}\right)\right] + \alpha^2 \tag{16}$$

Differentiating eq (16) with respect to α, we obtain

$$\alpha = -\frac{1}{2}t^{(b/t+1)}\exp\left[\frac{b}{t}+\frac{N_S(x)}{a}\right]$$

Putting the value of α again in equation (16), we obtain the envelope

$$F_2^S(x,t)\exp\left[M_S(x)\right] = -\frac{1}{4}\left[t^{(b/t+1)}\exp\left(\frac{b}{t}+\frac{N_S(x)}{a}\right)\right]^2$$

Therefore,

$$F_2^S(x,t) = -\frac{1}{4}t^{2(b/t+1)}\exp\left[\frac{2b}{t}+\frac{2N_S(x)}{a}-M_S(x)\right], \quad (17)$$

which is merely a particular solution

Now, defining

$$F_2^S(x,t_0) = -\frac{1}{4}t_0^{2(b/t_0+1)}\exp\left[\frac{2b}{t_0}+\frac{2N_S(x)}{a}-M_S(x)\right],$$

at $t = t_0$, where $t_0 = \ln\left(Q_0^2/\Lambda^2\right)$ at any lower value $Q = Q_0$ we get from eq (17),

$$F_2^S(x,t) = F_2^S(x,t_0)\left(\frac{t^{(b/t+1)}}{t_0^{(b/t_0+1)}}\right)^2\exp\left[2b\left(\frac{1}{t}-\frac{1}{t_0}\right)\right], \quad (18)$$

which gives the t-evolution of singlet structure function $F_2^S(x,t)$ in NLO for $\beta = \alpha^2$

Proceeding exactly in the same way, and defining

$$F_2^{NS}(x,t_0) = -\frac{1}{4}t_0^{2(b/t_0+1)}\exp\left[\frac{2b}{t_0}+\frac{2N_{NS}(x)}{a}-M_{NS}(x)\right],$$

where $N_{NS}(x) = \int\frac{dx}{A_S(x)+T_0B_S(x)}$

and $M_{NS}(x) = \int\frac{A_0(x)+T_0B_0(x)}{A_S(x)+T_0B_S(x)}dx$,

we get for non-singlet structure function in NLO as

$$F_2^{NS}(x,t) = F_2^{NS}(x,t_0)\left(\frac{t^{(b/t+1)}}{t_0^{(b/t_0+1)}}\right)^2\exp\left[2b\left(\frac{1}{t}-\frac{1}{t_0}\right)\right] \quad (19)$$

which gives the t-evolution of non-singlet structure function $F_2^{NS}(x,t)$ in NLO for $\beta = \alpha^2$

In an earlier communication [14], we suggested that for low x in LO for $\beta = \alpha^2$,

$$F_2^S(x,t) = F_2^S(x,t_0)\left(\frac{t}{t_0}\right)^2 \quad (20)$$

and

$$F_2^{NS}(x,t) = F_2^{NS}(x,t_0)\left(\frac{t}{t_0}\right)^2 \quad (21)$$

We observe that if b tends to zero, eqs (18) and (19) tend to eqs (20) and (21), respectively, *i.e.* solutions of NLO equations go over to those of LO equations. Physically, b tends to zero means number of flavours is high

Again defining

$$F_2^S(x_0,t) = -\frac{1}{4}t^{(b/t+1)}\exp\left[\frac{2b}{t}+\frac{2N_S(x)}{a}-M_S(x)\right]_{x=x_0},$$

we obtain from eq (17)

$$F_2^S(x,t) = F_2^S(x_0,t)\exp\int_{x_0}^{x}\left[\frac{2}{a}\frac{1}{L_2(x)+T_0M_2(x)}\right.$$

$$\left.-\frac{L_1(x)+T_0M_1(x)}{L_2(x)+T_0M_2(x)}\right]dx, \quad (22)$$

which gives the x-evolution of singlet structure function $F_2^S(x,t)$ in NLO for $\beta = \alpha^2$. Similarly, defining $F_2^{NS}(x_0,t) = -\frac{1}{4}t^{(b/t+1)}\times\exp\left[\frac{2b}{t}+\frac{2N_{NS}(x)}{a}-M_{NS}(x)\right]_{x=x_0}$, we get

$$F_2^{NS}(x,t) = F_2^{NS}(x_0,t)\exp\int_{x_0}^{x}\left[\frac{2}{a}\frac{1}{A_S(x)+T_0B_S(x)}\right.$$

$$\left.-\frac{A_0(x)+T_0B_0(x)}{A_S(x)+T_0B_S(x)}\right]dx, \quad (23)$$

which gives the x-evolution of non singlet structure function $F_2^{NS}(x,t)$ in NLO for $\beta = \alpha^2$

In an earlier communication [14], we suggested that for low-x in LO for $\beta = \alpha^2$,

$$F_2^S(x,t) = F_2^S(x_0,t)\exp\left[\int_{x_0}^{x}\left(\frac{2}{A_f M(x)}-\frac{L(x)}{M(x)}\right)dx\right] \quad (24)$$

and

$$F_2^{NS}(x,t) = F_2^{NS}(x_0,t)\exp\left[\int_{x_0}^{x}\left(\frac{2}{A_f Q(x)}-\frac{L(x)}{M(x)}\right)dx\right], \quad (25)$$

where

$$A_f = 4/(33-2N_f),\ P(x) = 3+4\ln(1-x)-(1-x)(x+3)$$

$$Q(x) = x(1-x^2)-2x\ln x,$$

$$L(x) = P(x) + K(x)C(x) + D(x)\frac{\partial K(x)}{\partial x}$$

and $M(x) = Q(x) + K(x)D(x)$, where again

$$C(x) = 1/2N_f(1-x)(2-x+2x^2)$$

and $D(x) = N_f x\left[-1/2(1-x)(5-4x+2x^2)+(3/2)\ln(1/x)\right]$

Of course, unlike for the t evolution equations, we could not have for the x-evolution equations in LO as some limiting case of NLO equations. Deuteron, proton and neutron structure functions measured in deep inelastic electro production can be written in terms of singlet and non singlet quark distribution functions [5] as

$$F_2^d(x,t) = 5/9\, F_2^S(x,t), \tag{26}$$

$$F_2^p(x,t) = 5/18\, F_2^S(x,t) + 3/18\, F_2^{NS}(x,t) \tag{27}$$

and

$$F_2^n(x,t) = 5/18\, F_2^S(x,t) - 3/18\, F_2^{NS}(x,t) \tag{28}$$

Now using eqs (22) in eq (26), we will get x evolution of deuteron structure function $F_2^S(x,t)$ at low x in NLO for $\beta = \alpha^2$ as

$$F_2^d(x,t) = F_2^d(x_0,t)\exp\int_{x_0}^{x}\left[\frac{2}{a}\,\frac{1}{L_2(x)+T_0M_2(x)} - \frac{L_1(x)+T_0M_1(x)}{L_2(x)+T_0M_2(x)}\right]dx \tag{29}$$

where, the input function is $F_2^d(x_0,t) - \frac{5}{9}F_2^S(x_0,t)$. The corresponding result for a particular solution of DGLAP evolution equations in LO for $\beta = \alpha^2$ obtained earlier [14] is

$$F_2^d(x,t) = F_2^d(x_0,t)\exp\left[\int_{x_0}^{x}\left(\frac{2}{A_f M(x)} - \frac{I(x)}{M(x)}\right)dx\right] \tag{30}$$

The determination of x evolutions of proton and neutron structure functions like those of deuteron structure function is not possible by this methodology because to extract the x evolution of proton and neutron structure functions we are to use eqs (22) and (23) in eqs (27) and (28). But the functions inside the integral sign of eqs (22) and (23) are different and we need to separate the input functions $F_2^S(x_0,t)$ and $F_2^{NS}(x_0,t)$ from the data points to extract the x evolutions of the proton and neutron structure functions which may contain large errors.

For the complete solution of eq (12) we take $\beta = \alpha^2$ in eq (15). If we take $\beta = \alpha$ in eq (15) and differentiate with respect to α as before, we get $0 = t^{(b/t+1)}\exp\left(\frac{b}{t}+\frac{N_S(x)}{a}\right)+1$, from which we can not determine the value of α. But if we take $\beta = \alpha^2$ in eq (15) and differentiate with respect to α we get $\alpha = \sqrt{-\frac{1}{3}t^{(b/t+1)}\exp\left(\frac{b}{t}+\frac{N_S(x)}{a}\right)}$ which is imaginary. Putting this value of α in eq (15) we get ultimately

$$F_2^S(x,t) = t^{(b/t+1)^2}\left\{\left(\frac{1}{3}\right)^{1/2} + \left(\frac{1}{3}\right)^{3/2}\right\} \times \exp\left[\left(\frac{b}{t}+\frac{N_S(x)}{a}\right)^{3/2} - M_S(x)\right]$$

Now, defining

$$F_2^S(x,t_0) = t_0^{(b/t+1)^2}\left\{\left(-\frac{1}{3}\right)^{1/2} + \left(-\frac{1}{3}\right)^{3/2}\right\} \times \exp\left[\left(\frac{b}{t_0}+\frac{N_S(x)}{a}\right)^{3/2} - M_S(x)\right]$$

we get

$$F_2^S(x,t) = F_2^S(x,t_0)\left(\frac{t^{(b/t+1)}}{t_0^{(b/t_0+1)}}\right)^{3/2}\exp\left[\frac{3}{2}b\left(\frac{1}{t}-\frac{1}{t_0}\right)\right]$$

Proceeding exactly in the same way we also get for non singlet structure function

$$F_2^{NS}(x,t) = F_2^{NS}(x,t_0)\left(\frac{t^{(b/t+1)}}{t_0^{(b/t_0+1)}}\right)^{3/2}\exp\left[\frac{3}{2}b\left(\frac{1}{t}-\frac{1}{t_0}\right)\right]$$

Then using eqs (26), (27) and (28) we get t evolutions of deuteron, proton and neutron structure functions

$$F_2^{d,p,n}(x,t) = F_2^{d,p,n}(x,t_0)\left(\frac{t^{(b/t+1)}}{t_0^{(b/t_0+1)}}\right)^{3/2}\exp\left[\frac{3}{2}b\left(\frac{1}{t}-\frac{1}{t_0}\right)\right]$$

Proceeding in the same way we get x evolution of deuteron structure function as

$$F_2^d(x,t) = F_2^d(x_0,t)\exp\int_{x_0}^{x}\left(\frac{3/2}{a}\,\frac{1}{L_2(x)+I_0M_2(x)} - \frac{I_1(x)+I_0M_1(x)}{L_2(x)+I_0M_2(x)}\right)dx$$

Similarly we can show that if we take $\beta = \alpha^4$ we get

$$F_2^{d,p,n}(x,t) = F_2^{d,p,n}(x,t_0)\left(\frac{t^{(b/t+1)}}{t_0^{(b/t_0+1)}}\right)^{4/3}\exp\left[\frac{4}{3}b\left(\frac{1}{t}-\frac{1}{t_0}\right)\right]$$

and

$$F_2^d(x,t) = I_2^d(x_0,t)\exp\int_x^1\left(\frac{4/3}{u}\,\frac{1}{I_3(u)+I_0M_3(u)}\right.$$

$$\left.-\frac{L_1(u)+I_0M_1(u)}{I_2(u)+I_0M_2(u)}\right)du$$

Similarly if we take $\beta=\alpha^5$ we get

$$F_3^{d\,p\,n}(x,t) = F_3^{d\,p\,n}(x,t_0)\left(\frac{t^{(b/t+1)}}{t_0^{(b/t+1)}}\right)^{5/4}\exp\left[\frac{5}{4}b\left(\frac{1}{t}-\frac{1}{t_0}\right)\right]$$

and

$$I_2^d(x,t) = I_2^d(x_0,t)\exp\int_x^1\left(\frac{5/4}{u}\,\frac{1}{I_3(u)+I_0M_3(u)}\right.$$

$$\left.-\frac{L_1(u)+I_0M_1(u)}{L_3(u)+I_0M_3(u)}\right)du$$

and so on

Thus we observe that if we take $\beta-\alpha$ in eq (15) we can not obtain the value of α and also the required solution But if we take $\beta=\alpha^2\ \alpha^3\ \alpha^4\ \alpha^5$ and so on we see that the powers of $t^{(b/t+1)}/t_0^{(b/t+1)}$ and coefficient of $b(1/t-1/t_0)$ of exponential part in t evolutions of deuteron proton and neutron structure functions are 2 3/2 4/3 5/4 and so on respectively as discussed above Similarly for x evolutions of deuteron structure functions we set that the numerators of the first term inside the integral sign are 2 3/2 4/3 5/4 and so on respectively for the same values of α Thus we see that if in the relation $\beta-\alpha^3$ x varies between 2 to a maximum value the powers of $t^{(1/t+1)}/t_0^{(1/t+1)}$ coefficient of $t^{(b/t+1)}/t_0^{(1/t+1)}$ of exponential part in t evolution and the numerator of the first term in the integral sign in x evolution varies between 2 to 1 Then it is understood that the solutions of eqs (12) and (13) obtained by this methodology are not unique and so the t evolutions of deuteron proton and neutron structure functions and x evolution of deuteron structure function obtained by this methodology are not unique

Thus by this methodology instead of having a single solution,we arrive at a band of solutions the range of these solutions being reasonably narrow

3 Results and discussion

For a quantitative analysis of x distributions of structure functions we calculate the integrals that occurred in eq (29) for $N_f=4$ In this case we neglect the first and second term of function $B_1(x)$ as x is small

In Figure 1 we present our results of x distribution of deuteron structure functions F_2^d from eq (29) for $K(x)=ax^b$ (dashed lines) and for $K(x)=ce^{-dx}$ (solid lines) in the relation $\beta=\alpha^3$ for x minimum (lower dashed and solid lines) and maximum (upper dashed and solid lines) where a b c and d are constants and for representative values of Q^2 given in each figure We compare them with NMC deuteron low x low Q^2 data [18] In each graph, the data point for x value just below 0 1 had been taken as input $F_2^d(x_0,t)$ If we take $K(x)=ax^b$ then agreement of the result for x minimum with experimental data is found to be excellent at $a=10$ $b=0\,016$ On the other hand if we take $K(x)=ce^{-dx}$ then agreement of the results for x minimum with experimental data is found to be good at $c=0\,5$ $d=-3\,8$ In this connection, earlier we observed [14] that agreement of the results with experimental data was excellent for $K(x)=4\,5$ (constant) $a=4\,5$ $b=0\,01$ $c=5$ $d=1$ for low x in leading order and there was no significant difference between the results for

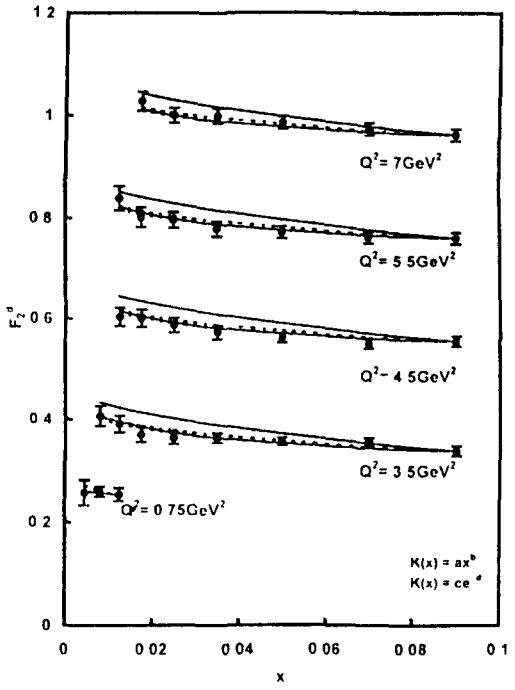

Figure 1 Results of x distribution of deuteron structure functions F_2^d from eq (29) for $K(x)=ax^b$ (dashed lines) and for $K(x)=ce^{-dx}$ (solid lines) in the relation for x minimum (lower dashed and solid lines) and maximum (upper dashed and solid lines) where a b c and d are constants and for representative values of Q given in each figure and compare them with NMC deuteron low x low Q^2 data [18] In each graph the data point for x value just below 0 1 has been taken as input $F_2^d(x_0,t)$ If we take $K(x)=ax^b$ then agreement of the result for x minimum with experimental data is found to be excellent at $a=10$ $b=0\,016$ On the other hand if we take $K(x)=ce^{-dx}$ then agreement of the results for x minimum with experimental data is found to be good at $c=0\,5$ $d=-3\,8$ For convenience value of each data point for one value of Q is increased by adding $0.2i$ where $i=0$ 1 2 3 are the numberings of curves counting from the bottom of the lowermost curve as the 0 th order

y minimum and maximum in the relation $\beta = \alpha'$. In the case of NLO, agreement of the results with experimental data is found to be very poor for any constant value of $K(x)$. Therefore, we do not present our result of x distribution at $K(x)$ = constant in NLO.

In Figure 2, we present our results of x evolution of deuteron structure function from eq (29) for $K(x) = ax^b$ (dashed lines) and $K(x) = ce^{-dx}$ (solid lines) in the relation $\beta = \alpha'$, for y maximum at different parameter values and for representative values of Q^2 given in each figure, and compare them with NMC deuteron low-x low-Q^2 data [18]. In each graph the data point for x value just below 0.1 has been taken as input $F_2^d(x_0, t)$. We observed that both the graphs coincide for each Q^2 value and are in excellent agreement with data when $a = 5.5$, $b = 0.016$, $c = 0.28$, $d = -3.8$.

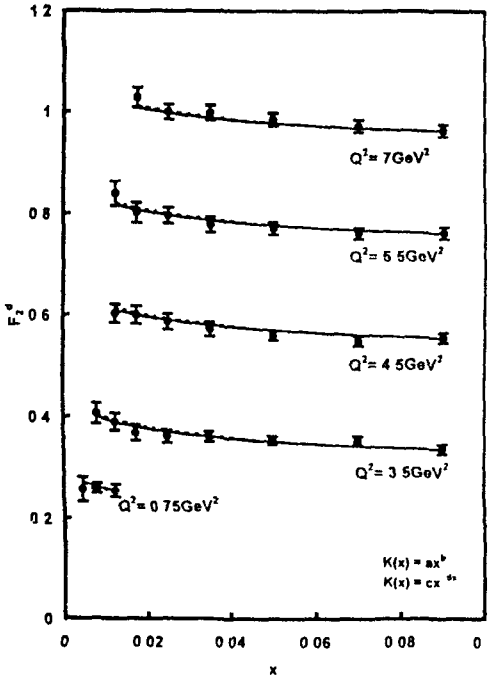

Figure 2. Results of x evolution of deuteron structure function from equation (29) for $K(x) = ax^b$ (dashed lines) and $K(x) = ce^{-dx}$ (solid lines) in the relation $\beta = \alpha'$ for y maximum at different parameter values and for representative values of Q^2 given in each figure and compare them with NMC deuteron low x low Q^2 data [18]. In each graph the data point for x value just below 0.1 has been taken as input $F_2^d(x_0, t)$. We observed that both the graphs coincide for each Q^2 value and are in excellent agreement with data when $a = 5.5$, $b = 0.016$, $c = 0.28$, $d = -3.8$. For convenience value of each data point for one value of Q^2 is increased by adding $0.2i$ where $i = 0, 1, 2, 3, \ldots$ are the numberings of curves counting from the bottom of the lowermost curve as the 0 th order.

In Figure 3, we present the sensitivity of our results from eq (29) for a, b, c, d in the relation $\beta = \alpha'$ for y minimum. In each graph (from top), if the absolute values of d, c, b or a respectively are increased, the curves shift upward and if the absolute values of d, c, b or a, respectively are decreased, the curves move in the opposite direction. For the sensitivity of a, we take $b = 0.016$ and we observe that at $a = 10$, agreement of the results with experimental data is found to be excellent. For the sensitivity of b, we take $a = 10$ and we observe that at $b = 0.016$ agreement of the results with experimental data is found to be excellent. On the other hand for the sensitivity of c, we take $b = -3.8$ and we observe that at $c = 0.5$, agreement of the results with experimental data is found to be good. For the sensitivity of d, we take $c = 0.5$ and we observe that at $d = -3.8$ agreemnt of the results with experimental data is found to be excellent.

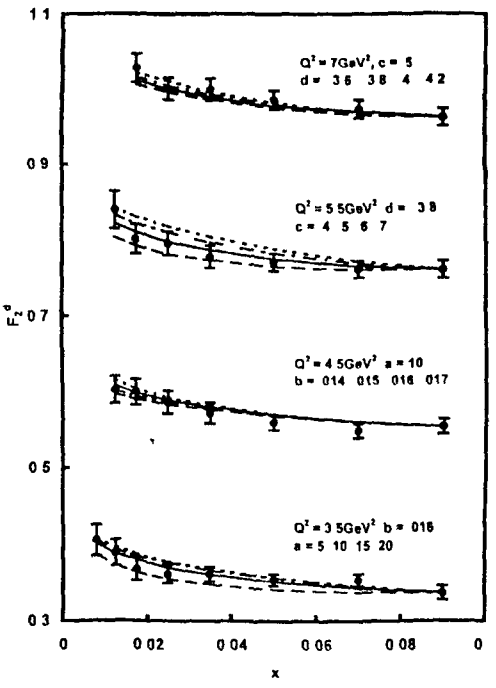

Figure 3. Sensitivity of our results of x distribution of deuteron structure function in the relation $\beta = \alpha'$ for y minimum for different values of a, b, c and d.

In Figure 4 we present the sensitivity of our results from eq (29) for different values of I_0 at best fit of $K(x) = ax^b$ and $K(x) = ce^{-dx}$ in the realtion $\beta = \alpha'$ for y minimum and for representative values of Q^2 given in each figure. Here $a = 10$, $b = 0.016$, $c = 0.5$, $d = -3.8$. We observed that if the value of I_0 is increased the curve moves slightly upward and if the value of I_0 is decreased, the curve moves slightly downward direction. But the nature of the curve remains same and difference between the curves are extremely small in both cases in the I_0 range mentioned in the figure.

In Figure 5 we present the results of x evolution of deuteron structure function for $K(x) = ax^b$ (dashed lines) and $K(x) = ce^{-dx}$ (solid lines) in the relation $\beta = \alpha'$ for y minimum in LO (lower dashed and solid lines) and in NLO (upper dashed and solid

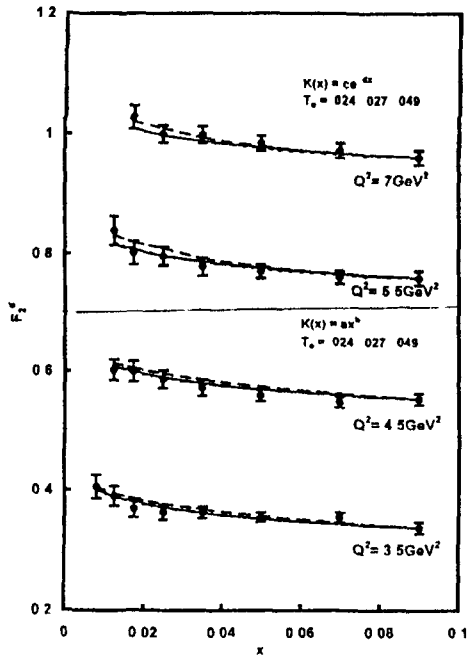

Figure 4 Sensitivity of our results of x distribution of deuteron structure function in the relation $\beta - \alpha^{\nu}$ for x minimum for different values of a b c and d

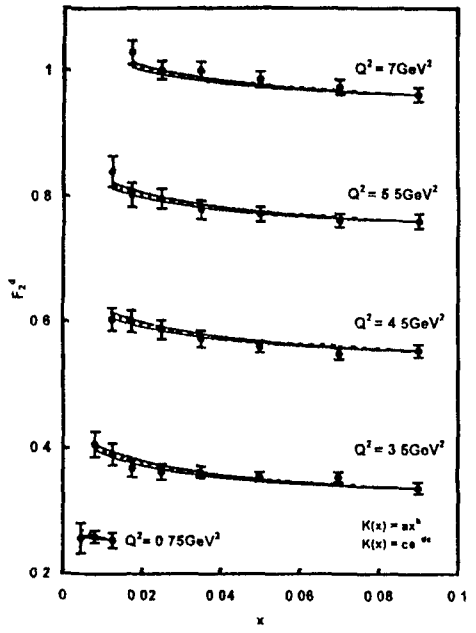

Figure 5 Results of x evolution of deuteron structure function for $K(x) = ax^b$ (dashed lines) and $K(x) = ce^{dx}$ (solid lines) in relation $\beta - \alpha^{\lambda}$ for x minimum in LO (lower dished and solid lines) and in NLO (upper dished and solid lines) for representative values of Q given in each figure and compare them with NMC deuteron low x low Q^2 data [18] In each graph the data point for x value just below 0 1 has been taken as input Agreement of the result with experimental data is found to be excellent for $a = 4\ 5$ $b = 0\ 01$ $c = 5$ $d = 1$ in LO and $a = 10$ $b = 0\ 016$ $c = 0\ 5$ $d = -3\ 8$ in NLO and all the curves in each graph almost coincide

lines) for representative values of Q^2 given in each figure and compare them with NMC deuteron low x low Q^2 data [18] In each graph, the data point for x value just below 0 1 has been taken as input Agreement of the result with experimental data is found to be excellent for $a = 4\ 5$ $b = 0\ 01$ $c = 5$ $d = 1$ in LO and $a = 10$ $b = 0\ 016$ $c = 0\ 5$ $d = -3\ 8$ in NLO and all curves in each graph almost coincide

In Figure 6 we plot $I(t)$ (solid line) and $I_0 I(t)$ (dashed line) where $T(t) = \alpha_s/2\pi$ against Q^2 in the Q^2 range $0\ 5 \le Q^2 \le 50$ GeV^2 We observed that for $T_0 = 0\ 027$ error becomes minimum in the Q^2 range $0\ 5 \le Q^2 \le 50$ GeV^2

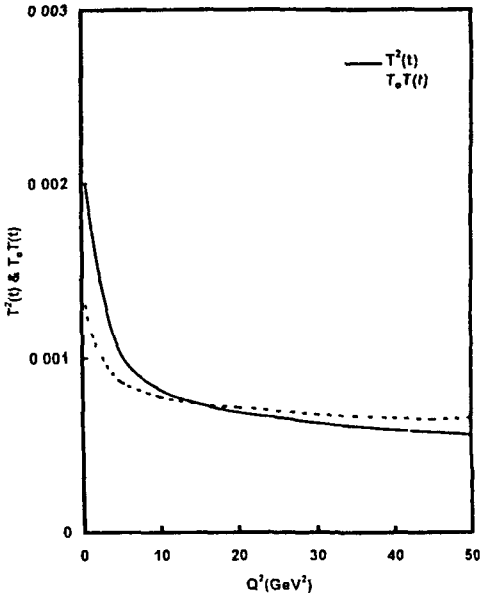

Figure 6 $I(t)$ (solid line) and $I_0 I(t)$ (dashed line where $I(t) = \alpha_s/2\pi$ against Q in the Q^2 range $0\ 5 < Q^2 < 50$ GeV We observed that for $I_0 = 0\ 027$ error becomes minimum in the Q range $0\ 5 < Q^2 < 50$ GeV

From our above discussion it has been observed that we can not establish a unique relation between singlet and gluon structure functions *i e* a unique expression for $K(x)$ in eq (9) by this method $K(x)$ in the forms of an exponential function of x or a power in x can equally produce required x distribution of deuteron structure functions But unlike x distribution function with many input parameters (generally used in the literature) our method required only one or two such parameters The explicit form of $K(x)$ can actually be obtained only by solving coupled DGLAP evolution equations for singlet and gluon structure functions and work is going on in this regard Traditionally the DGLAP equations provide a means of calculating the manner in which the parton distributions change at fixed x as Q^2 varies This change comes about because of the various types of parton branching emission processes and the x distributions are modified as the initial momentum is shared

among the various daughter partons However the exact rate of modifications of x-distributions at fixed Q^2 can not be obtained from the DGLAP equations, since it depends not only on the initial x but also on the rate of change of parton distributions with respect to x, $d^n F(x)/dx^n$ ($n = 1$ to ∞), up to infinite order Physically, this implies that at high-x the parton has a large momentum fraction at its disposal and as a result it radiates partons including gluons in innumerable ways some of them involving complicated QCD mechanisms However, for low x, many of the radiation processes will cease to occur due to momentum constraints and the x-evolutions get simplified It is then possible to visualize a situation in which the modification of the x-distribution simply depends on its initial value and its first derivative In this simplified situation the DGLAP equations give information on the shapes of the x distribution as demonstrated in this paper The clearer testing of our results of x evolution is actually the eq (23) which is free from the additional assumption [eq (9)] The required non singlet data is not adequately available in the low x region to test our result

Acknowledgment

One of us (JKS) is grateful to the University Grants Commission, New Delhi for the financial assistance to this work in the form of a major research project

References

[1] G Altarelli and G Parisi *Nucl Phys* **B126** 298 (1977)
[2] G Altarelli *Phys Rep* **81** 1 (1981)
[3] V N Gribov and L N Lipatov *Sov J Nucl Phys* **20** 94 (1975)
[4] Y L Dokshitzer *Sov Phys JETP* **46** 641 (1977)
[5] F Halzen and A D Martin *Quarks and Leptons An Introductory Course in Modern Particle Physics* (New York John and Wiley) (1984)
[6] A Ali and J Bartels (eds) *Proc DESY Topical Meeting on the Small x Behaviour of Deep Inelastic Structure Functions in QCD* (1990) (North Holland Amsterdam) (1991)
[7] G Jarlskog and D Rein (eds) *Proc Large Hardon Collider Workshop* (CERN report CERN 90-10) (1990)
[8] M Maruma and S Kumano *hep-ph/9505246*
[9] C Corianò and C Savkli JLAB-THY-98-09 WM-98-102 (1998)
[10] F Ayres (Jr) *Differential Equations* (Schaum's Outline Series) (New York McGraw Hill) (1952)
[11] D K Choudhury and J K Sarma *Pramana J Physics* **39** 273 (1992)
[12] J K Sarma D K Choudhury and G K Medhi *Phys Lett* **B403** 139 (1997)
[13] J K Sarma and B Das *Phys Lett* **B304** p323 (1993)
[14] R Rajkhowa and J K Sarma *hep-ph/0201263* (2002) *Indian J Phys* **78A** p365 (2004)
[15] R Rajkhowa and J K Sarma *hep-ph/0203070* (2002)
[16] R Rajkhowa and J K Sarma *J Cosmo* (2003)
[17] C Adloff H1 Collaboration DESY 98-169 *hep-ex/9811013* (1998)
[18] M Arneodo hep/961031 *NMC Nucl Phys* **B483** p3 (1997)
[19] F H Miller *Partial Differential Equation* (New York John and Willey) (1960)
[20] W Furmanski and R Petronzio *Nucl Phys* **B195** p237 (1982)
[21] W Furmanski and R Petronzio *Z Phys* **C11** 293 (1982) *Phys Lett* **B97** p437 (1980)
[22] A Deshamukhya and D K Choudhury *Proc 2nd Regional Conf Phys Research in North East* (Guwahati India October 2001) p34 (2001)
[23] I S Gradshteyn and I M Ryzhik *Tables of Integrals Series and Products* (ed) Alen Jeffrey (New York Academic) (1965)